LEABHARLANN CHOLÁISTE NA TRÍONÓIDE, BAILE ÁTHA CLIATH | TRINITY COLLEGE LIBRARY DUBLIN
Ollscoil Átha Cliath | The University of Dublin

Terms and Conditions of Use of Digitised Theses from Trinity College Library Dublin

Copyright statement

All material supplied by Trinity College Library is protected by copyright (under the Copyright and Related Rights Act, 2000 as amended) and other relevant Intellectual Property Rights. By accessing and using a Digitised Thesis from Trinity College Library you acknowledge that all Intellectual Property Rights in any Works supplied are the sole and exclusive property of the copyright and/or other IPR holder. Specific copyright holders may not be explicitly identified. Use of materials from other sources within a thesis should not be construed as a claim over them.

A non-exclusive, non-transferable licence is hereby granted to those using or reproducing, in whole or in part, the material for valid purposes, providing the copyright owners are acknowledged using the normal conventions. Where specific permission to use material is required, this is identified and such permission must be sought from the copyright holder or agency cited.

Liability statement

By using a Digitised Thesis, I accept that Trinity College Dublin bears no legal responsibility for the accuracy, legality or comprehensiveness of materials contained within the thesis, and that Trinity College Dublin accepts no liability for indirect, consequential, or incidental, damages or losses arising from use of the thesis for whatever reason. Information located in a thesis may be subject to specific use constraints, details of which may not be explicitly described. It is the responsibility of potential and actual users to be aware of such constraints and to abide by them. By making use of material from a digitised thesis, you accept these copyright and disclaimer provisions. Where it is brought to the attention of Trinity College Library that there may be a breach of copyright or other restraint, it is the policy to withdraw or take down access to a thesis while the issue is being resolved.

Access Agreement

By using a Digitised Thesis from Trinity College Library you are bound by the following Terms & Conditions. Please read them carefully.

I have read and I understand the following statement: All material supplied via a Digitised Thesis from Trinity College Library is protected by copyright and other intellectual property rights, and duplication or sale of all or part of any of a thesis is not permitted, except that material may be duplicated by you for your research use or for educational purposes in electronic or print form providing the copyright owners are acknowledged using the normal conventions. You must obtain permission for any other use. Electronic or print copies may not be offered, whether for sale or otherwise to anyone. This copy has been supplied on the understanding that it is copyright material and that no quotation from the thesis may be published without proper acknowledgement.

Genetic Mechanisms Establishing Thalamocortical Connectivity:

Novel Genes and a Role for Semaphorin6B

Olivia Bibollet-Bahena

A thesis submitted for the fulfillment of the Degree of Doctor in Philosophy to

Trinity College, University of Dublin

November 2015

DEAN OF GRADUATE STUDIES
20 JAN 2016
TRINITY COLLEGE, DUBLIN

THESIS
11037

50652434

Ph.D.
School of Genetics & Microbiology

TRINITY LIBRARY
27 JUL 2016
DUBLIN
11037

Declaration

I hereby declare that this thesis, submitted to the University of Dublin, Trinity College, is entirely my own work, unless stated otherwise, and has not been previously submitted to this or any other university. I give my permission to the library to lend or copy this thesis on request.

Acknowledgements

First and foremost, I would like to express my gratitude to my supervisor Dr. Kevin Mitchell for giving me the opportunity to undertake PhD studies in his laboratory. I had envisaged what type of training I would acquire during my stay; the number of techniques I have learned does not compare. Dr. Mitchell's enthusiasm for novel ways to explore developmental neurogenetics has been inspiring. This has been a great opportunity.

I would also like to thank past and present members of the Mitchell Lab for their help, support, and enthusiastic scientific and non-scientific discussions (in particular, Dr. Jackie Dolan, Niamh McGarry, Manuela Mitsogiannis, Ash Nicolas Watson, Dr. Graham Little, Dr. Daniel Shanley and Dr. Hiroshi Tawayarama)|. The department of Genetics as a whole, whether staff or students, has always been of great support (and in particular, Dr. Karsten Hokamp, Dr. Aoife McLysaght, Dr. Mario Fares and Maria Prats). In addition, I would like to thank the staff of the animal facility.

Personal thanks go to Declan Reilly, Andrew Costello, Caroline Igoe and Niall O'Brien.

I would also like to extend my gratitude to all the great friends I have made in Dublin throughout this journey.

Finally, unconditional support from my mother and sister cannot be thanked enough.

Summary

One of the main functions of the brain is to process information from the environment. All input to the neocortex passes through the thalamus in order to be handled. Therefore, proper connectivity between the thalamus and the neocortex is crucial. During brain development a staggeringly complex network of connections self-assembles between billions of neurons through a finely orchestrated series of stages. Extracellular proteins, known as guidance molecules, induce attractive or repulsive responses from extending axons leading them through their journeys towards their appropriate targets. Although different guidance molecules have been identified to date, it is speculated that many more are required to explain the observed complexity in brain connectivity.

Given the amount of available data and tools online, we first performed an *in silico* search for new potential candidates implicated in thalamocortical pathfinding. The Allen Brain Institute has generated a large dataset of mouse messenger RNA expression during development. Here, we use a bioinformatics approach to mine expression values for 2002 genes at 7 developmental ages relevant to different developmental stages: regional specification/patterning (E11.5), axon pathfinding (E13.5, E15.5 and E18.5), synaptogenesis (P4 and P14) and cortical plasticity (P28). Moreover, using different webtools (PSORTII, SignalP, big-PI predictor and TMHMM), we screened protein products for subcellular localization with an emphasis on the extracellular compartment where guidance molecules reside. We also included known functions associated to the genes in our dataset. We postulate a list of 43 new candidate genes involved in thalamocortical pathfinding.

To further pursue our search for genes involved in thalamocortical connectivity, we studied the *in vivo* implication of Sema6A, Sema6B, PlexinA2 and PlexinA4 in the somatosensory system. Previous work within the laboratory and elsewhere has already validated the developmental expression of Sema6A, Sema6B, PlexinA2 and PlexinA4, albeit in restricted time-points and brain regions. This body of work has also established roles in thalamocortical connectivity from the dorsal lateral geniculate nucleus for Sema6A, and axonal guidance in other brain regions for this protein, Sema6B and their binding partners PlexinA2 and PlexinA4. An interesting phenotype was reported by Suto, Ito et al. (2005) where adult *PlexinA4* mutant mice exhibit indistinct boundaries of

barrel formations in the somatosensory cortex. We therefore investigated the expression patterns of Sema6A, Sema6B, PlexinA2 and PlexinA4 at time-points relevant for barrel cortex formation (namely postnatal days 2, 4, 6 and 8). All four genes are expressed in the thalamus and the neocortex at those time-points. Moreover, their expression patterns intersect at the level of the ventral posteriomedial nucleus (VPM) of the thalamus, from which axons specifically project to the somatosensory cortex. Immunohistochemical studies have revealed PlexinA4 protein expression within thalamic (and cortical) axons at E15.5, as well as in the barrel neuropil at P8. In addition, *Sema6A*, *Sema6B* and *PlexinA2* mRNA expression is detected in the somatosensory cortex in cortical layers II/III above the characteristic barrel structures, but also in cortical layer IV between the barrels, during the first postnatal week.

We also present novel roles for *Sema6A*, *Sema6B* and *PlexinA4* in thalamocortical development towards the somatosensory cortex. We show that all three genes are required for thalamocortical axons to enter the cortex in the appropriate perpendicular orientation from the white matter layer by dye tracing experiments. *Sema6B* and *PlexinA4* null mice exhibit more severe and similar phenotypes, compared to *Sema6A*-/- mice. *Sema6A* and *Sema6B* appear to have additive effects. A striking defect in cell organization occurs in *Sema6B*-/- somatosensory cortex. We show that Cux-1 positive neurons fail to exit the barrel hollows, but do exit the septa. This type of phenotype has not been reported before and brings to light *Sema6B* as a gene involved in the exclusion of cortical layer IV neurons from the barrel hollows. The barrel neuropil is also differently organized in the *Sema6B*-/- mice. PlexinA4 positive fibers appear to avoid cells within the barrel hollows. Moreover, Cux-1 positive neurons are also found at abnormal positions in the somatosensory cortex of *Sema6A*-/- mice. In these mice, Cux-1 expressing neurons migrate beyond their target layer into the marginal zone (preliminary work suggests that the same phenotype is mimicked in *PlexinA2/PlexinA4* double knockout mutant mice). Taken together, these data implicate *Sema6A*, *Sema6B*, *PlexinA2* and *PlexinA4*, in proper VPM thalamocortical connectivity to the somatosensory cortex. Sema6A and Sema6B are required for correct cortical invasion of thalamocortical axons, as well as differentially delimitating the target areas of Cux-1 expressing neurons in cortical layer IV. Most likely, they are functioning through repellent actions via their binding partners PlexinA2 and PlexinA4.

List of Abbreviations

bHLH	basic helix-loop-helix
Cp	cortical plate
Ctx	cortex
devABA	developing Allen Brain Atlas
dLGN	dorsal lateral geniculate nucleus
DTB	diencephalon-telencephalon boundary
dTH	dorsal thalamus
FGF	fibroblast growth factor
Gad67	glutamic acid decarboxylase 67
GPCR	G-protein coupled receptor
GPI	glycosylphosphatidylinositol
ic	internal capsule
ISH	*in situ* hybridization
MAOA	monoamine oxidase type A
MZ	marginal zone
NMDAR	N-methyl-d-aspartate receptor
PSPB	pallium-subpallium boundary
pTH-C	caudal progenitor domain of the thalamus
pTH-R	rostral progenitor domain of the thalamus
Rt	reticular nucleus
S1	primary somatosensory cortex
Shh	Sonic hedgehog
SP	subplate
TCA	thalamocortical axon
VB	ventrobasal complex
VGluT2	vesicular glutamate transporter 2
vLGN	ventral lateral geniculate nucleus
VP	ventral posterior nucleus
VPM	ventral posteriomedial nucleus
vTel	ventral telencephalon
WM	white matter
WT	wild-type
ZLI	Zona Limitans Intrathalamica

Table of Contents

Declaration ..... **Error! Bookmark not defined.**

Acknowledgements ii

Summary iii

List of Abbreviations v

Table of Contents vi

List of Figures x

List of Tables xiii

Chapter 1 1

Introduction 1

1.1 Introduction 2

1.1.1 The Thalamocortical System 2

1.1.2 Thalamic development 6

1.1.3 Development of the thalamocortical projections 10

1.1.4 Aims 17

Chapter 2 19

Materials and Methods 19

2.1 Data acquisition and preprocessing 20

2.2 Clustering analyses 24

2.3 Enrichment analyses 24

2.4 Animals 24

2.5 DNA extraction, purification and genotyping 25

2.6 Histology 27

2.7 *In situ* hybridization probe construction 27

2.8 *In situ* hybridization 28

2.9 Immunohistochemistry 29

2.10 Fiber tracing with carbocyanine dyes 31

Chapter 3 32

Bioinformatics Analyses of Developmental Gene Expression Patterns in the Thalamus 32

3.1 Introduction 33

3.1.1 The mouse developing Allen Brain Atlas 33

3.1.2 Webtools to predict protein subcellular localization 34

3.1.3 Extracellular proteins expressed during thalamic development 36

3.1.4 Aims 39

3.2 Results 40

3.2.1 Clustering analyses of developmental gene expression patterns in the thalamus 40

3.2.2 Distribution of proteins by localization 45

3.2.3 Enrichment analyses of proteins based on localization 45

3.2.4 Distribution of proteins by function 50

3.2.5 Enrichment analyses of genes based on function 51

3.2.6 Genes involved in thalamic development 56

3.2.7 Extracellular axon guidance molecules 70

3.3 Discussion 83

3.3.1 Gene expression data from the Allen Brain Atlas 83

3.3.2 Enrichment analyses of localization and function 84

3.3.3 Novel candidates of thalamic axon pathfinding 85

3.3.4 Perspectives 87

Chapter 4 88

Expression of Semaphorin6A, Semaphorin6B, PlexinA2 and PlexinA4 in the Postnatal Thalamocortical System 88

4.1 Introduction 89

4.1.1 Semaphorins 89

4.1.2 Plexins 92

4.1.3 Class 6 Semaphorin and class A Plexin roles in the developing nervous system 95

4.1.4 Aims of this study 96

4.2 Results 98

4.2.1 Messenger RNA expression patterns of Sema6A, Sema6B, PlexinA2 and PlexinA4 at postnatal day 2 98

4.2.2 Messenger RNA expression patterns of Sema6A, Sema6B, PlexinA2 and PlexinA4 at postnatal day 4 105

4.2.3 Messenger RNA expression patterns of Sema6A, Sema6B, PlexinA2 and PlexinA4 at postnatal day 6 110

4.2.4 Messenger RNA expression patterns of Sema6A, Sema6B, PlexinA2 and PlexinA4 at postnatal day 8 116

4.2.5 Protein expression patterns of PlexinA4 from late-embryonic to early postnatal stages 121

4.3 Discussion 126

4.3.1 Combinatorial expression patterns of Sema6A, Sema6B, PlexinA2 and PlexinA4 in thalamic nuclei 126

4.3.2 Combinatorial expression patterns of Sema6B, Sema6A, PlexinA2 and PlexinA4 in the somatosensory cortex 127

4.3.3 Perspectives 128

Chapter 5 130

Investigating Thalamocortical Connectivity in the Early Postnatal Somatosensory Cortex 130

5.1 Introduction 131

5.1.1 Barrel cortex development 131

5.1.2 Activity-dependent mechanisms of barrel refinement 133

5.1.3 Barrel cortex phenotypes 136

5.1.4 Aims of this study 139

5.2 Results 140

5.2.1 Thalamocortical axons have abnormal trajectories through the somatosensory cortex of *Sema6B*-/- mice 140

5.2.2 *Sema6A* and *PlexinA4* null mutant mice also exhibit defects in thalamocortical axons trajectories through the somatosensory cortex 143

5.2.3 Preplate splitting occurs normally in *Sema6B*-/- mice 145

5.2.4 Cux-1 positive cells are found at abnormal positions in the barrel cortex of *Sema6B*-/- mice 146

5.2.5 Barrelettes and barreloids are unaffected in *Sema6B*-/- mice at P8 151

5.3 Discussion 156

5.3.1 Thalamocortical axons follow irregular trajectories within the somatosensory cortex of *Sema6A*, *Sema6B* and *PlexinA4* null mutant mice 156

5.3.2 *Sema6B*-/- mice display normal preplate splitting 156

5.3.3 Cux-1 expressing neurons are found at abnormal positions in the barrel cortex of *Sema6B*-/- mice 156

5.3.4 Barrelettes and barreloids do not show defects in *Sema6B*-/- mice 158

5.3.5 Perspectives and future directions 158

Chapter 6 162

Final Conclusions And Future Directions 162

6.1 Major findings and their implications 163

6.2 Future directions 166

List of Figures

Figure 1. Mature somatosensory thalamocortical system 5

Figure 2. Thalamic development 7

Figure 3. Neocortical development of projection neurons 12

Figure 4. Axon guidance molecules expressed along the thalamocortical path 16

Figure 5. Shh canonical and noncanonical signaling pathways 37

Figure 6. Wnt canonical and noncanonical signaling pathways 38

Figure 7. Hierarchical clustering of the developmental dataset 40

Figure 8. K-means clustering of the developmental dataset 40

Figure 9. Summaries of K-means Clustering Analyses of the Developmental Dataset . 44

Figure 10. Protein localization and function determination of the developmental dataset 45

Figure 11. Observed Over Expected Distributions of Protein Localization per Cluster 49

Figure 12. Observed Over Expected Distribution of Groups per Cluster 55

Figure 13. Shh and Ptch1 Expression at E11.5 61

Figure 14. Wnt3a, Wnt5a and Wnt8b Expression at E11.5 63

Figure 15. Celsr1, Fzd10 and Ryk Expression at E11.5 65

Figure 16. Rspo1/2/3 Expression at E11.5 67

Figure 17. FGF8/9/15 Expression at E11.5 69

Figure 18. Cntn2, Robo2 and Sema6a Expression at E15.5 76

Figure 19. Cadm1 and Ntng2 Expression at E15.5 77

Figure 20. Cbln4 and Kit Expression at E18.5 79

Figure 21. Dlk1 Expression at E15.5 80

Figure 22. Bmp3, Cbln2 and Cdh11 Expression at E18.5 82

Figure 23. Phylogenetic tree of Semaphorin sequences 90

Figure 24. Classes of the Semaphorin family 91

Figure 25. Semaphorin neuronal receptors 94

Figure 26. Expression levels of Sema6A in the mouse brain at P2 100

Figure 27. Expression levels of Sema6B in the mouse brain at P2 101

Figure 28. Expression levels of PlexinA2 in the mouse brain at P2 103

Figure 29. Expression levels of PlexinA4 in the mouse brain at P2 104

Figure 30. Expression levels of Sema6A in the mouse brain at P4 106

Figure 31. Expression levels of Sema6B in the mouse brain at P4 107

Figure 32. Expression levels of PlexinA2 in the mouse brain at P4 108

Figure 33. Expression levels of PlexinA4 in the mouse brain at P4 109

Figure 34. Expression levels of Sema6A in the mouse brain at P6 111

Figure 35. Expression levels of Sema6B in the mouse brain at P6 112

Figure 36. Expression levels of PlexinA2 in the mouse brain at P6 114

Figure 37. Expression levels of PlexinA4 in the mouse brain at P6 115

Figure 38. Expression levels of Sema6A in the mouse brain at P8 117

Figure 39. Expression levels of Sema6B in the mouse brain at P8 118

Figure 40. Expression of PlexinA2 in the mouse brain at P8 119

Figure 41. Expression levels of PlexinA4 in the mouse brain at P8 120

Figure 42. PlexinA4 expression in the mouse brain at E15.5 122

Figure 43. PlexinA4 expression in the mouse brain at P2 123

Figure 44. PlexinA4 expression in the mouse brain at P8 124

Figure 45. Maturation of the barrel cortex 132

Figure 46. Activity-regulated signaling pathways during maturation of thalamocortical synapses 134

Figure 47. Barrel cortex phenotypes 137

Figure 48. Thalamocortical axons grow into the cortical plate at abnormal positions in *Sema6B*-/- mice at P8 142

Figure 49. Thalamocortical projections in *Semaphorin* and *PlexinA4* null mutant mice at P7 144

Figure 50. Proper preplate splitting occurs in *Sema6B*-/- mice 145

Figure 51. Cortical layer IV neurons are found at abnormal positions within the barrels in *Sema6B*-/- mice at P8 148

Figure 52. PlexinA4 is expressed in the barrels of *Sema6B*-/- mice similar to wild-type 149

Figure 53. PlexinA4 expressing fibers avoid Cux-1 expressing cells in *Sema6B*-/- mouse barrel cortex at P8 150

Figure 54. Barrelettes are normal in *Sema6B*-/- mice at P8 153

Figure 55. Barreloids are normal in *Sema6B*-/- mice at P8 155

Figure 56. Cux-1 expressing cells are found within the marginal zone of the somatosensory cortex in *Sema6A*-/- mice at P4 160

Figure 57. Model of Sema6A, Sema6B, PlexinA2 and PlexinA4 in the developing barrel cortex 161

List of Tables

Table 1 Pronuclear markers in the wild-type thalamus at E18.5 10

Table 2 Developmental dataset 20

Table 3 Developmental dataset protein screens 21

Table 4 PCR Primer Sequences for Sema6B Genotyping 26

Table 5 PCR Genotyping Program for Sema6B 27

Table 6 Probes 28

Table 7 RNA Transcription and DIG Labeling 28

Table 8 Primary and Secondary Antibodies and Dilutions 30

Table 9 Features detected by PSORTII 35

Table 10 Number of Genes per Localization 45

Table 11 Observed / Expected Values per Localization 46

Table 12 Enrichment Analyses per Localization 50

Table 13 Number of Genes per Group 51

Table 14 Observed / Expected Values per Group 51

Table 15 Enrichment Analyses per Group 56

Table 16 Clustering Results for Shh, Wnts and FGFs, and their Binding Partners at K-mean 10 58

Table 17 Genes of Interest in Clusters Relevant to Axon Pathfinding 71

Table 18 Genes of Interest 72

Table 19 Genes Previously Implicated in Thalamocortical Development or Axon Guidance or Other 74

Chapter 1

Introduction

1.1 Introduction

One of the main functions of the brain is to process information from the environment. All input to the neocortex passes through the thalamus in order to be handled, such as sensory (except olfaction) and motor input. The communication between the thalamus and the neocortex is via axonal projections going both ways between these two structures, known as thalamocortical and corticothalamic projections. This system comes to be along with the rest of brain development, where a staggeringly complex network of connections self-assembles between billions of neurons through a finely orchestrated series of stages. The accuracy of this process is essential for the correct functioning of the nervous system; and, consequently, defects in this process are thought to underlie many serious psychiatric and neurological disorders. Interestingly, brain development relies on a highly conserved genetic program across species, which has allowed the use of different animal models to study it. A turning point in developmental neuroscience research has been the discovery of guidance molecules, extracellular proteins that through attractive or repulsive interactions lead axons through their journeys towards their appropriate targets. Although different guidance molecules have been identified to date, it is speculated that many more are required to explain the observed complexity in connectivity.

1.1.1 The Thalamocortical System

The thalamus is now thought to be key for relaying higher order information, underlying processes such as perceptual binding, cognitive integration and consciousness (Llinas et al., 1998), and no longer simply a conveyor for sensory information from the periphery to the neocortex. Projections are highly organized, with axons entering and leaving more than 30 different thalamic nuclei. Seminal work from the last century has demonstrated that the gateway to the neocortex is the thalamus. Local lesions induced to cortical terminals produce rapid retrograde degeneration of thalamic cells (Murray Sherman and Guillery 2001). This experimental procedure was extensively used to study connectivity between the neocortex and the thalamus. Small localized cortical lesions destroyed small localized areas of the thalamus, and larger damaged areas induced degeneration of a wider range of thalamic nuclei. However, in some cases the effects were not as easily correlated as subsequent research demonstrated that specific thalamic nuclei can project to multiple areas of the neocortex, and only producing lesions in parallel would damage the entire thalamic

nucleus. In addition, lesions covering the entirety of the neocortex produced damage in all thalamic nuclei except for the thalamic reticular nucleus, parts of the epithalamus, and the midline and intralaminar nuclei (Jones 1985). Although we now know through retrograde and anterograde transported markers that only the thalamic reticular nucleus and the ventral lateral geniculate nucleus do not project to the neocortex (and together these regions are known as the ventral thalamus or prethalamus), data from those experiments pioneered our understanding of thalamocortical connectivity and raised questions about other brain regions being innervated by the thalamus and thus allowing the thalamus to maintain some integrity following cortical lesions (Murray Sherman and Guillery 2001). Moreover, the idea of cortical axons projecting to the thalamus and possibly trophically supporting thalamic neurons came later.

Thalamocortical cells represent 70 to 99% of all mammalian thalamic cells, with variations due to thalamic nuclei and species specificities (Murray Sherman and Guillery 2001). Moreover, these cells are glutamatergic. As they relay sensory information, they have been deemed first order projections or 'drivers', and have been divided into five categories: visual from the lateral geniculate nucleus (LGN), auditory from the medial geniculate nucleus, somatosensory from the ventral posterior nucleus (VP) of the ventrobasal group (VB), motor from the ventrolateral and ventral anterior groups, and cingulate/affective from the anterior thalamic nuclei. Thalamic axons project to the neocortex, the striatum (Powell and Cowan 1954, Francois, Percheron et al. 1991, Gimenez-Amaya, McFarland et al. 1995) or the amygdala (LeDoux, Ruggiero et al. 1985) through the thalamic reticular nucleus and the internal capsule. Thalamocortical neurons are also involved in higher order projections, connectivity between different cortical areas through corticothalamocortical tracts (Murray Sherman and Guillery 2001, Guillery and Sherman 2002). The rest of the thalamic populations comprise, among others, interneurons or 'modulators'. These cell numbers vary considerably between different nuclei and also species. For instance, the LGN of rats, cats and monkeys have significant populations of interneurons, whereas the VP of rats possess little interneurons compared to the significant numbers in cats and monkeys (Arcelli, Frassoni et al. 1997). Thalamic neuron activity can also be regulated by neurons projecting from the brainstem, the thalamic reticular nucleus, the hypothalamus and the cortex (Murray Sherman and Guillery 2001).

Thalamocortical axons (TCAs) vary according to their terminal arbors and distribution of their terminal arbors in different cortical areas and cortical layers (Murray Sherman and Guillery 2001). First order projections mainly target cortical layer IV, however their projections can spill over to cortical layer III and seldom cortical layer V (Figure 1) (Murray Sherman and Guillery 2001, Wu, Ballester Rosado et al. 2011, Grant, Hoerder-Suabedissen et al. 2012). TCAs can also terminate in cortical layers I and VI, but do so to a lesser extent and tend to be of higher order projections (Murray Sherman and Guillery 2001, Grant, Hoerder-Suabedissen et al. 2012). Dye tracing experiments targeting small numbers or individual thalamic cells of the LGN and VP showed that small thalamic cells mainly innervate cortical layer I, whereas large thalamic cells predominantly project to cortical layer IV, of their modality matched cortical areas (Carey, Fitzpatrick et al. 1979, Penny, Itoh et al. 1982). Cortical drivers to the thalamus are localized in layer V, while cortical modulators of thalamic activity arise from layer VI (Sherman and Guillery 1998, Guillery and Sherman 2002, Grant, Hoerder-Suabedissen et al. 2012).

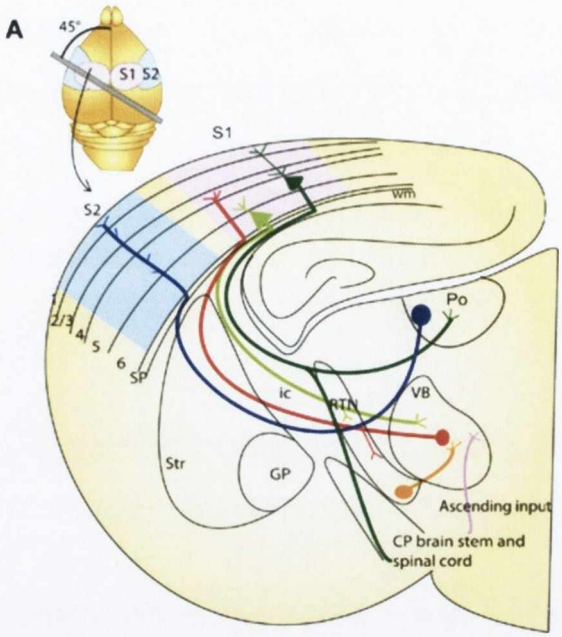


Figure 1. Mature somatosensory thalamocortical system

(A) *Inset*: outline of the mouse brain with the line indicating the plane of section to obtain thalamocortical slice containing the primary somatosensory cortex (S1) with intact thalamocortical projections. For clarity, secondary association somatosensory cortex (S2) connectivity is also indicated in the idealized section, although a different plane of section would be required to maintain connections. *Main image*: section schematic depicts the different types of connections between the thalamus and cortex using in the somatosensory system. The first order VB thalamic nucleus receives somatosensory peripheral input (pink). The VB then projects axons (red) to cortical layer IV of S1 (light blue). Cortical layer VI modulator neurons (light green) in S1 project back to the VB. Cortical layer V neurons (dark green) in S1 project to subcerebral structures and make a collateral branch to a higher order thalamic nucleus, for example the posterior thalamic nucleus (Po). The higher order nucleus then projects (dark blue) to an area of cortex that is different from the one it received input from (for example S2; light pink). This projection pattern generates an open loop with many possible functional circuits generated. CP, cerebral peduncle; GP, globus pallidus; ic, internal capsule; RTN, reticular thalamic nuclei; SP, subplate; Str, striatum; Po, posterior thalamic nuclei; VB, ventrobasal thalamic nuclei; wm, white matter.

Adapted from Grant, Hoerder-Suabedissen et al. (2012).

The classification of thalamocortical cells remains cumbersome as cells from different thalamic nuclei can have similar characteristics with regards to morphology, synaptic relationships, cable properties, voltage-dependent membrane conductances, etc. However, these cells follow accurate projections towards the neocortex. We postulate that their guidance specificities required through development could establish a reliable way of discriminating between populations of different thalamic nuclei through expression of specific extracellular proteins, however transient these might be.

1.1.2 Thalamic development

The brain emerges from the anterior part of the neural tube following its folding and closure early in embryonic development. The brain is then composed of three main parts: the forebrain (the prosencephalic vesicle), the midbrain (the mesencephalic vesicle) and the hindbrain (the rhombencephalic vesicle). The former part grows into two telencephalic vesicles, which will each contain a hemisphere of the cerebral cortex and the basal ganglia, and between them a central diencephalic vesicle, which will become the prethalamus (the ventral thalamus), the thalamus (the dorsal thalamus), the epithalamus and the hypothalamus [reviewed in (Price, Clegg et al. 2012)]. Thalamic progenitors are born in the ventricular zone along the third ventricle around mouse embryonic day (E) 10.5-11.5 for the neurons of first order projecting nuclei, and E12.5 for neurons of the other nuclei (Angevine 1970). There, they divide and generate postmitotic neurons who, in turn, migrate to the thalamic mantle zone and aggregate into specific nuclei. In light of Jessell's concept of neural induction based on positional identity (Jessell 2000), different morphogenetic signaling molecules and transcription factors have been linked to the various populations of thalamic neurons.

The prethalamus and the thalamus are separated by a transverse ventricular ridge that appears at the neural tube stages called the Zona Limitans Intrathalamica (ZLI), a zone that has been described morphologically in a wide variety of vertebrates (Kuhlenbeck 1938). The ZLI is particularly interesting as it has been found to act as a local organizer by expressing Sonic hedgehog (Shh), Wnts and fibroblast growth factors (FGFs) (Ishibashi and McMahon 2002, Kobayashi, Kobayashi et al. 2002, Braun, Etheridge et al. 2003, Zhou, Pinson et al. 2004, Vieira, Garda et al. 2005, Scholpp, Wolf et al. 2006, Kataoka and Shimogori 2008). More specifically, gradients of Shh, Wnts and FGF8 produced by the ZLI and surrounding areas delimit the area where the thalamus is formed (Shh is also expressed in the ventral midline of the prethalamus,

thalamus and pretectum primordium at a slightly earlier time-point; and, FGF8 is not produced by the ZLI although other FGFs are). These cues differentially induce specific thalamic transcription factors on cells that are already heterogeneous thereby further increasing molecularly distinct domains [reviewed by Scholpp and Lumsden (2010), Hagemann and Scholpp (2012), Nakagawa and Shimogori (2012)].

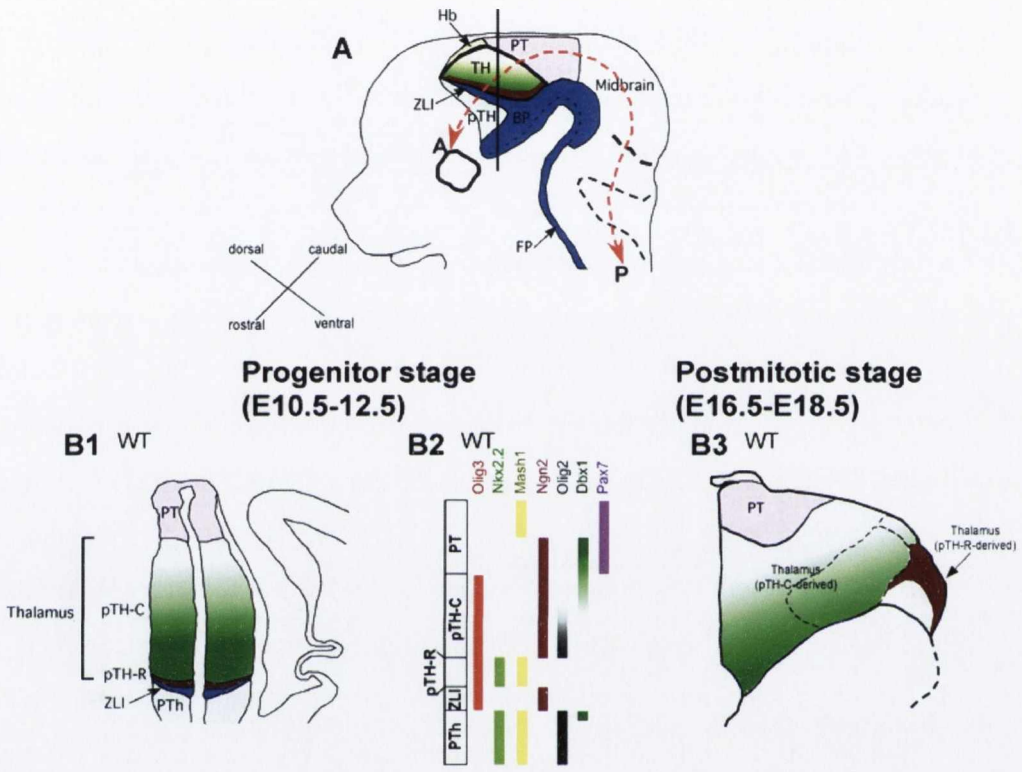


Figure 2. Thalamic development

Schematic of a sagittal view of the embryonic thalamus (A). The curved anterior-posterior (A–P) axis of the brain is shown in a red dotted line. The black vertical line indicates the orientation of frontal sections used in B1, B2 and B3. Frontal section schematic depicting the progenitor domains at early embryonic stages in wild type (WT) mice (B1). Green gradients within pTH-C indicate the graded differential patterns of gene expression within this domain. Spatial gene expression patterns in WT (B2). Frontal section schematic showing the postmitotic thalamus at late embryonic stages (B3). The graded color of pTH-C-derived thalamus corresponds to the overall lineage relationship with the progenitor domains shown in B1. BP, basal plate; FP, floor plate; Hb, habenula; PT, pretectum; pTH, prethalamus; TH, thalamus; ZLI, Zona Limitans Intrathalamica.

Adapted from Vue, Bluske et al. (2009).

Indeed, the prethalamus anlage is tanscription factor Fez-positive, whereas the thalamus anlage is transcription factor Irx-positive (Kiecker and Lumsden 2004, Hirata, Nakazawa et al. 2006, Jeong, Einhorn et al. 2007). These factors allow for differentially competent fields, since they differentially modulate cellular responses to Shh from the ZLI (Scholpp and Lumsden 2010). Moreover, Shh shows a graded pattern across the thalamus, from strong expression in the pTH-R domain (the rostral progenitor domain of the thalamus) and the prethalamus to low in the posteriodorsal pTH-C domain (the caudal progenitor domain of the thalamus). This allows for the complementary induction of important proneural basic helix-loop-helix (bHLH) transciption factors: Ascl1 in the pTH-R and the prethalamus, and Neurog1/2 in the pTH-C. The former transcription factor promotes GABAergic inhibitory neuron specification, while the latter promotes glutamatergic relay neuron differentiation (Vue, Aaker et al. 2007). The prethalamus will give rise to the thalamic reticular nucleus; the pTH-R domain to the intergeniculate leaflet (IGL) and the ventrolateral geniculate nucleus (both are retinorecipient nuclei but do not project to the cortex); and, the pTH-C domain to all the projecting nuclei to the neocortex. Shh is involved in further thalamic nuclei specification through the induction of more transcription factors: Gad1, Gbx2, Nkx2.2, Olig2, RORα, Sox2, Sox14 and Tal1 from high Shh concentrations in pTH-R or rostral pTH-C; Dbx1, Lhx2 and Olig3, from low Shh concentrations in caudal pTH-C (Barth and Wilson 1995, Ishibashi and McMahon 2002, Hashimoto-Torii, Motoyama et al. 2003, Kiecker and Lumsden 2004, Scholpp, Wolf et al. 2006, Szabo, Zhao et al. 2009, Vue, Bluske et al. 2009). More specifically, Dbx1 and Olig2 have complementary expression patterns within the pTH-C domain with Dbx1 concentration gradient high caudodorsally to low rostroventrally. Dbx1-expressing progenitors preferentially give rise to caudodorsal nuclei (the centrolateral nucleus, the mediodorsal nucleus and the centromedial nucleus). In addition, Olig3 is highly expressed throughout the thalamic ventricular zone and the ZLI, and much less in the caudal tip of the prethalamus. Experimental manipulations changing the patterns of expression or the area of influence of Shh in the thalamus have emphasized the spatiotemporal importance of Shh effects in properly patterning the rostral-caudal axis of the mouse thalamus (Szabo, Zhao et al. 2009, Vue, Bluske et al. 2009, Jeong, Dolson et al. 2011). Moreover, it is interesting to note that *Shh* mutant mice have severe defects and lack a distinguishable thalamus altogether, with embryos dying at or just before birth (Chiang, Litingtung et al. 1996).

Much less is known about the roles of Wnts and FGFs in thalamic development

once thalamic identity has been established. Nevertheless, it has been found that Wnt signaling through β-catenin differentially activates transcription throughout the thalamus (Bluske, Kawakami et al. 2009, Quinlan, Graf et al. 2009). In addition, Wnts' reach is complimentary to Shh's, with high-to-low dorsal-to-ventral influence in the pTH-C domain, as well as low in the pTH-R domain (Bluske, Kawakami et al. 2009). Not surprisingly, Wnts were found to induce expression of Neurog1/2 (Bluske, Vue et al. 2012). In contrast, FGF8's range of activity is mainly on the dorsal pTH-R, also controling proper rostral-caudal patterning of thalamic nuclei (Kataoka and Shimogori 2008). Whereas Wnt activity is antagonistic to Shh activity, FGF8 signaling is most likely downstream of Shh (Hagemann and Scholpp 2012).

Subdivisions of the thalamus emerge from five pronuclei, or undifferentiated cell masses, visible at E18.5 that express different markers, such as Calb2-Calretinin, Gbx2, Lhx2, Neurog2 and Cdh6. Szabo and colleagues (2009) compiled established thalamic expression of these five markers with their own data to distinguish the five pronuclei: the central pronucleus (anterior and ventral groups), the medial pronucleus (medial and intralaminar groups), the dorsal pronucleus (lateral and posterior groups), the lateral geniculate pronucleus and the medial geniculate pronucleus (Table 1). In addition, they demonstrated that Shh first promotes neuronal aggregation into specific thalamic nuclei partially through Gbx2 (the lateral and medial geniculate pronuclei specification is Gbx2 independent, whereas the medial pronucleus specification requires Gbx2 and is Shh independent), and then promotes thalamocortical connectivity.

Table 1 Pronuclear markers in the wild-type thalamus at E18.5

Pronuclei	Nuclei	Calb2	Gbx2	Lhx2	Neurog2	Cdh6
Central	ATN				+	+
	VP				+	+
	VM			+	+	+
	VMb	+	+	+		+
Medial	PV, PT, MV	+	+	+		
	MD		+			
	CM	+	+	+		+
	CL	+	+	+		
Dorsal	LD	+		+	+	
	LP	+	+	+		+
	Po					+
Lateral geniculate	LGd				+	+
Medial geniculate	MG	+	+	+		+

+ indicates expression. ANT, anterior thalamic nuclei; VP, ventral group; VM, ventromedial nucleus; VMb, ventromedial basal nucleus; PV, paraventricular nucleus; PT, paratenial nucleus; MV, medioventral nucleus; MD, mediodorsal nucleus; CM, centromedial nucleus; CL, centrolateral nucleus; LD, laterodorsal nucleus; LP, lateral posterior nucleus; Po, posterior nucleus; LGd,dorsal lateral geniculate nucleus; and MG, medial geniculate.

Adapted from Szabo, Zhao et al. (2009).

1.1.3 Development of the thalamocortical projections

Following the acquirement of thalamic identity, axons of projecting neurons initiate their long and convoluted journey to the cortex, before the thalamus even receives afferent innervation from the periphery. Thalamic organization into specific nuclei occurs concomitantly to thalamocortical connectivity suggesting that both require intertwined mechanisms (Price, Clegg et al. 2012). At embryonic day (E) 13 axonal projections from the dorsal thalamus extend ventrally through the thalamic reticular

nucleus towards the diencephalon-telencephalon boundary (DTB). The telencephalon is composed of the cerebral cortex dorsally (known as the pallium) and the basal ganglia centrally [known as the subpallium; Price, Clegg et al. (2012)]. The TCAs take a sharp turn into the internal capsule after which they fan out, continue on dorsally through the striatum and cross the pallium-subpallium boundary (PSPB). They reach the intermediate zone and the subplate at around E15.5-E16 in a rostroventral to caudodorsal gradient (Auladell, Perez-Sust et al. 2000). There, they pause for 2-3 days below their appropriate target area before invading the cortical plate in a dorsal to ventral gradient (Angevine 1970, Lund and Mustari 1977). Around birth, axons extend towards cortical layer IV. Extensive maturation occurs then up until P8 (Miller, Chou et al. 1993). In parallel, around E11, the cortex is composed of the ventricular zone, the subventricular zone and the preplate, the latter being the first layer of postmitotic cells to appear during corticogenesis (Figure 3) (Berry and Rogers 1965, Rakic, Davis et al. 2006, Molyneaux, Arlotta et al. 2007). At E12, the preplate splits into the marginal zone (or cortical layer I) and the subplate by the invasion of cortical neurons. It is between these two layers that the deep cortical plate starts to develop. When the TCAs reach the subplate around E15.5-E16, the deep cortical plate is still present and further maturation needs to occur before the TCAs can extend to cortical layer IV. Neurons generated in the ventricular and subventricular zones of the lateral ventricle migrate into the cortical plate and form its different layers in an inside-out manner, with layer VI established first around E18.5 and so on (Angevine and Sidman 1961, Berry and Rogers 1965). Layer II neurons are the last to be born and reach their appropriate layer by P5 [for reviews on thalamocortical connectivity see Molnar and Blakemore (1995), Lopez-Bendito and Molnar (2003), Price, Kennedy et al. (2006), Erzurumlu and Gaspar (2012)].

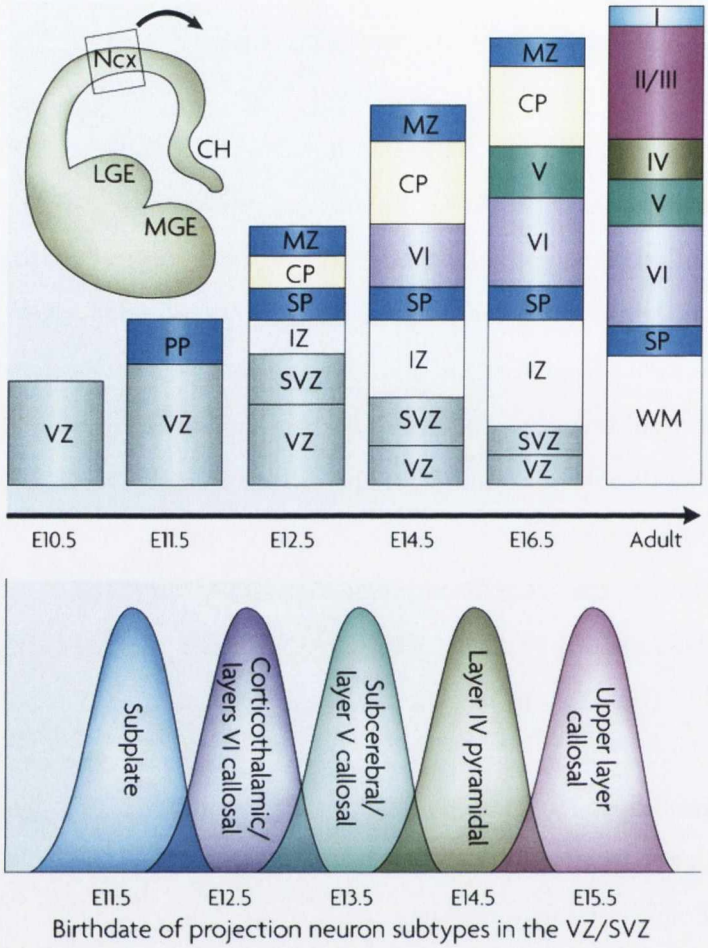


Figure 3. Neocortical development of projection neurons

The earliest born neurons from the ventricular zone (VZ) form the preplate (PP), which is later split into the marginal zone (MZ) and the subplate (SP). The cortical plate (CP), which will give rise to the multilayered neocortex, develops between these two layers in an inside-out fashion, such that later born neurons arriving at the cortical plate migrate past earlier born neurons. Different classes of projection neurons are born in overlapping temporal waves. All times listed are approximations due to the neurogenic gradients that exist across the cortex, where rostrolateral neurogenesis precedes caudomedial neurogenesis. CH, cortical hem; E, embryonic day; Ncx, neocortex; IZ, intermediate zone; LGE, lateral ganglionic eminence; MGE, medial ganglionic eminence; SVZ, subventricular zone; WM, white matter.

From Molyneaux, Arlotta et al. (2007).

Different populations of cells are generated along the path TCAs will have to navigate through, from proximal to distant regions to the thalamus these are thalamic reticular nucleic cells, cells from the ventral part of the ganglionic eminences, perirhinal cortical cells and subplate cells (Lopez-Bendito and Molnar 2003, Molnar, Garel et al. 2012). It had therefore been hypothesized that they must be required for proper thalamocortical connectivity to occur. Subplate cells were found to establish transient projections traversing the internal capsule and ultimately reaching the dorsal thalamus, prior to cortical drivers and modulators reaching the thalamus (McConnell, Ghosh et al. 1989). This and other studies led to the 'handshake hypothesis' which postulates that axons from the thalamus and the subplate intimately associate in the ventral telecephalon to guide TCAs across otherwise non-permissive terrain towards the neocortex (Molnar and Blakemore 1995). This hypothesis has received a lot of attention, and has recently been tested and confirmed directly (Chen, Magnani et al. 2012). Moreover, projections from the thalamic reticular nucleus towards the thalamus and the cortex were first reported in the embryonic rat (Mitrofanis and Baker 1993). Shortly after, guidepost cells from the ganglionic eminences were shown to extend pioneering projections towards the dorsal thalamus in order to guide the thalamocortical (and corticothalamic) axons through the internal capsule in hamster embryos (Metin and Godement 1996). Importantly, similar cell populations have been described in human embryonic development (Letinic and Kostovic 1996). More recently, corridor cells have been identified. These cells have short-range guidepost activity at the level of the internal capsule in the medial ganglionic eminence although they originate and migrate from the lateral ganglionic eminence (Lopez-Bendito, Cautinat et al. 2006).

A tightly controlled genetic program orchestrates all the stages through which TCAs need to go through in order to reach their final destinations. Axons require the ability to recognize the environment they are traveling through. Furthermore, they need to be able to quickly adapt their route discriminating between permissive and non-permissive territories. Different transgenic mouse models have revealed the importance of a range of transcription factors for proper thalamocortical development to take place. The defects observed occur at different locations along the thalamocortical journey. *Ascl1* mutant mice elicit wandering TCAs that cannot enter the ventral telencephalon (Tuttle, Nakagawa et al. 1999). Moreover, corticothalamic axons show the same defect coming from the opposite direction. Lack of retrograde labeling from the dorsal thalamus demonstrates that internal capsule cells are missing. The same occurs in *Pax6*

mutant mice (Hevner, Miyashita-Lin et al. 2002, Pratt, Quinn et al. 2002). Guidepost cells in *Emx2* and *Lhx2* mutant mice are displaced attracting TCAs to incorrect areas, these cells are also found in smaller numbers in these mutants (Lopez-Bendito, Chan et al. 2002, Bishop, Garel et al. 2003, Lakhina, Falnikar et al. 2007). Lakhina, Falnikar et al. (2007) observed an increased area of Sema6A expression in the ventral telencephalon of *Lhx2* mutant mice thereby creating a greatly repulsive region for caudally headed thalamic axons. Corridor cells express a set of markers that distinguish them from the surrounding internal capsule, which makes them interesting to study. For instance, *Ebf1* mutant mice exhibit a disorganized internal capsule where proper sorting of TCAs (and coticothalamic axons) in order to reach their appropriate target regions is shifted (Garel, Marin et al. 1999, Garel, Yun et al. 2002). Interestingly, these mutant mice have strong defects specifically affecting dLGN axons as these do not reach their targets. These defects have been attributed to the lack of Sema6A expression in the globus pallidus. Nkx2.1 expression is characteristic of the medial ganglionic eminence. Mutant mice for this gene have a surprising phenotype. TCAs project normally to the cortex; however, corticothalamic axons are differentially affected as cortical layer VI axons reach their targets in the thalamus, whereas cortical layer V axons do not (Marin, Baker et al. 2002). This illustrates interesting differences between the connectivity of drivers and modulators.

These transcriptional programs control the expression of guidance molecules, either secreted or membrane-bound proteins, as alluded with the work on *Lhx2* and *Ebf1* mutant mice and single-pass transmembrane protein Sema6A expression. Class 6 Semaphorins have been shown to interact with PlexinA members to mediate axonal guidance (Suto, Ito et al. 2005, Tawarayama, Yoshida et al. 2010, Andermatt, Wilson et al. 2014). A number of families of guidance molecules have been associated with these transcriptional programs. Lhx2 also differentially modulates the expression levels of the Robo1 and Robo2 receptors across different populations of thalamic neurons, thereby participating in the establishment of specific connectivity (Marcos-Mondejar, Peregrin et al. 2012). These receptors cooperatively mediate the repulsive actions of secreted molecules Slit1 and Slit2 on thalamocortical and corticothalamic projections (Lopez-Bendito, Flames et al. 2007). Cell adhesion molecules have also been implicated in normal development of thalamocortical projections. For instance, L1 and its close homolog (CHL1) play roles, albeit in quite different ways. The former is required for thalamocortical and corticothalamic axons to fasciculate normally at the level of the

internal capsule and subsequent pathfinding (Ohyama, Tan-Takeuchi et al. 2004, Wiencken-Barger, Mavity-Hudson et al. 2004). L1-deficient mice exhibit hyperfasciculation and misrouting of a subset of the most caudal TCAs. No corticothalamic axons reach the dorsal thalamus in these mice. CHL1, however, is not involved in proper fasciculation. It interacts with Neuropilin1 to mediate Sema3A responses guiding TCAs from the VP to the somatosensory cortex (Wright, Demyanenko et al. 2007). Mutant mice for either CHL1 or Neuropilin1 elicit misrouted VP axons into the visual cortex. L1 and CHL1 exhibit different expression patterns within the thalamus, therefore they affect different populations of axons. Still, a recent study has revealed specific cooperation of these two factors in a subset of TCAs projecting to the motor cortex by associating with the ephrinA/EphA and inducing growth cone collapse (Demyanenko, Siesser et al. 2011). What's more, a combinatorial code of thalamocortical connectivity has been established between the differentially expressed Eph receptors in the thalamus and membrane-bound ephrins in the cortex to allow proper targeting between and within cortical areas from the thalamus (Dufour, Seibt et al. 2003). Some of the molecules discussed here exhibit graded expression patterns establishing topography along the thalamocortical path (Figure 4). In addition, *Sema6A-/-* mice exhibit misrouted TCAs from the dLGN (Little, Lopez-Bendito et al. 2009). However, they eventually reach their target area in the visual cortex through navigating long distances in the marginal zone from the ventral telencephalon bypassing the turn into the internal capsule. This study further supports the role of intrinsic targeting cues within thalamic axons and cortical areas. It also demonstrates that the subplate is probably a permissive territory and can be bipassed for proper sorting. And perhaps it shows that the primitive system of thalamocortical connectivity is still in place in mammals (birds have no permissive corridor at the level of the internal capsule).

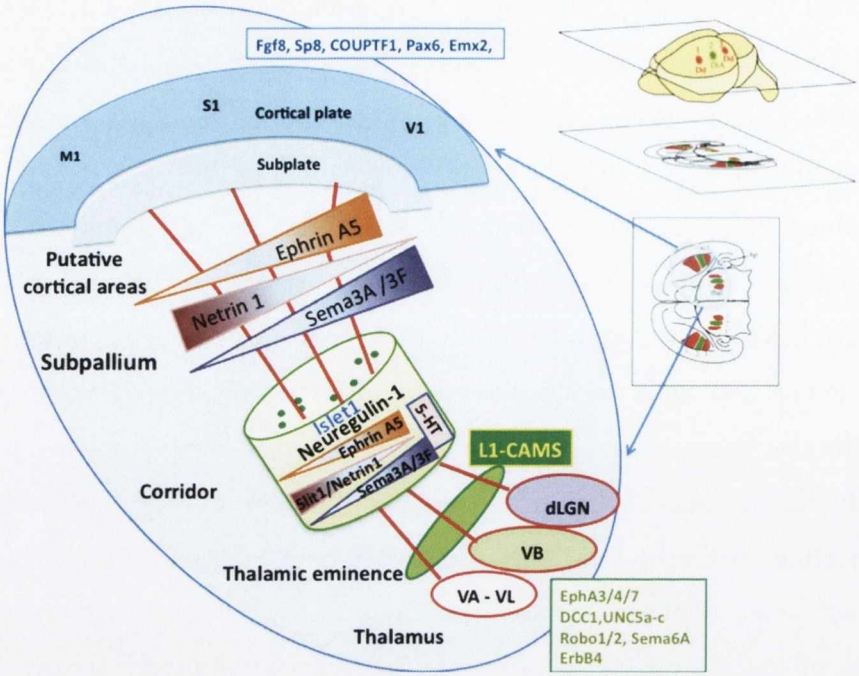


Figure 4. Axon guidance molecules expressed along the thalamocortical path

Upper right inset: Diagram of multiple dye placements in the cerebral neocortex positioned along an anterioposterior axis showing the arrangements of backfilled dorsal thalamic neurons in a mediolateral fashion. The schematic panels indicate the appropriate sections with labeling. The right hemisphere is enlarged to depict some of the molecules that are involved in the guidance of the TCAs across the thalamic eminence, corridor and subpallium to reach the target regions in the neocortex.

TCAs from different nuclei in the thalamus navigate through the thalamic eminence towards the neocortex. They are topographically sorted within a corridor of Islet1-expressing cells along the rostrocaudal axis (E13.5 to E15.5 in the mouse). As TCAs express different combinations of axon guidance cue receptors (listed in the box within the dorsal thalamus), they are guided by gradients of repulsive and attractive cues (EphrinA5, Netrin1, Sema3A, Sema3F and Slit1), influenced by Neuregulin-1 and serotonin (5-HT). Similar gradients are present in the ventral pallium, except for Slit1. TCAs target cortical areas that will contribute to the putative primary motor cortex (M1), somatosensory cortex (S1) and visual cortex (V1), but their entry to the cortex is regulated by the subplate. A few of the various gradients in the subplate and cortical plate are listed (Fgf8, Sp8, COUPTF1, Pax6 and Emx2). Additional molecular cues and

activity-dependent mechanisms promote the final synaptic targeting of TCAs within the neocortex. This initial topography can be considerably rearranged when TCAs enter the cortical plate. VA/VL, ventroanterior/ventrolateral nuclei; VB, ventrobasal complex; dLGN, dorsal lateral geniculate nucleus.

From Molnar, Garel et al. (2012).

Although much progress has been made in understanding what molecules guide TCAs along their path to the cortex, the picture is far from being complete since their mechanisms of action and combinatorial effects are only starting to be elucidated. In addition, many more molecules are probably involved in the process as we are still far from explaining the observed complexity that proper brain wiring requires. Many questions remain unanswered as we still cannot explain how connectivity is specified between individual thalamic nuclei and appropriate cortical areas.

1.1.4 Aims

The interest of this study relies on guidance molecules at the level of thalamocortical connectivity during development in mice. Although different molecules involved in the guidance of neurons have been identified to date, it is speculated that many more are implicated. Given the amount of available data and tools online, we first aim to perform an *in silico* search for new potential candidates in thalamocortical pathfinding. The Allen Brain Institute has generated a large dataset of mouse messenger RNA expression during development (developing Allen Brain Atlas). Here, we intend to use a bioinformatics approach to mine expression values for 2002 genes at 7 developmental ages relevant to different developmental stages: regional specification/patterning (E11.5), axon pathfinding (E13.5, E15.5 and E18.5), synaptogenesis (P4 and P14) and cortical plasticity (P28). Our goal is to postulate new candidate genes involved in thalamocortical pathfinding by clustering analyses of similar patterns of expression with peak expression at time-points relevant to thalamocortical axon guidance. Moreover, using different webtools, we aim to screen protein products for subcellular localization with an emphasis on the extracellular compartment where guidance molecules reside. To this information, we will add known functions associated to the genes in our dataset. We will extensively curate each set of results obtained to create a platform useable for this and further investigation.

Combining localization and function information, we will then validate our final dataset with known genes involved in particular functions of thalamic development. But, most importantly, we aim to extrapolate new candidate genes for thalamocortical pathfinding.

To further pursue our search for genes involved in thalamocortical connectivity, we aim to study the implication of Sema6A, Sema6B, PlexinA2 and PlexinA4 in the somatosensory system. Previous work within the laboratory and elsewhere has already validated the developmental expression of Sema6A, Sema6B, PlexinA2 and PlexinA4, albeit in restricted time-points and brain regions. Moreover, this body of work has established roles in dLGN thalamocortical connectivity for Sema6A, and axonal guidance in other brain regions for this protein, Sema6B and their binding partners PlexinA2 and PlexinA4 (discussed in Chapter 4). An interesting phenotype was reported by Suto, Ito et al. (2005) where adult *PlexinA4* mutant mice exhibit indistinct boundaries of barrel formations in the somatosensory cortex. We therefore aim to investigate the expression patterns of Sema6A, Sema6B, PlexinA2 and PlexinA4 at time-points relevant for barrel cortex formation (namely postnatal days 2, 4, 6 and 8). These time-points have not been studied previously in the context of these genes and the somatosensory system. In addition, we hypothesize that this group of genes is important for proper development of the somatosensory cortex. We have the intention to explore the developing somatosensory cortex by investigating TCA invasion and cellular organization of different null mutant mice for these genes through dye tracing experiments and immunohistochemistry. We speculate that Sema6A, Sema6B, PlexinA2 and PlexinA4 are differentially expressed within the thalamus and the cortex, possibly differentially intersecting in some areas, thereby creating a combinatorial code of connectivity.

Chapter 2

Materials and Methods

2.1 Data acquisition and preprocessing

The Allen Brain Atlas (ABA) provides a survey of gene expression in the brain from mid-gestation through aging in different species. Of interest to us is the data on the mouse brain. The detailed process of mouse brain data acquisition is explained in Lein, Hawrylycz et al. (2007). Briefly, *in situ* hybridization (ISH) data was recorded from coronal or sagittal sections and quantified per unit from a given spatial location for each gene (expression values per voxels). Voxels were assigned regional labels through age-matched anatomic reference atlases. We used the developmental dataset found on the ABA portal (www.brain-map.org) in order to do our clustering analyses.

The developmental dataset comprises expression values of 2002 genes obtained from ISH images in the sagittal plane across four embryonic (E11.5, E13.5, E15.5 and E18.5) and three early postnatal ages (P4, P14 and P28) found on the Allen Developing Mouse Brain Atlas (devABA)(Thompson, Ng et al. 2014). These time-points are developmentally relevant to regional specification/patterning (E11.5), axon pathfinding (E13.5, E15.5 and E18.5), synaptogenesis (P4 and P14) and cortical plasticity (P28). One animal was used per time-point per gene. Per-region data was quantified from ISH images by combining all voxels (3D pixels) with the same regional label. Liscovitch and Chechik (2013) extracted data from 36 anatomically delineated regions of the developing brain, which encompass the entire brain. The data is readily available for download at http://chechiklab.biu.ac.il/~lior/cerebellum.html. From the folder hg_data_text, we obtained data for the thalamus at all the time-points. The data is expressed as expression density (Table 2 in the Digital Appendix). For each brain region R, the expression density is defined as the sum of expressing pixels in R divided by the total number of pixels that intersect R (taken from the Technical White Paper: Informatics Data Processing for the Allen Developing Brain Atlas found at http://developingmouse.brain-map.org/docs/InformaticsDataProcessing.pdf). Each set of values is dependent on specific gene expression. A gene that is highly expressed throughout time-points, but has low levels of variation, has high expression densities. In contrast, a gene that is punctually turned on has low expression densities for all the time-points but the one that it is expressed at. We are interested in patterns of gene expression, and less in absolute values, so we normalized the data to reflect variations of expression. To do so, we calculated the average expression density for each gene at all time-points. We then divided each expression density from E11.5 to P28 by the

averaged expression density of the corresponding gene. A value of 1 indicates average expression levels whereas a value below or above 1 indicates decreased or increased expression levels compared to average, respectively. With this normalized data, we generated the developmental matrix of 2002 genes x 7 time-points. However, this matrix was reduced to 1996 genes x 7 time-points as 6 genes had no expression values throughout. These genes are Chrna1, Hoxd9, Lef1, Nrp2, Pbx1 and Rnd2.

The 2002 genes of the developmental dataset fall into one of these five categories (taken from the Technical White Paper: Allen Developing Mouse Brain Atlas found at http://developingmouse.brain-map.org/docs/Overview.pdf):

1. *Transcription factors*. Approximately one third of the genes are transcription factors, with extensive coverage of homeobox, basic helix-loop-helix, forkhead, nuclear receptor, high mobility group and POU domain genes.

2. *Neuropeptides, neurotransmitters, and their receptors*. Extensive coverage of genes in dopaminergic, serotonergic, glutamatergic, and gabaergic signaling, as well as neuropeptides and their receptors.

3. *Neuroanatomical marker genes*. Characterizing region- or cell type specific marker genes over development can provide information about the origins of a brain region or cell type, and may help to identify precursor regions at earlier time points.

4. *Gene ontologies/signaling pathways relevant to brain development*. Gene ontologies include axon guidance, receptor tyrosine kinases and their ligands. Pathways include Wnt signaling and Notch signaling pathways.

5. *Genes of general interest*. This category includes highly studied genes such as common drug targets, ion channels, cell adhesion, genes involved in neurotransmission, G-protein-coupled receptors, or involved in neurodevelopmental diseases, which are expressed in the brain in the adult and/or in development.

We screened protein products for cellular localization with an emphasis on the extracellular compartment (Table 3 in the Digital Appendix). More specifically, we looked for signal peptides, transmembrane domains and glycosylphosphatidylinositol (GPI)-anchors. Since genes were listed with their Allen gene name in the dataset, we looked for the MGI symbol and Ensembl gene identifiers (through http://www.ncbi.nlm.nih.gov/gene) to subsequently find their protein counterparts. Where multiple isoforms exist, the longest sequence was used for further analyses. We

screened fasta format sequences through PSORTII to find cellular localization of the protein products and the number of predicted helices of transmembrane proteins (http://psort.hgc.jp)(Horton and Nakai 1997, Nakai and Horton 1999). PSORTII predicted protein localization in the following compartments: cytoplasm, cytoskeleton, endoplasmic reticulum, Golgi, mitochondria, nucleus, plasma membrane, peroxisomes, vacuoles and vesicles of the secretory system. In addition, we ran the SignalP prediction program to determine whether a protein contains a signal peptide or not - indicative of extracellular localization (http://www.cbs.dtu.dk/services/SignalP/, version 4.1)(Nielsen, Engelbrecht et al. 1997, Petersen, Brunak et al. 2011). A GPI modification site prediction, the big-PI predictor was run to identify protein products with potential GPI-anchors (http://mendel.imp.ac.at/sat/gpi/gpi_server.html, version last modified June 17th 2005) (Eisenhaber, Bork et al. 1998, Eisenhaber, Bork et al. 1999, Sunyaev, Eisenhaber et al. 1999, Eisenhaber, Bork et al. 2000). When any of the three programs suggested extracellular localization, the protein was deemed found in the extracellular compartment. The TMHMM program was run to assess the presence and number of transmembrane domains (http://www.cbs.dtu.dk/services/TMHMM/, version 2.0)(Sonnhammer, von Heijne et al. 1998, Krogh, Larsson et al. 2001). When the number of transmembrane domains varied between PSORTII and TMHMM results, manual curation was performed (unless both programs picked up over two transmembrane domains and the protein was simply considered multi-pass). PFAM (http://pfam.xfam.org)(Finn, Bateman et al. 2014) and SMART A (http://smart.embl-heidelberg.de, version 2.12.1 released on August 6th 2012)(Schultz, Milpetz et al. 1998, Letunic, Doerks et al. 2014), motif recognition programs, allowed screening for important protein domains, which can be amalgamated through InterPro (http://www.ebi.ac.uk/interpro/search/sequence-search, version 49.0 released on November 20th 2014)(Mulder, Apweiler et al. 2002). SignalP, PFAM, SMART A and InterPro short description were readily accessed together through MartView from BioMart version 0.7 (http://www.biomart.org/biomart/martview/151674fc4104a8a6e4349733fab97115)(Kasprzyk 2011).

Finally, we updated the gene annotations of the dataset from Thompson, Ng et al. (2014). Thompson and colleagues had 1385 genes out of the 2002 falling into one or more of these categories: axon guidance pathway, cell adhesion, receptor tyrosine kinases (RTKs) and their ligands, Notch signaling, Wnt signaling, transcription factor

activity, basic helix-loop-helix transcription factor, forkhead transcription factor, homeobox transcription factor, nuclear receptor, POU domain genes, neurotransmitter pathway, ion channel, and G-protein coupled receptors (GPCRs). We screened genes for the following gene ontology (GO) term annotations (http://www.geneontology.org)(Ashburner, Ball et al. 2000) through MartView:

1) Axon Guidance GO:0007411;

2) Synapse GO:0045202;

3) Patterning: - Regionalization GO:0003002;

- Pattern Specification Process GO:0007389;

- Neural Tube Patterning GO:0021532;

- Rostrocaudal Neural Tube Patterning GO:0021903;

4) Transcription Factor Activity:

- Protein Binding Transcription Factor Activity GO:0000988;

- Nucleic Acid Binding Transcription Factor Activity GO:0001071;

- Sequence-Specific DNA Binding Transcription Factor Activity GO:0003700.

We found 99 genes with GO:0007411, 68 with GO:0045202, 1 with GO:0003002, 36 with GO:0007389, 1 with GO:0021532, 1 with GO:0021903, 122 with GO:0000988, 468 with GO:0001071 and 384 with GO:0003700. We also complemented the annotations by manual curation. Since many genes had more than one annotation, we grouped them as follows:

- Group 1: axon guidance pathway and cell adhesion;
- Group 2: synapse;
- Group 3: receptor tyrosine kinases and their ligands, and patterning;
- Group 4: neurotransmission pathway (GPCRs, ion channels, gap junctions);
- Group 5: chromatin and transcription factor activity
- Group 6: other (cytoskeleton, extracellular matrix, myelin, metabolic enzymes and signal transduction) and unannotated.

We only had 206 unannotated genes. Each gene belonged to only one group. When a gene fell into more than one group, we prioritized the groups as presented.

2.2 Clustering analyses

We performed clustering analyses on the developmental dataset using two online microarray analysis tools: the TM4:MeV program for hierarchical clustering (http://www.tm4.org/mev.html - version 4.9 released April 4th 2013)(Saeed, Sharov et al. 2003) and the clustering module integrated in ArrayPipe for k-means clustering (http://www.pathogenomics.ca/arraypipe - version 1.7)(Hokamp, Roche et al. 2004). In the latter tool, we used 1000 iterations as default for k-means Euclidian distance clustering. The developmental matrix was reduced to 1996 genes x 7 time-points as 6 genes had no expression values throughout and skewed the clustering process. These genes are Chrna1, Hoxd9, Lef1, Nrp2, Pbx1 and Rnd2.

2.3 Enrichment analyses

We performed chi square statistics to determine whether our developmental dataset was proportionally distributed in regards to cellular localization and groups across the 10 clusters obtained during k-means clustering analyses or enriched in particular clusters:

$$\text{Chi square} = \Sigma\ (\text{observed} - \text{expected})^2 / \text{expected, where}$$

$$\text{expected} = (\text{total \# of genes in cluster of interest} / \text{total \# of genes}) * \text{total \# of genes in group of interest}$$

Statistical significance was determined at p-value < 0.05. For the whole dataset, this required a value above 50.998 at 36 degrees of freedom [df = (column # -1) (row # -1) = (5-1) (10-1) = 4 * 9] and 61.656 at 45 degrees of freedom. Where multiple tests were performed on the same dataset, the Bonferroni correction was taken into account. A chi square value above 16.919 determined significance at p-value < 0.05, where degrees of freedom = n – 1 = 10 clusters – 1 = 9.

2.4 Animals

All procedures involving mice were performed in accordance with Statutory Instrument No 566 of 2002 (Amendment of Cruelty to Animals Act, 1876). A strain of C57/black6 (C57BL/6; Jackson Laboratories) inbred mice was used for these experiments. Four additional mouse lines were also used in these studies: 1) a strain of

C57BL/6 inbred mice carrying a genetrap insertion in the Sema6A gene (Leighton, Mitchell et al. 2001), 2) Sema6B knockout mice obtained from Dr. Yutaka Yoshida (Tawarayama, Yoshida et al. 2010), 3) PlexinA2 knockout mice obtained from Dr. Alain Chédotal (Suto, Tsuboi et al. 2007), and 4) PlexinA4 knockout mice in CD1 background obtained from Dr. Avraham Yaron (Yaron, Huang et al. 2005). The latter were backcrossed into C57BL/6 background. Some of these lines were crossed to obtain double knockout mice. All mice were maintained and bred in 12-hour light/12-hour dark cycles, in a specific pathogen free animal unit.

For experiments, animals were time-mated. Conception was determined by the presence of a vaginal plug on embryonic day (E) 0. For embryonic experiments, pregnant mice were sacrificed by cervical dislocation. Embryos were removed and chilled until movement had stopped in ice-cold phosphate buffered saline (PBS). Brains were then dissected, washed in cold PBS and fixed in 4% paraformaldehyde (PFA) in PBS at 4°C for 4-18 hours. Three to five millimeters of fresh tail tissue was taken from embryos obtained from mutant lines for DNA extraction, purification and genotyping. Newborn to postnatal day (P) 3 old mice were sacrificed by decapitation on the required day. Heads were transferred in ice-cold PBS, where dissections proceeded. Fixation was also in 4% PFA in PBS at 4°C for 4 hours or until used. Three to five millimeters of fresh tail tissue was taken from mice obtained from mutant lines for DNA extraction, purification and genotyping. Finally, older mice (P4 to adult) were administered a lethal dose of pentobarbital to anesthetize them. Three to five millimeters of fresh tail tissue was taken from mice obtained from mutant lines for DNA extraction, purification and genotyping. Then, mice were sacrificed by transcardial perfusion with 4% PFA in PBS. Decapitation ensued, and dissections proceeded in ice-cold PBS. Whole brains or flattened cortices were fixed in 4% PFA in PBS at 4°C for 4 hours, overnight (O/N) or until used. For all brains, if a specific duration of fixation was required, brains were washed and transferred into PBS at 4°C for up to 6 months.

2.5 DNA extraction, purification and genotyping

Approximately 4mm of fresh tail tissue was digested in 200µL of Boston buffer (50mM Tris pH 8.0, 50mM KCl, 2.5mM EDTA, 0.45% NP40, 0.45% Tween-20; Sigma) with 14-22mg/mL of Proteinase K (Roche) O/N at 56°C.

The DNA was purified through a phenol/chloroform extraction. Briefly, equal volume of phenol/chloroform/isoamyl alcohol mixture (25:24:1, v/v; Sigma) was added to the digested tissue in Boston buffer, and centrifuged for 5 minutes at 4°C at 17,000 g or over (Sigma). The supernatant was transferred to a new tube where 500µL of chloroform were subsequently added. This was centrifuged once again for 5 minutes at 4°C at 17,000 g or over, and the supernatant was collected. Equal volume of isopropanol and 10% of the total volume of 3M of sodium acetate were added to the supernatant, and the mixture was allowed to precipitate at -20°C O/N. The DNA was subsequently pelleted by centrifugation (at 4°C at 17,000 g or over for 30 minutes). The supernatant was discarded, and the DNA pellet was washed with 500µL of 70% ethanol (at 4°C at 17,000 g or over for 10 minutes). As much as possible of the supernatant was discarded. To ensure all ethanol was removed, the pellet was briefly dried and then resuspended in 100-200µL of H_2O. The concentration of each DNA sample was measured by spectrophotometer, where 1 OD_{260} = 50µg/mL. The concentration was adjusted to 50ng/µL with H_2O.

One microliter of DNA was used as template for polymerase chain reaction (PCR). The PCRs were carried out with KAPA2G Fast HS Ready Mix + dye (2X; Nalgene) on a thermal cycler (DNAEngine Peltier Thermal Cycler, Bio-Rad; see Tables 2.2 and 2.3).

Table 4 PCR Primer Sequences for Sema6B Genotyping

Primer	Sequence 5'->3'
Sema6B forward	CTCACATGTGGTCTTAAAGTCGCTTG
Sema6B reverse	TGATATCGCAGCTCCGTGGAAGTGG
Neo-4 reverse	CCATTGCTCAGCGGTGCTGTCCATC

Table 5 PCR Genotyping Program for Sema6B

Program
95°C for 2 minutes
39 cycles of:
Denaturing: 94°C for 45 seconds
Annealing: 60°C for 45 seconds
Extension: 72°C for 1.5 minutes
72°C for 2 minutes

2.6 Histology

Fixed brains were cut using a vibrating microtome (Leica VT1000s) into 40-100μm sections. To do so, fixed brains were embedded in 4% agarose (Sigma) in PBS, percent weight/volume. The block of agarose was trimmed with a sharp blade to orient the brain in the appropriate plane of sectioning on the vibratome stage. Brain slices were collected in PBS.

2.7 *In situ* hybridization probe construction

Plasmids were used for the production of Digoxigenin (DIG)-labeled riboprobes for *in situ* hybridization (ISH). First, these plasmids were linearized overnight at 37°C with the corresponding restriction enzymes, except for Neto-1 where a PCR product was used as template (see Table 2.4). They were then used as templates for the transcription of DIG-labeled RNA probes (see Table 2.5). The reaction mixture was incubated for 2 hours at 37°C. The quality of the RNA was checked by electrophoresis (an aliquot was run on an agarose gel). Transcribed RNA products were treated with 1U of RNase-free DNase I for 15 minutes at 37°C to remove the template. This reaction was stopped with 2μL of 0.2M EDTA pH 8.0. To precipitate the RNA, 2.5μL of 4M LiCl and 75μL of ethanol were added and allowed to incubate at -20°C for over an hour. The RNA was subsequently pelleted by centrifugation (at 4°C at 17,000 g or over [Sigma] for 20 minutes). The supernatant was discarded, and the RNA pellet was washed with 150μL of 70% ethanol (at 4°C at 17,000 g or over for 2 minutes). As much as possible of the supernatant was discarded. To ensure all ethanol was removed, the

pellet was centrifuged once again and the supernatant carefully discarded. The pellet was briefly dried and then resuspended in 55μL of 1mM sodium citrate solution at pH 6.35. The concentration of each RNA probe was measured by spectrophotometer, where 1 OD_{260} = 40μg/mL. The concentration was adjusted to 200ng/μL with sodium citrate. An equal volume of formamide was added to protect the RNA from RNase activity. The probes were stored at -20°C.

Table 6 Probes

Probe Name	Obtained from	Size (b)	Linearize	Transcribe	Product
SD89 (Sema6A)	Kevin J Mitchell	280	XhoI	T3	as-Sema6A
Sema6B	Graham E Little	756	BamHI	T7	as-Sema6B
PlexinA2	Alain Chédotal	315	XhoI	T3	as-PlxnA2
PlexinA4	Alain Chédotal	1260	EcoRV	T3	as-PlxnA4
Neto1	Tatsuya Okafuji	823	-	T7	as-Neto1

Table 7 RNA Transcription and DIG Labeling

Reagent	Amount
RNA transcription buffer (10X)	2.0μL
Linearized plasmid template	1.0μg
DIG labeling mix (10X, Roche)	2.0μL
Rnase OUT (40U/μL, Invitrogen)	0.5μL
Polymerase (T3 or T7, see Table 2.2)	20U
dH_2O	to 20μL

2.8 *In situ* hybridization

Fixed brains were embedded in 4% weight of low melting point agarose/volume of DEPC-treated PBS (g/mL). Brains were cut into 60μm sections, and the latter were collected in DEPC-treated PBS (RNase free environment). Free-floating sections were washed twice for five minutes in DEPC-treated PBS containing 0.1% Tween-20 (PBT). Sections were then permeabilized for 30 minutes in 0.5% Triton X-100 and 0.2%

Tween-20 in DEPC-treated PBS. A five-minute wash in PBT followed. Half the volume of PBT was subsequently removed and replaced by prehybridization solution (50% formamide, 5X SSC, 1% SDS, 2.5mg of yeast tRNA, 2.5mg of heparin in DEPC-treated H_2O) pre-warmed at 65°C. The brain sections were incubated in this mixture for ten minutes at room temperature. A wash with prehybridization solution for ten minutes at room temperature was performed afterward. The sections were then incubated in prehybridization solution for at least an hour at 65°C. Prehybridization solution containing probe at a concentration of 1μg/mL was next added to the sections for an overnight incubation at 65°C. The following morning, three 30-minute washes in solution I (50% formamide, 5X SSC, 1% SDS) and three more 30-minute washes in solution III (50% formamide, 2X SSC, 0.1% Tween-20) were carried out at 65°C. The sections were then washed three times for five minutes in Tris-buffered saline (TBS) containing 1% Tween-20 (TBST) back at room temperature. After that, they were incubated in blocking buffer (TBST containing 10% heat-inactivated sheep serum) for at least an hour. The blocking buffer was then replaced with antibody solution (1:2,000 anti-DIG-AP Fab fragment, from Roche, in blocking buffer) for an overnight incubation at 4°C. The next day, the sections were washed three times for five minutes in TBST at room temperature. Three two-hour washes in TBST followed. Then, the sections were washed in NTMT (0.1M Tris-HCl pH 9.5, 0.1M NaCl, 50mM $MgCl_2$, 1% Tween-20 in H_2O) three times for ten minutes. The colour development was done in NBT/BCIP solution (20μL NBT/BCIP stock solution from Roche per mL of NTMT) in the dark. Washing the sections with PBS stopped the reaction. Finally, the sections were mounted on slides and cover-slipped with AquaPolymount (Polysciences Inc). Steps carried out at 65°C were performed in a tightly sealed chamber humidified with 50% formamide in H_2O to prevent evaporation. All steps were done on a shaker with gentle rocking. Data was analyzed with an Olympus IX51 microscope. Contrast and exposure of images were enhanced for better visualization.

2.9 Immunohistochemistry

Free-floating brain sections were washed three times for ten minutes in PBS containing 0.2% triton X-100 (PBS-Triton). This was followed by a one- to three-hour incubation in blocking buffer (10% normal serum in PBS-Triton). The sections were then put in primary antibody in PBS at 4°C for 18-48 hours with gentle agitation (see

Table 2.6 for antibodies and dilutions). After three ten-minute washes in PBS, sections were incubated with fluorescently tagged secondary antibody in PBS for 2-4 hours. Sections were then washed three times for ten minutes in PBS before doing a counter stain with 4',6-diamidino-2-phenylindole (DAPI) diluted in dH_2O. A quick wash in PBS followed. Lastly, sections were mounted on slides and cover-slipped with AquaPolymount. All steps up to the counter stain were done with gentle rocking. Results were mostly documented with an epifluorescent microscope (Zeiss Axioplan2, Carl Zeiss Ltd. UK). Pictures were taken with a digital CCD camera (DP70.Olympus) connected to the microscope and using AnalysisB software (Olympus). Images were also obtained with Zeiss Confocal LSM700 Microscope using Zen software.

Table 8 Primary and Secondary Antibodies and Dilutions

Antibody	Dilution
BLBP (rabbit; Abcam ab32423)	1:300
Cux-1 (rabbit; Santa Cruz sc13024)	1:500
GAD67 (mouse; Millipore MAB5406)	1:1000
GFAP (rabbit; DakoCytomation Z0334)	1:2000
NeuN (mouse; Millipore MAB377)	1:200
Neurofilament (mouse; DSHB 3H2)	1:250
PlexinA4 (Armenian hamster; Courtesy of Dr.Suto)	1:500
SERT (rabbit; Calbiochem)	1:2000
VGluT2 (mouse; Millipore MAB5504)	1:1000
goat anti-Armenian hamster Cy3 (Jackson ImmunoResearch 127-165-160)	1:500
goat anti-mouse Alexa Fluor 488 (Invitrogen - Molecular Probes A11001)	1:500
goat anti-mouse Alexa Fluor 555 (Invitrogen - Molecular Probes A21422)	1:500
goat anti-rabbit Cy5 (Jackson ImmunoResearch 111-175-003)	1:500
goat anti-rabbit Alexa Fluor 488 (Invitrogen - Molecular Probes A11008)	1:500
goat anti-rabbit Alexa Fluor 555 (Invitrogen - Molecular Probes A21428)	1:500

2.10 Fiber tracing with carbocyanine dyes

In order to label axonal projections, holes were punched into the fixed brain tissue at the required site of dye injections with a tungsten dissection probe (World Precision Instruments Inc., Sarasota, Florida, USA). Then, two fluorescent lipophilic carbocyanine dyes, 1,1'-dioctadecyl-3,3,3'3'-tetramethylindocarbocyanine perchlorate (DiI) and 4-[4-(dihexadecylamino)styryl]-N-methylpyridinium iodide (DiA), were inserted into these holes at the appropriate depth for diffusion into cells or axons of interest (one type of dye per hole). Brains were kept in 1% PFA in PBS at room temperature for up to 12 weeks to allow complete labeling of the tracts. Brains were sectioned as described above in histology. Slices were then counterstained with DAPI, quickly washed in PBS, mounted and imaged.

Chapter 3

Bioinformatics Analyses of Developmental Gene Expression Patterns in the Thalamus

3.1 Introduction

Brain function relies on the proper development of a staggeringly complex network of connections established between billions of neurons. This process requires a highly conserved genetic program in which the expression of numerous genes is controlled spatiotemporally. One such category of genes expresses guidance cues, extracellular proteins that induce attractive or repulsive responses to lead axons towards their appropriate targets. Different guidance molecules have been identified to date; however, many more are thought to be required to explain the observed complexity in connectivity. The focus of this study relies on *in silico* discovery of guidance molecules at the level of thalamocortical connectivity during mouse development. A few gene expression datasets have been made available online, of particular interest the developing Allen Brain Atlas. There are also a few online tools dedicated to protein domain screens. Bridging together the information of various websites, we propose novel candidate genes in thalamocortical connectivity.

3.1.1 The mouse developing Allen Brain Atlas

The Allen Institute for Brain Science is dedicated to unraveling brain function through collaborative work. A considerable amount of effort has gone into generating public resources available through their portal (www.brain-map.org). Different maps of gene expression have been put together for the mouse, non-human primate and human adult brain, as well as the developing mouse and human brain. The data available for the developing mouse brain is more complete than that for the developing human brain as it contains expression data for more genes at more time-points and brain regions. Therefore, the mouse developing Allen Brain Atlas (devABA) can be used to make inferences into human development, and it is expression data from this atlas that we are interested in. To generate the devABA, gene expression was mapped through *in situ* hybridization (ISH) of sequential sagittal sections for 2002 genes at 7 developmental ages (Lein, Hawrylycz et al. 2007, Thompson, Ng et al. 2014). The time-points selected are relevant to regional specification/patterning (E11.5), axon pathfinding (E13.5, E15.5 and E18.5), synaptogenesis (P4 and P14) and cortical plasticity (P28). Messenger RNA expression data was quantified and recorded per three-dimensional units, or voxels. These voxels were assigned regional labels through age-matched anatomic reference atlases allowing for precise location and direct comparison of gene expression. The genes whose expression was acquired were selected according to previous functional

work implicating them in brain development or disorders of the brain. The quantified data is available through their application programming interface.

3.1.2 Webtools to predict protein subcellular localization

In order to focus on extracellular protein products, online prediction tools are invaluable. Computational prediction of subcellular localization relies on sorting signals (signal peptides), amino acid composition, between localization sites and functional motifs. PSORTII is a popular program that uses a series of consensus sequences to compare to the amino acid sequence of the protein of interest (Table 9). This program calculates the probabilities of being in each localization (cytoplasm, cytoskeleton, endoplasmic reticulum, Golgi apparatus, mitochondria, nucleus, plasma membrane, peroxisomes, vacuoles and vesicles of the secretory system) by using a two-fold *k*-nearest neighbor (*k*-NN) algorithm (Horton and Nakai 1997). To assess the predictive accuracy of PSORTII, Nakai and Horton (1999) compared their results to those from the SWISS-PROT and YPD databanks for 1531 *Saccharomyces cerevisiae* sequences. They obtained 57% accuracy, which they explain due to the available knowledge of protein biology and proteins whose localization can be found in multiple sites. Therefore, although much progress has been made in predicting subcellular localization, combining the outputs of different algorithms, from different websites, increases the probabilities of determining the correct localization, in addition to manual curation. So, accuracy can be increased by running programs like the SignalP prediction program, the big-PI predictor and the TMHMM program, if the intention is to focus on proteins localized extracellularly. The former screens for the N-terminal signal peptide, which is required for proteins to enter the secretory pathway, and is characterized by an amino acid sequence of a positively charged n-region, followed by a hydrophobic h-region and a neutral but polar c-region (Nielsen, Engelbrecht et al. 1997). The SignalP program uses neural network algorithms. Comparing accuracy with data from SWISS-PROT, Nielsen, Engelbrecht et al. (1997) originally achieved 70% accuracy for 1831 eukaryotic sequences; new refinements, however, have brought the accuracy up above 80% (Petersen, Brunak et al. 2011). The big-PI predictor screens protein sequences for a transamidase binding site at the C-terminal (ω-site), since cleavage by this enzyme is necessary for glycosylphosphatidylinositol anchoring to occur, through a knowledge-based algorithm (Eisenhaber, Bork et al. 1998, Eisenhaber, Bork et al. 1999). Results obtained for *Caenorhabditis elegans* indicate that the method used is above 80%

accurate when comparing data to the literature and SWISS-PROT annotated sequences (Eisenhaber, Bork et al. 2000). Finally, the TMHMM program screens for transmembrane (TM) helices in proteins through a hidden Markov model (HMM) (Sonnhammer, von Heijne et al. 1998, Krogh, Larsson et al. 2001). It incorporates search features such as hydrophobicity, charge bias, helix length and what they call grammatical constraints (correct sequential order of the different domains). Krogh, Larsson et al. (2001) reported single-sequence prediction accuracy of 78% when comparing data to various databanks.

Table 9 Features detected by PSORTII

Feature	Criteria
N-terminal signal peptide	Modified McGeoch's method and the cleavage-site consensus
Mitochondrial-targeting signal	Amino acid composition of the N-terminal 20 residues and some weak cleavage-site consensus
Nuclear-localization signals	Combined score for various empirical rules
ER-lumen-retention signal	The KDEL-like motif at the C-terminus
ER-membrane-retention signal	Motifs: XXRR-like (N-terminal) or KKXX-like (C-terminal)
Peroxisomal-targeting signal	PTS1 motif at the C-terminus and the PTS2 motif
Vacuolar-targeting signal	[TIK]LP[NKI] motif
Golgi-transport signal	The YQRL motif (preferentially at the cytoplasmic tail)
Tyrosine-containing motif	Number of tyrosine residues in the cytoplasmic tail
Dileucine motif	At the cytoplasmic tail
Membrane span(s)/topology	Maximum hydrophobicity and the number of predicted spans; charge difference across the most N-terminal transmembrane segment
RNA-binding motif	RNP-1 motif
Actinin-type actin-binding motifs	From PROSITE
Isoprenyl motif	CaaX motif at the C-terminus
GPI-anchor	Type-1a membrane protein with very short tail
N-myristoylation motif	At the N-terminus
DNA-binding motifs	63 motifs from PROSITE
Ribosomal-protein motifs	71 motifs from PROSITE
Prokaryotic DNA-binding motifs	33 motifs from PROSITE
Amino acid composition	Neural network score that discriminates between cytoplasmic and nuclear proteins
Coiled-coil structure	Number of residues in the predicted coiled-coil state
Length	Length of the sequence

Adapted from Nakai and Horton (1999).

3.1.3 Extracellular proteins expressed during thalamic development

A few molecules involved in thalamic development have been introduced in Chapter 1. The gene set from the devABA includes a range of morphogens, such as Shh, Wnts, FGFs and bone morphogenetic proteins (BMPs). Interestingly, morphogenetic cues have recently been found to also act as guidance cues as they can direct growth cone turning and can modulate response to other guidance cues (Yam and Charron 2013). And they do so through noncanonical signaling pathways (Figures 5 and 6). Wnts interact with a wide range of receptors making their effects context-dependent as opposed to intrinsic. Some of them are introduced in Figure 6, but Wnt can also bind R-Spondin family of receptors and ROR2, and Wnt activity can be modulate through the secreted Fz-related proteins (Sfrp)(Niehrs 2012). Recent studies have established that Shh expression by the midline floor plate promotes growth cone sensitivity of spinal cord commissural axons to the secreted repellent Sema3B during midline crossing (Parra and Zou 2010). Moreover, these effects require that the glial cell-derived neurotrophic factor (gdnf) and neuronal cell adhesion molecule (NrCAM) promote availability of Sema3B receptor PlexinA1 in commissural neurons (Nawabi, Briancon-Marjollet et al. 2010, Charoy, Nawabi et al. 2012). Some of these morphogenetic cues have not been studied much in the context of thalamocortical connectivity. Establishing their expression patterns in the thalamus in ages subsequent to patterning can introduce novel functions.

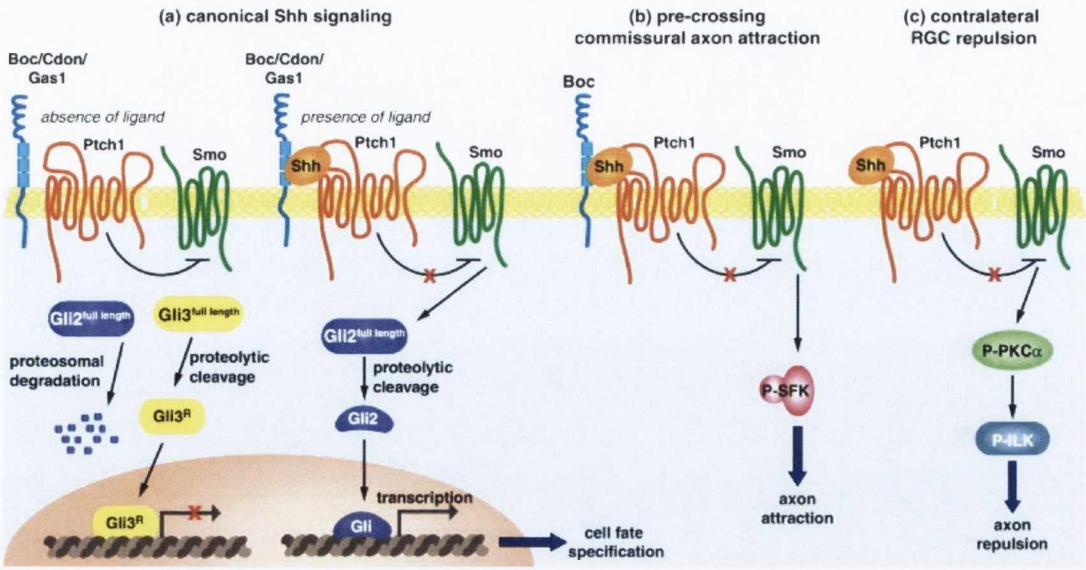


Figure 5. Shh canonical and noncanonical signaling pathways

Shh canonical signaling (A). In the absence of ligand, Ptch1 inhibits Smo thereby promoting full-length Gli2 degradation by proteosomes and full-length Gli3 cleavage to generate the Gli3 repressor form ($Gli3^R$) which blocks transcription. Shh binding to its receptors Ptch1 together with Boc, Cdon, or Gas1, relieves Ptch1-mediated inhibition of Smo. Smo can then induce the proteolytic cleavage of Gli2 and its translocation to the nucleus where it induces transcription of target genes. Noncanonical Shh signaling pathways involved in axon guidance (B and C). Shh binding to Boc induces Smo activation and Src-family-kinases (SFK) activity in pre-crossing commissural axon attraction (B). Shh acts through a Smo-dependent pathway to repel retinal ganglion cell (RGC) axons through protein kinase C-α (PKCα) and integrin-linked kinase (ILK) in contralateral RGCs (C).

Adapted from Yam and Charron (2013).

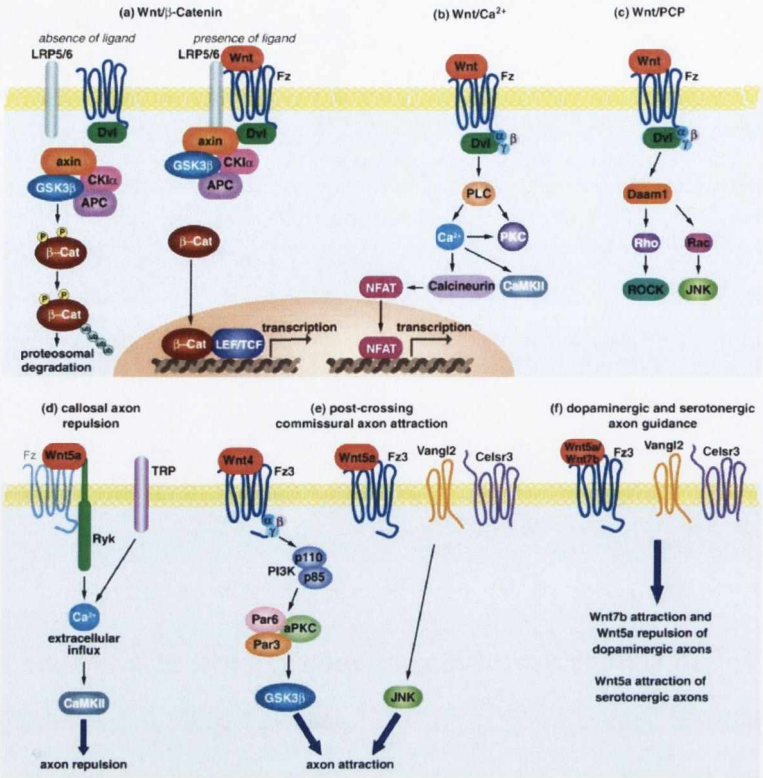


Figure 6. Wnt canonical and noncanonical signaling pathways

Wnt/β-catenin canonical signaling (A). β-catenin (β-cat) is phosphorylated by GSK3β and CKIα thereby flagging it for degradation, when Wnt is absent. Wnt binding to its receptor Frizzled (Fz) and coreceptors LRP5/6 activates Dishevelled (Dvl) and suppresses GSK3β activity inducing β-cat stabilization and accumulation in the nucleus where it intereacts with LEF/TCF to regulate gene transcription. Wnt noncanonical signaling pathways involved in axon guidance (B to F). Activation of the Wnt/Ca^{2+} pathway induces the activation of phospholipase C (PLC), the mobilization of intracellular Ca^{2+} and the activation of CaMKII, calcineurin, protein kinase C (PKC), and NFAT (B). In the Wnt/PCP pathway, Wnt–Fz interactions lead to Dvl-dependent activation of the small GTPases Rho and Rac, which in turn activate ROCK and JNK to regulate cell polarity (C). Wnt5a binding to its receptor Ryk, and possibly Fz, mediates repulsion of callosal axons and leads to extracellular influx of Ca^{2+} from TRP channels and CaMKII activation (D). Wnt4 binding to Fz3 induces a signaling cascade involving PI3K, aPKC/Par3/Par6 and GSK3β thereby attracting post-crossing commissural axons (E). Fz3, Vangl2, Celsr3 and JNK also regulate the guidance of these axons. Wnt5a and Wnt7b interact with Fz3, Vangl2 and Celsr3 to guide dopaminergic and serotonergic axons of the brainstem (F).

Adapted from Yam and Charron (2013).

3.1.4 Aims

In this study, we aim to identify novel axon guidance molecules involved in thalamocortical connectivity. To do so, we will use an *in silico* approach to mine expression values for 2002 genes at 7 developmental ages relevant to different developmental stages available from the devABA. We will perform clustering analyses of similar patterns of expression with peak expression at time-points relevant to thalamocortical axon guidance. Moreover, using PSORTII, SignalP, the big-PI predictor and TMHMM, we aim to screen protein products for subcellular localization with an emphasis on the extracellular compartment. To these results, we will add known functions associated to the genes in our dataset. We will extensively curate each set of results obtained to create a platform useable for this and further studies. Combining localization and function information, we aim to validate our final dataset with known genes involved in particular functions of thalamic development. But, most importantly, we aim to extrapolate new candidate genes for thalamocortical pathfinding.

3.2 Results

3.2.1 Clustering analyses of developmental gene expression patterns in the thalamus

In order to find genes expressed in the thalamus during time-points when axon guidance occurs, we normalized and clustered expression density values for 2002 developmental genes at E11.5, E13.5, E15.5, E18.5, P4, P14 and P28 found on the devABA (see sections 2.1 and 2.2 for details). These time-points are developmentally relevant to regional specification/patterning (E11.5), axon pathfinding (E13.5, E15.5 and E18.5), synaptogenesis (P4 and P14) and cortical plasticity (P28). We performed hierarchical and k-means clustering analyses (Figure 7 and Figure 8 in the Digital Appendix). The hierarchical clustering showed significant groups naturally occurring (Figure 7 in the Digital Appendix). This type of clustering groups genes by similarity, in this case of temporal expression patterns, and allows for clear segregation of extremes, with at opposite ends of the output completely different patterns of expression and in close proximity similar patterns of expression. However, establishing specific numbers of partitions that best describes the data as a whole can be cumbersome through this method. So, we further investigated the trends observed through hierarchical clustering by k-means clustering (Figure 8 in the Digital Appendix). This method clusters data within a preset number of groups (k-mean). We evaluated the flux across a range of k-mean values (6 to 18), since there is no right k-mean value for a particular dataset. As the value for the k-mean increased, clusters tended to get subdivided as opposed to reshuffled as seen on the flow chart (Figure 8 in the Digital Appendix). Clusters showed clear peaks of expression at different time-points that coincided with real biological trends (Figure 9 and text below). We selected k-mean 10 for further data analysis, since the data segregated into clusters differentially peaking at all embryonic time-points (Figure 9 in bold). There was enough separation between the different patterns. Moreover, k-mean values from 11 to 13 included fewer genes in embryonic peaking clusters, and we wanted to be as inclusive as possible (771 genes, 742 genes and 824 genes, respectively, compared to 825 genes found in embryonic peaking clusters for k-mean 10; Figure 9). Clusters for k-means 14 to 18 showed increased refinement of postnatal gene expression patterns and were therefore of less interest to us.

k-mean 6	E11.5	E13.5	E15.5	E18.5	P04	P14	P28	# genes
cluster 5	3.325	0.647	0.361	0.620	0.598	0.807	0.577	326
cluster 0	1.046	1.680	1.046	0.763	0.806	1.024	0.630	300
cluster 2	0.627	0.427	0.544	2.194	1.235	1.212	0.771	307
cluster 1	0.387	0.283	0.356	0.804	2.777	1.474	0.917	392
cluster 3	0.453	0.275	0.252	0.525	0.629	3.684	1.157	414
cluster 4	0.342	0.245	0.248	0.427	0.752	1.984	2.966	257

k-mean 7	E11.5	E13.5	E15.5	E18.5	P04	P14	P28	# genes
cluster 0	3.333	0.644	0.362	0.633	0.598	0.787	0.575	255
cluster 5	1.068	1.722	1.059	0.809	0.777	0.960	0.590	284
cluster 4	0.637	0.415	0.517	2.548	1.315	0.981	0.584	206
cluster 6	0.425	0.298	0.348	0.786	3.371	1.067	0.678	213
cluster 1	0.431	0.343	0.449	0.877	1.497	2.077	1.306	456
cluster 3	0.442	0.256	0.215	0.455	0.499	3.901	1.199	341
cluster 2	0.372	0.239	0.197	0.393	0.590	1.865	3.290	241

k-mean 8	E11.5	E13.5	E15.5	E18.5	P04	P14	P28	# genes
cluster 5	4.087	0.739	0.318	0.505	0.430	0.478	0.374	133
cluster 1	2.077	0.653	0.484	0.791	0.786	1.411	0.817	273
cluster 0	0.865	1.965	1.170	0.820	0.817	0.798	0.539	208
cluster 3	0.568	0.411	0.533	2.575	1.303	0.989	0.599	196
cluster 7	0.401	0.287	0.345	0.786	3.399	1.063	0.688	206
cluster 6	0.320	0.333	0.445	0.880	1.561	2.095	1.347	420
cluster 4	0.397	0.249	0.216	0.450	0.500	3.933	1.211	329
cluster 2	0.328	0.238	0.198	0.391	0.581	1.874	3.332	231

k-mean 9	E11.5	E13.5	E15.5	E18.5	P04	P14	P28	# genes
cluster 1	4.104	0.748	0.319	0.485	0.415	0.480	0.378	131
cluster 7	2.068	0.652	0.499	0.825	0.801	1.393	0.780	276
cluster 6	0.874	1.990	1.164	0.812	0.791	0.811	0.531	205
cluster 5	0.572	0.405	0.501	2.685	1.302	0.958	0.551	173
cluster 0	0.400	0.279	0.341	0.783	3.445	1.059	0.664	197
cluster 4	0.331	0.345	0.484	0.966	1.618	1.980	1.253	407
cluster 2	0.434	0.260	0.224	0.501	0.502	4.200	0.832	221
cluster 3	0.279	0.213	0.183	0.332	0.655	2.940	2.364	256
cluster 8	0.448	0.298	0.242	0.497	0.571	1.167	3.685	130

k-mean 10	E11.5	E13.5	E15.5	E18.5	P04	P14	P28	# genes
cluster 7	4.087	0.733	0.318	0.503	0.430	0.478	0.374	131
cluster 6	2.067	0.665	0.465	0.791	0.785	1.423	0.820	268
cluster 5	0.932	2.706	0.674	0.686	0.560	0.946	0.447	106
cluster 2	0.769	0.966	1.548	1.047	1.196	0.769	0.703	163
cluster 4	0.553	0.378	0.426	2.779	1.286	1.003	0.550	157
cluster 0	0.317	0.318	0.421	0.965	1.628	2.069	1.256	384
cluster 8	0.403	0.284	0.303	0.791	3.467	1.070	0.662	192
cluster 9	0.432	0.249	0.226	0.482	0.491	4.237	0.839	214
cluster 3	0.271	0.213	0.190	0.329	0.650	2.949	2.374	253
cluster 1	0.450	0.294	0.225	0.494	0.566	1.175	3.699	128

(Legend on p.44)

k-mean 11	E11.5	E13.5	E15.5	E18.5	P04	P14	P28	# genes
cluster 4	4.142	0.757	0.323	0.466	0.405	0.473	0.361	124
cluster 0	2.204	0.643	0.459	0.836	0.846	1.181	0.817	232
cluster 6	0.948	2.756	0.672	0.693	0.600	0.847	0.428	100
cluster 1	0.760	0.982	1.594	1.048	1.172	0.772	0.671	157
cluster 5	0.526	0.383	0.442	2.766	1.291	1.012	0.555	158
cluster 8	0.319	0.298	0.410	0.917	1.870	1.795	1.364	332
cluster 10	0.395	0.257	0.284	0.756	3.635	1.080	0.556	162
cluster 9	0.689	0.550	0.438	0.885	0.718	2.775	0.933	225
cluster 2	0.349	0.187	0.179	0.355	0.444	4.547	0.896	162
cluster 3	0.252	0.155	0.150	0.295	0.684	2.923	2.496	226
cluster 7	0.447	0.302	0.222	0.485	0.520	1.154	3.773	118

k-mean 12	E11.5	E13.5	E15.5	E18.5	P04	P14	P28	# genes
cluster 0	4.127	0.752	0.322	0.465	0.410	0.473	0.380	126
cluster 6	2.251	0.660	0.472	0.850	0.851	1.250	0.663	215
cluster 8	0.911	2.734	0.685	0.688	0.600	0.888	0.421	101
cluster 11	0.777	0.956	1.646	1.069	1.246	0.737	0.568	142
cluster 7	0.526	0.383	0.442	2.766	1.291	1.012	0.555	158
cluster 1	0.412	0.268	0.271	0.739	3.738	0.996	0.536	142
cluster 2	0.283	0.262	0.384	0.910	2.027	1.861	1.251	299
cluster 10	0.629	0.471	0.433	0.894	0.764	2.843	0.927	211
cluster 5	0.354	0.189	0.178	0.350	0.442	4.544	0.904	163
cluster 9	0.209	0.142	0.139	0.280	0.694	2.937	2.549	210
cluster 4	0.837	0.657	0.500	0.844	0.843	1.215	2.081	144
cluster 3	0.380	0.224	0.171	0.319	0.470	1.216	4.133	85

k-mean 13	E11.5	E13.5	E15.5	E18.5	P04	P14	P28	# genes
cluster 6	4.163	0.766	0.322	0.465	0.387	0.469	0.352	121
cluster 9	2.315	0.629	0.443	0.814	0.846	1.178	0.754	210
cluster 11	0.900	2.756	0.674	0.669	0.608	0.888	0.430	98
cluster 5	0.911	1.005	1.770	1.041	1.118	0.673	0.484	117
cluster 12	0.574	0.425	0.431	3.075	0.977	0.989	0.515	107
cluster 8	0.466	0.309	0.480	1.611	2.324	1.094	0.668	171
cluster 1	0.362	0.260	0.251	0.473	3.989	1.042	0.588	104
cluster 3	0.214	0.204	0.291	0.667	1.973	2.218	1.413	239
cluster 0	0.797	0.591	0.446	0.964	0.681	2.731	0.763	179
cluster 4	0.357	0.186	0.186	0.359	0.453	4.558	0.855	158
cluster 10	0.257	0.164	0.169	0.306	0.558	3.026	2.449	217
cluster 2	0.594	0.655	0.633	0.949	1.053	1.330	1.782	177
cluster 7	0.429	0.235	0.169	0.378	0.477	1.213	4.000	98

k-mean 14	E11.5	E13.5	E15.5	E18.5	P04	P14	P28	# genes
cluster 4	4.223	0.743	0.306	0.453	0.360	0.475	0.369	114
cluster 7	2.297	0.726	0.559	1.015	1.067	0.715	0.593	159
cluster 2	2.016	0.652	0.394	0.547	0.515	2.075	0.846	129
cluster 6	0.885	2.792	0.665	0.658	0.620	0.881	0.430	94
cluster 3	0.743	1.034	1.907	0.966	1.110	0.732	0.508	99
cluster 10	0.562	0.421	0.429	3.080	0.969	1.012	0.519	106
cluster 13	0.423	0.309	0.508	1.665	2.288	1.107	0.664	158
cluster 11	0.362	0.255	0.247	0.512	4.018	0.999	0.569	102
cluster 5	0.235	0.218	0.298	0.680	2.078	2.092	1.380	221
cluster 12	0.479	0.464	0.425	0.995	0.819	2.865	0.911	177
cluster 1	0.363	0.187	0.187	0.355	0.447	4.559	0.861	158
cluster 9	0.223	0.156	0.150	0.275	0.603	3.004	2.514	207
cluster 8	0.616	0.651	0.607	0.968	1.056	1.295	1.808	176
cluster 0	0.434	0.234	0.172	0.364	0.478	1.204	4.012	96

k-mean 15	E11.5	E13.5	E15.5	E18.5	P04	P14	P28	# genes
cluster 8	4.231	0.742	0.304	0.451	0.355	0.475	0.370	113
cluster 5	2.319	0.727	0.552	0.995	1.034	0.734	0.603	163
cluster 1	1.964	0.657	0.394	0.517	0.522	2.180	0.831	132
cluster 6	0.882	2.785	0.661	0.657	0.617	0.902	0.430	95
cluster 10	0.784	1.061	1.926	0.969	0.991	0.771	0.502	93
cluster 0	0.562	0.425	0.439	3.140	0.999	0.919	0.508	98
cluster 3	0.455	0.344	0.597	1.620	2.337	0.965	0.630	157
cluster 14	0.367	0.254	0.223	0.469	4.039	1.020	0.588	98
cluster 4	0.240	0.226	0.307	0.731	2.094	2.077	1.302	224
cluster 2	0.447	0.420	0.436	1.395	0.866	2.628	0.819	137
cluster 13	0.365	0.199	0.206	0.373	0.402	4.710	0.707	126
cluster 7	0.332	0.228	0.212	0.352	0.621	3.475	1.714	162
cluster 12	0.190	0.155	0.139	0.261	0.731	2.613	2.863	148
cluster 9	0.633	0.676	0.605	0.948	1.055	1.269	1.814	168
cluster 11	0.475	0.228	0.178	0.390	0.420	1.080	4.108	82

k-mean 16	E11.5	E13.5	E15.5	E18.5	P04	P14	P28	# genes
cluster 7	4.270	0.759	0.304	0.414	0.345	0.476	0.355	108
cluster 6	1.967	0.641	0.408	0.569	0.517	2.144	0.803	127
cluster 4	1.838	1.496	0.590	0.990	0.823	0.769	0.501	154
cluster 10	0.893	2.823	0.671	0.663	0.578	0.874	0.426	91
cluster 5	0.864	1.085	1.979	0.979	0.914	0.680	0.490	85
cluster 1	0.546	0.410	0.428	3.081	1.036	0.971	0.514	108
cluster 3	0.528	0.461	0.642	1.475	2.500	0.763	0.595	129
cluster 11	0.394	0.210	0.179	0.431	4.484	0.795	0.462	59
cluster 2	0.307	0.193	0.237	0.767	2.706	1.919	0.863	145
cluster 14	0.404	0.608	0.675	1.285	1.236	1.677	1.120	191
cluster 13	0.476	0.370	0.346	0.780	0.782	3.216	0.982	182
cluster 0	0.321	0.186	0.160	0.288	0.387	4.771	0.846	122
cluster 12	0.233	0.180	0.286	0.547	1.678	2.126	1.916	159
cluster 15	0.206	0.157	0.129	0.270	0.475	3.086	2.610	166
cluster 9	0.967	0.593	0.453	0.831	0.775	0.930	2.391	89
cluster 8	0.366	0.224	0.167	0.309	0.451	1.248	4.184	81

k-mean 17	E11.5	E13.5	E15.5	E18.5	P04	P14	P28	# genes
cluster 9	4.215	0.751	0.300	0.445	0.351	0.491	0.373	115
cluster 15	2.337	0.734	0.568	1.004	1.015	0.725	0.570	156
cluster 10	1.929	0.633	0.407	0.569	0.526	2.158	0.807	127
cluster 13	0.887	2.816	0.671	0.657	0.602	0.871	0.424	92
cluster 7	0.795	1.081	2.035	0.945	0.961	0.681	0.493	81
cluster 3	0.542	0.414	0.433	3.134	0.966	0.987	0.514	100
cluster 14	0.531	0.385	0.574	1.725	2.349	0.794	0.622	127
cluster 4	0.383	0.298	0.227	0.478	4.283	0.798	0.489	72
cluster 16	0.323	0.217	0.279	0.756	2.657	1.873	0.840	144
cluster 0	0.411	0.622	0.731	1.194	1.203	1.662	1.176	178
cluster 2	0.238	0.189	0.277	0.548	1.734	2.113	1.863	152
cluster 6	0.460	0.405	0.339	1.118	0.830	3.105	0.681	119
cluster 1	0.369	0.191	0.169	0.287	0.381	4.802	0.762	114
cluster 8	0.298	0.208	0.203	0.336	0.600	3.457	1.843	154
cluster 5	0.200	0.178	0.135	0.265	0.516	2.583	3.065	119
cluster 11	0.958	0.602	0.438	0.843	0.788	0.914	2.406	85
cluster 12	0.410	0.221	0.183	0.327	0.438	0.989	4.357	61

k-mean 18	E11.5	E13.5	E15.5	E18.5	P04	P14	P28	# genes
cluster 7	4.276	0.764	0.306	0.404	0.342	0.477	0.353	107
cluster 11	2.495	0.596	0.539	1.018	1.055	0.686	0.573	131
cluster 5	2.029	0.579	0.405	0.571	0.532	2.108	0.836	120
cluster 15	1.223	1.932	0.676	0.880	0.713	1.016	0.528	112
cluster 3	0.722	3.722	0.769	0.436	0.446	0.517	0.335	34
cluster 1	0.752	0.941	2.303	0.956	0.940	0.644	0.444	60
cluster 16	0.539	0.393	0.424	3.069	1.050	0.994	0.523	110
cluster 14	0.565	0.448	0.633	1.466	2.476	0.768	0.603	133
cluster 4	0.376	0.226	0.178	0.437	4.334	0.882	0.524	70
cluster 10	0.288	0.193	0.243	0.808	2.628	1.966	0.858	132
cluster 17	0.391	0.615	0.761	1.210	1.221	1.630	1.172	173
cluster 9	0.236	0.182	0.287	0.575	1.707	2.114	1.865	155
cluster 13	0.524	0.442	0.358	1.122	0.784	3.043	0.681	126
cluster 6	0.356	0.194	0.172	0.290	0.394	4.811	0.744	112
cluster 0	0.315	0.207	0.201	0.337	0.611	3.487	1.793	154
cluster 12	0.191	0.173	0.134	0.260	0.512	2.627	3.045	122
cluster 2	0.934	0.557	0.427	0.834	0.783	0.941	2.455	85
cluster 8	0.415	0.221	0.183	0.314	0.431	0.983	4.375	60

Figure 9. Summaries of K-means Clustering Analyses of the Developmental Dataset

Normalized expression densities were averaged per cluster to see the trends of expression from k-means 6 to 18 (k-mean indicated at top left corner of each table). Clusters were organized chronologically with early peaks of expression at the top and later peaks of expression at the bottom. Heatmap's 3 colour scale of gene expression data: 0.2, red; 1, white; blue, 5. Cluster numbers and gene numbers in blue have embryonic expression (see text). K-mean 10 was used for further analyses; the corresponding tableframe is in bold.

3.2.2 Distribution of proteins by localization

We used two different approaches with the aim of finding genes not previously known to be involved in axon guidance by cell-cell communication within the developmental dataset. First, we screened protein products for cellular localization with an emphasis on the extracellular environment combining the outputs of different tools available online (PSORTII, SignalP, Big-PI Predictor and TMHMM – see details in section 2.1). Our dataset predominantly expressed proteins found in the nucleus (906 proteins), followed by 292 secreted proteins, 283 GPI-anchored or single-pass transmembrane proteins, 266 cytoplasmic (or in organelles) proteins and 240 multi-pass transmembrane proteins (Table 10; Figure 10 in the Digital Appendix). Nine genes could not be annotated: C030002O17Rik, Frat1, Hbb-b2, Itlnb, LOC433436, LOC545810, mCG146432, Pcdha7 and Tigd5.

Table 10 Number of Genes per Localization

	Secreted	Single-Pass & GPI	Multi-Pass	Cytoplasm	Nucleus	Total
# Genes	292	283	240	266	906	1987

3.2.3 Enrichment analyses of proteins based on localization

We then hypothesized that different protein localizations are enriched in clusters relevant to specific developmental functions. In order to determine whether certain categories of protein localization were enriched in our dataset, we first calculated the expected values for each category (Table 11):

expected = (total # of genes in cluster of interest / total # of genes) * total # of genes in category of interest

For instance, the expected number of genes in cluster 7 that express secreted proteins is:

expected = (131 genes in cluster 7 / 1987 genes) * 292 genes in category of secreted proteins

= 19 genes

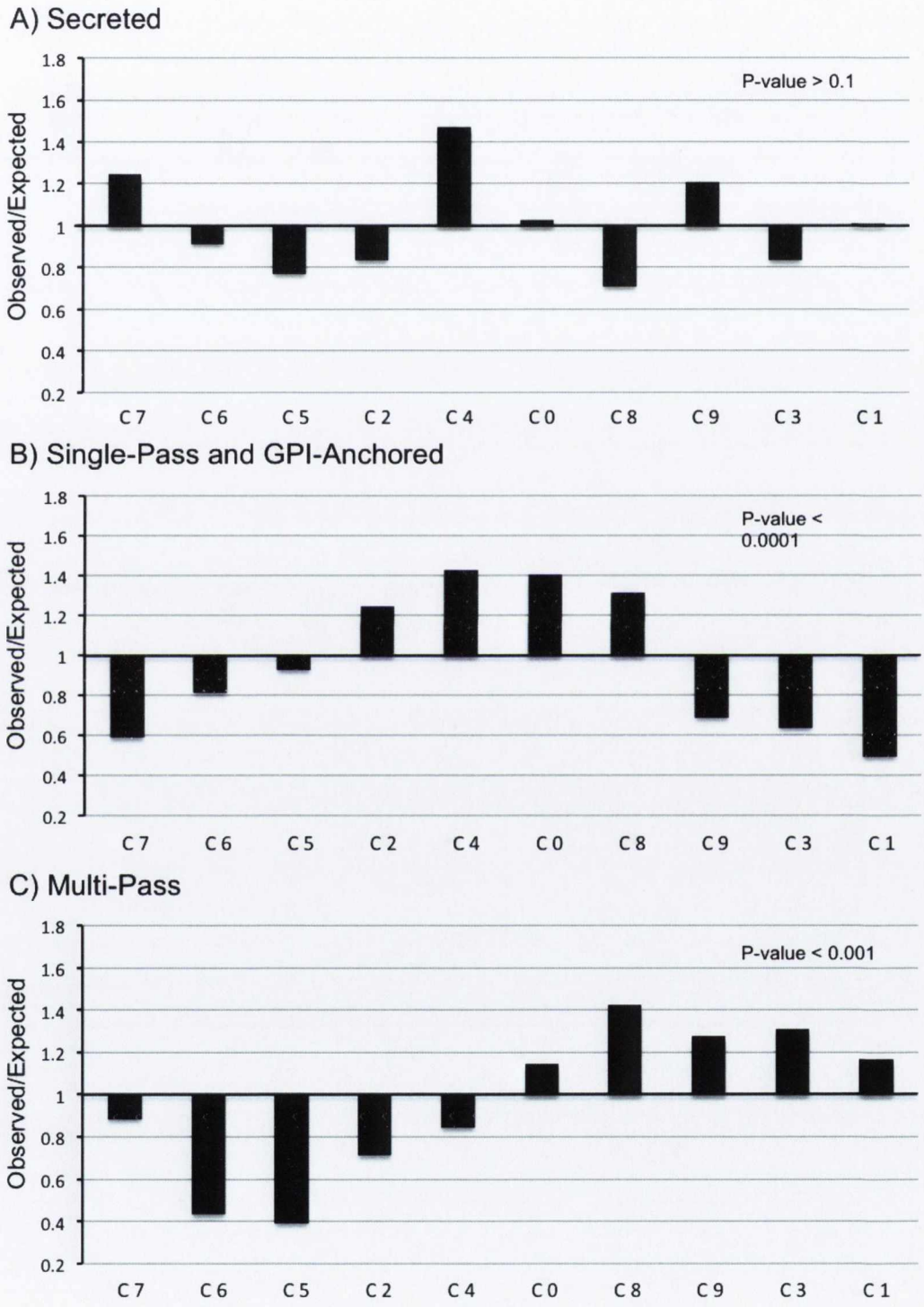
The numbers of genes per cluster for k-mean 10 are indicated in Figure 9.

Table 11 Observed / Expected Values per Localization

Cluster	Secreted	Single-Pass & GPI	Multi-Pass	Cytoplasm	Nucleus
Cluster 7	24 / 19	11 / 19	14 / 16	15 / 18	66 / 60
Cluster 6	36 / 39	31 / 38	14 / 32	30 / 36	157 / 122
Cluster 5	12 / 16	14 / 15	5 / 13	8 / 14	66 / 48
Cluster 2	20 / 24	29 / 23	14 / 20	15 / 22	83 / 74
Cluster 4	34 / 23	32 / 22	16 / 19	20 / 21	53 / 72
Cluster 0	58 / 56	77 / 55	53 / 46	56 / 51	140 / 175
Cluster 8	20 / 28	36 / 27	33 / 23	30 / 26	72 / 88
Cluster 9	38 / 31	21 / 30	33 / 26	27 / 29	94 / 98
Cluster 3	31 / 37	23 / 36	40 / 31	46 / 34	112 / 115
Cluster 1	19 / 19	9 / 18	18 / 15	19 / 17	63 / 58

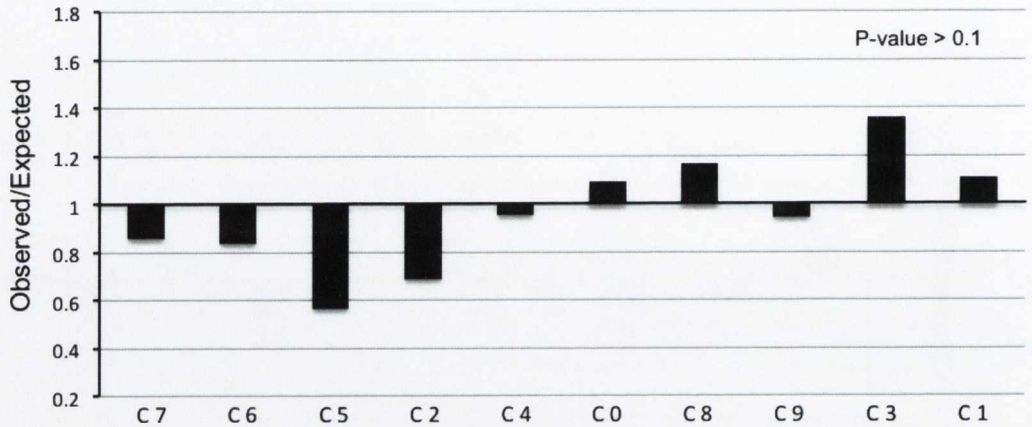
Different trends emerged from the observed/expected ratios (Figure 11 A-E). Chi square statistics on the whole dataset showed deviation from expected by random distribution at p-value < 0.001 (Table 12). Further statistics were done on individual categories to establish which ones were enriched in particular clusters. The Bonferroni correction was taken into account due to multiple testing lowering the threshold to $p \leq 0.01$. The trends observed with secreted and cytoplasmic proteins did not reach statistical significance (p-value > 0.1). However, the distribution of single-pass transmembrane and GPI-anchored proteins, multi-pass transmembrane proteins and nuclear proteins were significant at p-value < 0.0001, p-value < 0.001 and p-value < 0.001, respectively. Interestingly, proteins localized to the nucleus are enriched in clusters peaking at early time-points, whereas single-pass transmembrane and GPI-anchored proteins are enriched in clusters peaking from E15.5 to P4, and multi-pass transmembrane proteins are enriched in clusters peaking from P4 to P28 (Figure 11 F). This nicely correlates with the extensive requirement of transcription factors during patterning and axon guidance early on (localized in the nucleus), followed by axon guidance molecules expressed extracellularly during axon pathfinding, and finally synaptogenesis and

neurotransmission postnatally (many molecules involved in these processes are known to be multi-pass transmembrane proteins). Although we could already infer function from these analyses, we further characterized the genes from our dataset by known biological roles.

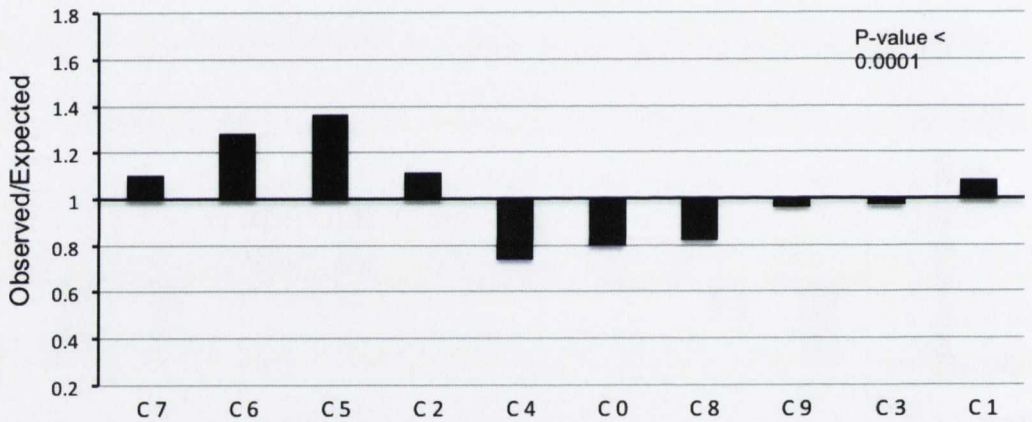


(Legend on p.49)

D) Cytoplasm



E) Nucleus



F) All Significant Categories

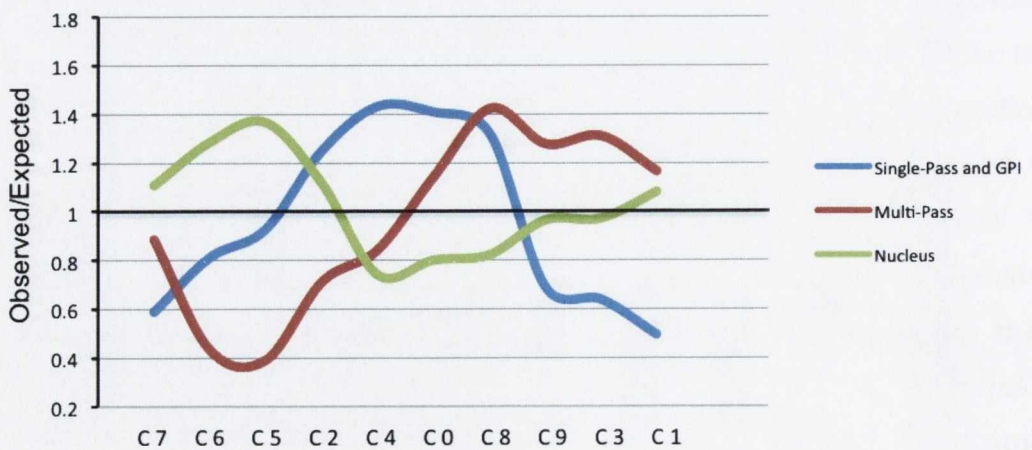


Figure 11. Observed Over Expected Distributions of Protein Localization per Cluster

Observed/expected values show different trends in all categories: secreted proteins (A), single-pass transmembrane or GPI-anchored proteins (B), multi-pass transmembrane proteins (C), cytoplasmic proteins (D) and nuclear proteins (E). A value of 1 indicates observed data matches expected values, whereas a value below or above 1 indicates decreased or increased counts compared to expected values, respectively. Clusters 0-9 are organized chronologically. C, cluster. P-values from chi square analyses are shown in upper right corner of each graph. All significant distributions by chi square analyses are shown for better comparison in F.

Table 12 Enrichment Analyses per Localization

	Chi Square	Degrees of Freedom	P-Value	Bonferroni Correction	Conclusion
All	120.426	36	< 0.001	No	Enrichment
Secreted	12.942	9	> 0.1	Yes	No Enrichment
Single-Pass and GPI	34.341	9	< 0.0001	Yes	Enrichment
Multi-Pass	27.904	9	< 0.001	Yes	Enrichment
Cytoplasm	11.983	9	> 0.1	Yes	No Enrichment
Nucleus	33.257	9	< 0.001	Yes	Enrichment

Degrees of freedom: All, (columns # - 1) (row # - 1) = (5 - 1) (10 - 1) = 36; Per Localization, n - 1 = 10 - 1 = 9. Bonferroni correction: $p \leq \alpha$ / # tests = 0.05 / 5 = 0.01

3.2.4 Distribution of proteins by function

We expanded the number of annotations of the dataset from Thompson and colleagues (2014) using GO term annotations and systematic manual curation (see details in section 2.1 and last column of Table 3 in the Digital Appendix). The dataset was then divided into 6 groups:

- Group 1: axon guidance pathway and cell adhesion;
- Group 2: synapse;
- Group 3: receptor tyrosine kinases and their ligands, and patterning;
- Group 4: neurotransmission pathway (GPCRs, ion channels, gap junctions);
- Group 5: chromatin and transcription factor activity
- Group 6: other (cytoskeleton, extracellular matrix, myelin, metabolic enzymes and signal transduction) and unannotated.

When a gene fell into more than one group, an order of priority was used (the order in which the groups are presented). Our dataset predominantly included genes involved with chromatin and transcription factor activity (676 genes in group 5); followed by 360 genes expressing receptor tyrosine kinases and their ligands, and genes involved in

patterning (group 3); 286 genes involved in the axon guidance pathway and cell adhesion (group 1); 270 in the neurotransmission pathway (group 4); and, 91 genes involved with synapses (group 2; Table 13; Figure 10 in the Digital Appendix). Group 6 contained 107 genes involved with or part of the cytoskeleton, extracellular matrix, myelin, signal transduction pathways or expressed metabolic enzymes. This group also included 206 unannotated genes totaling 313 genes.

Table 13 Number of Genes per Group

	Group 1	Group 2	Group 3	Group 4	Group 5	Group 6	Total
# Genes	286	91	360	270	676	313	1996

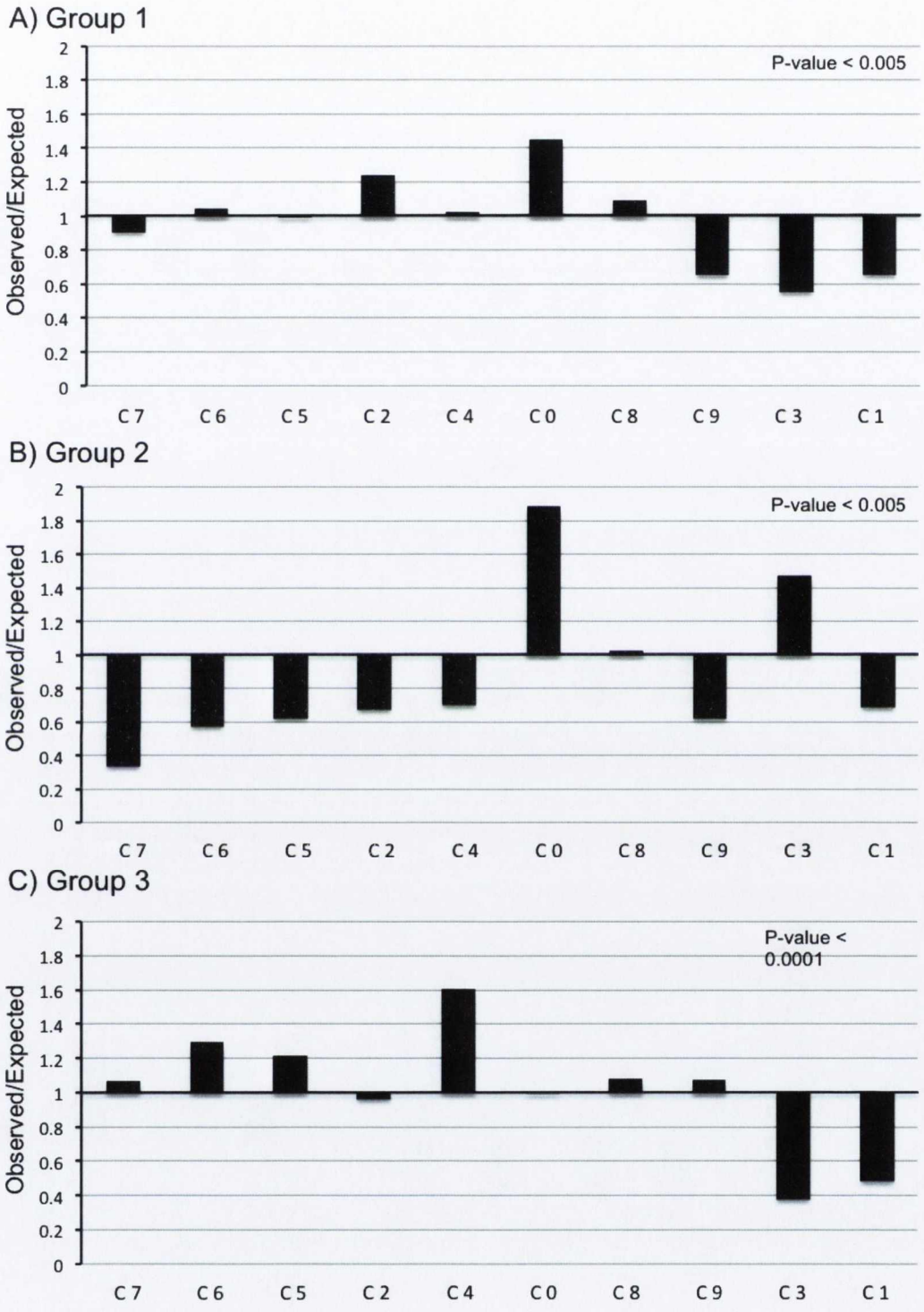
3.2.5 Enrichment analyses of genes based on function

In order to determine whether certain functional groups were enriched in our dataset, we first calculated the expected values for each group as in section 3.2.3 (Table 14).

Table 14 Observed / Expected Values per Group

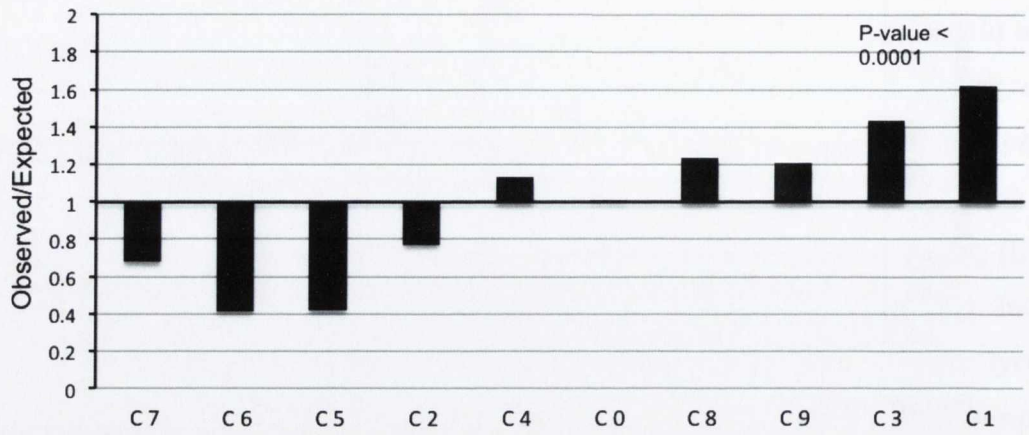
Cluster	Group 1	Group 2	Group 3	Group 4	Group 5	Group 6
Cluster 7	17 / 19	2 / 6	25 / 24	12 / 18	57 / 44	18 / 21
Cluster 6	40 / 38	7 / 12	62 / 48	15 / 36	122 / 91	22 / 42
Cluster 5	15 / 15	3 / 5	23 / 19	6 / 14	48 / 36	11 / 17
Cluster 2	29 / 23	5 / 7	28 / 29	17 / 22	67 / 55	17 / 26
Cluster 4	23 / 22	5 / 7	45 / 28	24 / 21	37 / 53	23 / 25
Cluster 0	80 / 55	33 / 18	68 / 69	52 / 52	88 / 130	63 / 60
Cluster 8	30 / 28	9 / 9	37 / 35	32 / 26	45 / 65	39 / 30
Cluster 9	20 / 31	6 / 10	41 / 39	35 / 29	77 / 72	35 / 34
Cluster 3	20 / 36	17 / 12	17 / 46	49 / 34	87 / 86	63 / 40
Cluster 1	12 / 18	4 / 6	11 / 23	28 / 17	51 / 43	22 / 20

Different trends emerged from the observed/expected ratios (Figure 12 A-F). Chi square statistics on the whole dataset showed deviation from expected by random distribution at p-value < 0.001 (Table 15). Further statistics were done on individual groups to establish which ones were enriched in particular clusters. The Bonferroni correction was taken into account due to multiple testing lowering the threshold to $p \leq 0.008$. All trends observed reached statistical significance at p-value < 0.005 for group 1 and group 2, and p-value < 0.0001 for group 3 to group 6. Like with our protein localization data, it is noteworthy that the five groups correlate nicely with real biological timelines [regional specification/patterning (E11.5), axon pathfinding (E13.5, E15.5 and E18.5), synaptogenesis (P4 and P14) and cortical plasticity (P28)]. Indeed, group 3 is enriched at E11.5 to E13.5 and includes genes expressing receptor tyrosine kinases and their ligands, and genes involved in patterning. Group 5, which is composed of genes expressing molecules involved with chromatin and transcription factor activity, is also enriched at early time-points (E11.5 to E15.5). Group 1 (axon guidance pathway and cell adhesion) is enriched from E15.5 to P4. Groups 2 (synapse) and 4 (neurotransmission pathway) are enriched from P4 to P28, with group 2 being mainly enriched at P14 – the time when eye opening occurs in mouse pups creating an influx of activity-dependent signals and mechanism refinements. Taken together, our protein localization and functional enrichment analyses validate our clustering analyses. What's more, founded extrapolations can be made for genes that little is known of. However, before doing the latter, we looked into individual genes that have previously been characterized.

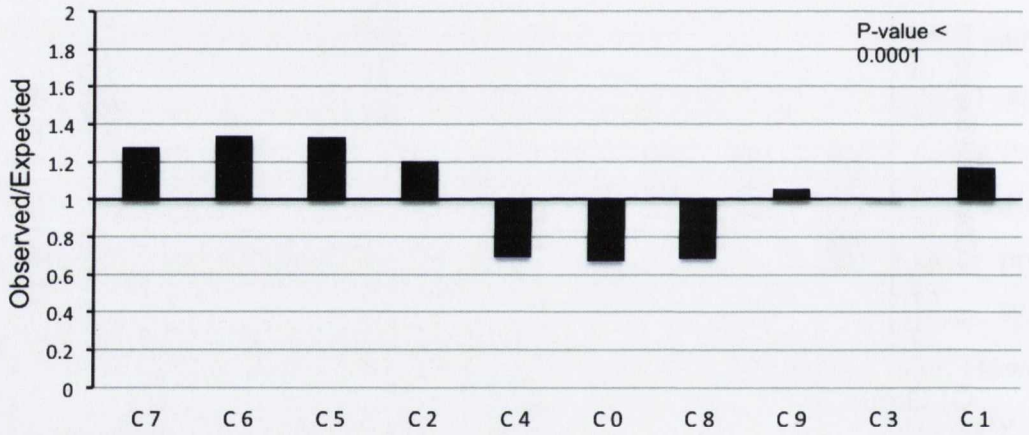


(Legend on p.55)

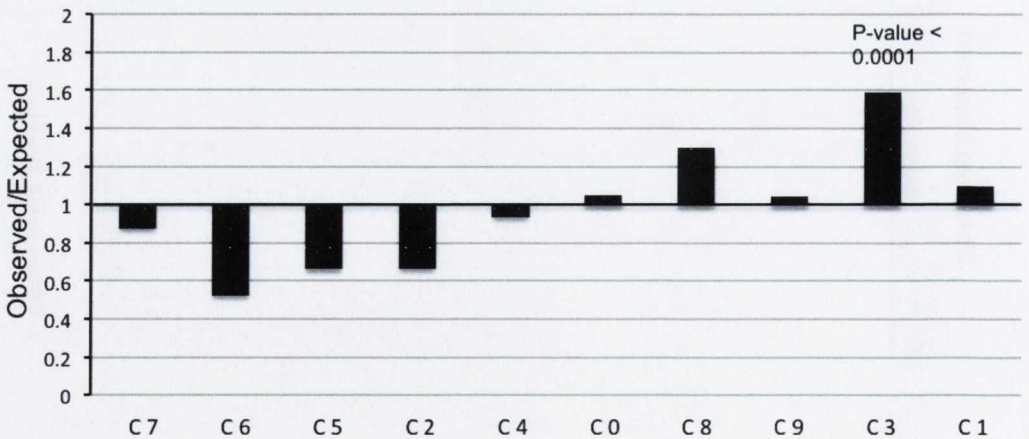
D) Group 4



E) Group 5



F) Group 6



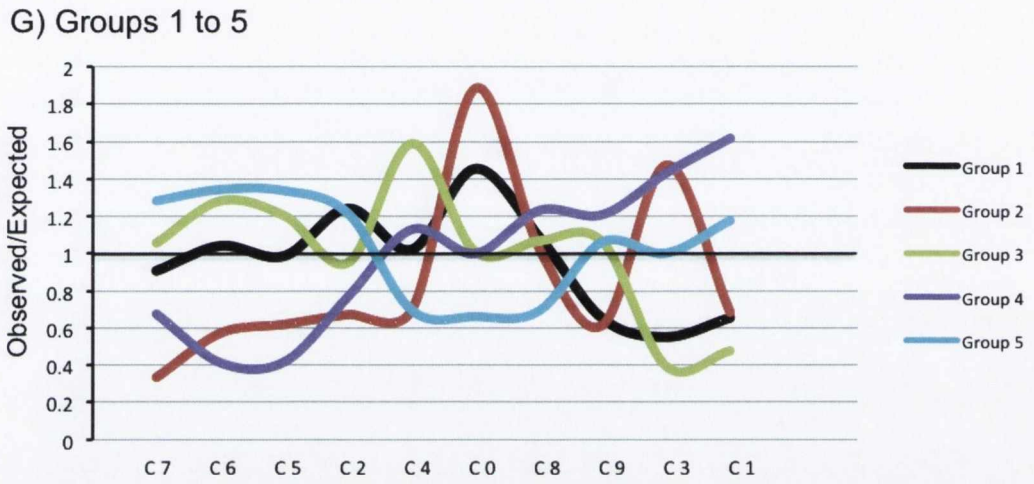


Figure 12. Observed Over Expected Distribution of Groups per Cluster

Observed/expected values show significant enrichment in all groups: Group 1 - axon guidance pathway and cell adhesion (A); Group 2 – synapse (B); Group 3 - receptor tyrosine kinases and their ligands, and patterning (C); Group 4 - neurotransmission pathway (GPCRs, ion channels, gap junctions; D); Group 5 - chromatin and transcription factor activity (E); and, Group 6 - other (cytoskeleton, extracellular matrix, myelin, metabolic enzymes and signal transduction) and unannotated (F). A value of 1 indicates observed data matches expected values, whereas a value below or above 1 indicates decreased or increased counts compared to expected values, respectively. Clusters 0-9 are organized chronologically. C, cluster. P-values from chi square analyses are shown in upper right corner of each graph. Distributions of Groups 1-5 are shown for better comparison in G.

Table 15 Enrichment Analyses per Group

	Chi Square	Degrees of Freedom	P-Value	Bonferroni Correction	Conclusion
All	205.292	45	< 0.001	No	Enrichment
Group 1	26.361	9	< 0.005	Yes	Enrichment
Group 2	25.343	9	< 0.005	Yes	Enrichment
Group 3	39.253	9	< 0.0001	Yes	Enrichment
Group 4	36.309	9	< 0.0001	Yes	Enrichment
Group 5	47.280	9	< 0.0001	Yes	Enrichment
Group 6	30.745	9	< 0.0001	Yes	Enrichment

Degrees of freedom: All, (columns # - 1) (row # - 1) = (6 - 1) (10 - 1) = 45; Per Group, n - 1 = 10 - 1 = 9. Bonferroni correction: $p \leq \alpha$ / # tests = 0.05 / 6 = 0.008

3.2.6 Genes involved in thalamic development

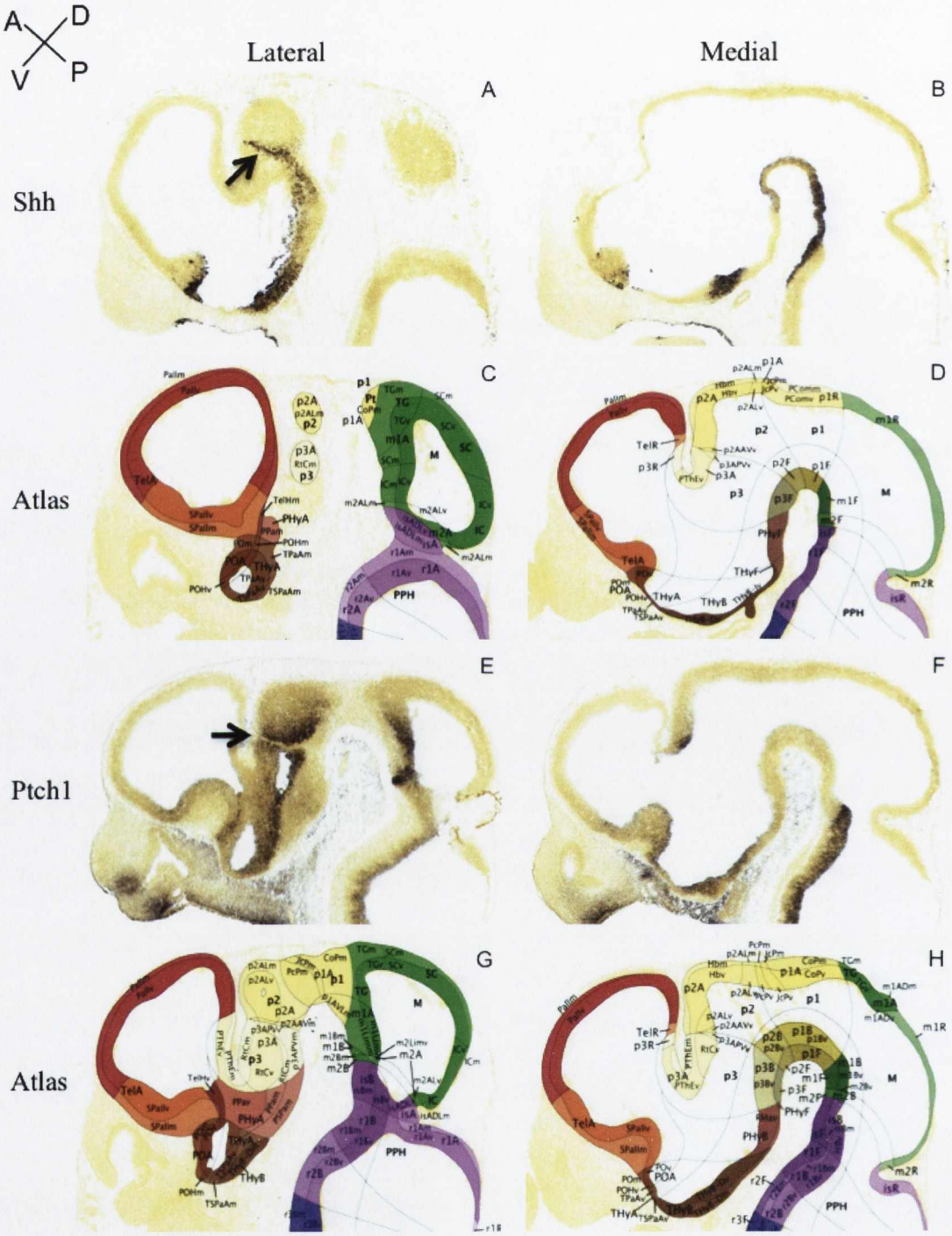
It is difficult to dissociate genes involved in thalamic regional specification from those involved in connectivity from the thalamus to the cortex as processes overlap and develop in parallel. However, we considered E11.5 as the time-point mainly relevant to regional specification and patterning. A few transcription factors and morphogens implicated in these developmental stages have been discussed in previous sections. We used these as validation of our system on an individual basis. First, we introduced the roles of Shh, Wnts and FGF8 in the patterning of the thalamus. As expected, Shh, a few Wnts, FGF8 and some of their binding partners are clustered together (Table 16). Of interest for early regionalization are clusters 6 and 7, which show peak expression at E11.5 (cluster 6 differs from cluster 7 by a second peak of expression at P14). Shh and receptor Ptch1 were found in cluster 7 and cluster 6, respectively. At E11.5, Shh was expressed in the ZLI (Figure 13A) and the floor plate of the thalamus (Figure 13B), while Ptch1 was expressed on both sides of the ZLI (Figure 13E). In regards to the thalamus, the highest levels of Ptch1 expression were caudoventral. In addition, Wnt3a, Wnt5a, Wnt5b, Wnt6 and Wnt8b had peak expression at E11.5. At this time-point, Wnt3a was weakly expressed laterally in the ventral part of the thalamus (Figure 14A) and much strongly expressed medially in the roof plate of the thalamus (Figure 14B). Wnt5a was mainly expressed in the floor plate of the thalamus (Figure 14F). Wnt8b was

strongly detected in the eminentia thalami, which is located ventral of prosomere 3 and is not technically part of the thalamus (Figure 14 I to J). Wnt5b and Wnt6 expression levels were almost undetectable throughout the thalamus. Wnt receptors Celsr1, Fzd10 and Ryk, and secreted binding partners Rspo1, Rspo2 and Rspo3 were found in cluster 7. Celsr1 was weakly expressed throughout the thalamus (Figure 15 A and B) compared to Ryk (Figure 15 I to J). Fzd10 was strongly expressed throughout the thalamus, except medially in the alar plate and the floor plate of the thalamus (Figure 15 E and F). As for Rspo1-3, they were mainly expressed in the roof plate of the thalamus (Figure 16). Finally, FGF3, FGF7, FGF8. FGF9, FGF15 and FGF16 were found to be mostly expressed at E11.5. FGF8 was specifically expressed in the roof plate of the thalamus (Figure 17B), whereas FGF9 was expressed ubiquitously in the thalamus (Figure 17 E and F). Interestingly, FGF9 has not previously been directly linked to thalamic development. High levels of FGF15 were detected laterally in the rostral part of the thalamus avoiding the ZLI (Figure 17I) as well as medially in the roof plate of the thalamus (Figure 17J). FGF3, FGF7 and FGF16 had almost undetectable levels of expression throughout the thalamus. None of their receptors clustered with these FGFs. However, these clustering results are indicative of highest expression levels compared to average, not of absolute expression levels. Their targets might also be outside the thalamus.

Table 16 Clustering Results for Shh, Wnts and FGFs, and their Binding Partners at K-mean 10

Gene	Cluster	Embryonic Peak	Embryonic Time-Point	Localization	Group
Shh	C7	Yes	E11.5	Secreted	1
Boc	C4	Yes	E18.5	Single-Pass	1
Cdon	C5	Yes	E13.5	Single-Pass	1
Gas1	C8	No		Anchored	1
Ptch1	C6	Yes	E11.5	Multi-Pass	3
Smo	C4	Yes	E18.5	Multi-Pass	3
Wnt1	C0	No		Secreted	3
Wnt2	C8	No		Secreted	3
Wnt2b	C5	Yes	E13.5	Secreted	3
Wnt3	C9	No		Secreted	1
Wnt3a	C7	Yes	E11.5	Secreted	1
Wnt4	C9	No		Secreted	3
Wnt5a	C6	Yes	E11.5	Secreted	1
Wnt5b	C6	Yes	E11.5	Secreted	3
Wnt6	C6	Yes	E11.5	Secreted	3
Wnt7a	C5	Yes	E13.5	Secreted	3
Wnt7b	C8	No		Secreted	3
Wnt8a	C0	No		Secreted	3
Wnt8b	C7	Yes	E11.5	Secreted	3
Wnt9a	C2	Yes	E15.5	Secreted	3
Wnt9b	C3	No		Secreted	3
Wnt10a	C9	No		Secreted	3
Wnt10b	C0	No		Secreted	3
Wnt11	C4	Yes	E18.5	Secreted	3
Wnt16	C0	No		Secreted	3
Celsr1	C7	Yes	E11.5	Multi-Pass	1
Celsr2	C1	No		Multi-Pass	1
Celsr3	C0	No		Multi-Pass	1
Fzd1	C9	No		Multi-Pass	3
Fzd2	C4	Yes	E18.5	Multi-Pass	3
Fzd3	C5	Yes	E13.5	Multi-Pass	3
Fzd4	C3	No		Multi-Pass	3
Fzd5	C0	No		Multi-Pass	3
Fzd6	C1	No		Multi-Pass	3
Fzd7	C0	No		Multi-Pass	3
Fzd8	C2	Yes	E15.5	Multi-Pass	3
Fzd9	C8	No		Multi-Pass	3
Fzd10	C7	Yes	E11.5	Multi-Pass	3
Lrp1	C0	No		Single-Pass	2
Lrp5	C5	Yes	E13.5	Single-Pass	2
Lrp6	C5	Yes	E13.5	Single-Pass	2

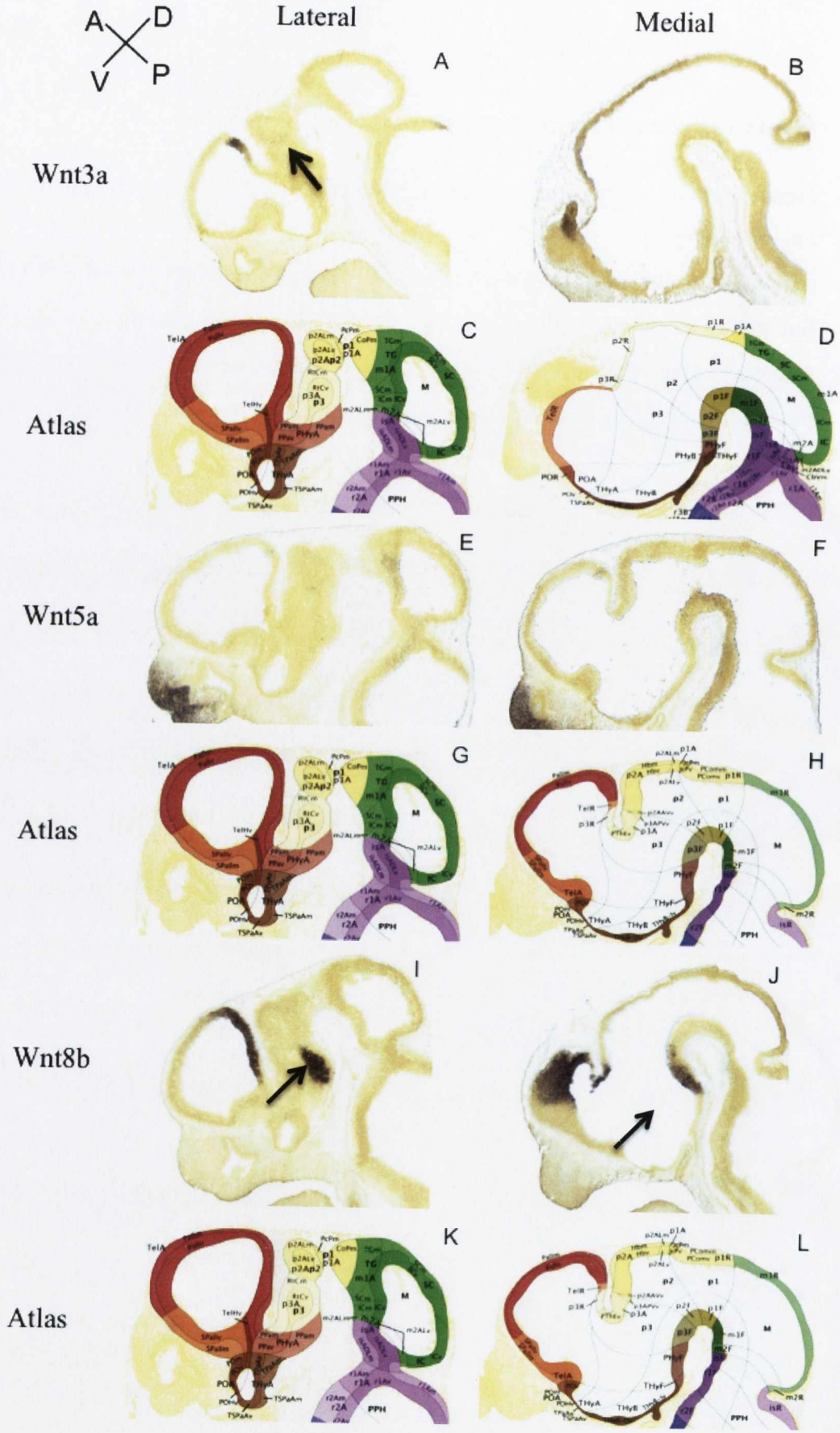
Gene	Cluster	Embryonic Peak	Embryonic Time-Point	Localization	Group
Lrp8	C0	No		Single-Pass	2
ROR1	C2	Yes	E15.5	Single-Pass	3
ROR2	C2	Yes	E15.5	Single-Pass	3
Rspo1	C7	Yes	E11.5	Secreted	3
Rspo2	C7	Yes	E11.5	Secreted	3
Rspo3	C7	Yes	E11.5	Secreted	3
Rspo4	C4	Yes	E18.5	Secreted	3
Ryk	C7	Yes	E11.5	Single-Pass	1
Sfrp1	C3	No		Secreted	1
Sfrp2	C6	Yes	E11.5	Secreted	3
Sfrp4	C4	Yes	E18.5	Secreted	3
Sfrp5	C9	No		Secreted	3
FGF1	C0	No		Secreted	3
FGF2	C4	Yes	E18.5	Secreted	3
FGF3	C6	Yes	E11.5	Secreted	3
FGF4	C1	No		Secreted	3
FGF5	C4	Yes	E18.5	Secreted	3
FGF6	C4	Yes	E18.5	Secreted	3
FGF7	C6	Yes	E11.5	Secreted	3
FGF8	C7	Yes	E11.5	Secreted	3
FGF9	C6	Yes	E11.5	Secreted	3
FGF10	C9	No		Secreted	3
FGF12	C3	No		Secreted	3
FGF14	C9	No		Secreted	3
FGF15	C7	Yes	E11.5	Secreted	3
FGF16	C6	Yes	E11.5	Secreted	3
FGF17	C4	Yes	E18.5	Secreted	3
FGF18	C8	No		Secreted	3
FGF20	C3	No		Secreted	3
FGF23	C0	No		Secreted	3
FGFBP1	C4	Yes	E18.5	Secreted	3
FGFR1	C0	No		Single-Pass	3
FGFR2	C1	No		Single-Pass	3
FGFR3	C9	No		Single-Pass	3
FGFR4	C5	Yes	E13.5	Single-Pass	3
FGFRL1	C9	No		Single-Pass	3



(Legend overleaf)

Figure 13. Shh and Ptch1 Expression at E11.5

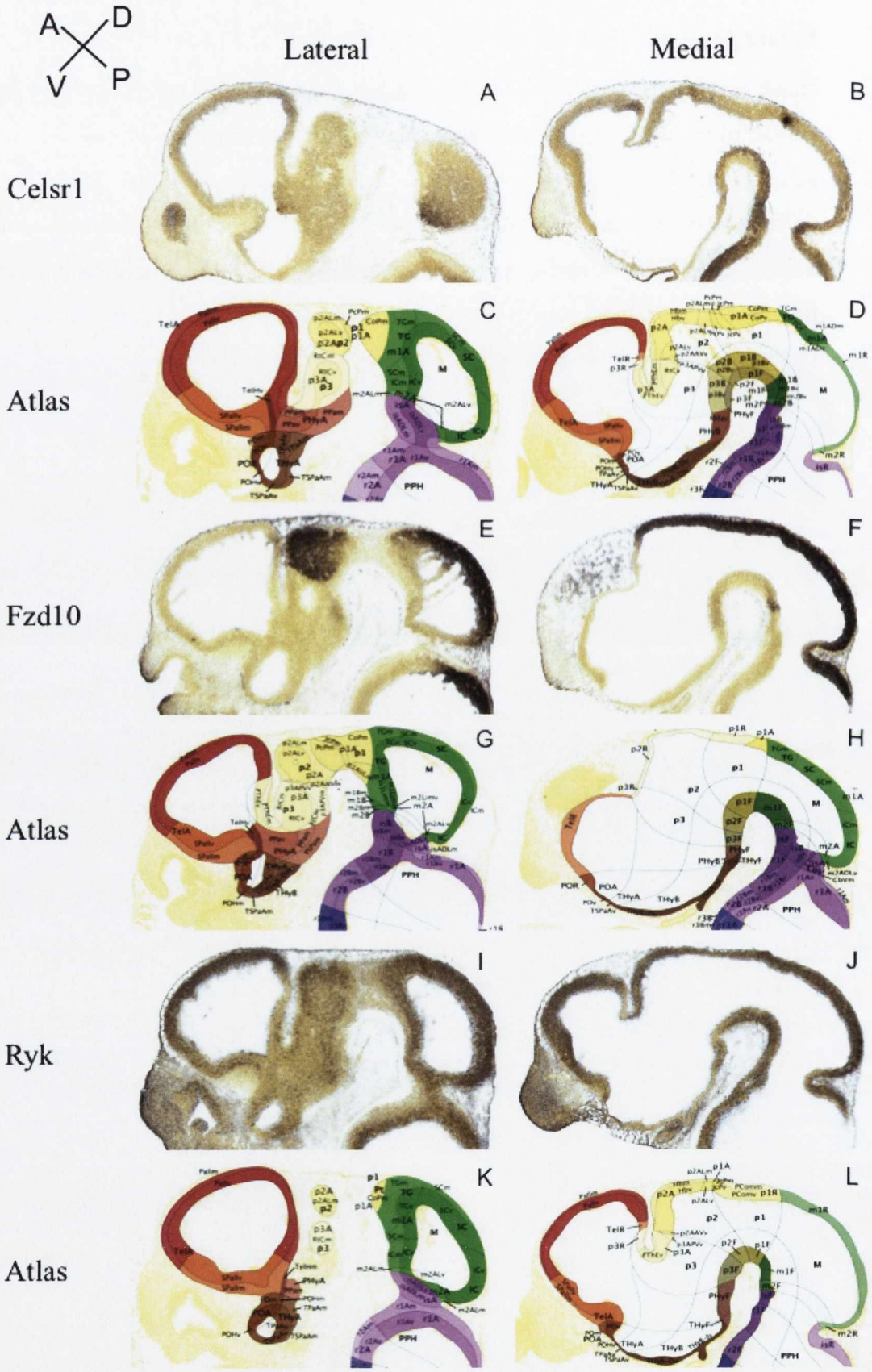
Head sagittal sections of *in situ* hybridization at E11.5 revealed strong thalamic expression of Shh in the ZLI (A, arrow) and the floor plate (B). Ptch1 was strongly expressed caudoventrally in the lateral part of the thalamus avoiding the ZLI (E, arrow), but not detected medially (F). C, D, G and H are corresponding images from the reference atlas provided for A, B, E and F, respectively. A, anterior/rostral; P, posterior/caudal; V, ventral; D, dorsal. Images taken from the developing Allen Brain Atlas.



(Legend overleaf)

Figure 14. Wnt3a, Wnt5a and Wnt8b Expression at E11.5

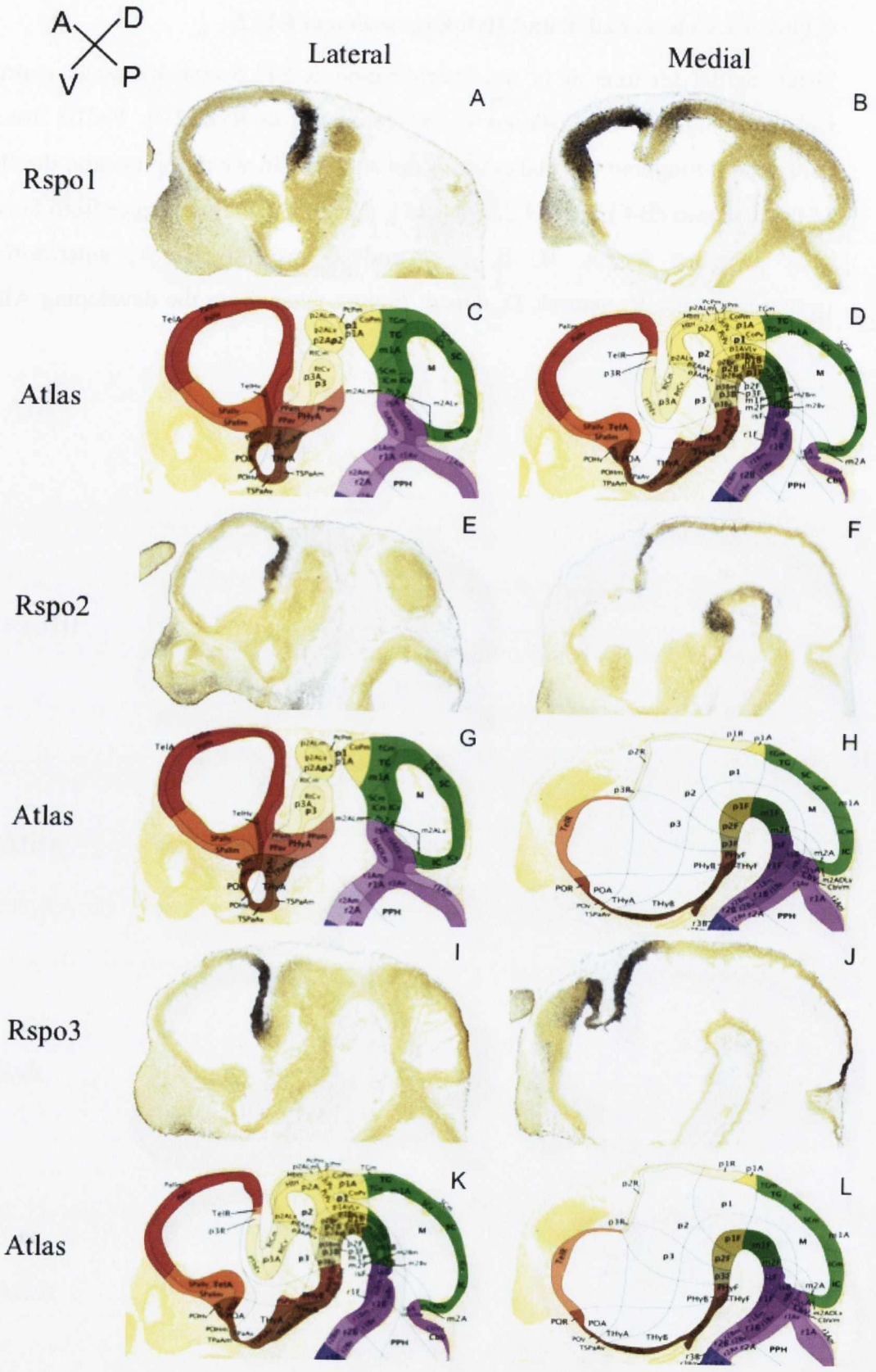
Head sagittal sections of *in situ* hybridization at E11.5 revealed weak expression of Wnt3a in the ventral part of the thalamus (A, arrow) and strong expression in the roof plate of the thalamus (B). Wnt5a was mainly expressed in the floor plate of the thalamus (E-F), while Wnt8b was strongly detected in the eminentia thalami (I-J, arrow). C, D, G, H, K and L are corresponding images from the reference atlas provided for A, B, E, F, I and J, respectively. A, anterior/rostral; P, posterior/caudal; V, ventral; D, dorsal. Images taken from the developing Allen Brain Atlas.



(Legend overleaf)

Figure 15. Celsr1, Fzd10 and Ryk Expression at E11.5

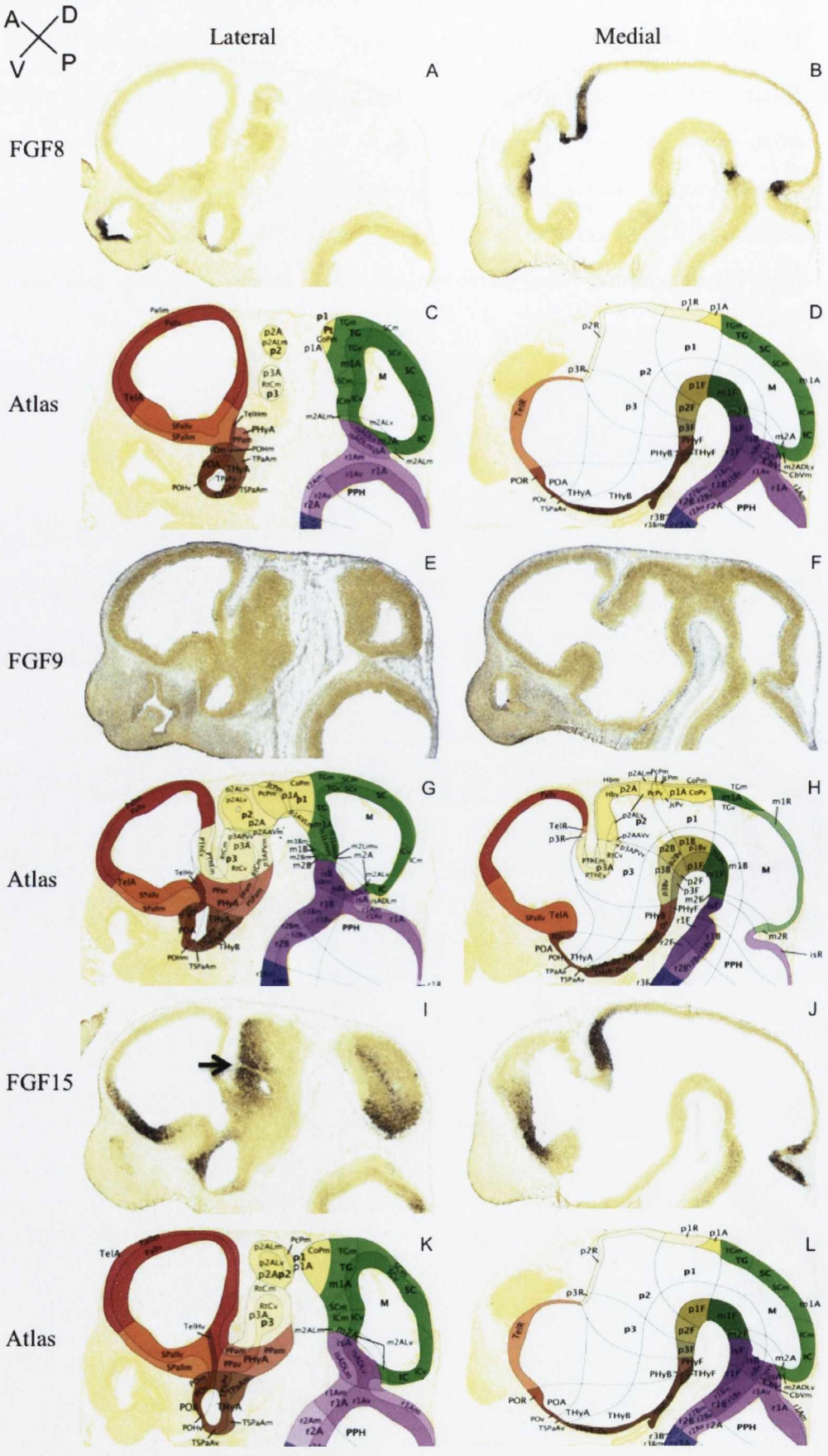
Head sagittal sections of *in situ* hybridization at E11.5 revealed weak expression of Celsr1 throughout the thalamus (A-B) compared to Ryk (I-J). Fzd10 was strongly expressed throughout the thalamus except medially in the alar plate and the floor plate of the thalamus (E-F). C, D, G, H, K and L are corresponding images from the reference atlas provided for A, B, E, F, I and J, respectively. A, anterior/rostral; P, posterior/caudal; V, ventral; D, dorsal. Images taken from the developing Allen Brain Atlas.



(Legend overleaf)

Figure 16. Rspo1/2/3 Expression at E11.5

Head sagittal sections of *in situ* hybridization at E11.5 revealed expression of Rspo1/2/3 in the roof plate of the thalamus (A, B, E, F, I and J). C, D, G, H, K and L are corresponding images from the reference atlas provided for A, B, E, F, I and J, respectively. A, anterior/rostral; P, posterior/caudal; V, ventral; D, dorsal. Images taken from the developing Allen Brain Atlas.



(Legend overleaf)

Figure 17. FGF8/9/15 Expression at E11.5

Head sagittal sections of *in situ* hybridization at E11.5 revealed FGF8 expression only in the roof plate of the thalamus (A-B), whereas FGF9 expression was ubiquitous in the thalamus (E-F). High levels of FGF15 were detected in the rostral part of the thalamus avoiding the ZLI (I, arrow) as well as in the roof plate of the thalamus (J). C, D, G, H, K and L are corresponding images from the reference atlas provided for A, B, E, F, I and J, respectively. A, anterior/rostral; P, posterior/caudal; V, ventral; D, dorsal. Images taken from the developing Allen Brain Atlas.

Moreover, the thalamus anlage is Irx-positive (see section 1.1.2 for details), and Irx1, Irx2 and Irx5 were found in clusters peaking at E11.5, E13.5 and E11.5, respectively (however, Irx3/4/6 had peak expression postnatally according to our dataset; Digital Appendix Figure 10). Fez, which is present in the prethalamus anlage but not the thalamus anlage, did not have high levels of thalamic expression embryonically finding itself in cluster 0 (showing highest expression at P14). Shh induced transcription factor Ascl1 was found in cluster 7, and Neurog1/2 were found in clusters peaking at E13.5 and E11.5, respectively. Further thalamic specification occurs through the induction of a range of transcription factors. These clustered as follows: Dbx1 and Olig3 (and Tal2) were found in cluster 7 indicating peak expression levels at E11.5; Gbx2, Lhx2, Tal1 and Sox14 were found in cluster 5 with highest recorded expression levels at E13.5; Sox2 was found in cluster 2 with peaking expression at E15.5; Gad1 and Olig1 were found in cluster 0 with highest levels of expression postnatally (although the pattern for this cluster shows increased expression levels above basal levels from E18.5 on); Nkx2.2 and Olig2 were found in cluster 8 indicating peak expression levels at P4; and, RORα was found in cluster 3 with highest expression levels at P14. The other thalamic markers at E18.5 Calb2 and Cdh6 were found in cluster 0 with a pattern of expression increasing from E18.5 onward reaching the highest levels at P14. In addition, the following transcription factors were found in either cluster 6 or 7 both having strongest expression levels at E11.5: Emx1/2, Gli1/2/3, Id1/2/3, Otx2 and Pax3/4/6 (although Pax4 levels were very low and undetectable by eye). Given that axonal projections start their journey towards the cortex at E13, we further focused our attention on clusters with peaks of gene expression starting at E13.5.

3.2.7 Extracellular axon guidance molecules

Our developmental dataset included three time-points particularly relevant to axon pathfinding: E13.5, E15.5 and E18.5. Genes with highest expression levels at E13.5 were grouped in cluster 5, those at E15.5 in cluster 2 and those at E18.5 in cluster 4. These three clusters totaled 426 genes. To focus on cell-cell communication, we refined our set of genes to genes that express proteins found in the extracellular compartment (Table 17). This brought our gene count down to 176. We then performed two types of curations on those genes. First, we carried out manual validation of the expression data at the corresponding time-points from the devABA. Up to this point, we had been quite inclusive in our cut-offs; however, we switched gears to not allow false

positives on an individual basis. We discarded genes that were uniformly expressed throughout the thalamus, genes that showed faint or no visible expression and genes for which there were artifacts on the slides that might have skewed the expression values (bubbles, specks, bad tissue). Our final set included 72 genes of interest (Table 18). Then, we did extensive literature searches in peer-reviewed journals to establish whether or not a gene had previously been linked to thalamocortical development and/or axon guidance (Table 19). This allowed gathering further information complementing the 6 groups we had established earlier. Twenty-nine genes had previously been implicated in thalamocortical development and 19 more had been characterized in the context of axon guidance, though not in the thalamus nor the thalamocortical path. The last 24 genes had not been previously linked to either. We selected a few genes as representatives of these three categories: Cntn2, Robo2 and Sema6a in the first category (Figure 18); Cadm1 and Ntng2 (Figure 19), and Cbln4 and Kit (Figure 20) in the second category; and, Dlk1 (Figure 21) and Bmp3, Cbln2 and Cdh11 (Figure 22) in the last category. All genes showed differential expression patterns within the thalamus (as mentioned above in our screening methods), which implicate interesting dynamics. Furthermore, and most importantly, the second and third categories shed light on novel candidates involved in thalamic axon pathfinding.

Table 17 Genes of Interest in Clusters Relevant to Axon Pathfinding

Cluster	Expression Peak	Total # Genes	# Genes Expressing Extracellular Proteins
Cluster 5	E13.5	106	31
Cluster 2	E15.5	163	63
Cluster 4	E18.5	157	82

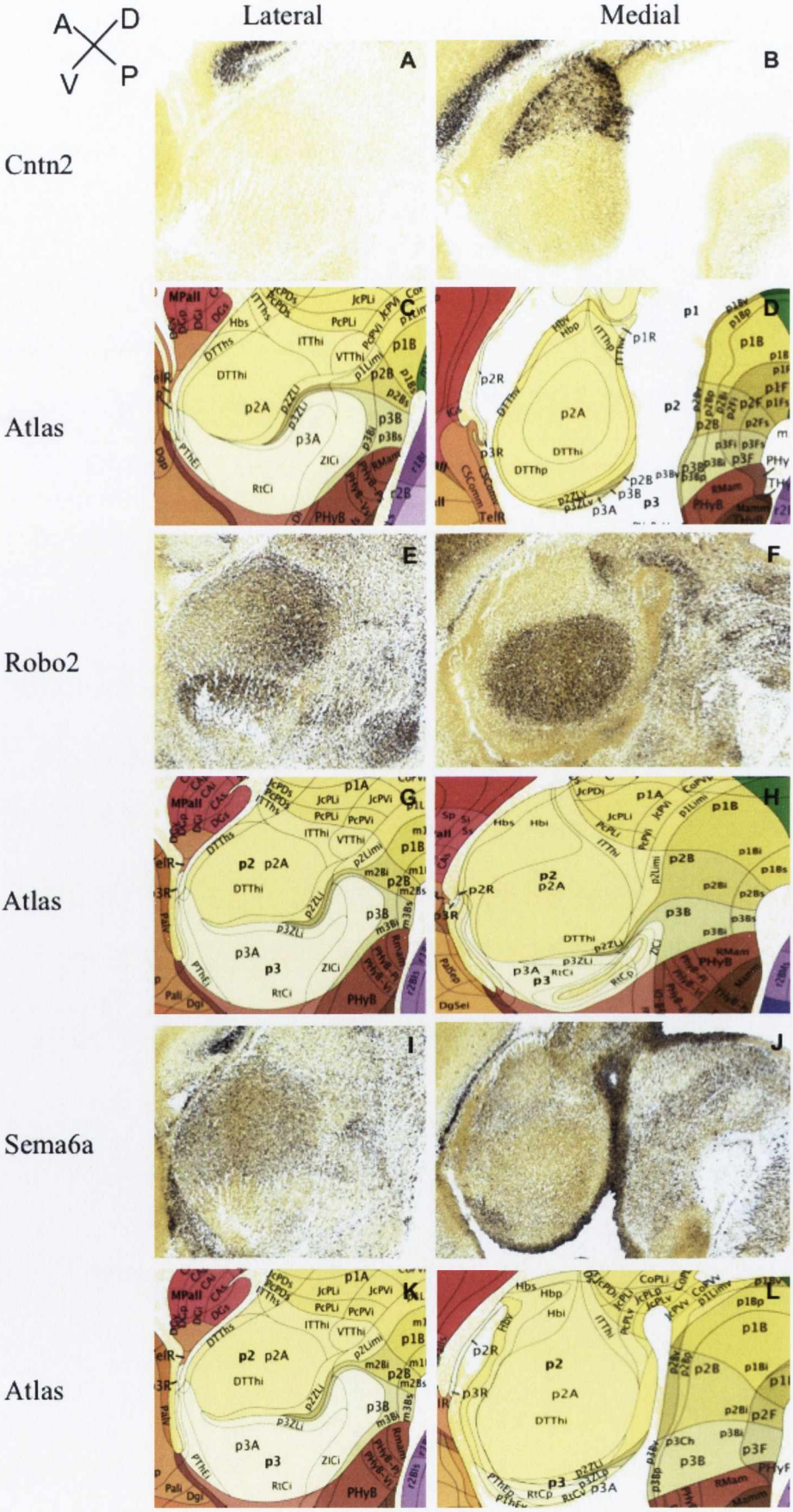
Table 18 Genes of Interest

Gene	Cluster	Embryonic Time-Point	Localization	Group
2610109H07Rik	C5	E13.5	Secreted	6
A2m	C4	E18.5	Secreted	6
Acvr2a	C4	E18.5	Single-Pass	3
Bmp3	C4	E18.5	Secreted	3
Cacna1h	C4	E18.5	Multi-Pass	4
Cadm1	C2	E15.5	Single-Pass	1
Cbln2	C4	E18.5	Secreted	2
Cbln4	C4	E18.5	Secreted	2
Cd24a	C2	E15.5	Anchored	1
Cdh11	C4	E18.5	Single-Pass	1
Cdh23	C4	E18.5	Single-Pass	1
Chl1	C2	E15.5	Single-Pass	1
Cnr1	C2	E15.5	Multi-Pass	4
Cntn2	C2	E15.5	Anchored	1
Col18a1	C5	E13.5	Secreted	6
Col2a1	C5	E13.5	Secreted	6
Col4a5	C5	E13.5	Secreted	6
Dcc	C2	E15.5	Single-Pass	1
Dlk1	C2	E15.5	Single-Pass	3
Efna3	C4	E18.5	Anchored	1
Efnb2	C4	E18.5	Single-Pass	1
Egfr	C4	E18.5	Single-Pass	3
Ephb1	C2	E15.5	Single-Pass	1
Erbb2	C2	E15.5	Single-Pass	3
Erbb4	C4	E18.5	Single-Pass	3
Fxyd6	C4	E18.5	Single-Pass	4
Fzd3	C5	E13.5	Multi-Pass	3
Gdf10	C2	E15.5	Secreted	3
Gpr161	C2	E15.5	Multi-Pass	4
Gpr98	C2	E15.5	Multi-Pass	1
Grik3	C2	E15.5	Multi-Pass	4
Grin2d	C4	E18.5	Multi-Pass	2
Grm3	C4	E18.5	Multi-Pass	4
Grm5	C4	E18.5	Multi-Pass	4
Itgav	C4	E18.5	Single-Pass	1
Kcng4	C4	E18.5	Multi-Pass	4
Kit	C4	E18.5	Single-Pass	3
L1cam	C2	E15.5	Single-Pass	1
Lefty2	C4	E18.5	Secreted	5
Lmtk3	C2	E15.5	Single-Pass	3
Lrp6	C5	E13.5	Single-Pass	2
Mdga1	C4	E18.5	Secreted	1
Mfap4	C5	E13.5	Secreted	3
Mfge8	C4	E18.5	Secreted	1

Gene	Cluster	Embryonic Time-Point	Localization	Group
Ngfr	C2	E15.5	Single-Pass	1
Notch1	C2	E15.5	Single-Pass	1
Notch3	C2	E15.5	Single-Pass	3
Npy	C4	E18.5	Secreted	4
Nrg1	C4	E18.5	Single-Pass	1
Nrp1	C4	E18.5	Single-Pass	1
Ntn1	C4	E18.5	Secreted	1
Ntng2	C2	E15.5	Anchored	1
Nts	C4	E18.5	Secreted	4
Odz3	C2	E15.5	Single-Pass	1
Pcdh18	C5	E13.5	Single-Pass	1
Plxna2	C4	E18.5	Single-Pass	1
Plxna4	C4	E18.5	Single-Pass	1
Plxnb1	C2	E15.5	Single-Pass	1
Reln	C4	E18.5	Secreted	1
Robo1	C2	E15.5	Single-Pass	1
Robo2	C2	E15.5	Single-Pass	1
Sema6a	C2	E15.5	Single-Pass	1
Slc18a2	C2	E15.5	Multi-Pass	4
Slc6a3	C4	E18.5	Multi-Pass	4
Tacr3	C4	E18.5	Multi-Pass	4
Tgfbr1	C5	E13.5	Single-Pass	3
Thbs3	C4	E18.5	Secreted	6
Tnc	C4	E18.5	Secreted	1
Vegfa	C4	E18.5	Secreted	3
Wnt7a	C5	E13.5	Secreted	3
Wnt9a	C2	E15.5	Secreted	3
Wnt11	C4	E18.5	Secreted	3

Table 19 Genes Previously Implicated in Thalamocortical Development or Axon Guidance or Other

		Previously Implicated in:		
Cluster	**Expression Peak**	**Thalamocortical Development**	**Axon Guidance**	**Other**
Cluster 5	E13.5	Lrp6	2610109H07Rik	Col2a1
		Fzd3	Col18a1	Mfap4
		Wnt7a	Col4a5	Pcdh18
			Tgfbr1	
Cluster 2	E15.5	Chl1	Cadm1	Cd24a
		Cnr1	Gpr98	Dlk1
		Cntn2	Notch1	Gdf10
		Dcc	Ntng2	Gpr161
		Ephb1	Plxnb1	Grik3
		Erbb2		Lmtk3
		L1cam		Notch3
		Ngfr		Wnt9a
		Odz3		
		Robo1		
		Robo2		
		Sema6a		
		Slc18a2		
Cluster 4	E18.5	Cacna1h	Cbln4	A2m
		Efna3	Efnb2	Acvr2a
		Egfr	Itgav	Bmp3
		Erbb4	Kit	Cbln2
		Grm3	Mdga1	Cdh11
		Grm5	Nts	Cdh23
		Npy	Plxna2	Fxyd6
		Nrg1	Plxna4	Grind2
		Nrp1	Vegfa	Kcgn4
		Ntn1	Wnt11	Lefty2
		Reln		Mfge8
		Slc6a3		Tacr3
		Tnc		Thbs3



(Legend overleaf)

Figure 18. Cntn2, Robo2 and Sema6a Expression at E15.5

Thalamic sagittal sections of *in situ* hybridization at E15.5 revealed differential patterns of expression of Cntn2 (A-B), Robo2 (E-F) and Sema6a (I-J). A, C, E, G, I and K are more lateral compared to B, D, F, H, J and L, respectively. C, D, G, H, K and L are corresponding images from the reference atlas provided for A, B, E, F, I and J, respectively. A, anterior/rostral; P, posterior/caudal; V, ventral; D, dorsal. Images taken from the developing Allen Brain Atlas.

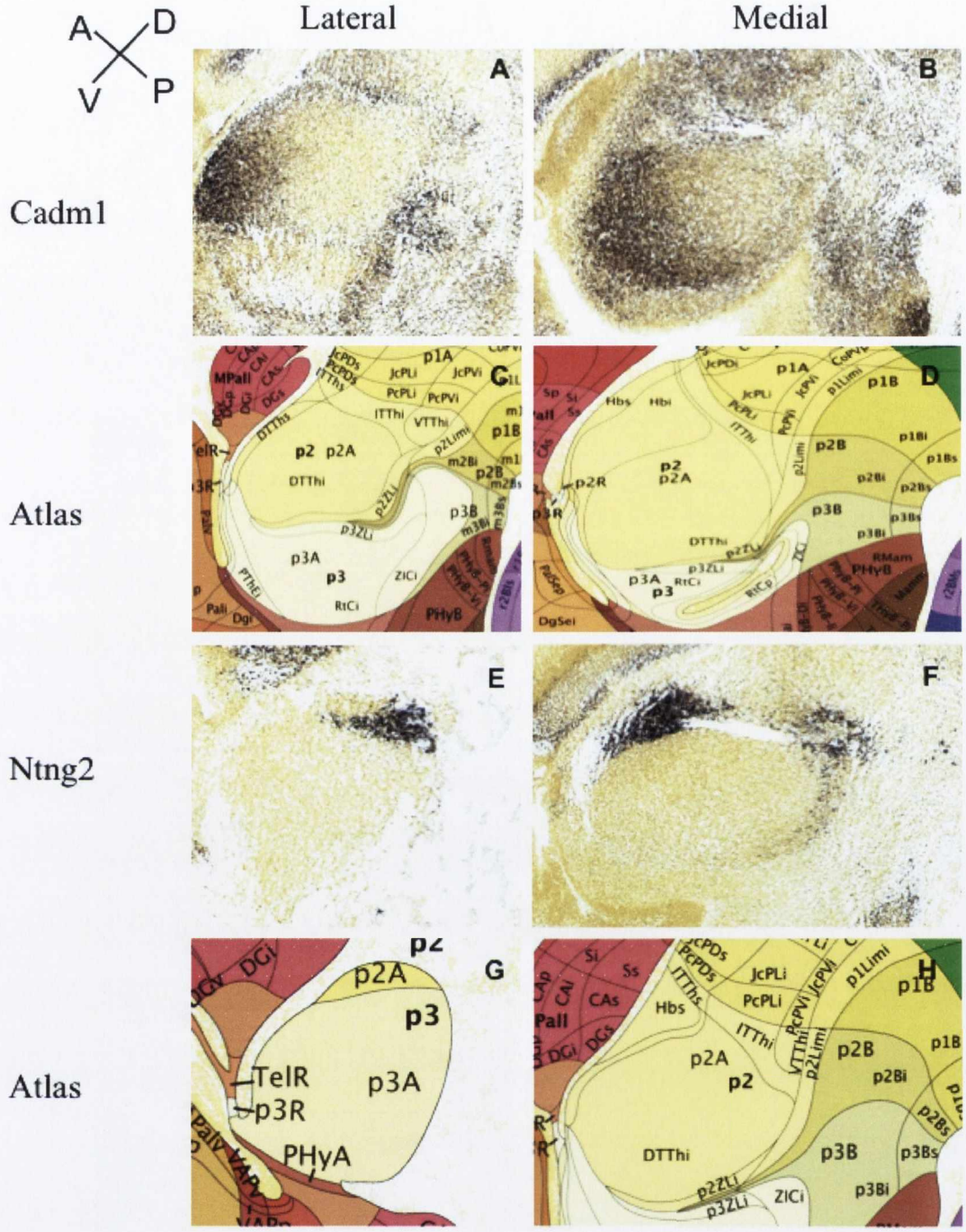
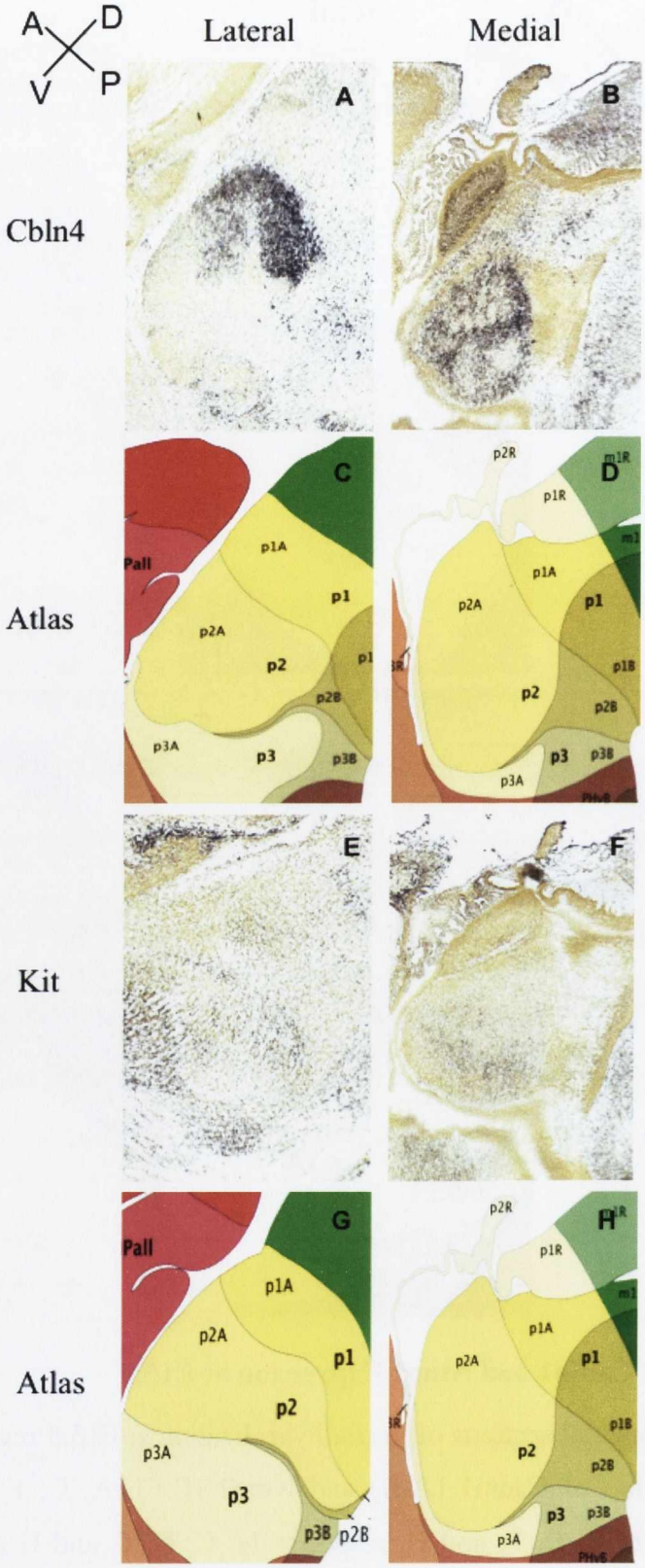


Figure 19. Cadm1 and Ntng2 Expression at E15.5

Thalamic sagittal sections of *in situ* hybridization at E15.5 revealed differential patterns of expression of Cadm1 (A-B) and Ntng2 (E-F). A, C, E, and G are more lateral compared to B, D, F, and H, respectively. C, D, G and H are corresponding images from the reference atlas provided for A, B, E and F, respectively. A, anterior/rostral; P, posterior/caudal; V, ventral; D, dorsal. Images taken from the developing Allen Brain Atlas.



(Legend overleaf)

Figure 20. Cbln4 and Kit Expression at E18.5

Thalamic sagittal sections of *in situ* hybridization at E18.5 revealed differential patterns of expression of Cbln4 (A-B) and Kit (E-F). A, C, E, and G are more lateral compared to B, D, F, and H, respectively. C, D, G and H are corresponding images from the reference atlas provided for A, B, E and F, respectively. A, anterior/rostral; P, posterior/caudal; V, ventral; D, dorsal. Images taken from the developing Allen Brain Atlas.

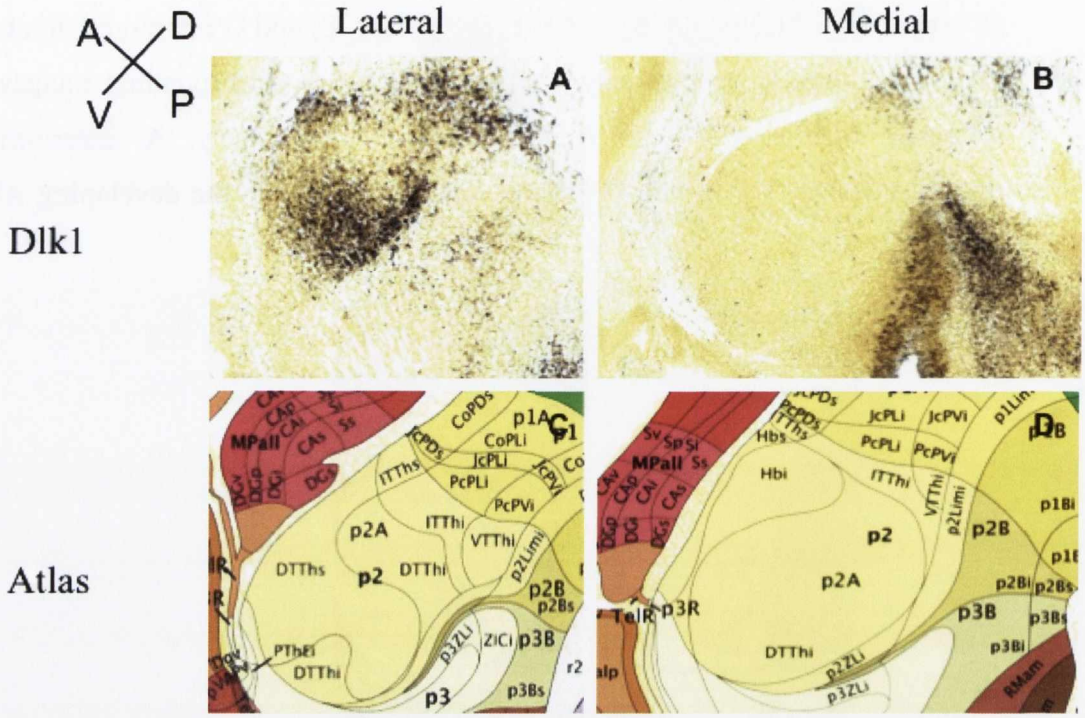
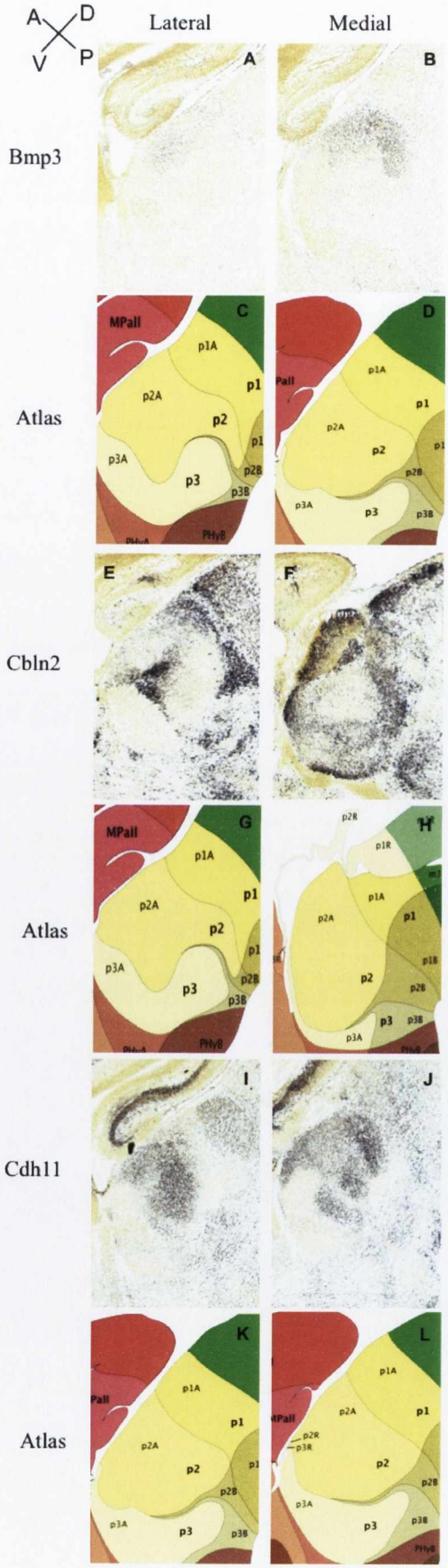


Figure 21. Dlk1 Expression at E15.5

Thalamic sagittal sections of *in situ* hybridization at E15.5 revealed differential patterns of expression of Dlk1 (A-B). A and C are more lateral compared to B and D, respectively. C and D are corresponding images from the reference atlas provided for A and B, respectively. A, anterior/rostral; P, posterior/caudal; V, ventral; D, dorsal. Images taken from the developing Allen Brain Atlas.



(Legend overleaf)

Figure 22. Bmp3, Cbln2 and Cdh11 Expression at E18.5

Thalamic sagittal sections of *in situ* hybridization at E18.5 revealed differential patterns of expression of Bmp3 (A-B), Cbln2 (E-F) and Cdh11 (I-J). A, C, E, G, I and K are more lateral compared to B, D, F, H, J and L, respectively. C, D, G, H, K and L are corresponding images from the reference atlas provided for A, B, E, F, I and J, respectively. A, anterior/rostral; P, posterior/caudal; V, ventral; D, dorsal. Images taken from the developing Allen Brain Atlas.

3.3 Discussion

This study bridges different online sources for the discovery of new functions of developmentally expressed genes in the thalamus. It also sets precedents for the same analyses to be carried out with expression data in different brain regions. We focused on thalamocortical connectivity and have found interesting new candidates potentially involved in this process.

3.3.1 Gene expression data from the Allen Brain Atlas

The Allen Brain Atlas (ABA) provides a survey of gene expression in the brain from mid-gestation through aging in mice, amongst other species. The data can be easily visualized through their portal, and there are now a few datasets available with quantified expression values. We used quantified expression density data of 1996 genes in our dataset. Each gene had an expression density value for the thalamus at each developmental age (E11.5, E13.5, E15.5, E18.5, P4, P14 and P28). This value was an averaged value of all the voxels within the whole area referenced as the thalamus. Already, this could mask strong expression of particular genes in small pockets of the thalamus. Moreover, ISH by nature is a qualitative assay. Therefore, wide ranges of expression values depend on individual genes and individual experiments. However, the quantified data is still indicative. To minimize the between-experiment variations, we opted for normalizing the data. This way, we compared temporal patterns of gene expression as opposed to high or low recorded expression values (which also circumvents having to establish a threshold for gene expression). Albeit not perfect, this dataset has the advantage of being directly linked to ISH images, where data can be validated or discarded on an individual basis. Indeed, we performed extensive manual curation to validate the data that we presented in this study. What's more, there is an ongoing initiative to validate the data with external sources to the ABA such as peer-reviewed literature sources and two online databases [the St. Jude Brain Gene Expression Map (BGEM) project (Magdaleno, Jensen et al. 2006) and the Gene Expression Nervous System Atlas (GENSAT) project (Gong, Zheng et al. 2003);(Henry and Hohmann 2012)].

We linked gene expression data to protein expression sequences that we annotated through various online tools. None of the tools we used are completely accurate with their algorithms, but are quite useful nonetheless to determine the

presence or absence of particular domains or functions. In order to obtain as good annotations as possible, we merged the results from different websites. Once again, manual curation was required. Thus, this study brings a platform to work from. We established subcellular localization of the protein products from our gene set, with an emphasis on the extracellular compartment (secreted, single-pass transmembrane, GPI-anchored and multi-pass transmembrane proteins). In addition, we updated and expanded the annotated gene function from Thompson and colleagues (2014).

Finally, we used two different web tools in order to perform clustering analyses on our normalized expression density dataset (the TM4:MeV program for hierarchical clustering and the clustering module integrated in ArrayPipe for k-means clustering).

3.3.2 Enrichment analyses of localization and function

The nature of the dataset led to hypothesize that particular types of proteins (secreted, single-pass transmembrane and GPI-anchored, multi-pass transmembrane, cytoplasmic and nuclear proteins) and specific protein functions (1- axon guidance pathway and cell adhesion; 2- synapse; 3- receptor tyrosine kinases and their ligands, and patterning; 4- neurotransmission pathway; and 5- chromatin and transcription factor activity) would be enriched at certain time-points (E11.5, E13.5, E15.5, E18.5, P4, P14 and P28). Indeed, our data correlated with biological timelines as proteins localized in the nucleus were found in clusters with highest expression levels at E11.5 and E13.5, which coincided with group 3 and group 5 enriched time-points. This can be translated by a high requirement of transcription factors during patterning and axon guidance early on. Then, single-pass transmembrane and GPI-anchored proteins were enriched in clusters peaking from E15.5 to P4, the same enriched time-points as group 1. Although secreted proteins did not reach statistical significance in the enrichment analyses, it is interesting to note that they clustered above expected values at E11.5, E18.5 and P14. At E11.5, extensive patterning is occuring as discussed with Shh, Wnts and FGFs. In addition, at E18.5 known axon guidance molecules are secreted, such as reelin and tensacin c; and, at P14, secreted proteins are expected to interact with the abundant number of multi-pass transmembrane proteins. Finally, multi-pass transmembrane proteins were enriched in clusters peaking from P4 to P28, which correlates with the enrichment patterns of groups 2 and 4. These proteomics analyses validated our dataset

and our clustering analyses. Hence, founded extrapolations could then be made for genes that had not been studied in the context of the thalamus.

3.3.3 Novel candidates of thalamic axon pathfinding

Ultimately, the goal of this project was to identify novel candidates potentially implicated in axon guidance by cell-cell communication. We confined our search to clusters that had peak expression from E13.5 to E18.5. After further validating our refined dataset, we narrowed our list of genes of interest to 72. Of those, 29 had already been studied in the context of thalamocortical development, 19 had previously been linked to axon guidance outside the thalamus or the thalamocortical path and 24 had not been associated to either. We selected a few genes as representatives of these three categories. As examples of genes implicated in thalamocortical axon pathfinding, expression data of Cntn2, Robo2 and Sema6A was presented. Their roles in thalamocortical connectivity have been described in section 1.1.3.

As for genes known to function as axon guidance molecules outside the thalamus, we focused on Cadm1, Cbln4, Kit and Ntng2. Cadm1, also known as SynCAM (synaptic cell adhesion molecule) or nectin-like molecule-1, was recently found to have a role in sensory axon pathfinding in the spinal cord of chick embryos by regulating axon-axon contacts (Frei, Andermatt et al. 2014). Cbln4, cerebellin-4 (a member of the C1q-tumor necrosis factor family) was previously shown to have interesting patterns of expression in the developing thalamus, with peaking levels at E18.5 (Miura, Iijima et al. 2006). It has also been identified as a ligand of Dcc (Wei, Pattarini et al. 2012, Haddick, Tom et al. 2014). Moreover, wandering axons have been observed in the spinal cord of *Cbln4* mutant mice at E11.5 (Haddick, Tom et al. 2014). Although the transmembrane tyrosine kinase receptor Kit, or proto-oncogene c-kit, has mainly been studied in the context of cancer, some groups have investigated its functions in the developing brain. Kit is expressed by commissural axons in the spinal cord and, through activation by kit ligand (kitl) expressed by midline floor plate cells, regulates midline exit in embryonic mice (Gore, Wong et al. 2008). Kitl expression in the developing thalamus has been established (Suzuki-Hirano, Ogawa et al. 2011), but less is known about Kit in the same area. Very little has been investigated regarding Cadm1, Cbln4 or Kit's involvement in axon guidance as attention has been directed towards synapse formation (Biederer, Sara et al. 2002, Kim, Im et al. 2003, Joo, Lee et al. 2011, Fujita, Tanabe et al. 2012, Yamada, Inoue et al. 2013, Ribic, Liu et al. 2014),

which makes them interesting candidates. Two separate groups identified Ntng2, netrin-G2 also known as laminet-2 (Nakashiba, Nishimura et al. 2002, Yin, Miner et al. 2002). Although we only detected it on Ntng1, both groups identified a GPI-anchor on Ntng2, which shows the importance of constantly validating the data obtained from screens with particular parameters. Furthermore, Ntng2 was shown to be expressed in the thalamus and to promote neurite outgrowth on dissociated cortical and thalamic neurons (Nakashiba, Nishimura et al. 2002); however, there is no *in vivo* data directly implicating Ntng2 to thalamocortical development.

The novel candidates possibly involved in thalamic axon projections we focused on were Bmp3, Cbln2, Cdh11 and Dlk1. The former, known as bone morphogenetic protein-3 or osteogenin-3, is a member of the transforming growth factor-β superfamily and has mainly been characterized in light of bone development and cancer. Little is known about Bmp3 in the brain; a few studies have focused on the closely related Bmp3b (or Gdf10) expression in the cerebellum (Cunningham, Jenkins et al. 1995, Takao, Hino et al. 1996). However, Bmp7 and the Bmp receptor Bmpr1b have been shown *in vitro* and *in vivo* to act as chemorepellent complexes in spinal cord commissural axon guidance during development (Augsburger, Schuchardt et al. 1999, Butler and Dodd 2003, Yamauchi, Phan et al. 2008) making Bmp3 an interesting candidate to investigate further. Cbln2 (another member of the C1q-tumor necrosis factor family) differential pattern of expression within the developing thalamus was previously shown with strongest expression at E18.5 (Miura, Iijima et al. 2006); nevertheless, no subsequent work has determined whether it is implicated in axonal guidance or not, but it has been determined that it is in synapse formation *in vitro* (Joo, Lee et al. 2011, Matsuda and Yuzaki 2011). As for Cdh11, although it has been implicated in osteogenesis and tumor progression [reviewed in (Corson and Gallie 2007, Marie, Hay et al. 2014)], it is also a known cell adhesion molecule of the central nervous system involved in synapse formation (Manabe, Togashi et al. 2000, Paradis, Harrar et al. 2007). Finally, Dlk1 (delta-like 1 homolog originally described in Drosophila), not to be confused with Dll1 or Dl1 (delta-like 1), has not been previously linked to axon guidance and has mainly been studied in the context of adipogenesis, tumorigenesis and myogenesis (Kilian and Beck-Sickinger 2015). Although its expression in the developing nigrostriatal system has been known for the last decade (Baladron, Ruiz-Hidalgo et al. 2005) and more recently in the developing hypothalamus

(Villanueva, Jacquier et al. 2012) and subventricular zone (Ferron, Charalambous et al. 2011), no focus has been given to the developing thalamus. Interestingly, Dlk1 has been shown to negatively regulate Notch1 through its epidermal growth factor (EGF)-like repeats (Baladron, Ruiz-Hidalgo et al. 2005).

3.3.4 Perspectives

This study has allowed to pinpoint genes whose functions can be inferred by spatial and temporal expression peaks (in this case extracellular molecules in the developmental thalamus). Moreover, we focused on a k-mean value of 10, but, in principle, more partitions through higher values of the k-mean should allow for greater expression pattern and function similarities.

In addition, we worked with individual genes, but great insight can be drawn on combinations of patterns of expression. Genes in the same family are more likely to interact with each other. We excluded ubiquitous mRNA expression patterns from our final refined set of genes of interest, therefore presenting an interesting and diversified set of spatial expression patterns. However, since our initial developmental dataset includes only 1996 genes, it is with precaution that global inferences should be made.

Chapter 4

Expression of Semaphorin6A, Semaphorin6B, PlexinA2 and PlexinA4 in the Postnatal Thalamocortical System

4.1 Introduction

In our quest to further identify and characterize relevant players of thalamocortical guidance, we narrowed our search to the Class 6 Semaphorins and the interacting Plexin-A proteins in the somatosensory system in mice, in particular Sema6A, Sema6B, PlexinA2 and PlexinA4. Sema6A is required to specify the guidance of a subset of thalamocortical axons (TCAs) specifically from the dorsal lateral geniculate nucleus at an intermediate choice point in the internal capsule (Leighton, Mitchell et al. 2001, Little, Lopez-Bendito et al. 2009). Genetic results from the laboratory also implicate the Sema6A-binding partners, PlexinA2 and PlexinA4, in this process. Little is known about the closely related protein Sema6B in thalamocortical development; however, Sema6B has been found to interact with PlexinA2 and PlexinA4 elsewhere (Suto, Ito et al. 2005, Suto, Tsuboi et al. 2007, Tawarayama, Yoshida et al. 2010). Here, we show dynamic expression patterns during the first postnatal week within the context of thalamocortical connectivity. We hypothesize that novel mechanisms of interaction between Semaphorins and Plexins may form the basis for a combinatorial code of connectivity.

4.1.1 Semaphorins

The first semaphorin, Fasciclin IV (now called Sema1a), was discovered over 20 years ago while performing a screen of differentially expressed cell surface molecules within the developing nervous system of the grasshopper (Kolodkin, Matthes et al. 1992). Shortly after, Collapsin (now termed Sema3A) was identified as a novel protein that induces neuronal growth cone collapse in the chick (Luo, Raible et al. 1993). Since then, over 20 proteins have been grouped as Semaphorins, a name that originates from the Greek word 'semaphore' meaning to transmit information via a signaling system (1999). The Semaphorin superfamily is highly conserved across species and phyla from nematode worms, insects, crustaceans, vertebrates and viruses (Figure 23 – note the close relation of Sema6A and Sema6B). So far, 20 Semaphorins have been identified in humans and mice, five in Drosophila and two from DNA viruses, making it one of the largest families of guidance cues (Yoshida 2012). These molecules are found in the extracellular compartment as either secreted, transmembrane or glycosylphosphatidylinositol (GPI)-anchored, and have been linked with functions ranging from neuronal connectivity to tumor progression, angiogenesis, immunoregulation and the development of many organ systems (Yazdani and Terman

2006). Despite their pleiotropic roles, all Semaphorins are defined by a highly conserved extracellular 'sema' domain of about 500 amino acids that contains stretches of specific amino acids and cysteine residues with the ability to form intrasubunit disulfide bonds. All Semaphorins, except for some viral Semaphorins, have another cysteine-rich motif called the plexin-semaphorin-integrin (PSI) domain adjacent to the carboxy-terminal side of the sema domain (Gherardi, Love et al. 2004). These proteins also possess N-linked glycosylation sites potentially for alternative splicing, but little is known about their relevance (Yazdani and Terman 2006). Functionally speaking, all Semaphorin signaling has been linked to cytoskeletal reorganization through modifications of actin filament and microtubule dynamics affecting motility (Huber, Kolodkin et al. 2003).

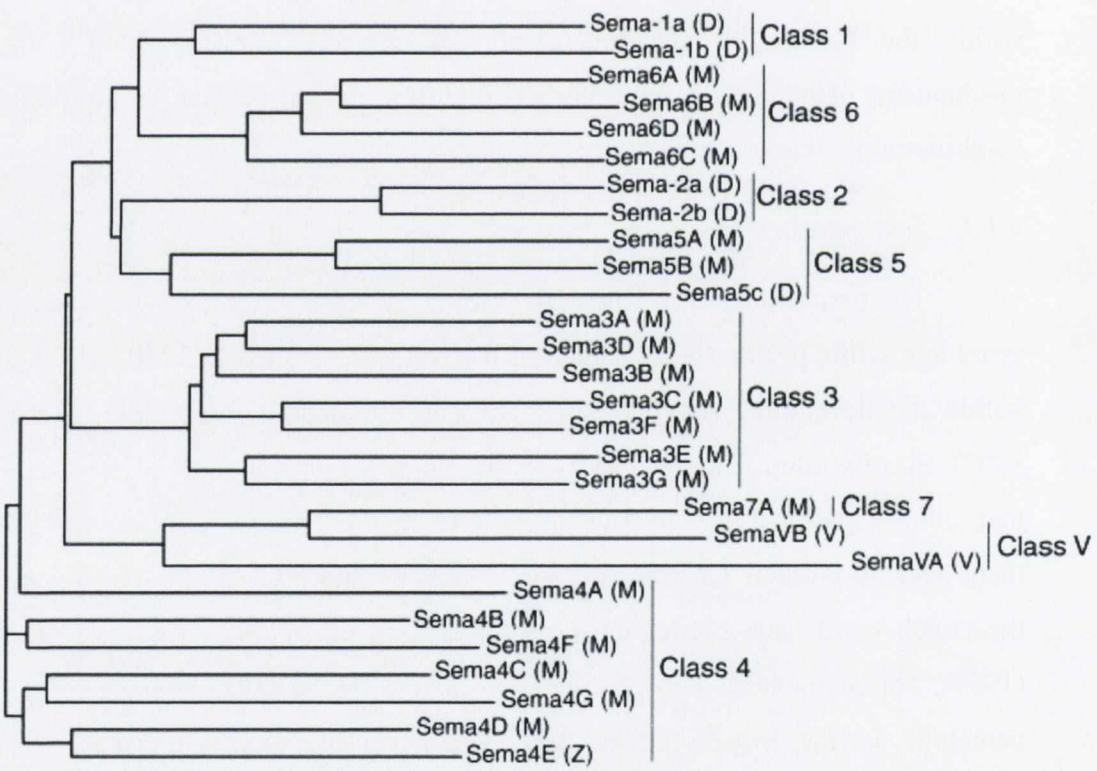


Figure 23. Phylogenetic tree of Semaphorin sequences

Groupings illustrate relation of Semaphorin genes, as well as their organization into different classes. D, *Drosophila*; M, mouse; V, viral; Z, zebrafish (sequence only identified in *Danio rerio*). From Yazdani and Terman (2006).

Based on phylogenetic tree analyses and the presence of particular protein motifs, Semaphorins have been subdivided into eight different classes termed 1-7 and V for virally encoded (Figure 24)(1999). Vertebrate Semaphorins fall into classes 3 to 7, except for Sema5C only found in zebrafish. Distinguishing structural features include the presence of immunoglobulin-like (Ig) domains, basic amino acids and 7 type 1 thrombospondin repeats (TSRs), besides their localization within the extracellular compartment. These domains confer, in part, functionality.

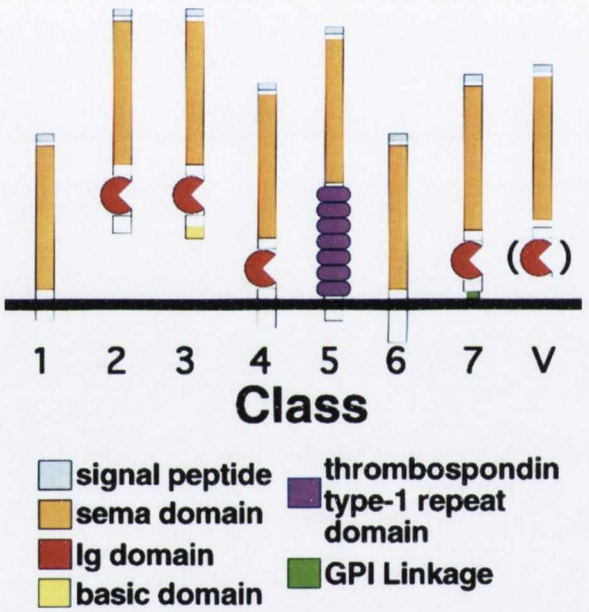


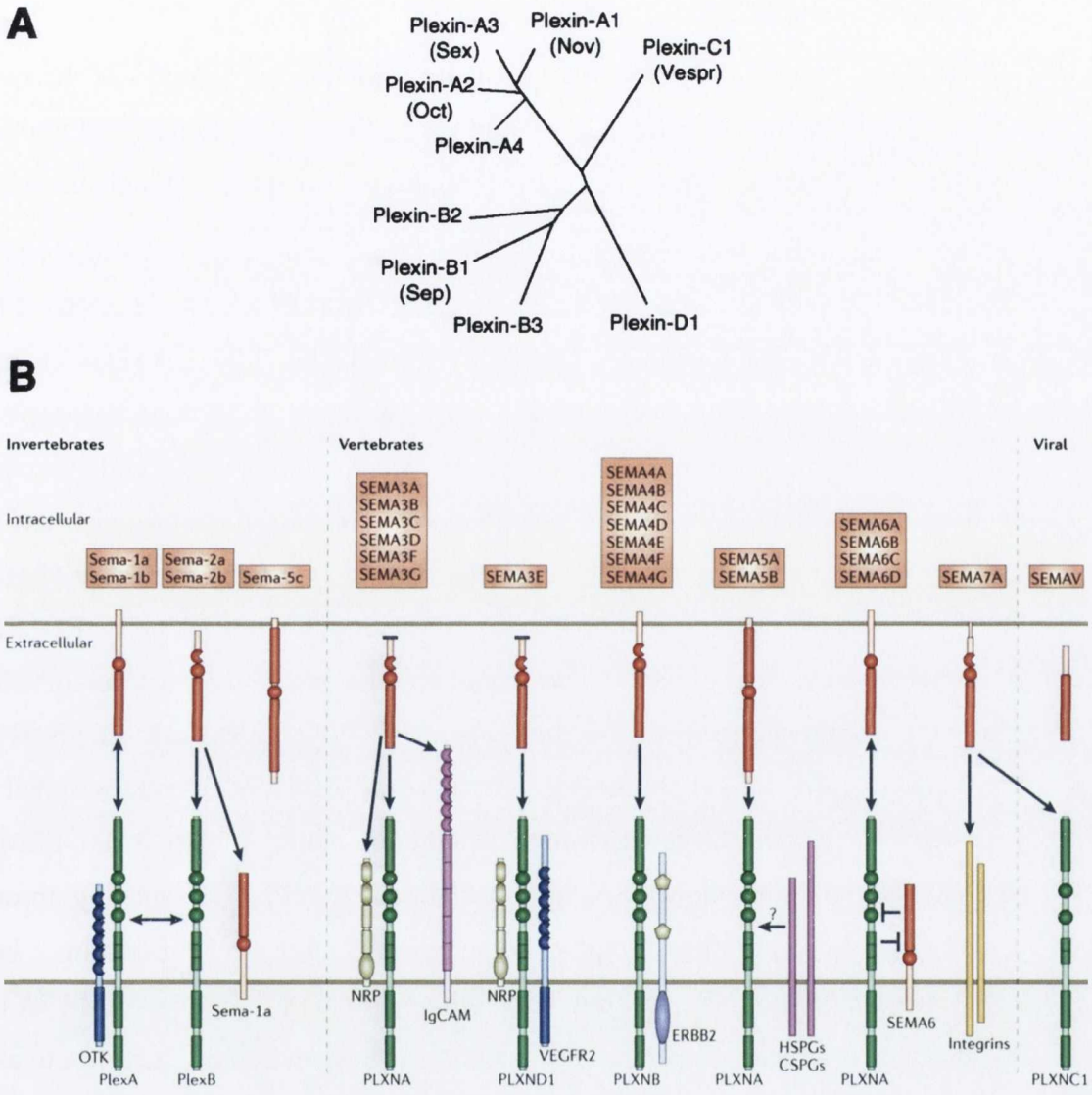
Figure 24. Classes of the Semaphorin family

Representative structures of each class of Semaphorins. Class 1 (single-pass transmembrane proteins) and class 2 (secreted proteins) are found in invertebrates. Class 3 (secreted proteins), classes 4-6 (single-pass transmembrane proteins) and class 7 (GPI-anchored) are found in vertebrates. Class V (secreted proteins) is virally encoded. From the Semaphorin Nomenclature Committee (1999).

There are no canonical signal transduction pathways for Semaphorins, adding to the complexity of their signaling capabilities and the difficulty to study them. Nonetheless, almost all Semaphorins have been shown to bind Plexins directly or through Neuropilin recruitment for secreted Semaphorins, with the exception of class 2 Semaphorins (Tamagnone, Artigiani et al. 1999, Huber, Kolodkin et al. 2003). Not only do Semaphorins function as ligands, but single-pass transmembrane Semaphorins possess a cytoplasmic domain that allows reverse signaling to occur. Of interest to us, Sema6A and Sema6B have been shown to mediate reverse signaling through enabled/vasodilator-stimulated phosphoprotein-like protein (Evl) and Src tyrosine kinase, respectively, both involved in cytoskeletal reorganization (Eckhardt, Behar et al. 1997, Klostermann, Lutz et al. 2000).

4.1.2 Plexins

Semaphorin interactions with Plexins occur through the sema domains on both proteins, although Plexin sema domains are much less conserved than those on their binding partners (Winberg, Noordermeer et al. 1998, Tamagnone, Artigiani et al. 1999, Gherardi, Love et al. 2004). Besides the Semaphorins and the Plexins, only the receptor tyrosine kinases MET and RON are known to possess a sema domain as well (Winberg, Noordermeer et al. 1998). The first Plexin was initially discovered in the nervous system of *Xenopus* tadpoles (Takagi, Tsuji et al. 1987, Ohta, Takagi et al. 1992, Ohta, Mizutani et al. 1995, Satoda, Takagi et al. 1995), and subsequently, many more were identified in invertebrates (Winberg, Noordermeer et al. 1998, Fujii, Nakao et al. 2002) and vertebrates (Kameyama, Murakami et al. 1996, Kameyama, Murakami et al. 1996, Maestrini, Tamagnone et al. 1996, Comeau, Johnson et al. 1998, Tamagnone, Artigiani et al. 1999, Suto, Murakami et al. 2003). The vertebrate Plexin superfamily now comprises 9 members divided as follows: PlexinA1-4, PlexinB1-3, PlexinC1 and PlexinD1 (Figure 35 A and B)(Tamagnone, Artigiani et al. 1999). Early studies already pointed towards a role in axon guidance in Drosophila (Winberg, Noordermeer et al. 1998). Although initially implicated in axonal repulsion, Semaphorin and Plexin effects are highly context dependent and can act as attractive cues as well (Song, Ming et al. 1998, Castellani, Chedotal et al. 2000, Castellani, De Angelis et al. 2002, Wolman, Liu et al. 2004).



(Figure legend overleaf)

Figure 25. Semaphorin neuronal receptors

Phylogenetic tree of the vertebrate Plexin family indicate groupings of the relation of Plexin genes, as well as their organization into different classes (A). Old nomenclature was overwritten as seen by names in brackets. From Tamagnone, Artigiani et al. (1999).

Most Semaphorins signal through Plexin receptor complexes in neurons (B). Nine Plexins have been identified in vertebrates (PLXNA1–PLXNA4, PLXNB1–PLXNB3, PLXNC1 and PLXND1) and two Plexins in invertebrates [Plexin A (PlexA) and Plexin B (PlexB)]. Sema1s and Sema2s signal through PlexA and PlexB, respectively, and these two Plexins can form heteromultimeric receptor complexes. The latter complexes can include various co-receptors that modulate receptor function, such as off-track (OTK) with PlexA receptors. In vertebrates, SEMA3s, SEMA5s and SEMA6s signal through PLXNAs, although SEMA3s require neuropilins (NRP1 or NRP2). SEMA3E directly interacts with PLXND1 and mediates attraction in the presence of NRP1 and vascular endothelial growth factor receptor 2 (VEGFR2). SEMA3E–PLXND1 binding mediates repulsion in the absence of NRP1. A few SEMA3s potentially signal directly through immunoglobulin super family cell adhesion molecules (IgCAMs). SEMA4s are PLXNBs binding partners. Proteoglycans modulate SEMA5 signaling through yet unknown receptors. Interestingly, some transmembrane Semaphorins, including SEMA6s and Sema1a, can function both as ligands and as receptors. SEMA7A interacts with neuronal integrin receptors to promote axon outgrowth (and PLXNC1 to affect the immune system). SEMAVs can also bind PLXNC1. In addition, SEMA6s and PLXNAs can make cis interactions that can negatively affect each other. CSPGs, chondroitin sulphate proteoglycans; HSPGs, heparan sulphate. From Pasterkamp (2012).

All Plexins are single-pass transmembrane proteins that share characteristic features in addition to their amino-terminal sema domains: three PSI domains and three to six IPT (Ig domain shared by Plexins and Transcription factors) domains extracellularly (Winberg, Noordermeer et al. 1998, Tamagnone, Artigiani et al. 1999, Suto, Murakami et al. 2003, Gherardi, Love et al. 2004, Janssen, Robinson et al. 2010). Moreover, the carboxy-terminal cytoplasmic SP (domain of SEX and Plexins) domain of approximately 600 amino acids is highly conserved as well, with 57% to 97% homology (Tamagnone, Artigiani et al. 1999). This domain contains putative tyrosine kinase phosphorylation sites, although not within previously identified canonical motifs. What's more, to date, the SP domain shares no homology with other proteins. Nonetheless, many downstream effectors have been identified. Not surprisingly, these are involved in cytoskeleton reorganization (Yamada, Sakisaka et al. 2005, Jeon, Kim et al. 2010, Hung, Pak et al. 2011, Pascoe, Wang et al. 2015). Crystal structure analyses have revealed the main mediators of Plexins (Pascoe, Wang et al. 2015): Rac1 and Rnd1 through weak interactions with the Rho GTPase-binding domain (RDB) (Hota and Buck 2009, Tong, Hota et al. 2009, Wang, Hota et al. 2011), Rap GTPase activating protein (GAP) through the GAP-like domain (Wang, He et al. 2012) and flavoprotein oxidoreductases MICAL through a novel binding site (Terman, Mao et al. 2002, Nadella, Bianchet et al. 2005, Siebold, Berrow et al. 2005).

4.1.3 Class 6 Semaphorin and class A Plexin roles in the developing nervous system

Differences in binding abilities to Semaphorins and within the Plexin SP domain have allowed the Semaphorin and Plexin interactions to have a broad range of functions. Genetic approaches have highlighted the importance of Semaphorin signaling in the guidance of axons and dendrites (Giger *et al.*, 2000; Polleux *et al.*, 2000; Leighton *et al.*, 2001; de Araujo *et al.*, 2003; Pasterkamp and Kolodkin, 2003; Sahay *et al.*, 2003), axon branching and pruning (Bagri *et al.*, 2003; Faulkner *et al.*, 2007), neuronal migration (Eickholt *et al.*, 2002; Kerjan *et al.*, 2005) and synaptic connectivity (Matthes, Sink et al. 1995, Winberg, Mitchell et al. 1998, Godenschwege, Hu et al. 2002, Suto, Tsuboi et al. 2007). Moreover, Semaphorins have roles in the adult brain in synaptic plasticity regulation, remodeling or sprouting (Sahay *et al.*, 2005). Of interest to us, class A Plexins and class 6 Semaphorins have been previously studied in the developing nervous system, albeit mainly outside the context of thalamocortical connectivity.

Our laboratory has been investigating the functions of Class 6 transmembrane Semaphorins and the interacting PlexinA proteins in thalamocortical connectivity development. Indeed, previous data from the laboratory demonstrates that Sema6A is required to guide TCAs specifically from the dorsal lateral geniculate nucleus, the primary visual nucleus of the thalamus that receives inputs from the retina and sends projections to the primary visual cortex, at the level of the internal capsule (Little et al., 2009). Genetic results also implicate the Sema6A-binding partners, PlexinA2 and PlexinA4, in this process. The Class 6 Semaphorins is composed of single-pass transmembrane proteins and it comprises four members, Sema6A-D, that have been shown to bind directly and specifically to members of the PlexinA subfamily. Sema6A and Sema6B have been shown to bind to PlexinA2 and PlexinA4 (Suto, Ito et al. 2005, Andermatt, Wilson et al. 2014), and Sema6C and Sema6D to PlexinA1 (Yoshida, Han et al. 2006). The functions of Sema6A are mediated by PlexinA2 and PlexinA4, though no canonical signal transduction pathway has been found, as the nature of their interactions is highly context-dependent. For instance, in the cerebellum, PlexinA2 acts as a receptor for Sema6A (Renaud *et al.*, 2008). However, in the corticospinal tract and the hippocampus, Sema6A functions as a repellent cue through PlexinA4 (Suto *et al.*, 2007; Runker *et al.*, 2008), while PlexinA2 in the hippocampus antagonizes Sema6A function (Suto *et al.*, 2007; Tawarayama *et al.*, 2010). Sema6B also cooperates in Sema6A function. For example, in the hippocampus, it has been shown to act in a partially redundant fashion to restrict mossy fibers to particular lamina by signaling through PlexinA4 (Tawarayama *et al.*, 2010). Moreover, PlexinA4 propagates repulsive signals of Sema6B, as well as Sema6A, in sympathetic ganglion axons *in vitro* (Suto, Ito et al. 2005). Interestingly, these molecules can bind in trans, but also in cis, adding to the complexity of their function and regulation (Suto, Tsuboi et al. 2007, Renaud, Kerjan et al. 2008, Haklai-Topper, Mlechkovich et al. 2010, Andermatt, Wilson et al. 2014). Haklai-Topper, Mlechkovich et al. (2010) recently found that Sema6B can directly relieve Sema6A inhibition of PlexinA4 function in dorsal root ganglion neurons, and that all these interactions occur in cis.

4.1.4 Aims of this study

In order to further explore potential roles of Sema6A, Sema6B, PlexinA2 and PlexinA4 in thalamocortical connectivity, detailed expression patterns of these genes are essential. Previous studies within the laboratory and elsewhere have demonstrated

the dynamic patterns that these genes exhibit at other time-points; therefore, we focus on the fist postnatal week at two-day intervals (P2, P4, P6 and P8). These time-points are relevant to proper invasion of TCAs into the cortical plate and further refinement. The lack of reliable antibodies to detect Sema6A, Sema6B and PlexinA2 protein expression has made comprehensive expression data analysis difficult. However, messenger RNA (mRNA) expression levels are indicative of potential protein presence and can allow determining which cells express the genes of interest. For PlexinA4 expression, we will not only present mRNA expression data, but also protein expression data. Particular focus is aimed at the somatosensory system, since it presents an interesting model to study thalamocortical connectivity.

4.2 Results

4.2.1 Messenger RNA expression patterns of Sema6A, Sema6B, PlexinA2 and PlexinA4 at postnatal day 2

Previous work in the laboratory established the expression patterns of Sema6A, Sema6B, PlexinA2 and PlexinA4 (and PlexinA1 and PlexinA3) in the thalamocortical system at embryonic day (E) 14.5, E16.5, at birth and postnatal day (P) 4. Briefly, at E14.5 both Sema6A and Sema6B are expressed in the dorsal thalamus; however, Sema6A expression follows a lateral^{high} to ventral^{low} gradient, whereas Sema6B expression is broad throughout the thalamus. In addition, both genes are expressed in the ventral telencephalon. Sema6B is also present in the cortical subplate. At E16.5, Sema6A is still persistent in the dorsal thalamus, with strongest expression caudally in the ventral and lateral geniculate nuclei (LGN), and the ventrobasal (VB) complex. Sema6B is primarily expressed rostrally in the dorsal thalamus. Both genes show high expression in the telencephalon, with Sema6A mainly localized to the globus pallidus, the neuroepithelium of the caudate putamen and the piriform cortex; and Sema6B predominantly localized to the basomedial and lateral amygdaloid nuclei. More specifically in the cortex, Sema6A is expressed in the marginal zone, the deep cortical plate, the subplate and the subventricular zone, whereas Sema6B is expressed in the marginal zone, the innermost part of the deep cortical plate, the subplate and the intermediate and subventricular zones. At these embryonic stages, both PlexinA2 and PlexinA4 expression is high medially in the dorsal thalamus. Moreover, PlexinA2 is expressed in the neuroepithelium of the caudate putamen, and cortically in the marginal zone, the deep cortical plate, the subplate and the intermediate zone at E14.5. By E16.5, PlexinA2 expression is limited to the basomedial amygdaloid nucleus, the deep cortical plate and the intermediate zone in the telencephalon. As for PlexinA4, it is expressed in the globus pallidus, a dorsal band to the internal capsule, and the subplate and the intermediate zone of the neocortex. At E16.5, high expression of PlexinA4 is also found in the cortical marginal zone.

At P0 and P4, Sema6A and Sema6B remain expressed in the dorsal thalamus. In addition, their expression in the neocortex has become more refined with differential patterns across the layers. At birth, in the primary somatosensory cortex, Sema6A is detected in higher levels in the cortical plate, layer VI and the subplate, while Sema6B is strongly detected in the cortical plate. At P4, Sema6A expression is strong in the

marginal zone, layers IV, V and VIb, and the subplate of the primary somatosensory cortex. Sema6B is expressed in a decreasing gradient from the marginal zone to the white matter layer of the same cortical area. PlexinA2 and PlexinA4 are still present in the dorsal thalamus at P0 and P4, with higher expression medially. In the primary somatosensory cortex, both genes elicit complementary expression patterns with PlexinA2 showing strong expression in layer VIb, and PlexinA4 showing strong expression in layers II, III and IV. However, both are expressed in the marginal zone. Interestingly, Sema6B and PlexinA4 exhibit similar patterns of expression postnatally.

At P2, axons start forming rows within the ventral posteriomedial nucleus (VPM) of the VB and will become visible barreloids by P3 (Erzurumlu and Gaspar 2012). Postnatal day 2 also marks the day that TCAs start organizing in patches within barrel rows in layer IV of the somatosensory cortex (Rebsam, Seif et al. 2002). Both Sema6A and Sema6B are strongly expressed in the VB (Figure 26B and C, and Figure 27B and C). Interestingly, patches in the VPM begin to be discernable with Sema6B expression patterns (Figure 27C). Only Sema6A is detected in the ventral and dorsal LGN (compare Figure 26B and C to Figure 27B and C). In the somatosensory cortex, Sema6A is expressed in the marginal zone and in a decreasing gradient from layer V to the white matter layer (Figure 26D to F). Sema6B is strongly detected rostrally in the outermost layers of the cortical plate and layer V (Figure 27D), and is mainly detected caudally in the marginal zone, the cortical plate and layer V of the somatosensory cortex (Figure 27E and F).

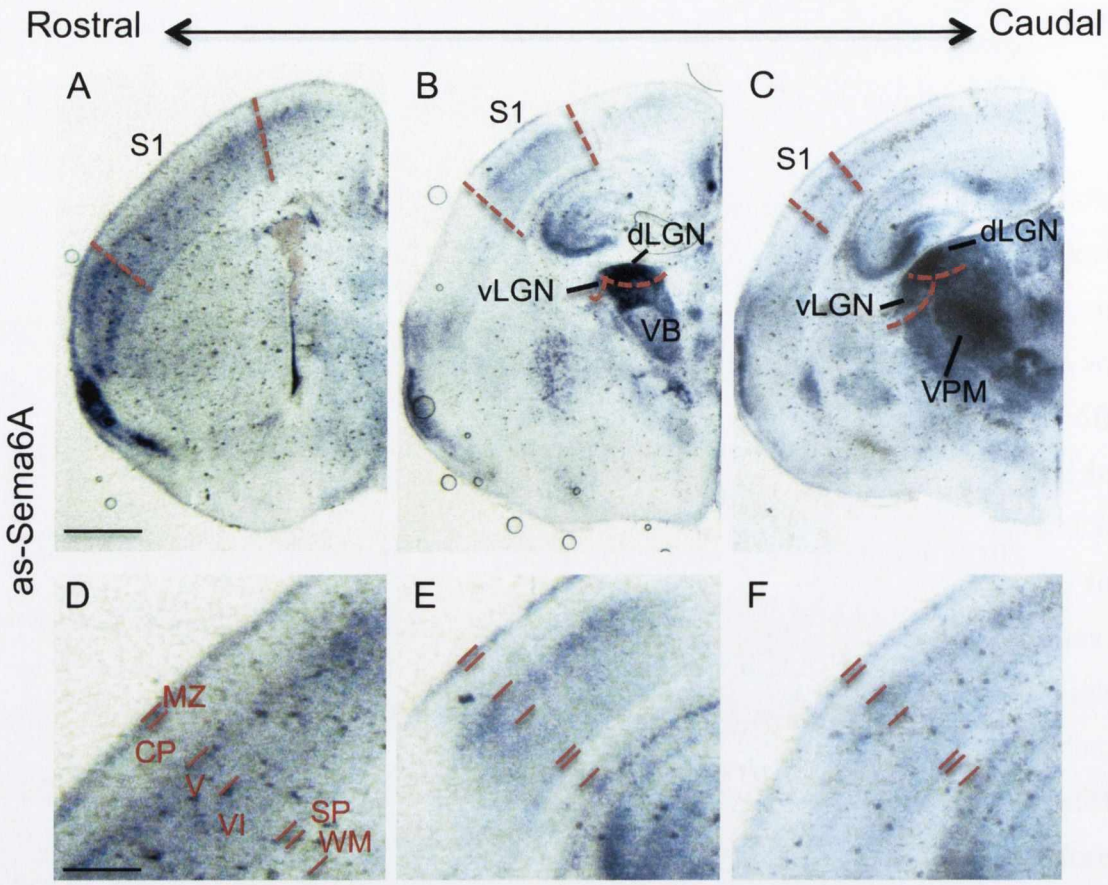


Figure 26. Expression levels of Sema6A in the mouse brain at P2

In situ hybridization revealed mRNA levels with antisense RNA probes against Sema6A. The latter is strongly expressed in the dorsal thalamic nuclei [ventrobasal complex (VB) of the thalamus, ventral lateral geniculate nucleus (vLGN) and dorsal lateral geniculate nucleus (dLGN), among other nuclei (B and C)]. In the somatosensory cortex (S1), Sema6A is expressed in the marginal zone (MZ) and in a decreasing gradient from cortical layer V (V) to the white matter layer (WM; D-F). D, E and F are higher magnifications of the cortex of A, B and C, respectively. CP, cortical plate; SP, subplate; VI, cortical layer VI; VPM, ventral posteriomedial nucleus.

Scale: A to C 500μm; D to F 200μm.

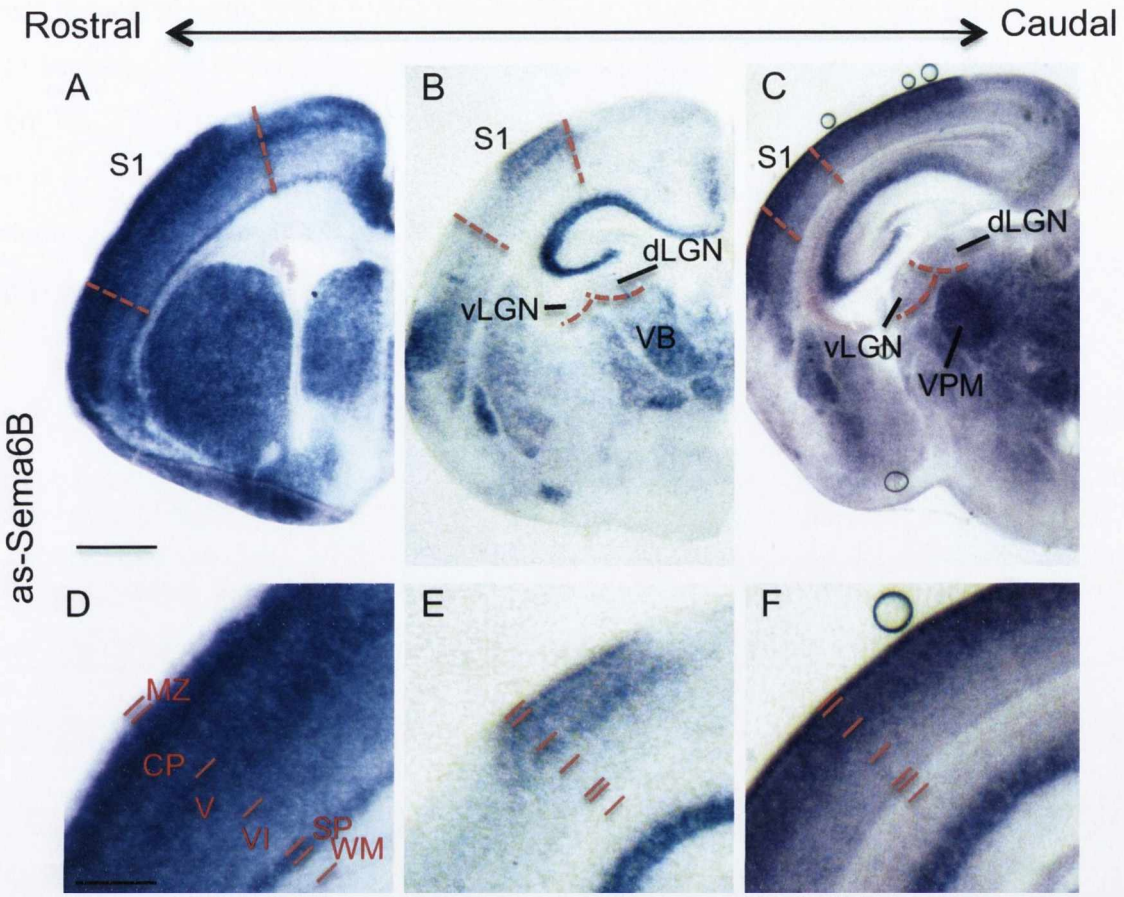


Figure 27. Expression levels of Sema6B in the mouse brain at P2

In situ hybridization revealed mRNA levels with antisense RNA probes against Sema6B. The latter is strongly expressed in the ventrobasal complex (VB) of the thalamus, and in particular in the ventral posteriomedial nucleus (VPM; B and C)]. Patches in the VPM are discernable with Sema6B expression patterns (C). In the somatosensory cortex (S1), Sema6B is strongly detected rostrally in the outermost layers of the cortical plate (CP) and cortical layer V (V; D), and is mainly detected caudally in the marginal zone (MZ), the cortical plate and cortical layer V of the somatosensory cortex (E and F). D, E and F are higher magnifications of the cortex of A, B and C, respectively. dLGN, dorsal lateral geniculate nucleus; vLGN, ventral lateral geniculate nucleus; SP, subplate; VI, cortical layer VI; WM, white matter layer.

Scale: A to C 500μm; D to F 200μm.

PlexinA2 and PlexinA4 expression in the thalamus is predominantly ventral, with no expression detected in the ventral or dorsal LGN (Figure 28B and C, and Figure 29B and C). Moreover, in the somatosensory cortex, PlexinA2 is expressed rostrally in the marginal zone and below the cortical plate in cortical layers V, VI and the subplate (Figure 28D and E). Caudally, PlexinA2 is only expressed in the marginal zone and the cortical layer VI (Figure 28F). PlexinA4 is expressed throughout the somatosensory cortex, but with stronger levels in the marginal zone and the cortical plate (Figure 29D to F).

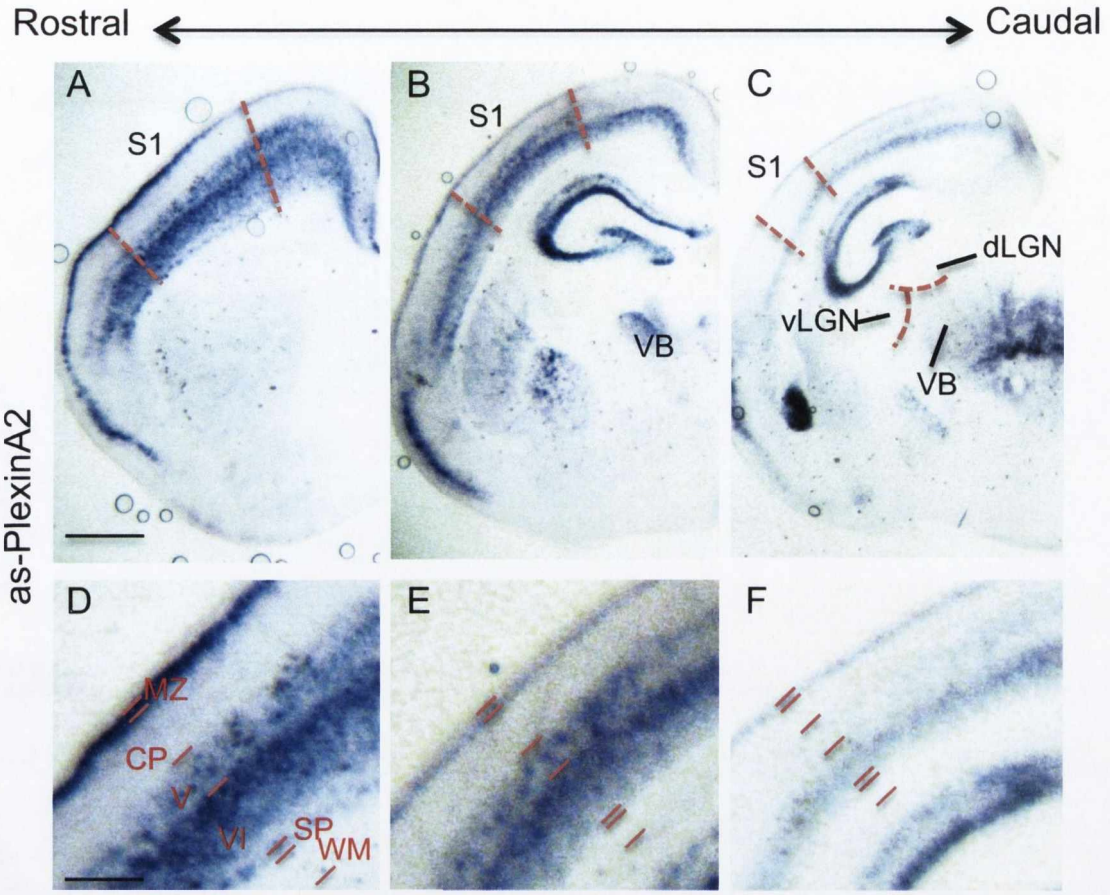


Figure 28. Expression levels of PlexinA2 in the mouse brain at P2

In situ hybridization revealed mRNA levels with antisense RNA probes against PlexinA2. The latter is predominantly expressed in the ventral thalamus (B and C). In the somatosensory cortex (S1), PlexinA2 is expressed rostrally in the marginal zone (MZ) and below the cortical plate (CP) in cortical layer V (V), cortical layer VI (VI), and the subplate (SP; D and E). Caudally, PlexinA2 is only expressed in the marginal zone and the cortical layer VI (F). D, E and F are higher magnifications of the cortex of A, B and C, respectively. dLGN, dorsal lateral geniculate nucleus; vLGN, ventral lateral geniculate nucleus; VB, ventrobasal complex; WM, white matter layer.

Scale: A to C 500μm; D to F 200μm.

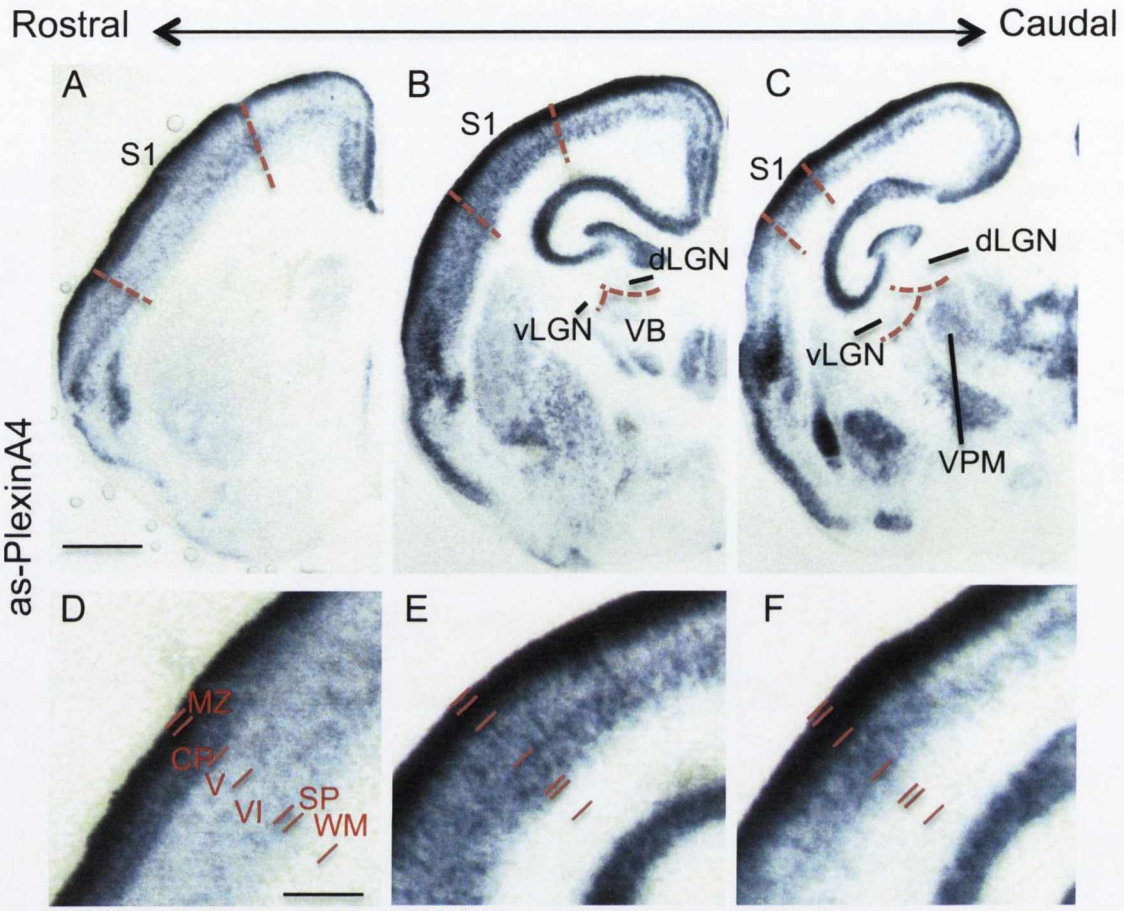


Figure 29. Expression levels of PlexinA4 in the mouse brain at P2

In situ hybridization revealed mRNA levels with antisense RNA probes against PlexinA4. The latter is predominantly expressed in the ventral thalamus (B and C). In the somatosensory cortex (S1), PlexinA4 is expressed throughout (D-F), but with stronger levels in the marginal zone (MZ) and the cortical plate (CP). D, E and F are higher magnifications of the cortex of A, B and C, respectively. dLGN, dorsal lateral geniculate nucleus; vLGN, ventral lateral geniculate nucleus; VB, ventrobasal complex; V, cortical layer V; VI, cortical layer VI; SP, subplate; WM, white matter layer.

Scale: A to C 500µm; D to F 200µm.

4.2.2 Messenger RNA expression patterns of Sema6A, Sema6B, PlexinA2 and PlexinA4 at postnatal day 4

Studies have shown that P4 is the end of the critical period for structural plasticity following either whisker follicle or infraorbital nerve damage, or whisker trimming (Durham and Woolsey 1984, Datwani, Iwasato et al. 2002, Rebsam, Seif et al. 2005, Erzurumlu and Gaspar 2012). Moreover, all cortical neurons have reached their target layer and barrel aggregates will become apparent shortly after this time-point. Although previous work in the laboratory had looked into this time-point, we wanted to address it in regards to thalamocortical connectivity to the somatosensory cortex. As previously mentioned, Sema6A is expressed throughout the thalamus (Figure 30B and C), and quite strongly in the ventral and dorsal LGN, and the VB. Sema6B is also widely expressed in the thalamus (Figure 31B and C), and we can see the barreloids nicely defined in the VPM (Figure 31C). In the somatosensory cortex, Sema6A expression is strongest in layers IV (Figure 30D-F), whereas Sema6B expression is strongest in the marginal zone with levels decreasing towards the white matter layer (Figure 31D-F).

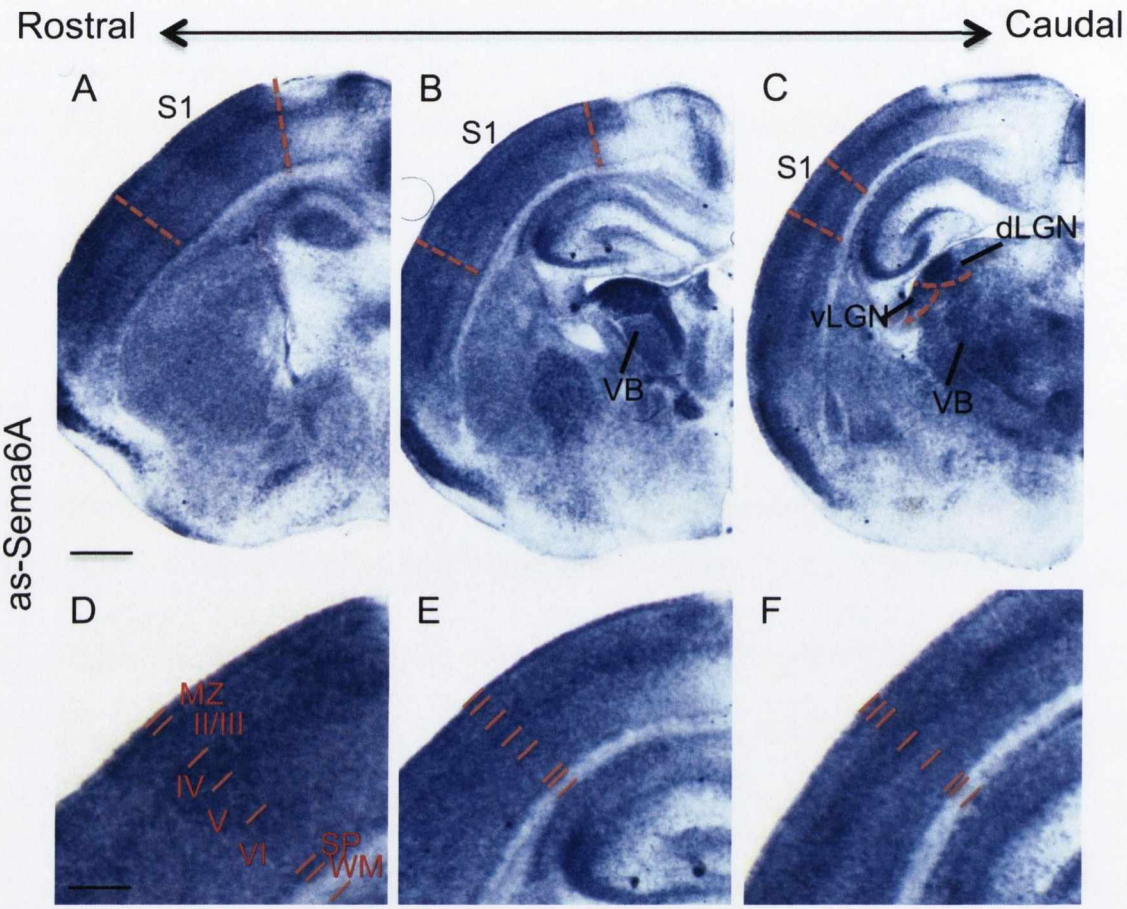


Figure 30. Expression levels of Sema6A in the mouse brain at P4

In situ hybridization revealed mRNA levels with antisense RNA probes against Sema6A. The latter is expressed throughout the thalamus (B and C), and quite strongly in the ventral and dorsal lateral geniculate nuclei (vLGN and dLGN), and the ventrobasal complex (VB). In the somatosensory cortex (S1), Sema6A expression is strongest in cortical layer IV (IV; D-F). D, E and F are higher magnifications of the cortex of A, B and C, respectively. MZ, marginal zone; II/III, cortical layers II and III; V , cortical layer V; VI, cortical layer VI; SP, subplate; WM, white matter layer.

Scale: A to C 500μm; D to F 200μm.

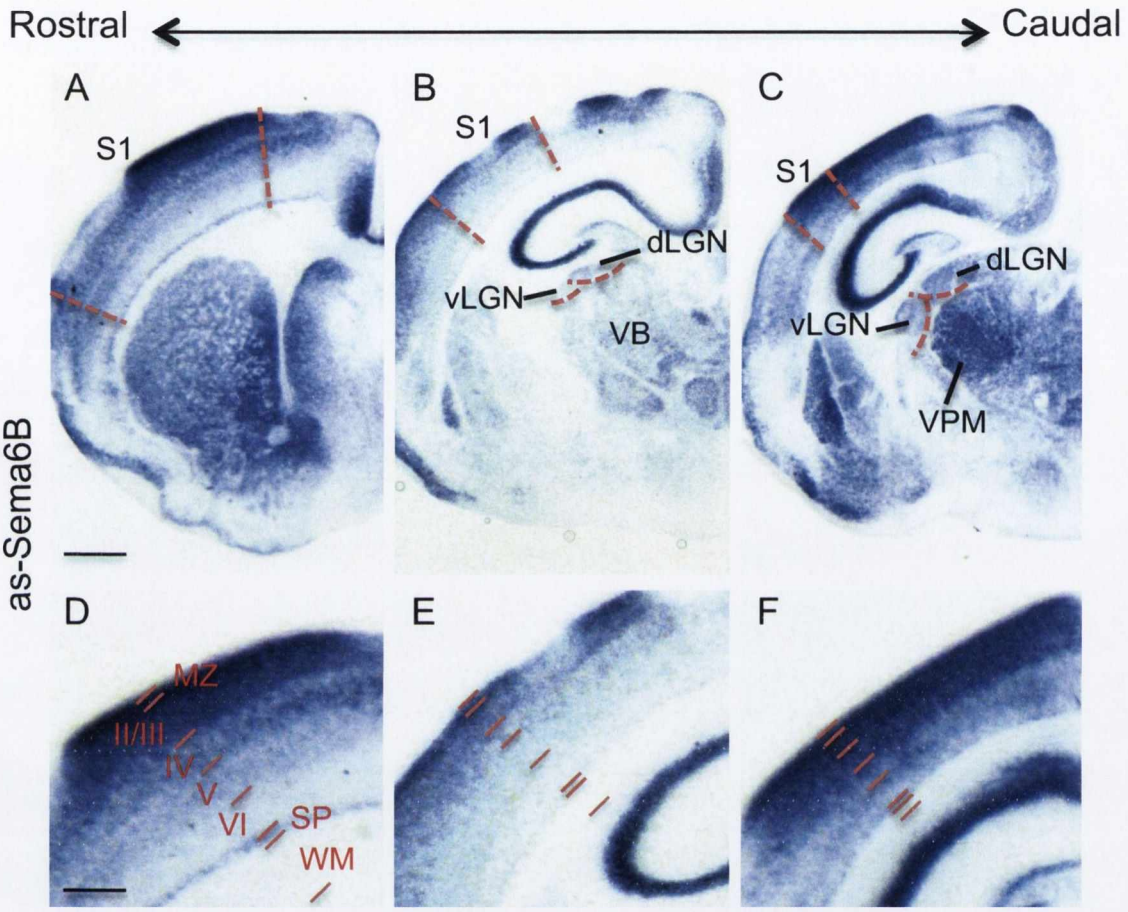


Figure 31. Expression levels of Sema6B in the mouse brain at P4

In situ hybridization revealed mRNA levels with antisense RNA probes against Sema6B. The latter is widely expressed throughout the thalamus (B and C). The barreloids are nicely defined in the ventral posteriomedial nucleus (VPM; C). In the somatosensory cortex (S1), Sema6B expression is strongest in the marginal zone (MZ) with levels decreasing towards the white matter layer (WM; D-F). D, E and F are higher magnifications of the cortex of A, B and C, respectively. vLGN, ventral lateral geniculate nucleus; dLGN, dorsal lateral geniculate nucleus; VB, ventrobasal complex; II/III, cortical layers II and III; IV, cortical layer IV; V, cortical layer V; VI, cortical layer VI; SP, subplate.

Scale: A to C 500μm; D to F 200μm.

PlexinA2 and PlexinA4 continue to be mainly expressed in the ventral thalamus, with clear expression in the VPM (Figure 32 B and C, and Figure 33 B and C). PlexinA2 is expressed throughout the cortical plate, but higher expression is localized to the marginal zone, layer VI and the subplate in the somatosensory cortex (Figure 32 D to F). PlexinA4 is also expressed in the marginal zone, but differs from PlexinA2 as it is expressed in layers II/III, and then with lower strength in deeper layers of the neocortex (Figure 33 D to F).

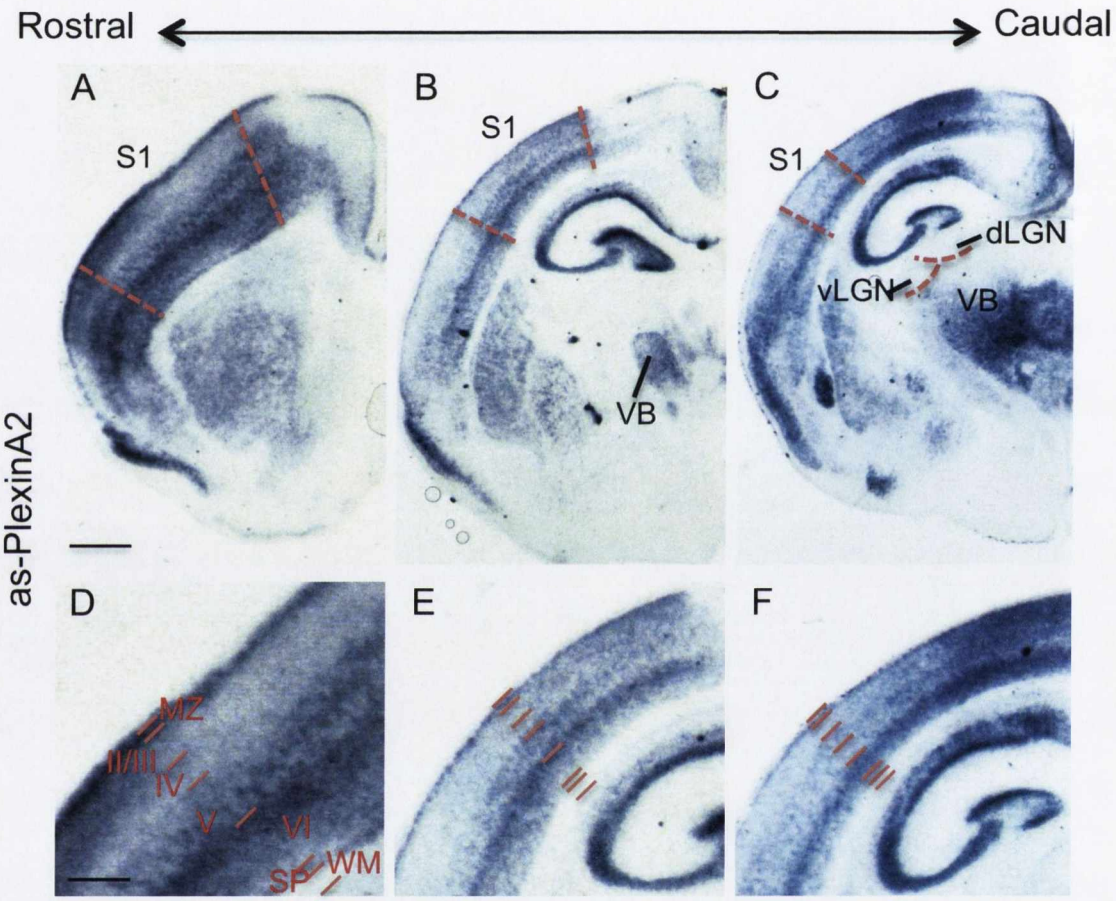


Figure 32. Expression levels of PlexinA2 in the mouse brain at P4

In situ hybridization revealed mRNA levels with antisense RNA probes against PlexinA2. The latter is predominantly expressed in the ventral thalamus (B and C). In the somatosensory cortex (S1), PlexinA2 is expressed throughout cortical plate, but higher expression is localized to the marginal zone (MZ), cortical layer VI (VI) and the subplate (SP; D-F). D, E and F are higher magnifications of the cortex of A, B and C, respectively. vLGN, ventral lateral geniculate nucleus; dLGN, dorsal lateral geniculate nucleus; VB, ventrobasal complex; II/III, cortical layers II and III; IV, cortical layer IV; V, cortical layer V; WM, white matter layer. Scale: A to C 500μm; D to F 200μm.

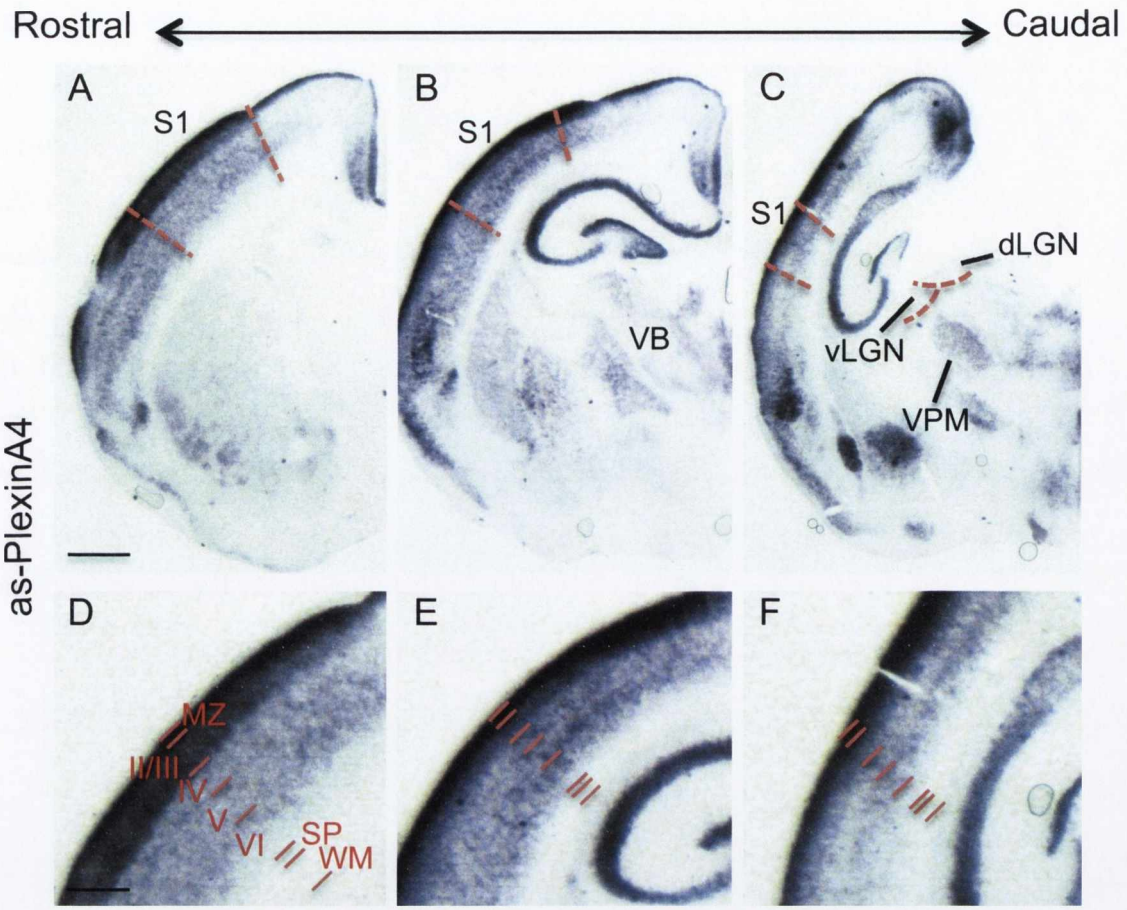


Figure 33. Expression levels of PlexinA4 in the mouse brain at P4

In situ hybridization revealed mRNA levels with antisense RNA probes against PlexinA4. The latter is predominantly expressed in the ventral thalamus (B and C), with clear expression in the barreloids within ventral posteriomedial nucleus (VPM; C). In the somatosensory cortex (S1), PlexinA4 is expressed in the marginal zone (MZ), but also in cortical layers II and III (II/III), and then with lower strength in deeper layers of the neocortex (D-F). D, E and F are higher magnifications of the cortex of A, B and C, respectively. vLGN, ventral lateral geniculate nucleus; dLGN, dorsal lateral geniculate nucleus; VB, ventrobasal complex; IV, cortical layer IV; V, cortical layer V; VI, cortical layer VI; SP, subplate; WM, white matter layer.

Scale: A to C 500µm; D to F 200µm.

4.2.3 Messenger RNA expression patterns of Sema6A, Sema6B, PlexinA2 and PlexinA4 at postnatal day 6

At P6, barrel organization becomes apparent in the somatosensory cortex (Rice, Gomez et al. 1985), and barrel cells acquire polarized dendritic morphology (Espinosa, Wheeler et al. 2009). Our expression data shows that Sema6A and Sema6B are continuously expressed in the thalamus (Figure 34 B and C, and Figure 35 B and C). Moreover, Sema6A expression is high in the marginal zone, cortical layers II, III, at the border between cortical layers IV and V, cortical layer VI and the subplate (Figure 34 D to F). Sema6B shows a similar pattern of expression in the somatosensory cortex (Figure 35 D to F). Interestingly, the area where the barrels form in cortical layer IV is devoid of Sema6A and Sema6B expression. What's more, the barrels are surrounded by the expression of these two genes.

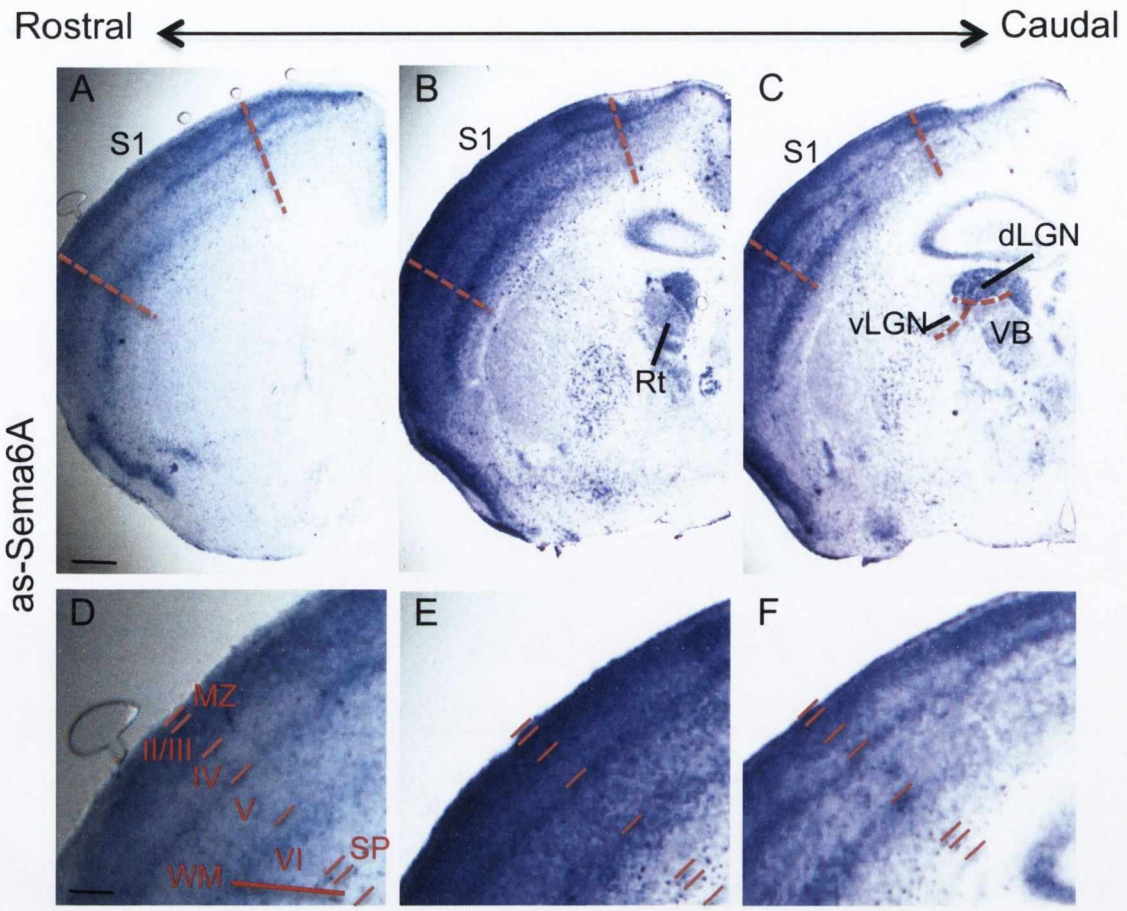


Figure 34. Expression levels of Sema6A in the mouse brain at P6

In situ hybridization revealed mRNA levels with antisense RNA probes against Sema6A. The latter is expressed throughout the thalamus (B and C), and quite strongly in dorsal lateral geniculate nucleus (dLGN). In the somatosensory cortex (S1), Sema6A expression is high in the marginal zone (MZ), cortical layers II and III (II/III), at the border between cortical layer IV (IV) and cortical layer VI (VI), and the subplate (SP; D-F). D, E and F are higher magnifications of the cortex of A, B and C, respectively. Rt, reticular nucleus; VB, ventrobasal complex; vLGN, ventral lateral geniculate nucleus; V, cortical layer V; WM, white matter layer.

Scale: A to C 500µm; D to F 200µm.

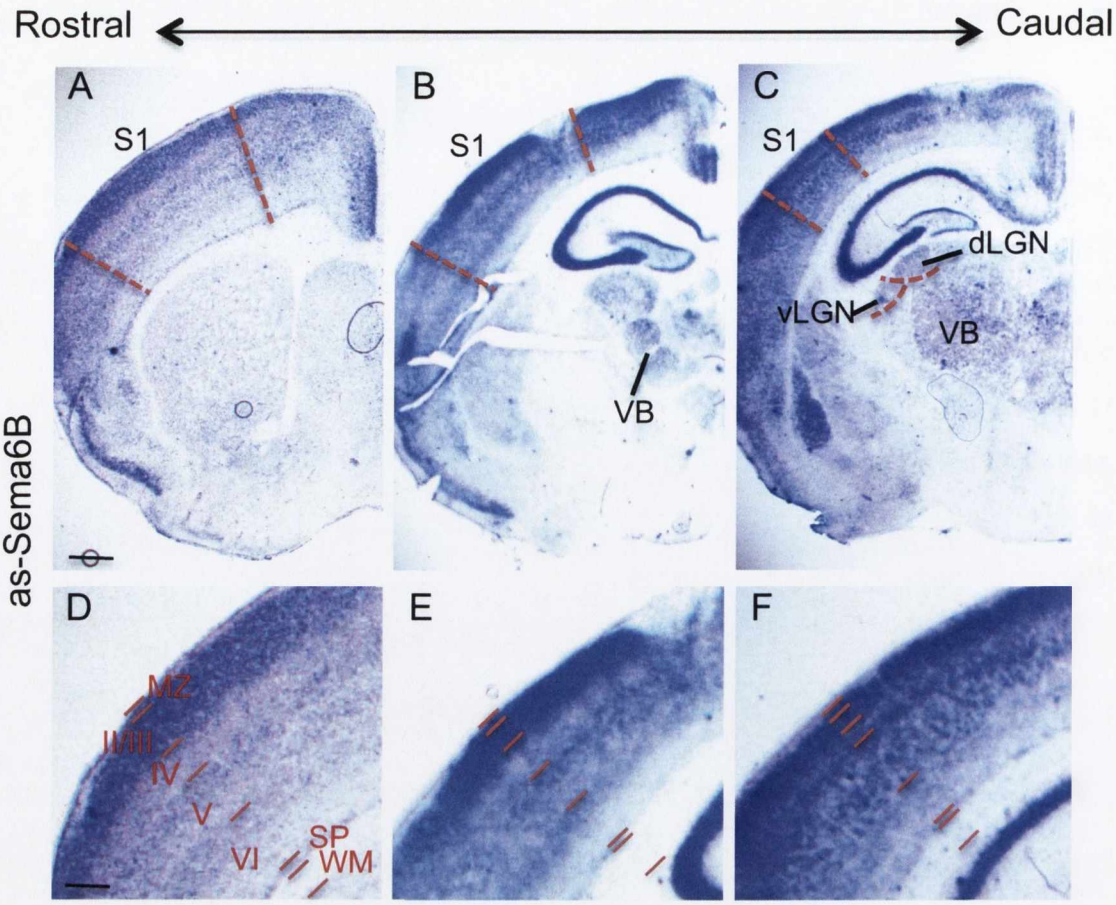


Figure 35. Expression levels of Sema6B in the mouse brain at P6

In situ hybridization revealed mRNA levels with antisense RNA probes against Sema6B. The latter is widely expressed throughout the thalamus (B and C). In the somatosensory cortex (S1), Sema6B expression is high in the marginal zone (MZ), cortical layers II and III (II/III), at the border between cortical layer IV (IV) and cortical layer V (V), and the subplate (SP; D-F). D, E and F are higher magnifications of the cortex of A, B and C, respectively. VB, ventrobasal complex; vLGN, ventral lateral geniculate nucleus; dLGN, dorsal lateral geniculate nucleus; VI, cortical layer VI; WM, white matter layer.

Scale: A to C 500µm; D to F 200µm.

At this time-point, PlexinA2 remains expressed in the thalamus, although not in the VPM (Figure 36 B and C). The thalamic expression is confined medially. Although there is weak expression medially of PlexinA4, the strongest thalamic expression is within the VPM as the barreloids can be readily distinguished (Figure 37 B and C). In the somatosensory cortex, PlexinA2 expression is similar to that of Sema6A and Sema6B with high levels in the marginal zone, cortical layers II and III, and the subplate (Figure 36 D to F). However, there is no strong divide between cortical layers IV and V. In the case of PlexinA2, the expression is within cortical layer IV surrounding the barrels. Strong expression is also apparent in cortical layer VI. PlexinA4 expression is the most contrasting comparing to Sema6A, Sema6B and PlexinA2, since it is actually strongly expressed within the barrels (Figure 37 D to F). It is also expressed in the marginal zone and in cortical layer VI, and weakly in the deeper layers below.

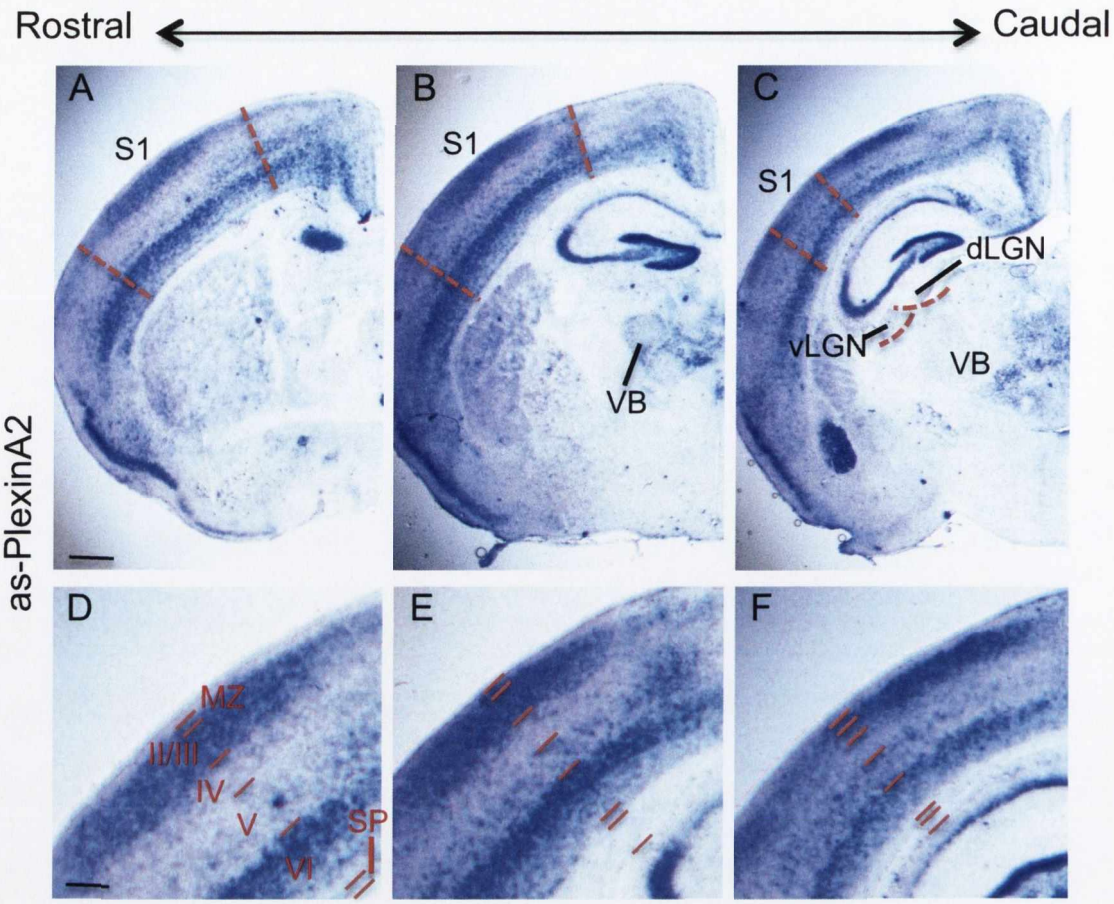


Figure 36. Expression levels of PlexinA2 in the mouse brain at P6

In situ hybridization revealed mRNA levels with antisense RNA probes against PlexinA2. The latter is predominantly expressed medially in the thalamus (B and C). In the somatosensory cortex (S1), PlexinA2 is expressed in the marginal zone (MZ), cortical layers II and III (II/III), cortical layer VI (VI) and the subplate (SP; D-F). D, E and F are higher magnifications of the cortex of A, B and C, respectively. VB, ventrobasal complex; vLGN, ventral lateral geniculate nucleus; dLGN, dorsal lateral geniculate nucleus; IV, cortical layer IV; V, cortical layer V; WM, white matter layer.

Scale: A to C 500µm; D to F 200µm.

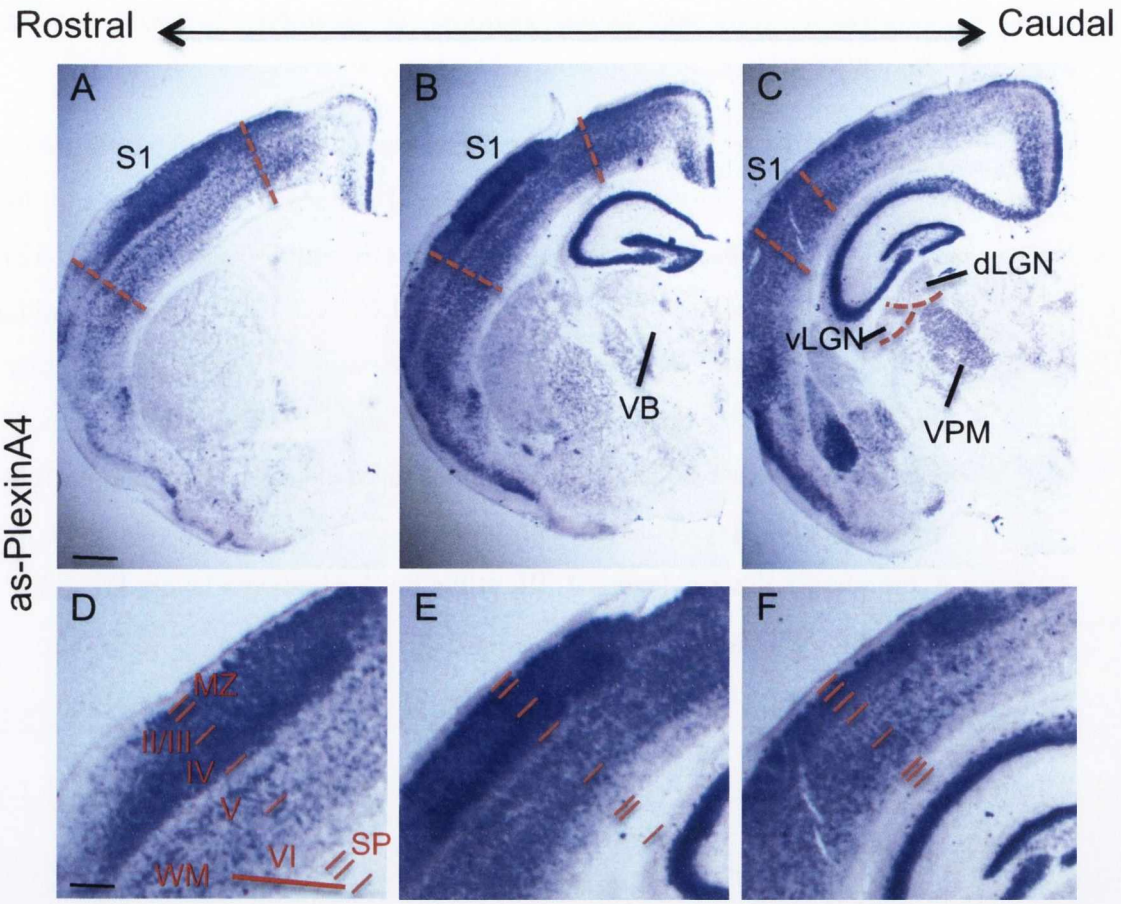


Figure 37. Expression levels of PlexinA4 in the mouse brain at P6

In situ hybridization revealed mRNA levels with antisense RNA probes against PlexinA4. The latter is predominantly expressed within the barreloids of the ventral posteriomedial nucleus (VPM) in the thalamus (C). In the somatosensory cortex (S1), PlexinA4 is expressed in the marginal zone (MZ), cortical layer IV (IV) and cortical layer VI (VI), and weakly in the deeper layers of S1 (D-F). D, E and F are higher magnifications of the cortex of A, B and C, respectively. VB, ventrobasal complex; vLGN, ventral lateral geniculate nucleus; dLGN, dorsal lateral geniculate nucleus; V, cortical layer V; II/III, cortical layers II and III; V, cortical layer V; VI, cortical layer VI; SP, subplate; WM, white matter layer.

Scale: A to C 500μm; D to F 200μm.

4.2.4 Messenger RNA expression patterns of Sema6A, Sema6B, PlexinA2 and PlexinA4 at postnatal day 8

After the first postnatal week, the barrel cortex is fully in place. What remains is the establishment of synapses between layer IV and layers II/III, and horizontal connections between neurons in layers II and III (Erzurumlu and Gaspar 2012). At P8, Sema6A thalamic expression is high in the dorsal LGN and in the VPM, and continues to be mainly expressed laterally (Figure 38 B and C). Sema6B remains widely expressed throughout the thalamus (Figure 39 B and C). In the somatosensory cortex, Sema6A is broadly expressed; still, it continues to be excluded from the barrels (Figure 38 D to F). Sema6B stays constant compared to its expression levels at P6 with high levels in the marginal zone, layers II, III, at the border between layers IV and V and the subplate (Figure 39 D to F).

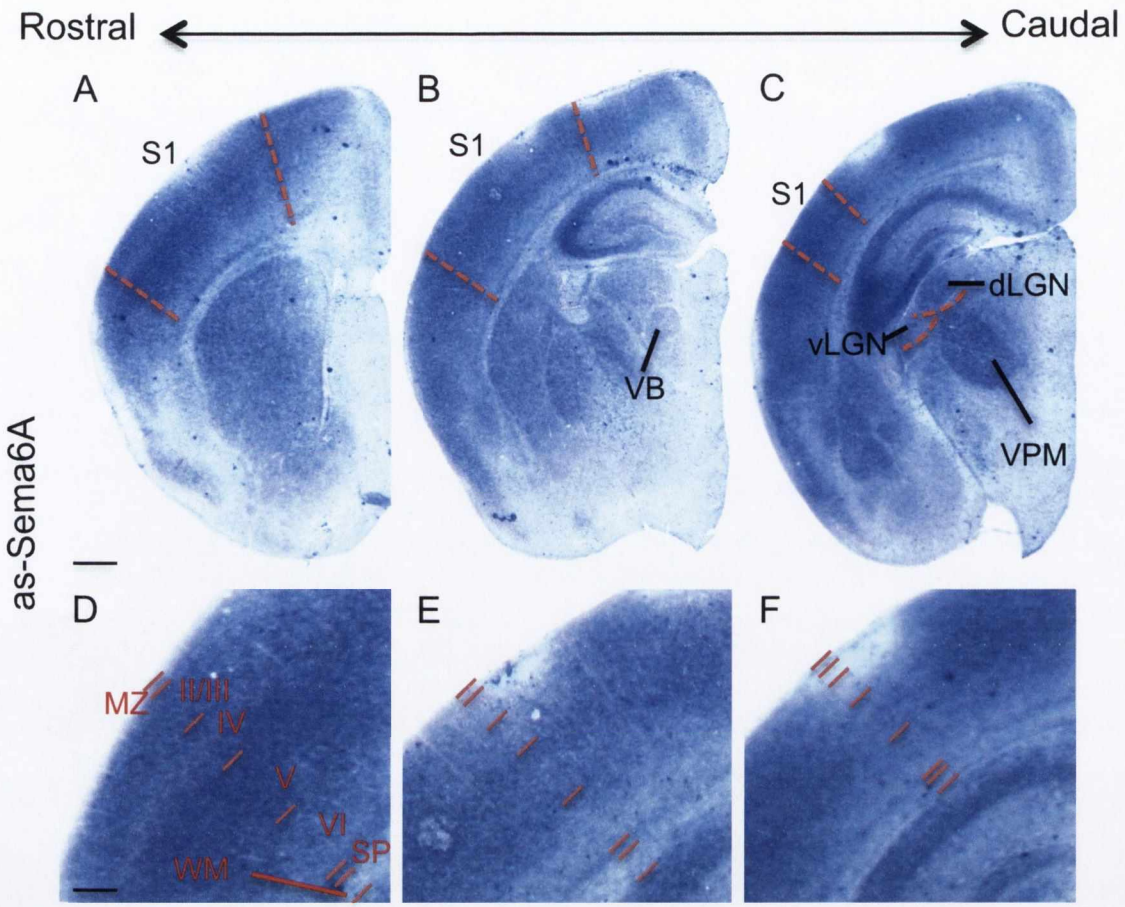


Figure 38. Expression levels of Sema6A in the mouse brain at P8

In situ hybridization revealed mRNA levels with antisense RNA probes against Sema6A. The latter is expressed throughout the thalamus (B and C), and quite strongly laterally in dorsal lateral geniculate nucleus (dLGN) and the ventral posteriomedial nucleus (VPM). In the somatosensory cortex (S1), Sema6A is broadly expressed, except in the barrels (D-F). D, E and F are higher magnifications of the cortex of A, B and C, respectively. VB, ventrobasal complex; vLGN, ventral lateral geniculate nucleus; MZ, marginal zone; II/III, cortical layers II and III; IV, cortical layer IV; V, cortical layer V; VI, cortical layer VI; SP, subplate; WM, white matter layer.

Scale: A to C 500μm; D to F 200μm.

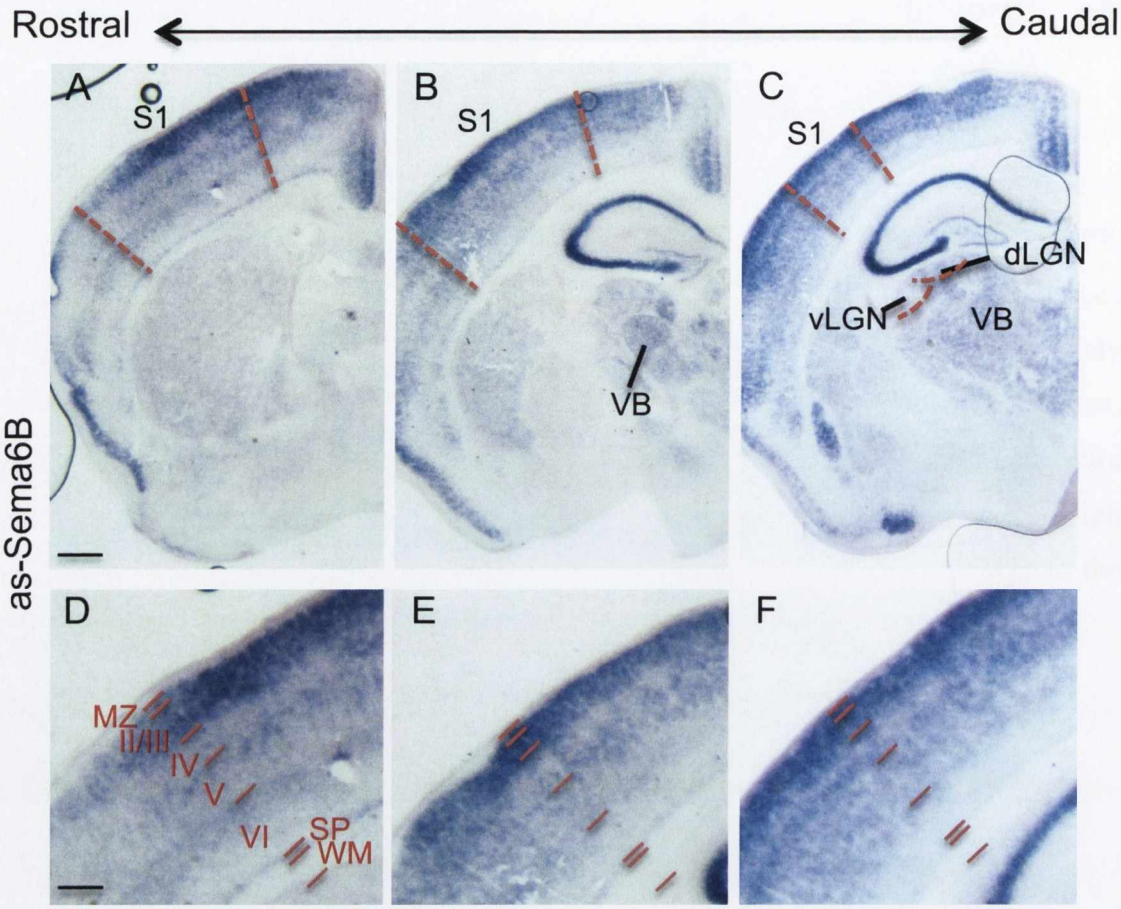


Figure 39. Expression levels of Sema6B in the mouse brain at P8

In situ hybridization revealed mRNA levels with antisense RNA probes against Sema6B. The latter is widely expressed throughout the thalamus (B and C). In the somatosensory cortex (S1), Sema6B expression is high in the marginal zone (MZ), cortical layers II and III (II/III), at the border between cortical layer IV (IV) and cortical layer V (V), and the subplate (SP; D-F). D, E and F are higher magnifications of the cortex of A, B and C, respectively. VB, ventrobasal complex; vLGN, ventral lateral geniculate nucleus; dLGN, dorsal lateral geniculate nucleus; VI, cortical layer VI; WM, white matter layer.

Scale: A to C 500µm; D to F 200µm.

Both Sema6A and PlexinA2 are weakly expressed at P8. PlexinA2 expression is characterized by higher levels in cortical layer VI of the somatosensory cortex (Figure 40 D to F). PlexinA4, however, is specifically expressed in the VPM (Figure 41C). In addition, its expression remains strong within the barrels and the cortical layers above (Figure 41 D to F). The outermost part of layer V shows no expression of PlexinA4, while layer VI and the subplate show weak expression.

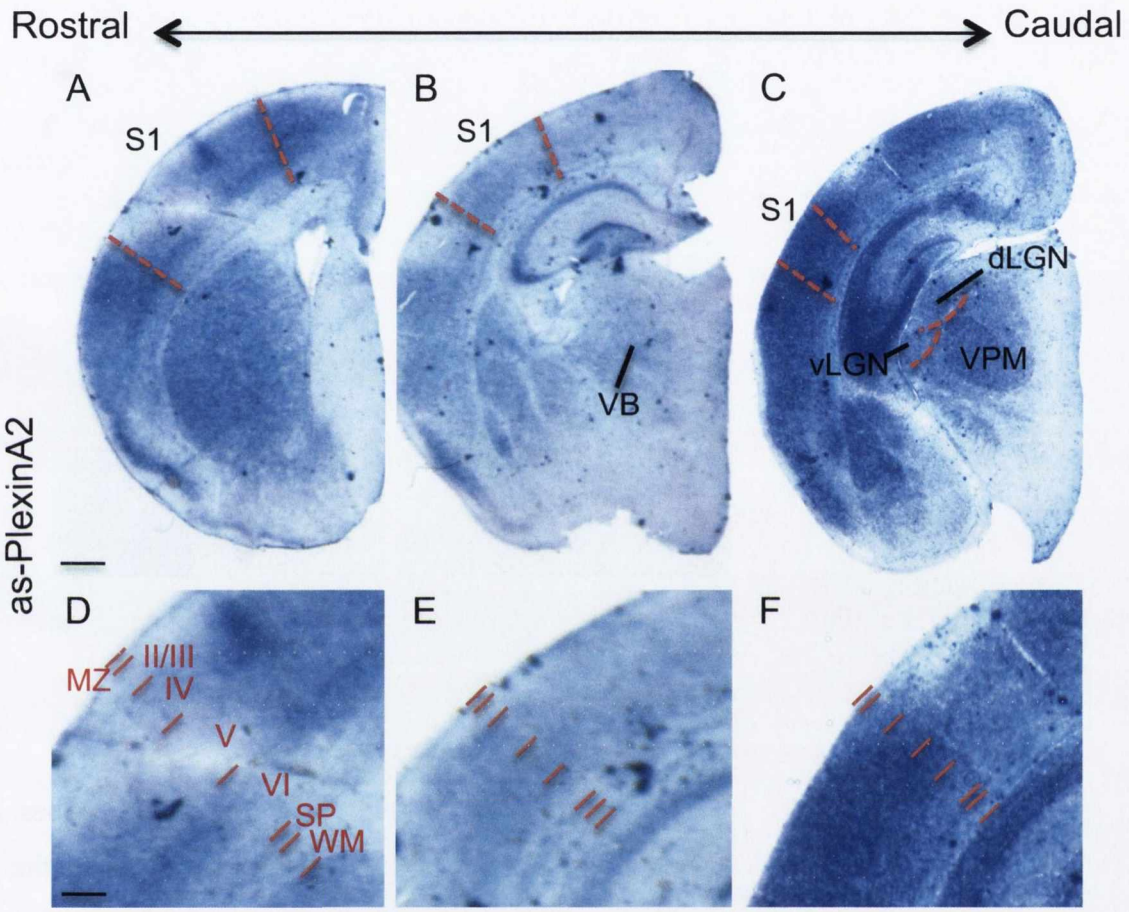


Figure 40. Expression of PlexinA2 in the mouse brain at P8

In situ hybridization revealed mRNA levels with antisense RNA probes against PlexinA2. The latter is weakly expressed throughout. In the somatosensory cortex (S1), PlexinA2 has higher expression in cortical layer VI (VI) compare to the other layers (D-F). D, E and F are higher magnifications of the cortex of A, B and C, respectively. VB, ventrobasal complex; vLGN, ventral lateral geniculate nucleus; dLGN, dorsal lateral geniculate nucleus; VPM, ventral posteriomedial nucleus; MZ, marginal zone; II/III, cortical layers II and III; IV, cortical layer IV; V, cortical layer V; SP, subplate; WM, white matter layer.

Scale: A to C 500μm; D to F 200μm.

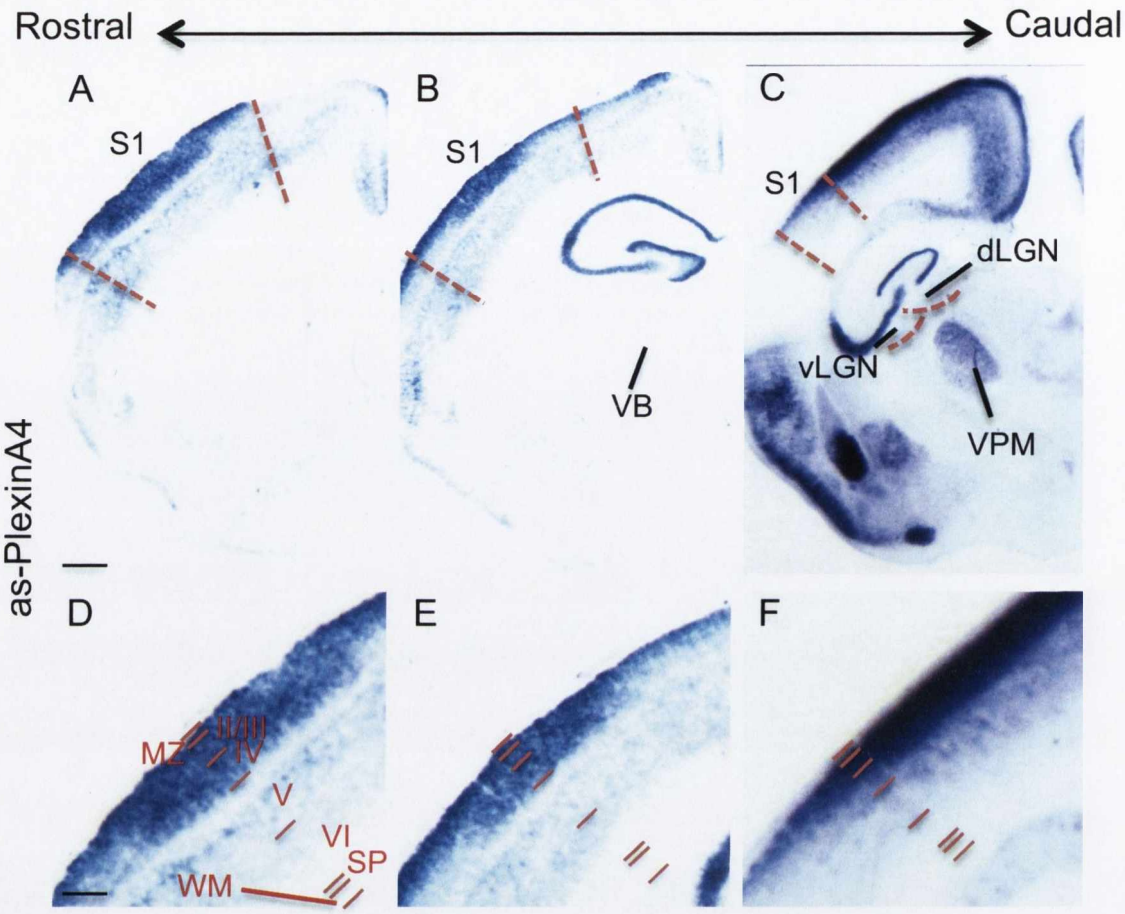


Figure 41. Expression levels of PlexinA4 in the mouse brain at P8

In situ hybridization revealed mRNA levels with antisense RNA probes against PlexinA4. The latter is predominantly expressed within the barreloids of the ventral posteriomedial nucleus (VPM) in the thalamus (C). In the somatosensory cortex (S1), PlexinA4 is expressed in the marginal zone (MZ), cortical layers II and III (II/III) and cortical layer IV (IV; D-F). The outermost part of cortical layer V (V) shows no expression of PlexinA4, while cortical layer VI (VI) and the subplate (SP) show weak expression. D, E and F are higher magnifications of the cortex of A, B and C, respectively. VB, ventrobasal complex; vLGN, ventral lateral geniculate nucleus; dLGN, dorsal lateral geniculate nucleus; WM, white matter layer.

Scale: A to C 500µm; D to F 200µm.

4.2.5 Protein expression patterns of PlexinA4 from late-embryonic to early postnatal stages

Although no functional antibodies for Sema6A, Sema6B or PlexinA2 were found reliable, we are able to provide protein expression patterns for PlexinA4 (Figures 20-22). PlexinA4 is strongly expressed in axons at E15.5 (Figure 42 B, C, E, F, H and I) and P2 (Figure 43 B, C, E, F, H and I) going from the thalamus to the cortex and the cortex to the thalamus. Moreover, the commissural projections also strongly express PlexinA4 (Figure 42 B and C, and Figure 43 B, C, E and F). At P8, PlexinA4 expression is predominantly within the barrel cortex (and the hippocampus; Figure 44 C and F). These data suggest that PlexinA4 is probably expressed in leading edges of TCAs, as only expression remains in the barrel cortex at P8. Moreover, it is interesting complementary data to the ISH data obtained in order to start teasing out which cells express PlexinA4 (ISH data) and where (IHC data).

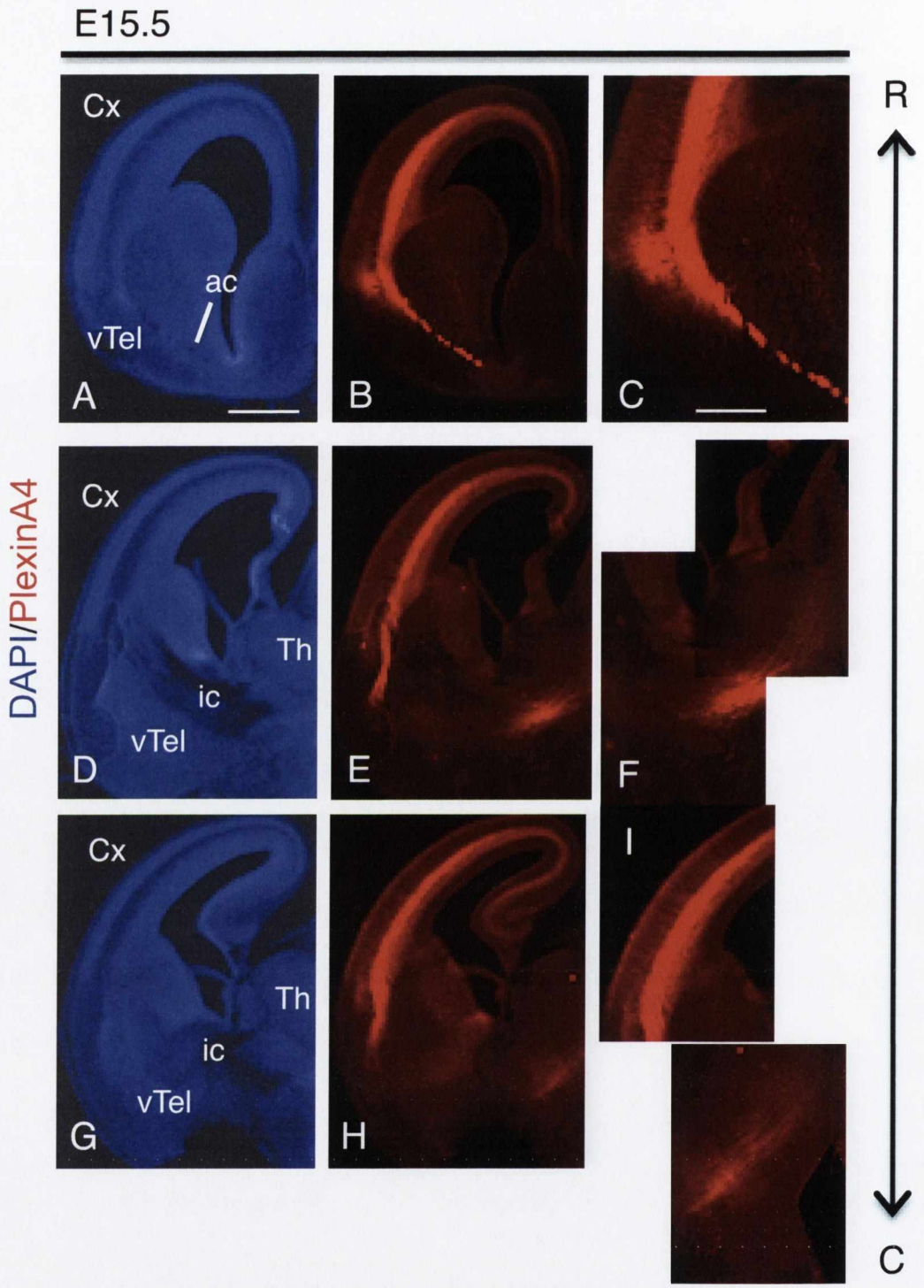


Figure 42. PlexinA4 expression in the mouse brain at E15.5

Immunohistochemistry revealed PlexinA4 protein expression in cortical and thalamic axons (B, C, E, F, H and I). A, D and G are DAPI staining. C, F and I are higher magnifications of B, E and H, respectively. Cx, cortex; ac, anterior commissure; vTel, ventral telencephalon; ic, internal capsule; Th, thalamus; R, rostral; C, caudal.

Scale: A, B, D, E, G and H 500μm; C, F and I 250μm.

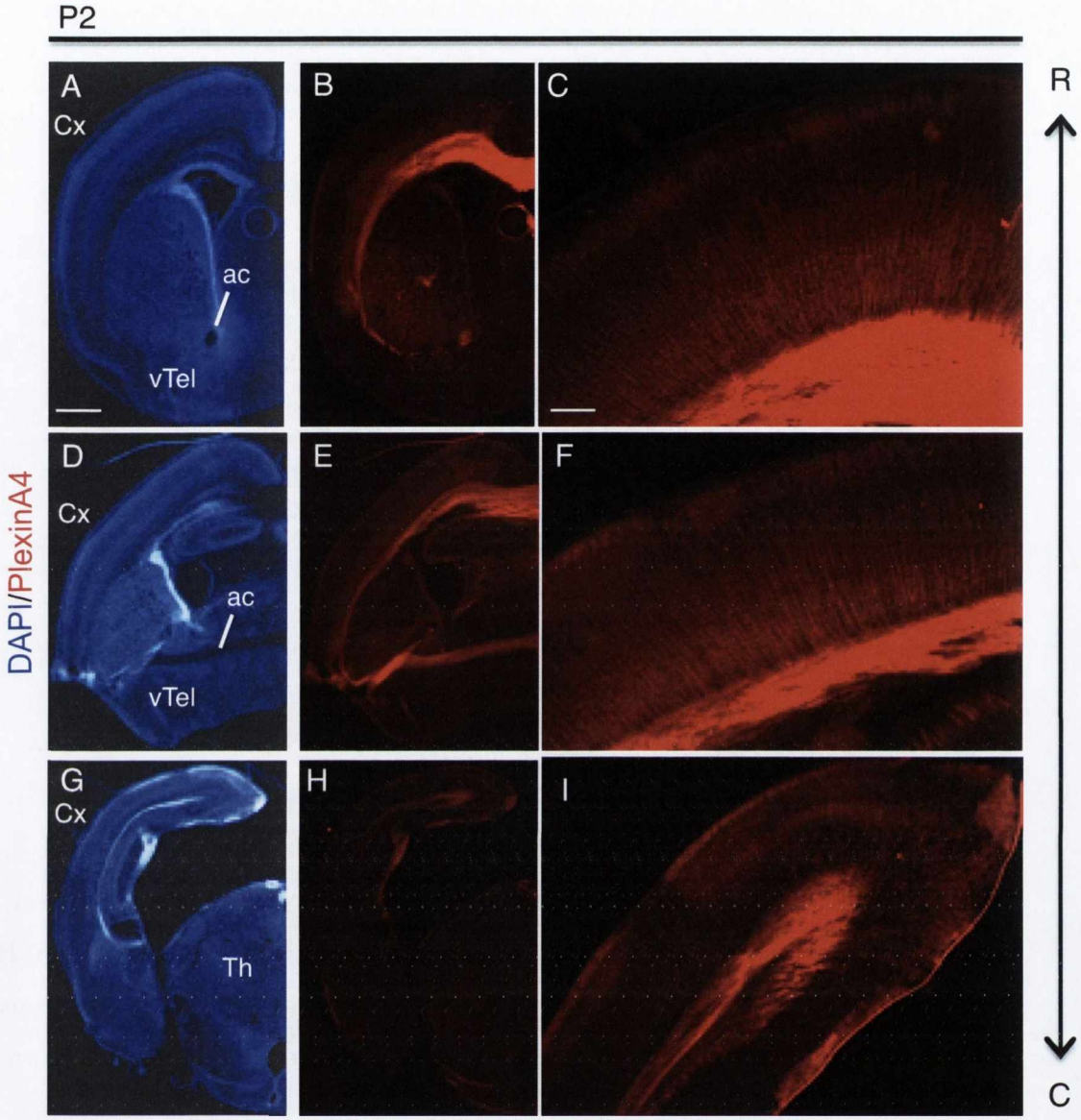


Figure 43. PlexinA4 expression in the mouse brain at P2

Immunohistochemistry revealed PlexinA4 protein expression in cortical and thalamic axons (B, C, E, F, H and I). A, D and G are DAPI staining. C, F and I are higher magnifications of B, E and H, respectively. Cx, cortex; ac, anterior commissure; vTel, ventral telencephalon; Th, thalamus; R, rostral; C, caudal.

Scale: A, B, D, E, G and H 500μm; C, F and I 125μm.

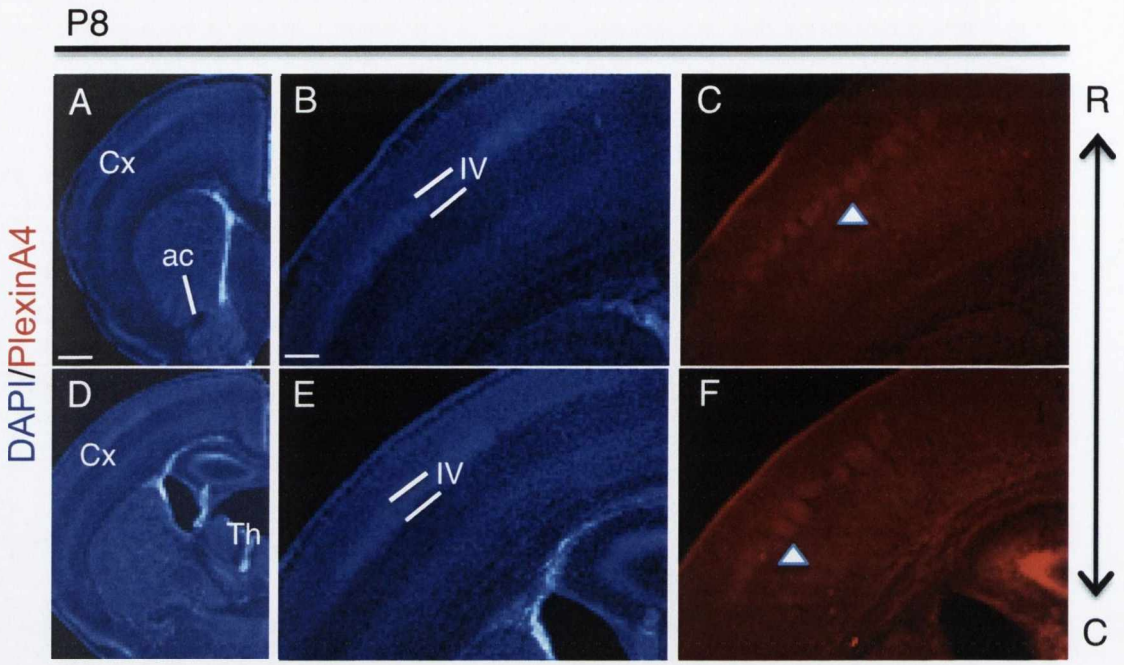


Figure 44. PlexinA4 expression in the mouse brain at P8

Immunohistochemistry revealed PlexinA4 protein expression in the barrels within cortical layer IV (IV) of the somatosensory cortex (arrowheads in C and F). A, B, D and E are DAPI staining. B and C are higher magnifications of A, while E and F are higher magnifications of D. Cx, cortex; ac, anterior commissure; Th, thalamus; R, rostral; C, caudal.

Scale: A and D 500μm; C and F 200μm.

These dynamic expression patterns suggest interesting roles of Sema6A, Sema6B, PlexinA2 and PlexinA4 in thalamic connectivity towards the somatosensory cortex (and cortical axons towards the thalamus) at time-points previously characterized as essential for proper development. Noteworthy are the striking patterns within the VPM, and within or around the barrels of the somatosensory cortex.

4.3 Discussion

This study presents expression data of Sema6A, Sema6B, PlexinA2 and PlexinA4 in the first postnatal week of life in the mouse brain. During this time in development, TCAs reach their targets in cortical layer IV, and extensive refinement occurs. Multiple cues are expected to be required to properly orchestrate these steps. So, extracellular molecules previously implicated in axon guidance with different patterns of expression in the areas of interest represent invaluable tools to further understand the yet elusive process of brain wiring.

Previous studies have looked into the expression patterns of members of the class A Plexins, however at different stages of development and different areas of the brain. Nonetheless, the expression of PlexinA4 in the somatosensory system has been reported previously. At E16.5, Suto and colleagues (2003) noted the expression of PlexinA4 in the VPL/VPM regions of the thalamus. In addition, they observed strong expression of PlexinA4 in the marginal zone at E15.5, which was maintained at P0, and a moderate ISH signal in layer IV of the somatosensory cortex at P16. No other time-points were investigated in that study regarding the somatosensory system. Moreover, a couple of years later, the same group described a defect in the barrel formation in adult PlexinA4 mutant mice through cytochrome oxidase histochemistry (Suto et al, 2005). The boundary of the barrels did not show clear definition as seen in wildtype control mice, and the authors suggested that the lack of PlexinA4 in the TCAs from the VPM, as predicted by ISH in their previous study, caused these axons to terminate diffusely within the barrel cortex. However, these studies determined PlexinA4 expression patterns only (and only through ISH). PlexinA2, Sema6A and Sema6B expression was not investigated.

In addition, previous work in our laboratory also laid some groundwork for this present study. Nonetheless, the highly changing thalamic and cortical environments during the first postnatal week prompted us to further investigate expression patterns at closer time-point intervals.

4.3.1 Combinatorial expression patterns of Sema6A, Sema6B, PlexinA2 and PlexinA4 in thalamic nuclei

Both Sema6A and Sema6B are widely expressed throughout the thalamus at all time-points investigated (P2, P4, P6 and P8). However, Sema6A persists as being a

marker of the dLGN, but also the vLGN and the VB. This gene would also appear to be expressed more laterally as the first postnatal week progresses. Although Sema6B is also widespread throughout the thalamus, its levels of expression in the VB are quite interesting. Barreloids in the VPM are nicely identifiable through Sema6B expression, already at P2 patches start being discernable. Sema6B is not strongly expressed in the vLGN nor the dLGN, however some expression is detectable constantly from P2 to P8. In addition, PlexinA2 and PlexinA4 are differentially expressed ventrally. The former gene is nicely expressed ventrally throughout the thalamus, and this expression pattern persists throughout the first postnatal week. PlexinA4 is widespread throughout the ventral thalamus at P2, but as the days go by, becomes nicely localized to the VB, and more specifically to the VPM. From P4 to P8, the barreloids are nicely discernable. Although ISH reveals the presence of specific mRNA, this data is only indicative of potential protein expression. However, taken together, this data suggests that during the first postnatal week Sema6B is widely expressed throughout the thalamus, as well as Sema6A, although Sema6A appears like a potential marker more laterally as the days go by. PlexinA2 is ubiquitously expressed ventrally. PlexinA4 initially shows a similar pattern of expression, but by P8 is localized in the VPM. In regards to thalamocortical connectivity to the barrel field of the somatosensory cortex, all four genes could play a role, as their expression intersects in the VPM. What's more, PlexinA4 is not expressed in the posterior nucleus of the thalamus after P2 (but all three other genes are), which is interesting because the projections from that nucleus to the somatosensory cortex terminate in the septum and not the barrel center. This adds to the specificity of barrel center TCAs.

4.3.2 Combinatorial expression patterns of Sema6B, Sema6A, PlexinA2 and PlexinA4 in the somatosensory cortex

Sema6A expression in the somatosensory cortex is characterized by expression in the marginal zone and in layer V from P2 to P8; however, its expression is dynamic. At P2, Sema6A is detected in decreasing levels from layer V to the white matter layer. At P4, expression appears in cortical layer IV. When barrels become visible, Sema6A expression is seen in cortical layers II and III, at the border between cortical layers IV and V, and in the subplate. At P8, Sema6A is not as easily detected but is widespread, except in the barrel field. As for Sema6B, at P2 its expression is detectable in the marginal zone, the outermost end of the cortical plate (which will become cortical

layers II and III) and cortical layer V. At P4, Sema6B is expressed throughout the cortex in descending intensity from the marginal zone to the white matter layer. Two days after, Sema6B exhibits a similar pattern of expression as Sema6A at the same time-point, which Sema6B maintains at P8. PlexinA2 is characteristically expressed in the marginal zone, cortical layer VI and the subplate throughout the time-points observed. However, expression is detected in all layers as well, except for cortical layer IV. Finally, PlexinA4 expression starts high in the marginal zone and decreases towards the white matter layer at P2 and P4. At P6, there is a switch where no more expression is visible in cortical layer V. The strongest expression remains from the marginal zone to cortical layer IV. Taken together, these data allow for some speculation. For instance, Sema6B is expressed within all layers of the somatosensory cortex at P2. However, at P6, its expression is found surrounding the barrel field, not only above and below cortical layer IV, but also medially and laterally. Given this data, Sema6B (and Sema6A, and PlexinA2 in a distinct combination) could be guiding the TCAs from the VPM to the appropriate target cortical layer by repulsing the TCAs from non-permissive areas (initially the immature cortical layers and subsequently the areas surrounding the barrels). Taken together, Sema6B expression is outside the barrels while PlexinA4 expression is within from P6. In addition, the immunohistochemistry results nicely demonstrate that PlexinA4 is expressed within the thalamic (and cortical) axons. It could also be expressed within dendrites in cortical layer IV (or even axonal mRNA). These data will allow for comprehensive analyses of phenotypic effects of these proteins *in vivo*.

4.3.3 Perspectives

Many studies have determined roles of transcription factors in thalamic and cortical arealization during development. However, the effectors of these factors, which actually mediate the cytoarchitectural reorganization, are only beginning to be unraveled. Focus has targeted ephrins, L1 and its close homolog (CHL1), and cadherins, as they were hypothesized to be involved in axon guidance due to their timing of expression and their functions in cell-cell adhesion. A combinatorial code of thalamocortical connectivity has been established between the differentially expressed Eph receptors in the thalamus and ephrins in the cortex to allow proper targeting between and within cortical areas from the thalamus (Dufour, Seibt et al. 2003). Although L1 and CHL1 had been implicated separately in axon guidance and synapse

plasticity, a recent study has revealed specific cooperation of these two factors in a subset of TCAs projecting to the motor cortex by associating with the ephrinA/EphA and inducing growth cone collapse (Demyanenko, Siesser et al. 2011). Suzuki, Inoue et al. (1997) found interesting combinatorial patterns of expression of type-II classic cadherins (namely Cdh6, 8 and 11) in both the thalamus and the cortex postnatally. In addition, more recent studies have added to the expression specificity of these cadherins within the somatosensory system. Indeed, Cdh8 was detected in the septa of the barrel cortex through ISH (Gil, Needleman et al. 2002), and another group corroborated and expanded the developmental time-points investigated for Cdh6 expression within the thalamus (Szabo, Zhao et al. 2009). Interestingly, it was found that subsets of axons within the same tracts differentially express Cdh2 and Cdh4, suggesting a finer refinement of target recognition as not all axons departing from the same area have the same destination (Obst-Pernberg, Medina et al. 2001). The idea of a combinatorial code of connectivity is emerging as a strong one for the Semaphorin6s and the PlexinAs as well as only a subset of dLGN TCAs are misrouted in the Sema6A mutant mice (Leighton, Mitchell et al. 2001, Little, Lopez-Bendito et al. 2009). With the same hypotheses in mind (dynamic spatiotemporal expression patterns and extracellular transducers of cytoskeletal reorganization), we ventured into thalamocortical development of the somatosensory cortex in *Sema6B* mutant mice, since very little is known about that molecule, keeping in mind possible interactions or redundancy with *Sema6A* and *PlexinA4*.

Chapter 5

Investigating Thalamocortical Connectivity in the Early Postnatal Somatosensory Cortex

5.1 Introduction

The dynamic spatiotemporal expression patterns of Sema6A, Sema6B, PlexinA2 and PlexinA4 during the first postnatal week in the somatosensory system prompted us to investigate possible functions for these genes in this context. Suto, Ito et al. (2005) described an interesting phenotype in the barrel cortex of *PlexinA4-/-* adult mutant mice. Indeed, they found through cytochrome oxidase labeling that the boundaries of individual barrels were indistinct in these mutant mice compared to clearly defined barrels in wild-type age-matched controls. The rodent somatosensory system presents interesting whisker-to-barrel features that allow us to use it as a great model for connectivity. Here, we present novel roles for *Sema6A*, *PlexinA2* and *PlexinA4*, and in particular for *Sema6B*, in proper invasion of thalamic axons into the cortical plate and cellular organization within cortical layer IV of the somatosensory cortex. We hypothesize that *Sema6B* could be a cell-surface effector of activity-dependent processes in the somatosensory cortex.

5.1.1 Barrel cortex development

The somatosensory system in mice is characterized, in part, by the lemniscal whisker-to-barrel isomorphic representation. Each individual cortical barrel mainly receives input from a single whisker (Armstrong-James and Fox 1987). Trigeminal nerve projections from the base of whiskers innervate the brainstem through discrete barrelettes, which in turn project to the contralateral barreloids in the ventral posteriomedial nucleus (VPM) of the thalamus (Agmon, Yang et al. 1995). Thalamocortical axons (TCAs) from the VPM organize in tight bundles in what are called barrel hollows. These are delimited by cortical layer IV cell bodies known as barrel walls. Cortical layer IV neuron dendrites are oriented towards the barrel hollows (Woolsey and Van der Loos 1970, Inan and Crair 2007). At birth, TCAs from the ventral posteriomedial nucleus of the thalamus begin to innervate the cortical plate through genetically specified mechanisms (Lopez-Bendito and Molnar 2003, Inan and Crair 2007). At this stage, TCAs and cortical cells are randomly spread in the developing cortical layer IV (Figure 45). Postnatal day 2 marks the day that TCAs start organizing in patches forming whisker-related clusters in layer IV of the somatosensory cortex, generating a rough topographic map of the whisker pad on the snout (Rebsam, Seif et al. 2002). In addition, axons start forming rows within the VPM and will become visible barreloids by P3 (Erzurumlu and Gaspar 2012). Studies have shown that P4 ends

the critical period for structural plasticity following surgical procedures such as whisker follicle or infraorbital nerve damage, or whisker trimming (Durham and Woolsey 1984, Datwani, Iwasato et al. 2002, Rebsam, Seif et al. 2005, Erzurumlu and Gaspar 2012). Moreover, all cortical neurons have reached their target layer and barrel aggregates will become apparent shortly after this time-point (Lopez-Bendito and Molnar 2003). Two days later, at P6, cortical layer IV neurons migrate toward the edges of the barrels and acquire polarized dendritic morphology, and thalamocortical connections to interneurons occur (Espinosa, Wheeler et al. 2009). Activity-dependent processes then refine these projections, restricting to specific barrels the arbors of TCAs receiving inputs from specific whiskers up until the end of the second postnatal week. It is well established that these processes can be disrupted by altering activity or by mutations affecting NMDA or serotonergic signaling. However, the effectors of these signals, which actually mediate the cytoarchitectural reorganization, are not known.

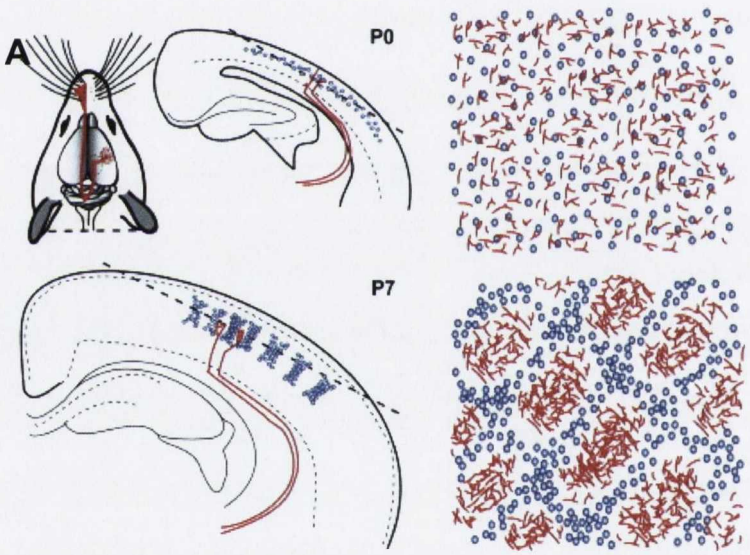


Figure 45. Maturation of the barrel cortex

Schematic of the lemniscal whisker-to-barrel pathway in the mouse brain (A). Around P0, TCAs reach the cortical plate, however, both TCAs and layer IV cells are evenly distributed. Around P7, TCAs organize in tight bundles in what are called barrel hollows around which layer IV cells form the barrel walls (barrel hollows are not completely devoid of cell bodies, however). Coronal cartoons depict the level of cortical layer IV where a tangential cut has been taken (broken line). Magnifications to the right show the organization of the barrel cortex at P0 and P7 in that tangential plane.

From Molnar and Molnar (2006).

5.1.2 Activity-dependent mechanisms of barrel refinement

As soon as the TCAs invade the cortical plate, the interplay between TCAs and cortical layer IV neurons becomes essential for proper development. Both genetic programs become interdependent, and neuronal activity becomes crucial for proper maturation (Inan and Crair 2007). Neurotransmission from presynaptic to postsynaptic cells is essential for the barrel field patterns to mature properly, and is characterized by presynaptic serotonergic receptor activity and postsynaptic glutamatergic receptor activity (Erzurumlu and Kind 2001). Downstream signaling pathways have been investigated through transgenic mouse models and have uncovered interesting roles for N-methyl-d-aspartate receptor (NMDAR) subunits 1 and 2B, metabotropic glutamate receptor 5 (mGluR5), adenylyl cyclase 1 (Adcy1), protein kinase A (PKA), phospholipase C (PLC), monoamine oxidase type A (MAOA), synaptic Ras GTPase-activating protein 1 (SynGAP1), serotonergic transporter (5-HTT), LIM domain-only 4 (Lmo4) and neurogenic differentiation factor 2 (NeuroD2) transcription factors, brain-derived neurotrophic factor (BDNF), tyrosine kinase receptor type 2 (TrkB), EphrinA5 and neurofibromin (Nf1; Figure 46), since mutant mice show barrel cortex defects (Inan and Crair 2007, Wu, Ballester Rosado et al. 2011). After the first postnatal week, the requirement for serotonin fades as shown by the lack of its signaling machinery (Inan and Crair 2007, van Kleef, Gaspar et al. 2012).

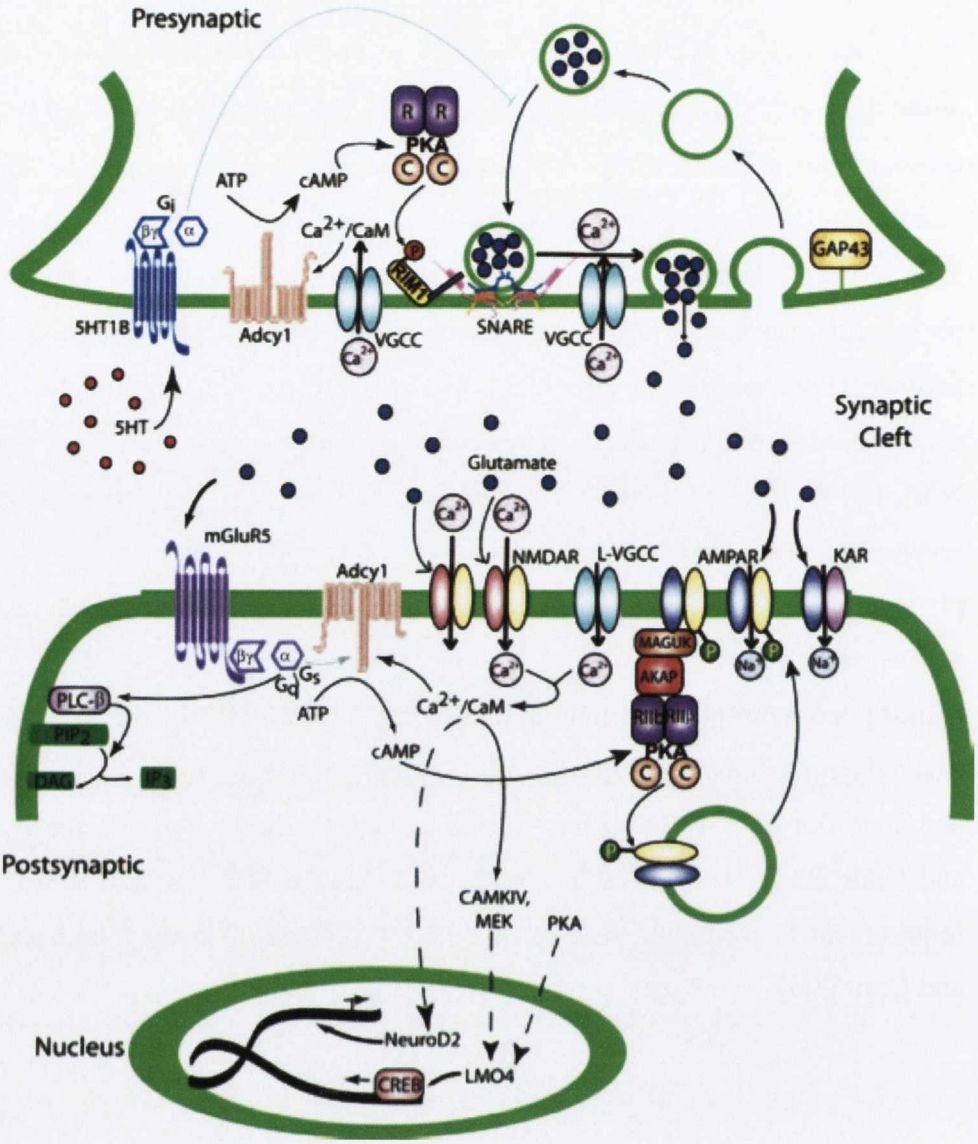


Figure 46. Activity-regulated signaling pathways during maturation of thalamocortical synapses

Presynaptic: When an action potential arrives at a thalamocortical axon (TCA) terminal, voltage-gated calcium channels (VGCC) are activated and let calcium enter thereby stimulating release of vesicles containing glutamate. Intracellular calcium binds to calmodulin (Ca2+/CaM) to activate Adcy1, which catalyzes cAMP formation. The latter binds to the regulatory subunits of protein kinase A (PKA-R) dissociating regulatory from catalytic subunits, thus activating the catalytic subunits (PKA-C). One target of PKA is Rim1α, which regulates vesicular release. Serotonin (5-HT) present at

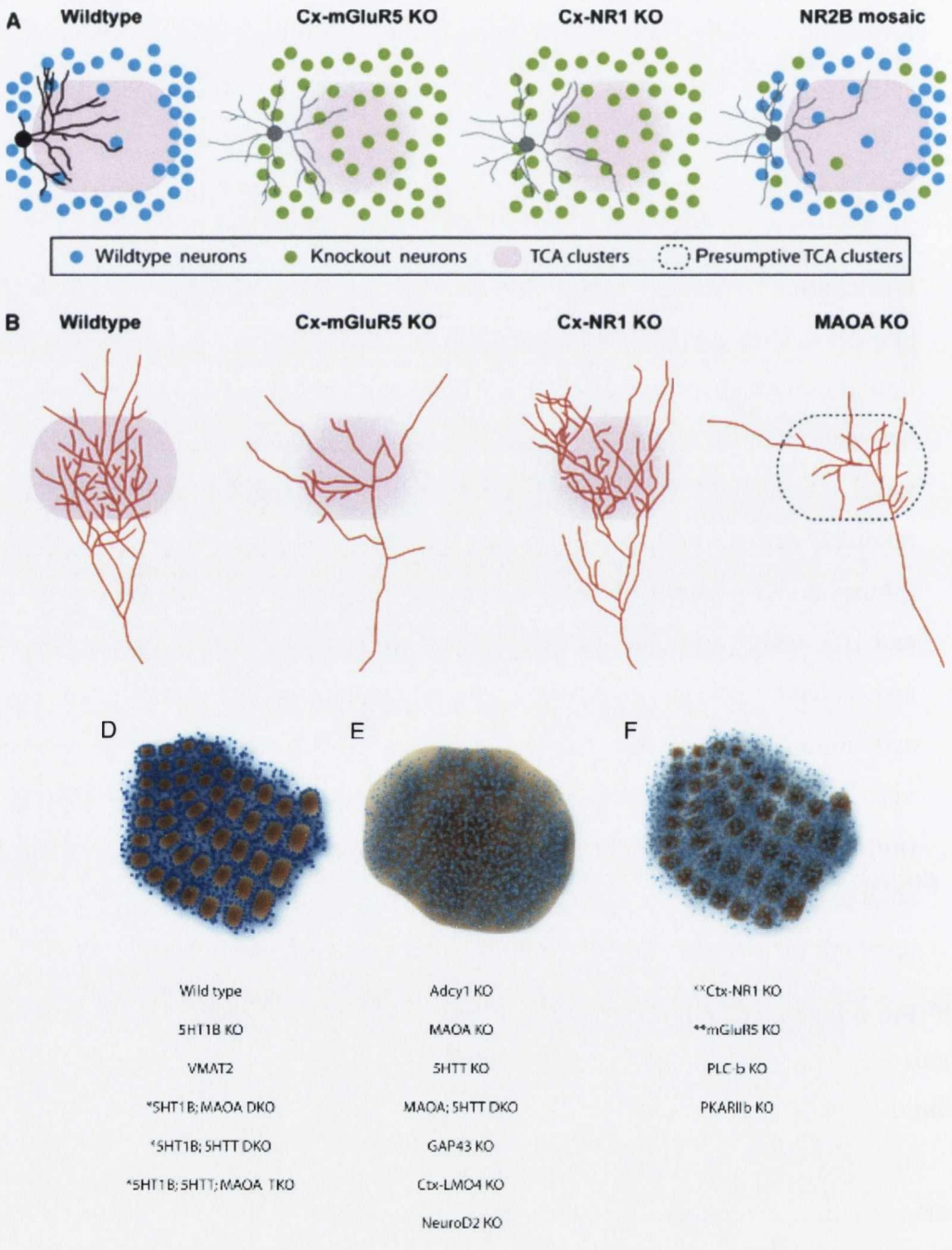
the synaptic cleft activates 5HT1B receptors, which may negatively regulate glutamate release via G-proteins (such as Gi). 5HT can also be transported into the TCA terminals by 5HTT and can be stored into vesicles by VMAT2.

Postsynaptic: Glutamate released from the presynaptic terminal activates ionotropic glutamate AMPA (amino-3-hydroxyl-5-methyl-4-isoxazolepropicreaseonate) and kainate receptors (KARs). Ion flow through these receptors depolarizes the postsynaptic membrane, consequently stimulating VGCCs. Depolarization and glutamate binding activates NMDARs and, in turn, calcium influx through NMDARs and VGCCs leads to formation of Ca2+/CaM, which can stimulate different signaling cascades. Ca2+/CaM activates Adcy1, which activates PKA signaling. PKA is localized in close proximity to glutamate receptors via interaction of its type II regulatory subunits (like PKARIIβ) with AKAPs (A-kinase anchoring proteins). AKAPs can bind to MAGUKs (membrane associated guanylate kinase) that interact with AMPARs and NMDARs. This localization provides specificity for PKA function. At the membrane, PKA phosphorylates AMPAR subunits (such as GluR1) leading to the insertion of AMPARs into the postsynaptic membrane. Although there is no evidence for an interaction between mGluR5 and cAMP signaling, Adcy1 function may be regulated by mGluR5, which stimulates G proteins (such as Gs) upon activation via glutamate binding. mGluR5 activates PLC-β by G proteins (such as Gq), which in turn cleaves PIP2 [phosphatidylinositol (4,5) bisphosphate] to generate two secondary messengers, DAG and IP3, which stimulate different signaling cascades such as protein kinase C (PKC) and calcium release from intracellular calcium stores. Ca2+/CaM also regulates activation of transcription factors such as NeuroD2 and LMO4. The latter is regulated via Ca2+/CaM stimulation of CaMKIV (Ca2+/CaM-dependent kinase IV) and MEK (mitogen-activated protein or extracellular signal-regulated kinase kinase). SNARE, soluble NSF (N-ethylmaleimide sensitive factor) attachment receptor; CREB, cAMP response element-binding. See text for additional abbreviations.

From Inan and Crair (2007).

5.1.3 Barrel cortex phenotypes

Transgenic mice with mutations in genes involved in activity-dependent mechanisms of barrel cortex development exhibit different types of phenotypes (Figure 47). They are mainly described according to their TCA clustering patterns, cortical layer IV cell organization and dendritic orientation. Seminal work from the last twenty years has brought an array of players to light (some presented in the previous section).



(Legend overleaf)

Figure 47. Barrel cortex phenotypes

Examples of reconstructed cortical layer IV spiny stellate neurons and single TCAs in wild type, Cx-mGluR5-KO, Cx-NR1-KO and NR2B mosaic mutant mice (A and B). Wild type mice layer IV spiny stellate neurons display polarized dendritic morphology with the majority of their dendrites projecting toward the barrel hollow (pink; A). In both Cx-mGluR5 and Cx-NR1 mutant mice, layer IV neurons are evenly distributed in the barrel field and have symmetric dendritic morphology. In NR2B mosaic mutant mice, layer IV neurons located in the barrel walls show non-polarized dendritic pattern. Wild type axon arbors in layer IV develop from a single axon, forming numerous axon collaterals, with a dominant orientation of the branches toward the barrel center; individual TCAs form highly branched and densely clustered arbors corresponding to the mapped facial whisker (B). In Cx-mGluR5 mice and MAOA mutant mice, the complexity of TCA arbors is much reduced, and collaterals grow in divergent directions instead of forming a narrow cluster. In Cx-NR1 mutant mice, TCAs have exuberant branches. Tangential schematics of the main classes of activity-dependent barrel cortex phenotypes with regards to TCA clustering and barrel wall formation compared to wild-type mice (D to F).

A and B from Wu, Ballester Rosado et al. (2011), and D to F from Inan and Crair (2007).

Spontaneous mutations introduced in CD1 mouse lines at the Université de Lausanne revealed a barrelless phenotype (Welker, Armstrong-James et al. 1996). These mice still present normal topological organization, although TCA arbors are exuberant and cortical layer IV cells do not form distinguishable barrel rings. Tight spatiotemporal relays were lost. The mutation was mapped to Adcy1 thereby implicating for the first time cAMP signaling pathways to brain patterning (Abdel-Majid, Leong et al. 1998). This finding led to the rationale of exploring transgenic mutant models of or pharmacologically blocking signaling molecules regulating Adcy1 activity. Much attention was focused on NMDARs, and a cortex-specific NR1 subunit knockout showed TCA clusters that were less defined than normal, although discernable, but no barrel wall formation (Iwasato, Datwani et al. 2000). Moreover, it was subsequently described that proper dendritic polarization towards barrel hollows was also lost in these mutant mice (Datwani, Iwasato et al. 2002). Activation of transcription factors in this pathway has also been implicated in barrel cortex development, such as LMO4 through conditional loss in the forebrain with defective clustering of TCAs and barrel ring formation (Kashani, Qiu et al. 2006), NeuroD2 through null mice with barrel cortex organization disruption (Ince-Dunn, Hall et al. 2006), BTB/POZ domain-containing 3 (Btbd3) through knockdown with shRNA with deregulated dendritic orientation of cortical layer IV neurons (Matsui, Tran et al. 2013), and LIM homeobox 2 (Lhx2) through a conditional cortex knockout with no recognizable barrel cortex features (Shetty, Godbole et al. 2013). Different reviews have detailed the phenotypes observed in molecules involved in this pathway (Erzurumlu and Kind 2001, Lopez-Bendito and Molnar 2003, Inan and Crair 2007, Wu, Ballester Rosado et al. 2011).

In addition, transgenic models affecting the serotonergic homeostasis during the first postnatal week have clearly demonstrated its role in barrel map formation, adding to the complexity of barrel cortex maturation. Mutant mice with excess serotonin induced by disrupted activity of MAOA or the serotonin transporter display severe whisker map phenotypes with lack of TCA clusters and barrel cellular organization (Cases, Vitalis et al. 1996, Salichon, Gaspar et al. 2001). However, mice with deficient levels of serotonin in the synaptic cleft elicit normal barrel map formation (Persico, Mengual et al. 2001).

Importantly, other molecules regulate barrel cortex organization independently of neurotransmission. Cell surface molecule neural cell adhesion molecule (NCAM) does so on barrels of the anterolateral barrel subfield and the most distal barrels of the posteriomedial barrel subfield as mutant mice exhibit no distinctive segregation of TCAs of those barrels through cytochrome oxidase labeling (Enriquez-Barreto, Palazzetti et al. 2012). In addition, RORβ is expressed in cortical layer IV during barrel cortex maturation and induces barrel wall cluster formation (Jabaudon, Shnider et al. 2012). Interestingly, RORβ overexpression as early as E18 (prior to TCA invasion of the cortex) induces the cytoarchitectural changes normally observed at later time-points.

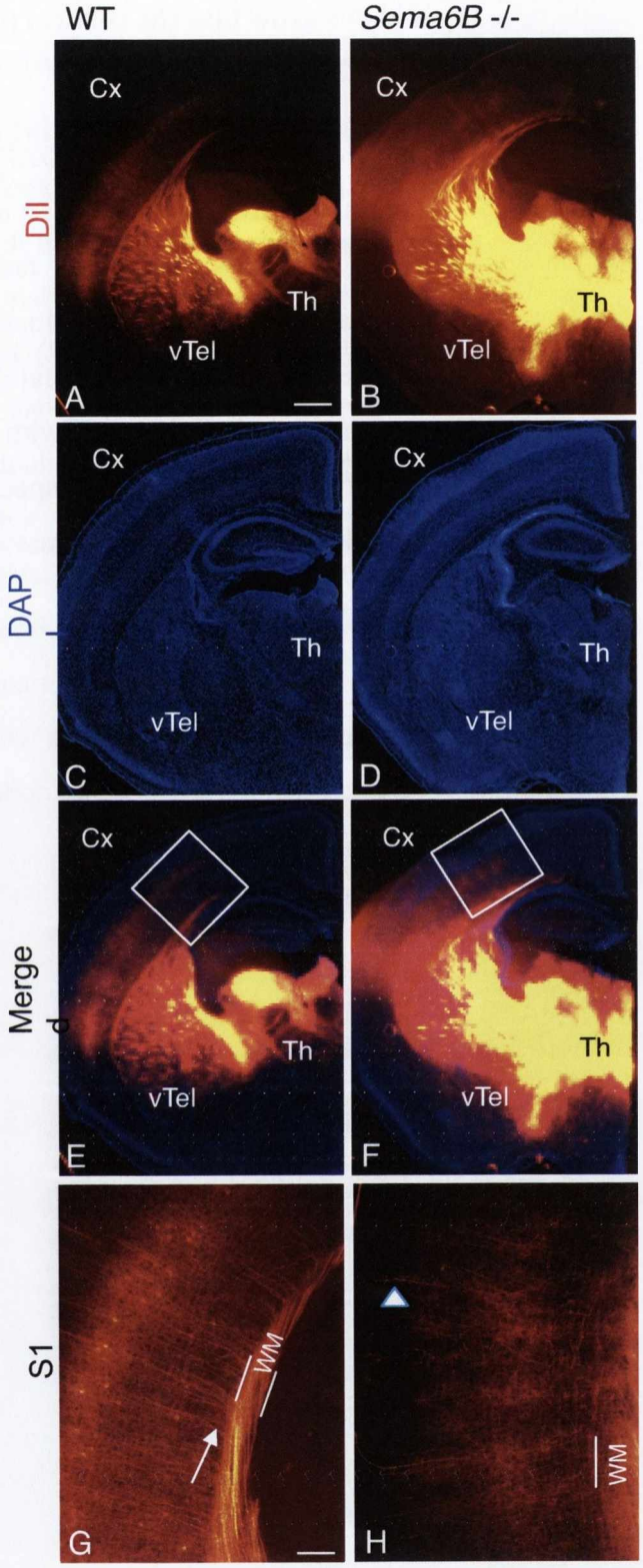
5.1.4 Aims of this study

Given the expression patterns that we observe for Sema6A, Sema6B, PlexinA2 and PlexinA4 from P2 to P8 in the VPM and the somatosensory cortex, and the phenotype reported in the adult *PlexinA4-/-* mouse barrel cortex (Suto, Ito et al. 2005), we aim to investigate key elements of barrel cortex formation, that is TCA clustering into barrels in cortical layer IV and cortical layer IV neuron formation of barrel walls, particularly in *Sema6B-/-* mice as very little is known about this gene. However, it is impossible to study the function of Sema6B without keeping in mind the closely-related protein Sema6A, and the binding partners PlexinA2 and PlexinA4. The somatosensory system also comprises barrelettes (brainstem) and barreloids (thalamus) in the brain, we intend to investigate their integrity in case defects are observed in *Sema6B-/-* mice.

5.2 Results

5.2.1 Thalamocortical axons have abnormal trajectories through the somatosensory cortex of Sema6B-/- mice

The interesting expression patterns from chapter 4 enticed us into looking into possible functions of *Sema6B* in thalamocortical connectivity development. Since very little is known about *Sema6B*, we explored different time-points relevant to key steps in proper TCA journey to the cortex. We did not find any striking defects embryonically; however, at P8, loss of *Sema6B* function became apparent in the somatosensory cortex through dye tracing experiments (Figure 48). Indeed, *Sema6B-/-* mice exhibit a few abnormalities. First, TCAs invade the cortical plate at abnormal locations following zigzag trajectories to reach their targets in layer IV (Figure 48H) compared to the highly ordered way in which TCAs normally innervate the cortical plate (Figure 48G). Second, some TCAs extend beyond cortical layer IV to cortical layers II/III (Figure 48H arrowhead).



(Legend overleaf)

Figure 48. Thalamocortical axons grow into the cortical plate at abnormal positions in *Sema6B*-/- mice at P8

Coronal sections of dye tracing from the thalamus and DAPI counterstain in wild-type (A and C) and *Sema6B*-/- (B and D) mouse brains at P8. In normal development, TCAs innervate the cortical plate in a highly organized fashion (G). Axons extend perpendicularly from the white matter (WM) at specific locations (arrow). However, in *Sema6B*-/- mice, the TCAs have extended into the cortical plate at abnormal positions (H) and into layers II/III (arrowhead) as can be seen with DiI tracing. G and H are higher magnifications of the square boxes in E and F, respectively. WT, wild-type; Cx, cortex; Th, thalamus; vTel, ventral telencephalon; S1, somatosensory cortex.

Scale: A to F 500μm; G and H 150μm.

5.2.2 Sema6A and PlexinA4 null mutant mice also exhibit defects in thalamocortical axons trajectories through the somatosensory cortex

Since Sema6B is closely related to Sema6A, and they both are known to interact with PlexinA4, we looked into the somatosensory cortices of *Sema6A* and *PlexinA4* null mutant mice (as well as *Sema6A/Sema6B* double knockouts) for potential phenotypes, together with our collaborators in Japan (Figure 49). Interestingly, all null mutants show the zigzag phenotype (Figure 2E, H, K and N), with *Sema6B* and *PlexinA4* null mutant mice exhibiting more drastic phenotypes compared to *Sema6A-/-* mice. *Sema6A/Sema6B* double knockout mice appear to have additive defects in the somatosensory cortex. Moreover, confocal microscopy allowed us to appreciate the extent of these defects, as well as evaluating the lack of definition in individual barrels in layer IV in *Sema6B*, *Sema6A*, *Sema6A/Sema6B* double knockout and *PlexinA4* null mutant mice (compare Figure 49C to Figure 49F, I, L and O). *Plexin-A1-/-* mice, however, do not show any phenotype in this context (data not shown, mutant mice only housed by our collaborators).

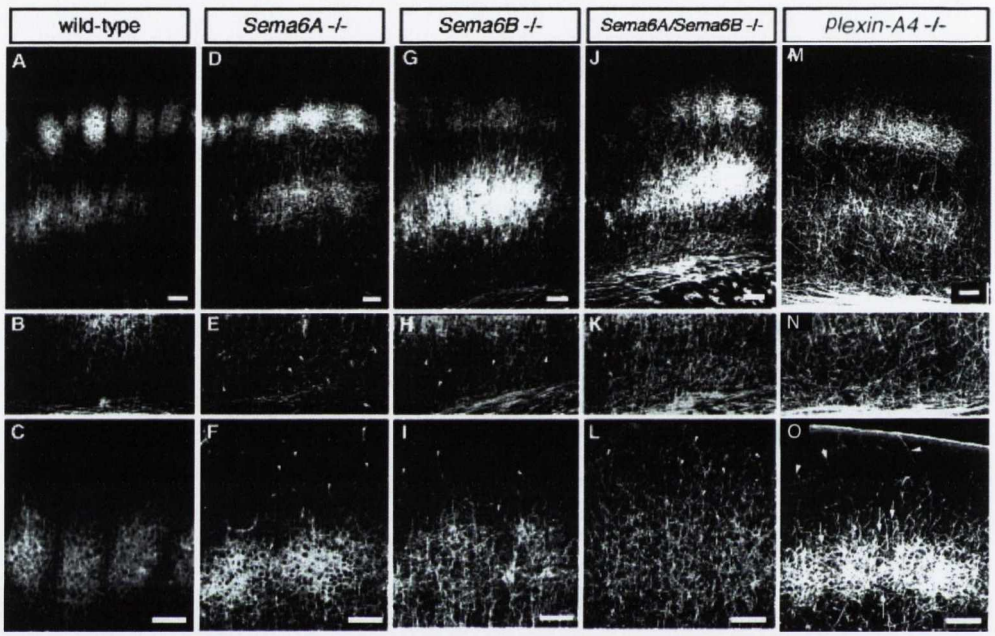


Figure 49. Thalamocortical projections in *Semaphorin* and *PlexinA4* null mutant mice at P7

Survey of thalamocortical projections in the somatosensory cortex of *Sema6A*, *Sema6B*, *Sema6A/Sema6B* and *PlexinA4* null mutant mice with DiI tracing from the ventral posteriomedial nucleus of the thalamus at P7. Null mutant mice exhibit several abnormalities. The boundary of individual barrels in layer IV is not clearly defined in all the mutants, compare wild-type (A or C) to *Sema6A-/-* (D or F), *Sema6B-/-* (G or I), *Sema6A/Sema6B* double knockout mice (J or L) and *PlexinA4-/-* (M or O). Moreover, these mutants display abnormal trajectories from the subplate to their target area in layer IV, compare B to E, H, K and N (arrowheads). Finally, several fibers project beyond layer IV to layers II/III, compare C to F, I, L and O (arrowheads).

Figure from Fujisawa's group in Japan. We obtained similar results.

5.2.3 Preplate splitting occurs normally in Sema6B-/- mice

We hypothesized that the zigzag phenotype we observe at P8 may result from (1) a failure of pleplate splitting or (2) the inability of TCAs to respond to subplate cues. We have found that Neto1 is a marker of subplate cells at E15.5. Other animal models suggest that improper preplate splitting can be observed by calretinin, a marker of Cajal-Retzius cells, labeling at E18.5 (Rakic, Davis et al. 2006). Both *in situ* hybridization and immunohistochemistry revealed that proper preplate splitting is occurring in *Sema6B-/-* mice (Figure 50). Thus, this data is more supportive of the latter hypothesis. However, although the subplate looks grossly normal, few populations of cells could have been displaced to the marginal zone. Subplate cells are heterogeneous and no pan marker is known for them. This could explain the phenotype.

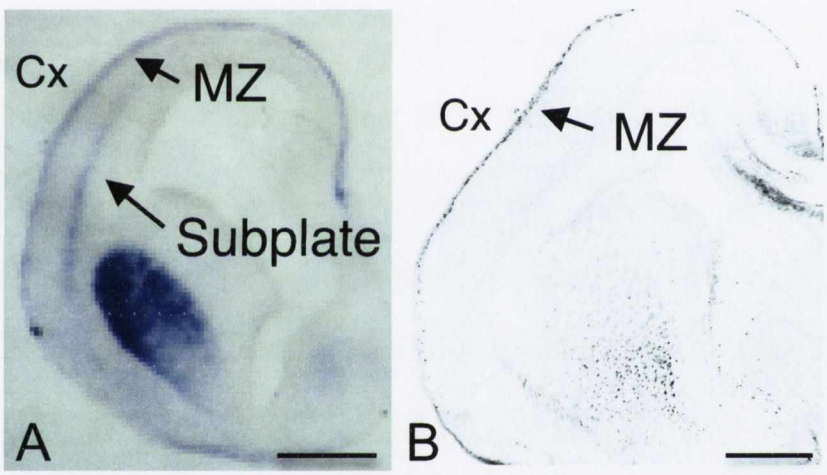


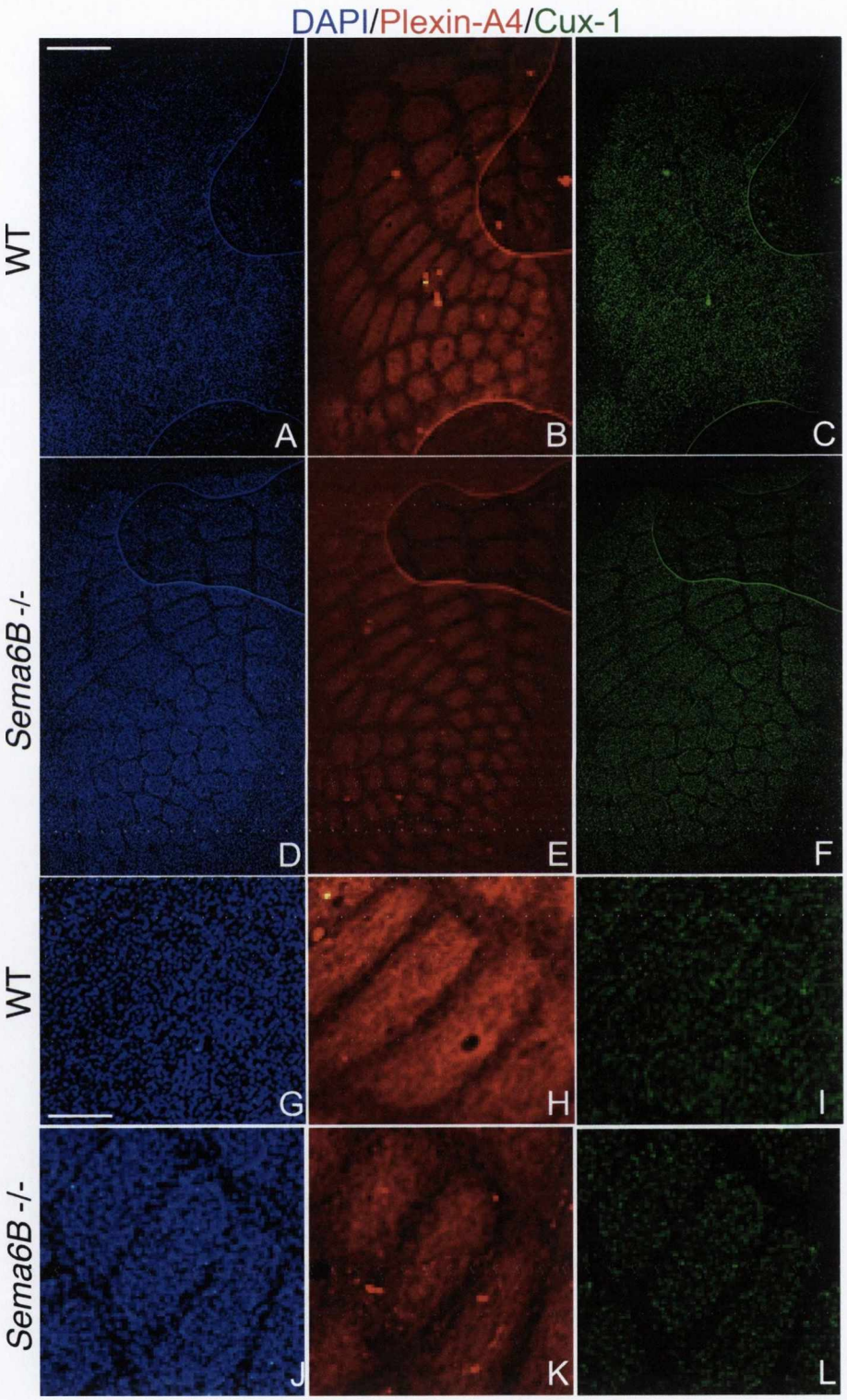
Figure 50. Proper preplate splitting occurs in *Sema6B-/-* mice

Proper preplate splitting takes place in *Sema6B-/-* mice. Neto1 expression patterns detected through *in situ* hybridization show normal distribution in *Sema6B-/-* mouse brain at E15.5 (A). Calretinin expression revealed by immunohistochemistry is localized to the marginal zone (MZ) in the cortex of *Sema6B-/-* mice as seen in wild-type mice at E18.5 (B).

Scale: A and B 500μm.

5.2.4 Cux-1 positive cells are found at abnormal positions in the barrel cortex of Sema6B-/- mice

In parallel to early defects that could explain the phenotypes observed, we continued exploring the environment of the somatosensory cortex at P8, more specifically cortical layer IV. Maturation of the barrel cortex involves TCAs to aggregate in tight bundles at the level of cortical layer IV, also known as barrels, after the first postnatal week. Moreover, layer IV neurons organize themselves around these barrels forming walls (there are still cells present in the hollows of the barrels, but higher densities are found within the walls). A previous study determined Cux-1 as a valuable marker of cortical layer IV neurons in the somatosensory cortex (Ferrere, Vitalis et al. 2006). In the context of *Sema6B-/-* mice, Cux-1 positive cells are found at abnormal positions within barrel hollows of the somatosensory cortex (Figure 51). We used PlexinA4 expression as a marker of the barrels (Figure 51B, E, H and K). Interestingly, PlexinA4 could be a marker of layer IV dendrites at P8, since the defect detected by dye tracing is not mimicked by PlexinA4 labeling. Both the VPM and the cortex express PlexinA4 mRNA at P8. In situ hybridization revealed that PlexinA4 expressing cells are not displaced in the barrel cortex of *Sema6B-/-* mice and remain mainly at the level of the barrel walls (Figure 52).



(Legend overleaf)

Figure 51. Cortical layer IV neurons are found at abnormal positions within the barrels in *Sema6B-/-* mice at P8

Layer IV cells are found at abnormal positions in the barrel cortex of *Sema6B-/-* mice. Immunohistochemistry revealed higher densities of Cux-1 positive cells in barrel hollows of flattened cortices of P8 *Sema6B-/-* mice (F and L) compared to wild-type mice (C and I). G to L are higher magnifications of A to F, respectively. A to C and G to I are sections from wild type mice, whereas D to F and J to L are from *Sema6B-/-* mice. WT, wild-type.

Scale: A to F 750μm; G to L 250μm.

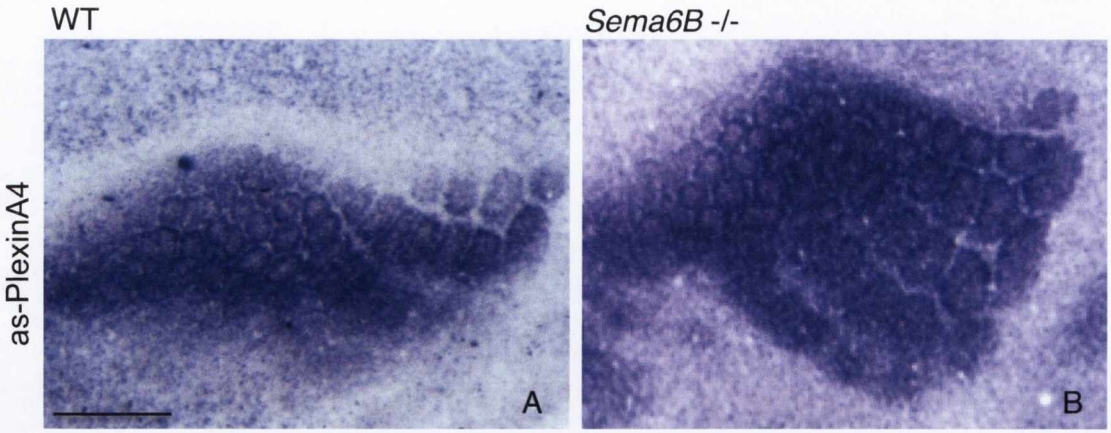


Figure 52. PlexinA4 is expressed in the barrels of *Sema6B-/-* mice similar to wild-type

In situ hybridization of flat cortices revealed that PlexinA4 expression patterns remain similar in *Sema6B-/-* (B) and wild-type mice (A).

Scale: A and B 500μm.

Confocal microscopy allowed further exploring cortical layer IV cell phenotype in individual barrels (Figure 53). Surprisingly, Plexin-A4 expressing fibers avoid Cux-1 positive cells in *Sema6B-/-* mice (Figure 53 I and J). What's more, this avoidance makes individual barrels look porous (Figure 53 E and F). In some ways, *Sema6B-/-* barrels seem more structured than the wild-type barrels. PlexinA4 and the vesicular glutamate transporter 2 (VGluT2), a marker of presynaptic glutamatergic axon terminals and of barrel interior (Nakamura, Hioki et al. 2005, Liguz-Lecznar and Skangiel-Kramska 2007), do not grossly colocalize (compare Figure 53 E and G).

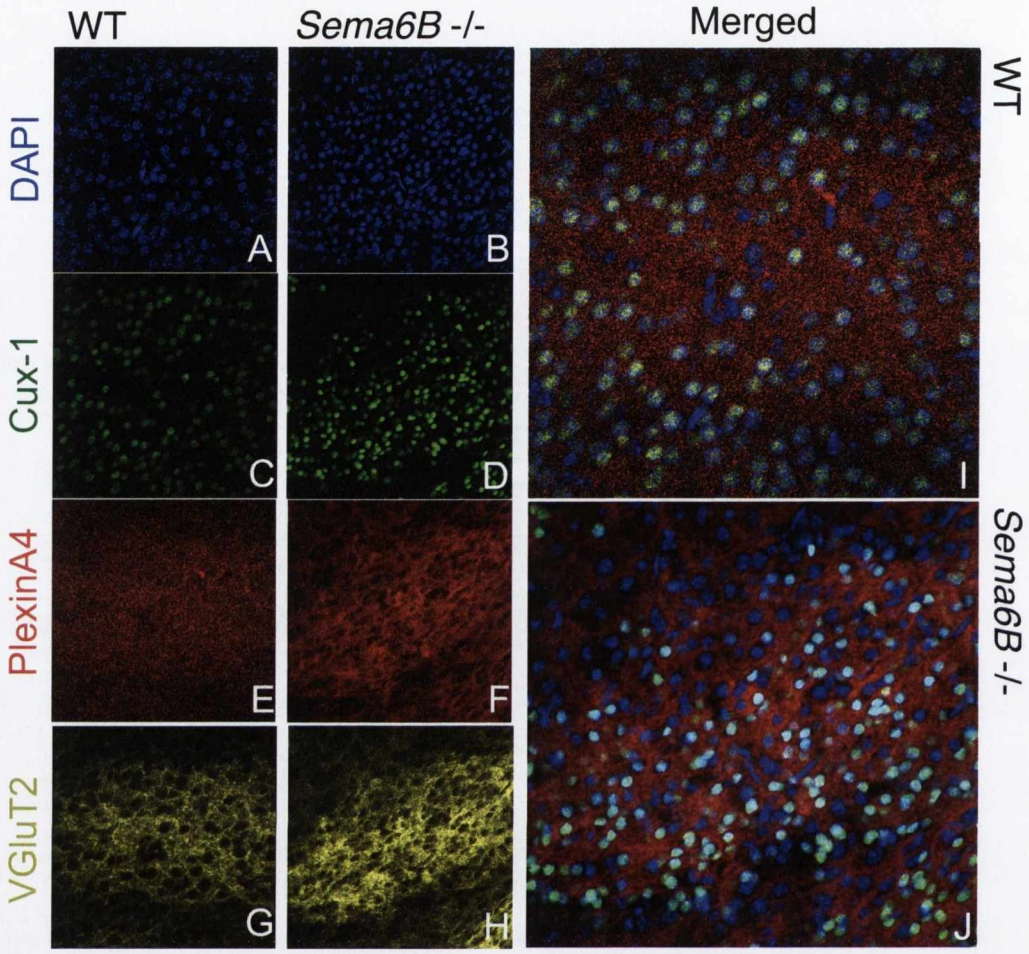
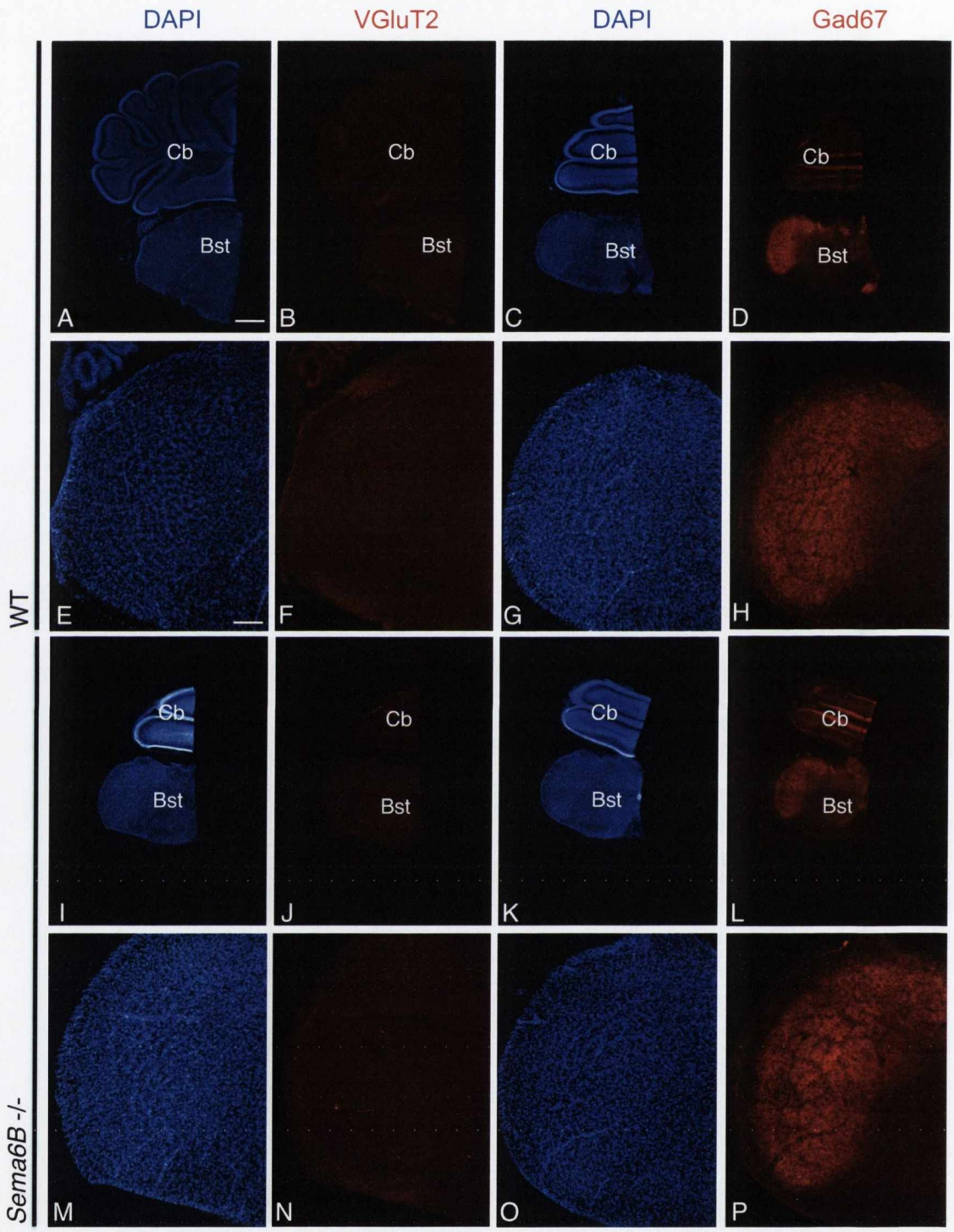


Figure 53. PlexinA4 expressing fibers avoid Cux-1 expressing cells in *Sema6B*-/- mouse barrel cortex at P8

Immunohistochemistry of individual barrels showed higher densities of layer IV Cux-1 positive cells within the barrel hollows (compare C and D). In addition, Plexin-A4 positive fibers avoid these cells (compare merged images of DAPI, PlexinA4 and Cux-1 I and J). Indeed, *Sema6B*-/- barrel in F is more porous than wild-type barrel in E. A, C, E, G and I are images from a representative wild-type barrel, whereas B, D, F, H and J are images from a representative barrel from *Sema6B*-/- mice. VGluT2, vesicular glutamate transporter 2; WT, wild-type.

5.2.5 Barrelettes and barreloids are unaffected in Sema6B-/- mice at P8

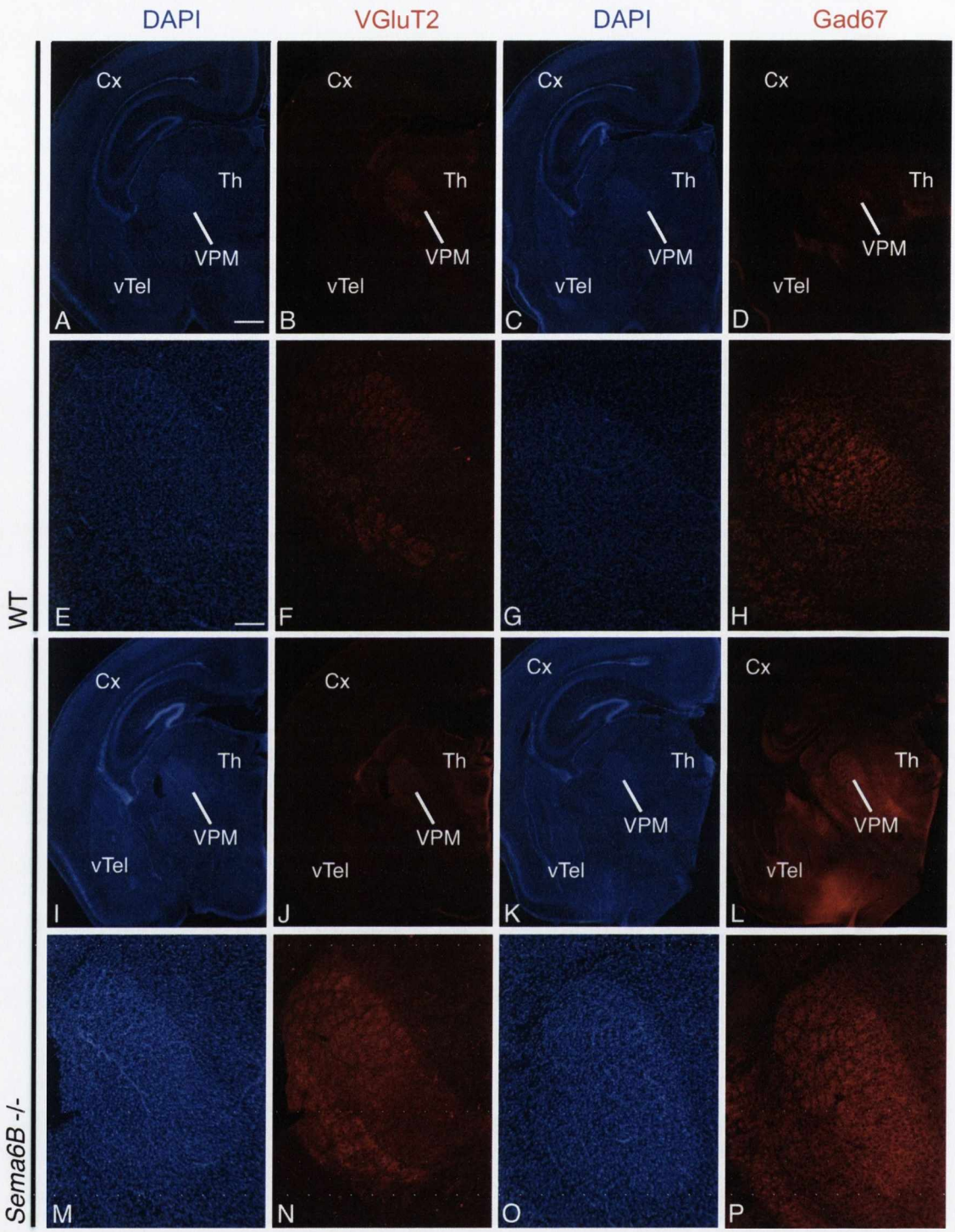
In the brain, the whisker-to-barrel somatosensory system comprises barrelettes in the brainstem and barreloids in the thalamus. The barrelettes, barreloids and barrels are all characterized by the one-to-one represention of individual whiskers. Moreover, they are all highly innervated by axons, and so are composed of areas of low cell densities surrounded by areas of higher cell densities or walls. As with the barrels, the vesicular glutamate transporter 2 is a marker of the interior of the barreloids (Nakamura, Hioki et al. 2005). Glutamic acid decarboxylase 67 (Gad67) has recently been added as a marker of the barreloids (Meyer, Egger et al. 2013). Although some body of work has been done on the barrelettes, it is mainly through cytochrome oxidase labeling. We investigated the integrity of barrelettes and barreloids in *Sema6B-/-* mice at P8. Here, we show that both VGluT2 and Gad67 are markers of the barrelettes (Figure 54 B and F for VGluT2, and Figure 54 D and H for Gad67). In addition, we report that there are no striking differences between wild-type and *Sema6B-/-* mouse barrelettes (Figure 54). The same is true for the barreloids of wild-type and *Sema6B-/-* mice (Figure 55).



(Legend overleaf)

Figure 54. Barrelettes are normal in *Sema6B*-/- mice at P8

Immunolabeling of coronal sections with vesicular glutamate transporter 2 (VGluT2) and glutamic acid decarboxylase 67 (Gad67) antibodies, and counterstained with DAPI in wild-type (A to H) and *Sema6B*-/- (I to P) mice. E to H are higher magnifications of the brainstem (Bst) of whole wild-type coronal sections in A to D, respectively. M to P are higher magnifications of the brainstem of whole *Sema6B*-/- coronal sections in I to L, respectively. WT, wild-type; Cb, cerebellum. Scale: A-D, I-L 500μm; E-H and M-P 150 μm.



(Legend overleaf)

Figure 55. Barreloids are normal in *Sema6B*-/- mice at P8

Immunolabeling of coronal sections with vesicular glutamate transporter 2 (VGluT2) and glutamic acid decarboxylase 67 (Gad67) antibodies, and counterstained with DAPI in wild-type (A to H) and *Sema6B*-/- (I to P) mice. E to H are higher magnifications of the ventral posteromedial nucleus (VPM) of whole wild-type coronal sections in A to D, respectively. M to P are higher magnifications of the VPM of whole *Sema6B*-/- coronal sections in I to L, respectively. WT, wild-type; Cx, cortex; vTel, ventral telencephalon; Th, thalamus.

Scale: A-D, I-L 500μm; E-H and M-P 150 μm.

5.3 Discussion

This study presents new phenotypes in *Sema6A*, *Sema6B*, *Sema6A/Sema6B* double knockout and *PlexinA4* null mutant mice in the context of thalamocortical connectivity in the somatosensory cortex at P8.

5.3.1 Thalamocortical axons follow irregular trajectories within the somatosensory cortex of Sema6A, Sema6B and PlexinA4 null mutant mice

Thalamocortical axons have abnormal trajectories from the white matter layer to their target cortical layer IV. Indeed, they exhibit a zigzag phenotype as opposed to invading the cortical plate in an orderly fashion perpendicular to the white matter layer. Moreover, TCA extensions into cortical layer II/III are more exuberant in the null mutant mice examined, and the barrel boundaries are less defined. *Sema6B* and *PlexinA4* null mutant mice show more severe phenotypes in single knockout mutant mice. However, *Sema6A*-/- mice also display the phenotypes at a lesser extent. Interestingly, *Sema6A/Sema6B* double knockout mutant mice appear to have additive effects, showing most drastic phenotypes. This data suggests potential interaction between *Sema6B* and *PlexinA4*, and some level of additive effects between *Sema6A* and *Sema6B* function.

5.3.2 Sema6B-/- mice display normal preplate splitting

Previous studies have reported premature and disorganized invasion of TCAs into the cortical plate of the *reeler* mouse due to improper preplate splitting (Caviness and Korde 1981, Molnar, Adams et al. 1998). We investigated whether the same was true in *Sema6B*-/- mice; however, our data suggests proper preplate splitting is occurring, and more likely that TCAs are lacking the ability to respond to subplate cues. Many studies have emphasized the lack of pan subplate markers, and we could have therefore missed populations of misplaced subplate cells, since we only looked into two different markers. Nonetheless, no exuberant projections are seen embryonically through the cortical plate in *Sema6B*-/- mice (data not shown).

5.3.3 Cux-1 expressing neurons are found at abnormal positions in the barrel cortex of Sema6B-/- mice

Fortunately, a few markers are available to explore the environment of cortical

layer IV. Cux-1 is a neuronal marker of cortical layers II to IV, with highest expression in layer IV in the somatosensory cortex. Many studies of the barrel cortex have utilized Cux-1 labeling as indication of neuronal localization. We find that in *Sema6B*-/- mice Cux-1 positive cell concentrations are abnormally high within the barrel hollows. More specifically, the densities of these cells do not appear to decrease from same barrel wall to wall. Surprisingly, the septa are maintained discernable through lower presence of cells. Other mutant mice exhibiting defects in the barrel cortex have not shown such a phenotype. These mutants have been divided in three groups of distinct charactersitics: 1) TCAs cluster normally within barrel hollows but barrel walls, although close to wild-type morphology, are comparatively less defined, 2) TCAs aggregate as in wild-type mice but layer IV cells do not show any particular organization, and 3) TCAs do not cluster within barrel hollows and barrel wall organization is disrupted (Inan and Crair 2007). Basically, barrel phenotypes are classified depending on TCA and barrel wall organization. From this, we can add a fourth category of defects as seen in *Sema6B*-/- mice: TCAs do not cluster normally and barrel hollows do not form. In both fronts, a repulsive signal appears to be missing. Taken together with the expression data from Chapter 4, the absence of Sema6B surrounding the barrels does not allow TCAs to be confined to the barrels be it extending exuberantly into layers II/III or the septa of the barrel cortex. Moreover, Sema6A presence does not compensate for the lack of Sema6B. In addition, Cux-1 expressing neurons are not repelled from the barrel hollows (although they are from the septa). Interestingly, PlexinA4 is expressed within the neuropil of the barrels. The absence of Sema6B and PlexinA4 interaction within the barrel hollows might explain the phenotype we see. Furthermore, PlexinA4 expressing cells do not appear to have changed localization in *Sema6B* mutant mice remaining in the barrel walls. On the other hand, we see colocalization of PlexinA4 and cortical layer IV cells in wild-type barrels, but not in *Sema6B*-/- mouse barrels. Not only are these cells irresponsive to PlexinA4, they avoid the neuropil expressing it. Perhaps Sema6B and PlexinA4 function in conjunction with other guidance molecules. The data we have gathered reveals quite a complex picture. Like in the case of L1 and CHL1 discussed in the previous chapter, a third player could specifically target TCAs and cortical layer IV cells in the barrel cortex in addition to Sema6B and PlexinA4. Future work will help elucidate this picture.

5.3.4 Barrelettes and barreloids do not show defects in Sema6B-/- mice

The whisker-to-barrel system comprises barrelettes in the brainstem and barreloids in the thalamus. We investigated their integrity through known and speculated markers. Both barrelettes and barreloids remain intact in *Sema6B*-/- mice as determined by DAPI, VGluT2 and Gad67 labeling. Gad67 nicely allows for clear visualization of the barrelettes in the brainstem, which was not previously reported.

5.3.5 Perspectives and future directions

Our data directly implicates *Sema6A*, *Sema6B* and *PlexinA4* in proper thalamocortical connectivity in the somatosensory cortex. We address particular interest to Sema6B, since little is known about this molecule in brain development, and clear phenotypes are revealed in mutant mice of this gene. It is impossible to study Sema6B function without also paying attention to the other potential players of this system. However, we are in early days of understanding its role in the barrel cortex.

We find novel phenotypes in the null mutant mice explored. Dye tracing allowed visualizing thalamocortical axons invading the somatosensory cortex. However, this technique is qualitative and the outcome highly dependent on the amount of dye absorbed by the neurons in the thalamus or the ventral posteriomedial nucleus of the thalamus. Data obtained in *PlexinA2-/-* mice was inconclusive due to the amount of labeling within the somatosensory cortex. We explored other possible venues to circumvent this issue. First, we spent time refining Golgi staining techniques, but no counterstain was successful. We therefore could not be certain of the cells labeled. We then performed *ex vivo* electroporations on whole brains prior to slicing. The efficiency of electroporation was extremely high, but the slice morphology was lost after a couple of days in culture and axons traveled through routes not normally accessible to them. The next step is *in utero* electroporations, we managed to get as far as few axons being electroporated in the thalamus. This will be an interesting avenue to further explore in the near future.

We have also investigated different expression patterns in wild-type and *Sema6B*-/- mouse somatosensory cortex from P2 to P8; however, no striking defects have been noticed (data not shown). More specifically, we were interested in glial organization within the somatosensory cortex, since Cooper and Steindler (1986) found

that the glial fibrillary acidic protein (GFAP) delineates the prospective barrels from P3 in wild-type mice, a few days before the barrels are discernable with Cresyl violet or DAPI. Moreover, they investigated the barrel cortex phenotype in the *reeler* mouse using this marker and established that glial defects are visible from P6 (O'Brien, Steindler et al. 1987). In addition, we are expanding the data obtained through Cux-1 labeling. No obvious defects are observed at early time-points in *Sema6B*-/- mice. However, *Sema6A*-/- mice exhibit striking defects in the somatosensory cortex at P4 (Figure 56). Preliminary data demonstrates that these defects are mimicked by *PlexinA2/PlexinA4* double knockout mutant mice, but not by single knockout mutant mice. Cux-1 positive cells are also found at abnormal positions; however, in this case, they are found within the marginal zone. These phenotypes are much more drastic than in *Sema6B*-/- mice, as the somatosensory cortex integrity in *Sema6A* and *PlexinA2/PlexinA4* double knockout mutant mice is quite disturbed. Previous work from the laboratory reported aberrant lamination in the somatosensory cortex of *Sema6A*-/- mice, but this was only demonstrated through NeuN labeling (Runker, O'Tuathaigh et al. 2011).

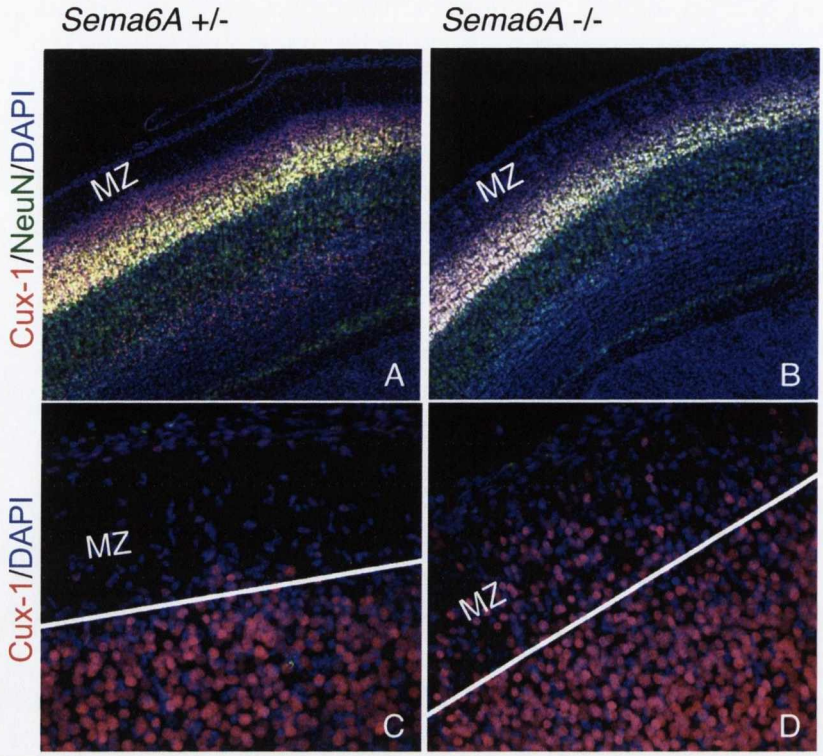


Figure 56. Cux-1 expressing cells are found within the marginal zone of the somatosensory cortex in *Sema6A-/-* mice at P4

Immunohistochemistry revealed the presence of Cux-1 positive cells in the marginal zone (MZ) of the somatosensory cortex of *Sema6A*-/- mice at P4 (B and D). *Sema6A* heterozygous mice were used as control as they exhibit no phenotype compared to wild-type mice. C and D are higher magnifications of A and B.

In conclusion, with the data collected so far, we hypothesize that Sema6A and Sema6B play a role in guiding TCAs and Cux-1 positive neurons to their appropriate positions in the barrel cortex. The former does so by keeping them within layer IV and not beyond, and the latter in more intricate ways by keeping TCAs within the barrel hollows and Cux-1 expressing neurons outside the barrel hollows. Some functions could be redundant, although double knockout mutants show additive effects. These actions are likely through their binding partners PlexinA2, but, more strikingly, PlexinA4 (Figure 57). However, this data raises an important question: are these proteins effectors of activity-dependent processes or part of a parallel morphogenetic program?

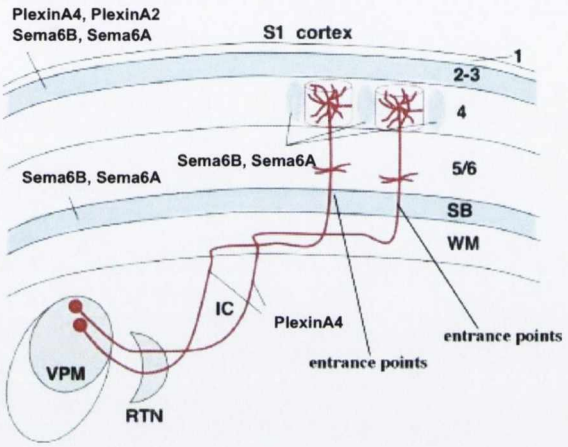


Figure 57. Model of Sema6A, Sema6B, PlexinA2 and PlexinA4 in the developing barrel cortex

See text for details. S1, somatosensory/barrel cortex; 1, marginal zone; 2-3, cortical layers II/III; 4, cortical layer IV; 5/6, cortical layers V/VI; SB, subplate; WM, white matter layer; VPM, ventral posteriomedial nucleus; RTN, reticular nucleus; IC, internal capsule.

Adapted from Dr. Hajime Fujisawa.

Chapter 6

Final Conclusions

And

Future Directions

6.1 Major findings and their implications

The task of unraveling the genetic program that determines proper brain wiring from the thalamus to the cortex is far from being achieved. However, we present here tools and data that are helping make the image clearer. First, we have compiled, annotated, clustered, curated and validated expression data of a set of genes of particular interest for brain development from the developing Allen Brain Atlas. A total of 1996 thalamic messenger RNA expression patterns were normalized across 8 time-points relevant to 7 developmental stages, namely region specification/patterning (E11.5), axon pathfinding (E13.5, E15.5 and E18.5), synaptogenesis (P4 and P14) and cortical plasticity (P28). Genes were annotated according to protein product cellular localization, with an emphasis on extracellular localization (either secreted, GPI-anchored, single- or multi-pass transmembrane proteins), and other previously known functions to facilitate context dependent discovery of novel thalamocortical axon guidance molecules. Through various available online tools and curations, we have created a high quality dataset ready to be used by the scientific community. Indeed, in doing so, we have found novel candidates potentially involved in thalamocortical axon pathfinding. Refining our gene set to those with peak expression at E13.5, E15.5 and E18.5, and protein localization to the extracellular compartment, we identified 72 genes of interest of which 29 had previously been implicated in thalamocortical development, 19 to axon guidance outside the thalamus or thalamocortical path and 24 to other functions. Importantly, these genes present differential expression patterns within the thalamus, which makes them good candidates for specific developmental functions.

In a further focused study, but no less interesting and insightful, we have investigated the expression patterns of Sema6A, Sema6B, PlexinA2 and PlexinA4 in mouse brain at P2, P4, P6 and P8. These time-points are highly relevant to thalamocortical connectivity. Due to the interesting, well studied and amenable model that the somatosensory system represents, we have explored it with great attention. All four genes are expressed in the thalamus and the cortex at those time-points. Moreover, they are specifically expressed in the ventral posteriomedial nucleus (VPM) of the thalamus, from which axons specifically project to the somatosensory cortex. The latter also expresses these genes in particular patterns. In more detail, axons from the thalamic barreloids project to cortical barrels. All four-gene expression patterns intersect at the level of the VPM, making projections from that particular nucleus quite interesting to

study. Immunohistochemical studies have revealed PlexinA4 protein expression within thalamic (and cortical) axons at E15.5, as well as in the barrel neuropil at P8. In addition, *Sema6A*, *Sema6B* and *PlexinA2* mRNA expression is detected in cortical layers II/III above the barrel structures, but also in cortical layer IV between the barrels, during the first postnatal week.

Not only have we provided novel expression data, we have also found novel roles for *Sema6A*, *Sema6B* and *PlexinA4* in thalamocortical development towards the somatosensory cortex. We show that all three genes are required for thalamocortical axons to enter the cortex in the appropriate perpendicular orientation from the white matter layer. *Sema6B* and *PlexinA4* null mutant mice exhibit more severe and similar phenotypes, compared to *Sema6A*-/- mice. Nonetheless, *Sema6A* and *Sema6B* appear to have additive effects. Despite the wandering trajectories in the somatosensory cortex, it would appear that the thalamic axons reach their appropriate targets to a certain extent; perhaps like the dorsal lateral geniculate nucleic thalamocortical axons do in *Sema6A*-/- mice (Little, Lopez-Bendito et al. 2009). In *Sema6A*-/- mice, thalamic axons are misrouted at the level of the internal capsule, but find a primitive route to the visual cortex. However, more work is required to determine this with certainty whether projections resolve themselves in a similar fashion in *Sema6B*-/- mice.

Further analyses were focused on *Sema6B* as little is known about this gene. Other studies have outlined the importance of proper preplate splitting for correct invasion of thalamic axons to take place (Caviness and Korde 1981, Molnar, Adams et al. 1998). We report no obvious defects in preplate splitting in *Sema6B*-/- mice. This implies that the thalamocortical axons are probably not responding correctly to subplate cues in *Sema6B*-/- mice. Moreover, the integrity of the somatosensory system appears normal until thalamocortical axons reach the cortex in *Sema6B*-/- mice: both barrelettes in the brainstem and barreloids in the thalamus display regular morphology, and no obvious defects are observed on the thalamocortical path before entering the cortex. Extensive work from other groups has been performed with cytochrome oxidase labeling of these structures. Although the vesicular glutamate transporter 2 and the glutamic acid decarboxylase 67 have been used to study the barreloids, we report here that these are also relevant and useful markers to evaluate barrelette structure.

A striking defect in cell organization occurs in *Sema6B*-/- somatosensory cortex. We show that Cux-1 positive neurons fail to exit the barrel hollows, but do exit the

septa. This type of phenotype has not been reported before and brings to light *Sema6B* as a gene involved in the exclusion of cortical layer IV neurons from the barrel hollows. What's more, the barrel neuropil is differently organized in the *Sema6B*-/- mice. PlexinA4 positive fibers appear to avoid cells within the barrel hollows. Moreover, Cux-1 positive neurons are also found at abnormal positions in the somatosensory cortex of *Sema6A*-/- mice. In these mice, Cux-1 expressing neurons migrate beyond their target layer into the marginal zone (preliminary works suggests that the same phenotype is mimicked in *PlexinA2/PlexinA4* double knockout mutant mice).

Taken together, these data implicate our genes of interest, namely *Sema6A*, *Sema6B*, *PlexinA2* and *PlexinA4*, in proper VPM thalamocortical connectivity to the somatosensory cortex. Sema6A and Sema6B are required for correct cortical invasion of thalamocortical axons, as well as differentially delimitating the target areas of Cux-1 expressing neurons in cortical layer IV. Most likely, they are functioning through repellent actions via their binding partners PlexinA2 and PlexinA4.

Moreover, genome-scan meta analyses have highlighted the potential involvement of Sema6A, Sema6B, PlexinA2 and PlexinA4 in different psychiatric disorders (Hovatta, Varilo et al. 1999, Lewis, Levinson et al. 2003, Cheng, Juo et al. 2006, Trikalinos, Karvouni et al. 2006). Most recently, Codina-Sola, Rodriguez-Santiago et al. (2015) have identified mutations leading to Sema6B overexpression in an autistic patient. Basic understanding of brain development is leading to better understanding of neurodevelopmental disorders. We are gaining valuable insight into disorders of brain connectivity such as autism and schizophrenia through fundamental research (Runker, O'Tuathaigh et al. 2011). Indeed, animal models with targeted gene mutations are great tools for understanding gene function. Studies in *Neuregulin1*, a susceptibility gene for schizophrenia, mutant mice have revealed impaired electrophysiological activity in the somatosensory cortex (Barz, Bessaih et al. 2014). Perhaps *Sema6B*-/- mice would reveal similar defects.

6.2 Future directions

The approach used to find novel candidate genes involved in thalamocortical development can be extended to other developmental contexts. It can also be used in thalamocortical development from different brain regions on the path to the cortex. For instance, we are hoping to explore patterns of gene expression at intermediate decision points, since cell populations in those areas are yet to be fully characterized. Moreover, another dataset is available through the Allen Brain Atlas, an adult dataset. This dataset comprises mRNA expression patterns of high quality for 3041 genes, which is bigger than the developmental dataset of 2002 genes. In addition, brain voxels are referenced to hierarchical subdivisions. For example, we can extract data for the whole thalamus or only the ventral posterior nucleus of the thalamus. This represents another avenue to explore in order to find genes potentially implicated in thalamocortical development in general or towards the somatosensory cortex. Like with the developmental dataset, different curations are necessary; but, with a platform already in place, reaching the discovery stages should occur rather quickly. Validation will be required to ensure that those genes are also expressed during development. Furthermore, it would be interesting to pursue investigation on the candidate genes we established through our developmental dataset. Green fluorescent protein targeting of our candidate genes would allow to follow projections from the thalamus to the cortex of the thalamic population that express those genes. This type of characterization would lay the foundation for further experimentation.

We have focused on cell-cell communication in our bioinformatics analyses. However, the genetic program from transcription factors to cell surface effector proteins is still greatly unknown. As presented in the introduction, the effects of a range of transcription factors on thalamic regionalization and thalamocortical axon guidance have been investigated. For instance, Neurog2 promotes glutamatergic relay neuron differentiation and cell-autonomously guides thalamic projections to frontal cortical areas (Seibt, Schuurmans et al. 2003, Vue, Aaker et al. 2007). However, except for extensive exploration of the transcriptional cascade - transcriptional activation of one transcription factor after another - downstream effectors of Neurog2 have not been identified to date (Molnar, Garel et al. 2012). Temporal and spatial expression data linking transcription factor presence with that of cell surface effectors therefore

becomes valuable. Nonetheless, our developmental dataset only includes 1996 genes, so global inferences are to be made with caution.

Our model of Sema6B function in the developing connectivity between the thalamus and the cortex is at early stages. Sema6B could have direct and indirect effects on the somatosensory system; therefore, additional markers of cell populations and cellular components should properly be investigated in the developing cortex. For instance, Gad67 proved to be a good marker of barrelettes and barreloids, and has previously been reported as being differentially expressed in the barrel cortex during the first postnatal week (Kiser, Cooper et al. 1998). Extensive work on the cortex of *reeler* mice has revealed a vast array of intricate defects. Moreover, investigating dendritic refinement in cortical layer IV has been cumbersome, but with new techniques such as the 'Supernova' system to sparsely and brightly label cortical layer IV cells presented by Mizuno, Luo et al. (2014), this hurdle could be overcome. This group also developed thalamocortical axon green fluorescent protein transgenic mice that allow to visualize presynaptic TCA clusters in the cortex. Together, these two systems allow for great exploration of the somatosensory system. We have probably only scratched the surface at this point in the *Sema6B*-/- mouse brain, whereas *Sema6A*-/- mice exhibit striking defects from embryonic stages on, Sema6B effects appear to be more subtle and required for fine-tuning.

We have gathered interesting expression data during the first postnatal week, when axons invade the cortical plate and extensive synaptogenesis occurs. In addition, striking phenotypes have been discussed. However, the lack of a reliable antibody to determine the localization of Sema6B protein is a limiting factor. Messenger RNA expression is indicative of possible protein expression, but it is not necessarily correlated. In order to gain more insight on its direct function, *in utero* electroporation of either thalamic or cortical cells altering its expression would be quite useful. In addition, generating conditional knockout mice targeting thalamic or cortical expression of Sema6B would be invaluable. The same is true for PlexinA4 function. Although we have shown which cells potentially express it and where the protein is localized, we cannot assess at the time being whether dendrites or thalamic axons or both express it in the cortex. We hypothesize that the leading edges of thalamic axons express PlexinA4 due to the temporal patterns of expression seen from E15.5 to P8, but more work is required to determine this with certainty. Needless to say that *in utero* electroporation

experiments and conditional knockout mice affecting Sema6A and PlexinA2 expression would also answer many questions. What's more, knocking out the expression of combinations of these genes through *in utero* electroporation or conditional knockout mice would clarify pressing questions on redundancies or additive effects of these genes. The fact that we found intersecting expression of these four genes in the VPM and that barreloids form normally in *Sema6B*-/- mice deserves further attention. This data suggests that Sema6B is exclusively implicated at the level of thalamocortical connectivity in the context of the somatosensory system.

Discriminating between the developmental genetic program and activity-dependent gene expression will be another interesting aspect to focus on. A first step in that direction is to investigate whether Sema6B is expressed in the somatosensory cortex after whisker-trimming or infraorbital nerve damage is performed. Analyzing the synaptic integrity of *Sema6B*-/- mice through immunohistochemistry would also be insightful (presence of pre- and postsynaptic markers, and signaling machinery). Moreover, establishing whether *Sema6B*-/- mice have a normally functioning somatosensory system could be explored through an array of sensory behavioral tasks.

(1999). "Unified nomenclature for the semaphorins/collapsins. Semaphorin Nomenclature Committee." Cell **97**(5): 551-552.

Abdel-Majid, R. M., W. L. Leong, L. C. Schalkwyk, D. S. Smallman, S. T. Wong, D. R. Storm, A. Fine, M. J. Dobson, D. L. Guernsey and P. E. Neumann (1998). "Loss of adenylyl cyclase I activity disrupts patterning of mouse somatosensory cortex." Nat Genet **19**(3): 289-291.

Agmon, A., L. T. Yang, E. G. Jones and D. K. O'Dowd (1995). "Topological precision in the thalamic projection to neonatal mouse barrel cortex." J Neurosci **15**(1 Pt 2): 549-561.

Andermatt, I., N. H. Wilson, T. Bergmann, O. Mauti, M. Gesemann, S. Sockanathan and E. T. Stoeckli (2014). "Semaphorin 6B acts as a receptor in post-crossing commissural axon guidance." Development **141**(19): 3709-3720.

Angevine, J. B., Jr. (1970). "Time of neuron origin in the diencephalon of the mouse. An autoradiographic study." J Comp Neurol **139**(2): 129-187.

Arcelli, P., C. Frassoni, M. C. Regondi, S. De Biasi and R. Spreafico (1997). "GABAergic neurons in mammalian thalamus: a marker of thalamic complexity?" Brain Res Bull **42**(1): 27-37.

Armstrong-James, M. and K. Fox (1987). "Spatiotemporal convergence and divergence in the rat S1 "barrel" cortex." J Comp Neurol **263**(2): 265-281.

Ashburner, M., C. A. Ball, J. A. Blake, D. Botstein, H. Butler, J. M. Cherry, A. P. Davis, K. Dolinski, S. S. Dwight, J. T. Eppig, M. A. Harris, D. P. Hill, L. Issel-Tarver, A. Kasarskis, S. Lewis, J. C. Matese, J. E. Richardson, M. Ringwald, G. M. Rubin and G. Sherlock (2000). "Gene ontology: tool for the unification of biology. The Gene Ontology Consortium." Nat Genet **25**(1): 25-29.

Augsburger, A., A. Schuchardt, S. Hoskins, J. Dodd and S. Butler (1999). "BMPs as mediators of roof plate repulsion of commissural neurons." Neuron **24**(1): 127-141.

Auladell, C., P. Perez-Sust, H. Super and E. Soriano (2000). "The early development of thalamocortical and corticothalamic projections in the mouse." Anat Embryol (Berl) **201**(3): 169-179.

Baladron, V., M. J. Ruiz-Hidalgo, M. L. Nueda, M. J. Diaz-Guerra, J. J. Garcia-Ramirez, E. Bonvini, E. Gubina and J. Laborda (2005). "dlk acts as a negative

regulator of Notch1 activation through interactions with specific EGF-like repeats." Exp Cell Res **303**(2): 343-359.

Barth, K. A. and S. W. Wilson (1995). "Expression of zebrafish nk2.2 is influenced by sonic hedgehog/vertebrate hedgehog-1 and demarcates a zone of neuronal differentiation in the embryonic forebrain." Development **121**(6): 1755-1768.

Barz, C. S., T. Bessaih, T. Abel, D. Feldmeyer and D. Contreras (2014). "Sensory encoding in Neuregulin 1 mutants." Brain Struct Funct.

Berry, M. and A. W. Rogers (1965). "The migration of neuroblasts in the developing cerebral cortex." J Anat **99**(Pt 4): 691-709.

Biederer, T., Y. Sara, M. Mozhayeva, D. Atasoy, X. Liu, E. T. Kavalali and T. C. Sudhof (2002). "SynCAM, a synaptic adhesion molecule that drives synapse assembly." Science **297**(5586): 1525-1531.

Bishop, K. M., S. Garel, Y. Nakagawa, J. L. Rubenstein and D. D. O'Leary (2003). "Emx1 and Emx2 cooperate to regulate cortical size, lamination, neuronal differentiation, development of cortical efferents, and thalamocortical pathfinding." J Comp Neurol **457**(4): 345-360.

Bluske, K. K., Y. Kawakami, N. Koyano-Nakagawa and Y. Nakagawa (2009). "Differential activity of Wnt/beta-catenin signaling in the embryonic mouse thalamus." Dev Dyn **238**(12): 3297-3309.

Bluske, K. K., T. Y. Vue, Y. Kawakami, M. M. Taketo, K. Yoshikawa, J. E. Johnson and Y. Nakagawa (2012). "beta-Catenin signaling specifies progenitor cell identity in parallel with Shh signaling in the developing mammalian thalamus." Development **139**(15): 2692-2702.

Braun, M. M., A. Etheridge, A. Bernard, C. P. Robertson and H. Roelink (2003). "Wnt signaling is required at distinct stages of development for the induction of the posterior forebrain." Development **130**(23): 5579-5587.

Butler, S. J. and J. Dodd (2003). "A role for BMP heterodimers in roof plate-mediated repulsion of commissural axons." Neuron **38**(3): 389-401.

Carey, R. G., D. Fitzpatrick and I. T. Diamond (1979). "Layer I of striate cortex of Tupaia glis and Galago senegalensis: projections from thalamus and claustrum revealed by retrograde transport of horseradish peroxidase." J Comp Neurol **186**(3): 393-437.

Cases, O., T. Vitalis, I. Seif, E. De Maeyer, C. Sotelo and P. Gaspar (1996). "Lack of barrels in the somatosensory cortex of monoamine oxidase A-deficient mice: role of a serotonin excess during the critical period." Neuron **16**(2): 297-307.

Castellani, V., A. Chedotal, M. Schachner, C. Faivre-Sarrailh and G. Rougon (2000). "Analysis of the L1-deficient mouse phenotype reveals cross-talk between Sema3A and L1 signaling pathways in axonal guidance." Neuron **27**(2): 237-249.

Castellani, V., E. De Angelis, S. Kenwrick and G. Rougon (2002). "Cis and trans interactions of L1 with neuropilin-1 control axonal responses to semaphorin 3A." EMBO J **21**(23): 6348-6357.

Caviness, V. S., Jr. and M. G. Korde (1981). "Monoaminergic afferents to the neocortex: a developmental histofluorescence study in normal and Reeler mouse embryos." Brain Res **209**(1): 1-9.

Charoy, C., H. Nawabi, F. Reynaud, E. Derrington, M. Bozon, K. Wright, J. Falk, F. Helmbacher, K. Kindbeiter and V. Castellani (2012). "gdnf activates midline repulsion by Semaphorin3B via NCAM during commissural axon guidance." Neuron **75**(6): 1051-1066.

Chen, Y., D. Magnani, T. Theil, T. Pratt and D. J. Price (2012). "Evidence that descending cortical axons are essential for thalamocortical axons to cross the pallial-subpallial boundary in the embryonic forebrain." PLoS One **7**(3): e33105.

Cheng, R., S. H. Juo, J. E. Loth, J. Nee, I. Iossifov, R. Blumenthal, L. Sharpe, K. Kanyas, B. Lerer, B. Lilliston, M. Smith, K. Trautman, T. C. Gilliam, J. Endicott and M. Baron (2006). "Genome-wide linkage scan in a large bipolar disorder sample from the National Institute of Mental Health genetics initiative suggests putative loci for bipolar disorder, psychosis, suicide, and panic disorder." Mol Psychiatry **11**(3): 252-260.

Chiang, C., Y. Litingtung, E. Lee, K. E. Young, J. L. Corden, H. Westphal and P. A. Beachy (1996). "Cyclopia and defective axial patterning in mice lacking Sonic hedgehog gene function." Nature **383**(6599): 407-413.

Comeau, M. R., R. Johnson, R. F. DuBose, M. Petersen, P. Gearing, T. VandenBos, L. Park, T. Farrah, R. M. Buller, J. I. Cohen, L. D. Strockbine, C. Rauch and M. K. Spriggs (1998). "A poxvirus-encoded semaphorin induces cytokine production from monocytes and binds to a novel cellular semaphorin receptor, VESPR." Immunity **8**(4): 473-482.

Cooper, N. G. and D. A. Steindler (1986). "Monoclonal antibody to glial fibrillary acidic protein reveals a parcellation of individual barrels in the early postnatal mouse somatosensory cortex." Brain Res **380**(2): 341-348.

Corson, T. W. and B. L. Gallie (2007). "One hit, two hits, three hits, more? Genomic changes in the development of retinoblastoma." Genes Chromosomes Cancer **46**(7): 617-634.

Cunningham, N. S., N. A. Jenkins, D. J. Gilbert, N. G. Copeland, A. H. Reddi and S. J. Lee (1995). "Growth/differentiation factor-10: a new member of the transforming growth factor-beta superfamily related to bone morphogenetic protein-3." Growth Factors **12**(2): 99-109.

Datwani, A., T. Iwasato, S. Itohara and R. S. Erzurumlu (2002). "Lesion-induced thalamocortical axonal plasticity in the S1 cortex is independent of NMDA receptor function in excitatory cortical neurons." J Neurosci **22**(21): 9171-9175.

Datwani, A., T. Iwasato, S. Itohara and R. S. Erzurumlu (2002). "NMDA receptor-dependent pattern transfer from afferents to postsynaptic cells and dendritic differentiation in the barrel cortex." Mol Cell Neurosci **21**(3): 477-492.

Demyanenko, G. P., P. F. Siesser, A. G. Wright, L. H. Brennaman, U. Bartsch, M. Schachner and P. F. Maness (2011). "L1 and CHL1 Cooperate in Thalamocortical Axon Targeting." Cereb Cortex **21**(2): 401-412.

Dufour, A., J. Seibt, L. Passante, V. Depaepe, T. Ciossek, J. Frisen, K. Kullander, J. G. Flanagan, F. Polleux and P. Vanderhaeghen (2003). "Area specificity and topography of thalamocortical projections are controlled by ephrin/Eph genes." Neuron **39**(3): 453-465.

Durham, D. and T. A. Woolsey (1984). "Effects of neonatal whisker lesions on mouse central trigeminal pathways." J Comp Neurol **223**(3): 424-447.

Eckhardt, F., O. Behar, E. Calautti, K. Yonezawa, I. Nishimoto and M. C. Fishman (1997). "A novel transmembrane semaphorin can bind c-src." Mol Cell Neurosci **9**(5-6): 409-419.

Eisenhaber, B., P. Bork and F. Eisenhaber (1998). "Sequence properties of GPI-anchored proteins near the omega-site: constraints for the polypeptide binding site of the putative transamidase." Protein Eng **11**(12): 1155-1161.

Eisenhaber, B., P. Bork and F. Eisenhaber (1999). "Prediction of potential GPI-modification sites in proprotein sequences." J Mol Biol **292**(3): 741-758.

Eisenhaber, B., P. Bork, Y. Yuan, G. Loffler and F. Eisenhaber (2000). "Automated annotation of GPI anchor sites: case study C. elegans." Trends Biochem Sci **25**(7): 340-341.

Enriquez-Barreto, L., C. Palazzetti, L. H. Brennaman, P. F. Maness and A. Fairen (2012). "Neural cell adhesion molecule, NCAM, regulates thalamocortical axon pathfinding and the organization of the cortical somatosensory representation in mouse." Front Mol Neurosci **5**: 76.

Erzurumlu, R. S. and P. Gaspar (2012). "Development and critical period plasticity of the barrel cortex." Eur J Neurosci **35**(10): 1540-1553.

Erzurumlu, R. S. and P. C. Kind (2001). "Neural activity: sculptor of 'barrels' in the neocortex." Trends Neurosci **24**(10): 589-595.

Espinosa, J. S., D. G. Wheeler, R. W. Tsien and L. Luo (2009). "Uncoupling dendrite growth and patterning: single-cell knockout analysis of NMDA receptor 2B." Neuron **62**(2): 205-217.

Ferrere, A., T. Vitalis, H. Gingras, P. Gaspar and O. Cases (2006). "Expression of Cux-1 and Cux-2 in the developing somatosensory cortex of normal and barrel-defective mice." Anat Rec A Discov Mol Cell Evol Biol **288**(2): 158-165.

Ferron, S. R., M. Charalambous, E. Radford, K. McEwen, H. Wildner, E. Hind, J. M. Morante-Redolat, J. Laborda, F. Guillemot, S. R. Bauer, I. Farinas and A. C. Ferguson-Smith (2011). "Postnatal loss of Dlk1 imprinting in stem cells and niche astrocytes regulates neurogenesis." Nature **475**(7356): 381-385.

Finn, R. D., A. Bateman, J. Clements, P. Coggill, R. Y. Eberhardt, S. R. Eddy, A. Heger, K. Hetherington, L. Holm, J. Mistry, E. L. Sonnhammer, J. Tate and M. Punta (2014). "Pfam: the protein families database." Nucleic Acids Res **42**(Database issue): D222-230.

Francois, C., G. Percheron, A. Parent, A. F. Sadikot, G. Fenelon and J. Yelnik (1991). "Topography of the projection from the central complex of the thalamus to the sensorimotor striatal territory in monkeys." J Comp Neurol **305**(1): 17-34.

Frei, J. A., I. Andermatt, M. Gesemann and E. T. Stoeckli (2014). "The SynCAM synaptic cell adhesion molecules are involved in sensory axon pathfinding by regulating axon-axon contacts." J Cell Sci **127**(24): 5288-5302.

Fujii, T., F. Nakao, Y. Shibata, G. Shioi, E. Kodama, H. Fujisawa and S. Takagi (2002). "Caenorhabditis elegans PlexinA, PLX-1, interacts with transmembrane

semaphorins and regulates epidermal morphogenesis." Development **129**(9): 2053-2063.

Fujita, E., Y. Tanabe, B. A. Imhof, M. Y. Momoi and T. Momoi (2012). "Cadm1-expressing synapses on Purkinje cell dendrites are involved in mouse ultrasonic vocalization activity." PLoS One **7**(1): e30151.

Garel, S., F. Marin, R. Grosschedl and P. Charnay (1999). "Ebf1 controls early cell differentiation in the embryonic striatum." Development **126**(23): 5285-5294.

Garel, S., K. Yun, R. Grosschedl and J. L. Rubenstein (2002). "The early topography of thalamocortical projections is shifted in Ebf1 and Dlx1/2 mutant mice." Development **129**(24): 5621-5634.

Gherardi, E., C. A. Love, R. M. Esnouf and E. Y. Jones (2004). "The sema domain." Curr Opin Struct Biol **14**(6): 669-678.

Gil, O. D., L. Needleman and G. W. Huntley (2002). "Developmental patterns of cadherin expression and localization in relation to compartmentalized thalamocortical terminations in rat barrel cortex." J Comp Neurol **453**(4): 372-388.

Gimenez-Amaya, J. M., N. R. McFarland, S. de las Heras and S. N. Haber (1995). "Organization of thalamic projections to the ventral striatum in the primate." J Comp Neurol **354**(1): 127-149.

Gong, S., C. Zheng, M. L. Doughty, K. Losos, N. Didkovsky, U. B. Schambra, N. J. Nowak, A. Joyner, G. Leblanc, M. E. Hatten and N. Heintz (2003). "A gene expression atlas of the central nervous system based on bacterial artificial chromosomes." Nature **425**(6961): 917-925.

Gore, B. B., K. G. Wong and M. Tessier-Lavigne (2008). "Stem cell factor functions as an outgrowth-promoting factor to enable axon exit from the midline intermediate target." Neuron **57**(4): 501-510.

Grant, E., A. Hoerder-Suabedissen and Z. Molnar (2012). "Development of the corticothalamic projections." Front Neurosci **6**: 53.

Guillery, R. W. and S. M. Sherman (2002). "Thalamic relay functions and their role in corticocortical communication: generalizations from the visual system." Neuron **33**(2): 163-175.

Haddick, P. C., I. Tom, E. Luis, G. Quinones, B. J. Wranik, S. R. Ramani, J. P. Stephan, M. Tessier-Lavigne and L. C. Gonzalez (2014). "Defining the ligand specificity of the deleted in colorectal cancer (DCC) receptor." PLoS One **9**(1): e84823.

Hagemann, A. I. and S. Scholpp (2012). "The Tale of the Three Brothers - Shh, Wnt, and Fgf during Development of the Thalamus." Front Neurosci **6**: 76.

Haklai-Topper, L., G. Mlechkovich, D. Savariego, I. Gokhman and A. Yaron (2010). "Cis interaction between Semaphorin6A and Plexin-A4 modulates the repulsive response to Sema6A." EMBO J **29**(15): 2635-2645.

Hashimoto-Torii, K., J. Motoyama, C. C. Hui, A. Kuroiwa, M. Nakafuku and K. Shimamura (2003). "Differential activities of Sonic hedgehog mediated by Gli transcription factors define distinct neuronal subtypes in the dorsal thalamus." Mech Dev **120**(10): 1097-1111.

Henry, A. M. and J. G. Hohmann (2012). "High-resolution gene expression atlases for adult and developing mouse brain and spinal cord." Mamm Genome **23**(9-10): 539-549.

Hevner, R. F., E. Miyashita-Lin and J. L. Rubenstein (2002). "Cortical and thalamic axon pathfinding defects in Tbr1, Gbx2, and Pax6 mutant mice: evidence that cortical and thalamic axons interact and guide each other." J Comp Neurol **447**(1): 8-17.

Hirata, T., M. Nakazawa, O. Muraoka, R. Nakayama, Y. Suda and M. Hibi (2006). "Zinc-finger genes Fez and Fez-like function in the establishment of diencephalon subdivisions." Development **133**(20): 3993-4004.

Hokamp, K., F. M. Roche, M. Acab, M. E. Rousseau, B. Kuo, D. Goode, D. Aeschliman, J. Bryan, L. A. Babiuk, R. E. Hancock and F. S. Brinkman (2004). "ArrayPipe: a flexible processing pipeline for microarray data." Nucleic Acids Res **32**(Web Server issue): W457-459.

Horton, P. and K. Nakai (1997). "Better prediction of protein cellular localization sites with the k nearest neighbors classifier." Proc Int Conf Intell Syst Mol Biol **5**: 147-152.

Hota, P. K. and M. Buck (2009). "Thermodynamic characterization of two homologous protein complexes: associations of the semaphorin receptor plexin-B1 RhoGTPase binding domain with Rnd1 and active Rac1." Protein Sci **18**(5): 1060-1071.

Hovatta, I., T. Varilo, J. Suvisaari, J. D. Terwilliger, V. Ollikainen, R. Arajarvi, H. Juvonen, M. L. Kokko-Sahin, L. Vaisanen, H. Mannila, J. Lonnqvist and L. Peltonen (1999). "A genomewide screen for schizophrenia genes in an isolated Finnish subpopulation, suggesting multiple susceptibility loci." Am J Hum Genet **65**(4): 1114-1124.

Huber, A. B., A. L. Kolodkin, D. D. Ginty and J. F. Cloutier (2003). "Signaling at the growth cone: ligand-receptor complexes and the control of axon growth and guidance." Annu Rev Neurosci **26**: 509-563.

Hung, R. J., C. W. Pak and J. R. Terman (2011). "Direct redox regulation of F-actin assembly and disassembly by Mical." Science **334**(6063): 1710-1713.

Inan, M. and M. C. Crair (2007). "Development of cortical maps: perspectives from the barrel cortex." Neuroscientist **13**(1): 49-61.

Ince-Dunn, G., B. J. Hall, S. C. Hu, B. Ripley, R. L. Huganir, J. M. Olson, S. J. Tapscott and A. Ghosh (2006). "Regulation of thalamocortical patterning and synaptic maturation by NeuroD2." Neuron **49**(5): 683-695.

Ishibashi, M. and A. P. McMahon (2002). "A sonic hedgehog-dependent signaling relay regulates growth of diencephalic and mesencephalic primordia in the early mouse embryo." Development **129**(20): 4807-4819.

Iwasato, T., A. Datwani, A. M. Wolf, H. Nishiyama, Y. Taguchi, S. Tonegawa, T. Knopfel, R. S. Erzurumlu and S. Itohara (2000). "Cortex-restricted disruption of NMDAR1 impairs neuronal patterns in the barrel cortex." Nature **406**(6797): 726-731.

Jabaudon, D., S. J. Shnider, D. J. Tischfield, M. J. Galazo and J. D. Macklis (2012). "RORbeta induces barrel-like neuronal clusters in the developing neocortex." Cereb Cortex **22**(5): 996-1006.

Janssen, B. J., R. A. Robinson, F. Perez-Branguli, C. H. Bell, K. J. Mitchell, C. Siebold and E. Y. Jones (2010). "Structural basis of semaphorin-plexin signalling." Nature **467**(7319): 1118-1122.

Jeon, C. Y., H. J. Kim, J. Y. Lee, J. B. Kim, S. C. Kim and J. B. Park (2010). "p190RhoGAP and Rap-dependent RhoGAP (ARAP3) inactivate RhoA in response to nerve growth factor leading to neurite outgrowth from PC12 cells." Exp Mol Med **42**(5): 335-344.

Jeong, J. Y., Z. Einhorn, P. Mathur, L. Chen, S. Lee, K. Kawakami and S. Guo (2007). "Patterning the zebrafish diencephalon by the conserved zinc-finger protein Fezl." Development **134**(1): 127-136.

Jeong, Y., D. K. Dolson, R. R. Waclaw, M. P. Matise, L. Sussel, K. Campbell, K. H. Kaestner and D. J. Epstein (2011). "Spatial and temporal requirements for sonic hedgehog in the regulation of thalamic interneuron identity." Development **138**(3): 531-541.

Jessell, T. M. (2000). "Neuronal specification in the spinal cord: inductive signals and transcriptional codes." Nat Rev Genet **1**(1): 20-29.

Jones, E. G. (1985). The thalamus, Plenum Press.

Joo, J. Y., S. J. Lee, T. Uemura, T. Yoshida, M. Yasumura, M. Watanabe and M. Mishina (2011). "Differential interactions of cerebellin precursor protein (Cbln) subtypes and neurexin variants for synapse formation of cortical neurons." Biochem Biophys Res Commun **406**(4): 627-632.

Kameyama, T., Y. Murakami, F. Suto, A. Kawakami, S. Takagi, T. Hirata and H. Fujisawa (1996). "Identification of a neuronal cell surface molecule, plexin, in mice." Biochem Biophys Res Commun **226**(2): 524-529.

Kameyama, T., Y. Murakami, F. Suto, A. Kawakami, S. Takagi, T. Hirata and H. Fujisawa (1996). "Identification of plexin family molecules in mice." Biochem Biophys Res Commun **226**(2): 396-402.

Kashani, A. H., Z. Qiu, L. Jurata, S. K. Lee, S. Pfaff, S. Goebbels, K. A. Nave and A. Ghosh (2006). "Calcium activation of the LMO4 transcription complex and its role in the patterning of thalamocortical connections." J Neurosci **26**(32): 8398-8408.

Kasprzyk, A. (2011). "BioMart: driving a paradigm change in biological data management." Database (Oxford) **2011**: bar049.

Kataoka, A. and T. Shimogori (2008). "Fgf8 controls regional identity in the developing thalamus." Development **135**(17): 2873-2881.

Kiecker, C. and A. Lumsden (2004). "Hedgehog signaling from the ZLI regulates diencephalic regional identity." Nat Neurosci **7**(11): 1242-1249.

Kilian, T. M. and A. G. Beck-Sickinger (2015). "Recombinant expression and characterization of biologically active protein delta homolog 1." Protein Expr Purif **110**: 72-78.

Kim, D., J. O. Im, Y. J. Won, S. Y. Yoon, E. J. Lee, J. H. Lee and H. N. Hong (2003). "Upregulation of c-Kit receptor and stem cell factor in cerebellar inhibitory synapses in response to kainic acid." J Neurosci Res **71**(1): 72-78.

Kiser, P. J., N. G. Cooper and G. D. Mower (1998). "Expression of two forms of glutamic acid decarboxylase (GAD67 and GAD65) during postnatal development of rat somatosensory barrel cortex." J Comp Neurol **402**(1): 62-74.

Klostermann, A., B. Lutz, F. Gertler and C. Behl (2000). "The orthologous human and murine semaphorin 6A-1 proteins (SEMA6A-1/Sema6A-1) bind to the enabled/vasodilator-stimulated phosphoprotein-like protein (EVL) via a novel carboxyl-terminal zyxin-like domain." J Biol Chem **275**(50): 39647-39653.

Kobayashi, D., M. Kobayashi, K. Matsumoto, T. Ogura, M. Nakafuku and K. Shimamura (2002). "Early subdivisions in the neural plate define distinct competence for inductive signals." Development **129**(1): 83-93.

Kolodkin, A. L., D. J. Matthes, T. P. O'Connor, N. H. Patel, A. Admon, D. Bentley and C. S. Goodman (1992). "Fasciclin IV: sequence, expression, and function during growth cone guidance in the grasshopper embryo." Neuron **9**(5): 831-845.

Krogh, A., B. Larsson, G. von Heijne and E. L. Sonnhammer (2001). "Predicting transmembrane protein topology with a hidden Markov model: application to complete genomes." J Mol Biol **305**(3): 567-580.

Kuhlenbeck, H. (1938). "The ontogenetic development and phylogenetic significance of the cortex telencephali in the Chick." Journal of Comparative Neurology **69**: pp. 273-301.

Lakhina, V., A. Falnikar, L. Bhatnagar and S. Tole (2007). "Early thalamocortical tract guidance and topographic sorting of thalamic projections requires LIM-homeodomain gene Lhx2." Dev Biol **306**(2): 703-713.

LeDoux, J. E., D. A. Ruggiero and D. J. Reis (1985). "Projections to the subcortical forebrain from anatomically defined regions of the medial geniculate body in the rat." J Comp Neurol **242**(2): 182-213.

Leighton, P. A., K. J. Mitchell, L. V. Goodrich, X. Lu, K. Pinson, P. Scherz, W. C. Skarnes and M. Tessier-Lavigne (2001). "Defining brain wiring patterns and mechanisms through gene trapping in mice." Nature **410**(6825): 174-179.

Lein, E. S., M. J. Hawrylycz, N. Ao, M. Ayres, A. Bensinger, A. Bernard, A. F. Boe, M. S. Boguski, K. S. Brockway, E. J. Byrnes, L. Chen, L. Chen, T. M.

Chen, M. C. Chin, J. Chong, B. E. Crook, A. Czaplinska, C. N. Dang, S. Datta, N. R. Dee, A. L. Desaki, T. Desta, E. Diep, T. A. Dolbeare, M. J. Donelan, H. W. Dong, J. G. Dougherty, B. J. Duncan, A. J. Ebbert, G. Eichele, L. K. Estin, C. Faber, B. A. Facer, R. Fields, S. R. Fischer, T. P. Fliss, C. Frensley, S. N. Gates, K. J. Glattfelder, K. R. Halverson, M. R. Hart, J. G. Hohmann, M. P. Howell, D. P. Jeung, R. A. Johnson, P. T. Karr, R. Kawal, J. M. Kidney, R. H. Knapik, C. L. Kuan, J. H. Lake, A. R. Laramee, K. D. Larsen, C. Lau, T. A. Lemon, A. J. Liang, Y. Liu, L. T. Luong, J. Michaels, J. J. Morgan, R. J. Morgan, M. T. Mortrud, N. F. Mosqueda, L. L. Ng, R. Ng, G. J. Orta, C. C. Overly, T. H. Pak, S. E. Parry, S. D. Pathak, O. C. Pearson, R. B. Puchalski, Z. L. Riley, H. R. Rockett, S. A. Rowland, J. J. Royall, M. J. Ruiz, N. R. Sarno, K. Schaffnit, N. V. Shapovalova, T. Sivisay, C. R. Slaughterbeck, S. C. Smith, K. A. Smith, B. I. Smith, A. J. Sodt, N. N. Stewart, K. R. Stumpf, S. M. Sunkin, M. Sutram, A. Tam, C. D. Teemer, C. Thaller, C. L. Thompson, L. R. Varnam, A. Visel, R. M. Whitlock, P. E. Wohnoutka, C. K. Wolkey, V. Y. Wong, M. Wood, M. B. Yaylaoglu, R. C. Young, B. L. Youngstrom, X. F. Yuan, B. Zhang, T. A. Zwingman and A. R. Jones (2007). "Genome-wide atlas of gene expression in the adult mouse brain." Nature **445**(7124): 168-176.

Letinic, K. and I. Kostovic (1996). "Transient neuronal population of the internal capsule in the developing human cerebrum." Neuroreport **7**(13): 2159-2162.

Letunic, I., T. Doerks and P. Bork (2014). "SMART: recent updates, new developments and status in 2015." Nucleic Acids Res.

Lewis, C. M., D. F. Levinson, L. H. Wise, L. E. DeLisi, R. E. Straub, I. Hovatta, N. M. Williams, S. G. Schwab, A. E. Pulver, S. V. Faraone, L. M. Brzustowicz, C. A. Kaufmann, D. L. Garver, H. M. Gurling, E. Lindholm, H. Coon, H. W. Moises, W. Byerley, S. H. Shaw, A. Mesen, R. Sherrington, F. A. O'Neill, D. Walsh, K. S. Kendler, J. Ekelund, T. Paunio, J. Lonnqvist, L. Peltonen, M. C. O'Donovan, M. J. Owen, D. B. Wildenauer, W. Maier, G. Nestadt, J. L. Blouin, S. E. Antonarakis, B. J. Mowry, J. M. Silverman, R. R. Crowe, C. R. Cloninger, M. T. Tsuang, D. Malaspina, J. M. Harkavy-Friedman, D. M. Svrakic, A. S. Bassett, J. Holcomb, G. Kalsi, A. McQuillin, J. Brynjolfson, T. Sigmundsson, H. Petursson, E. Jazin, T. Zoega and T. Helgason (2003). "Genome scan meta-analysis of schizophrenia and bipolar disorder, part II: Schizophrenia." Am J Hum Genet **73**(1): 34-48.

Liguz-Lecznar, M. and J. Skangiel-Kramska (2007). "Vesicular glutamate transporters VGLUT1 and VGLUT2 in the developing mouse barrel cortex." Int J Dev Neurosci **25**(2): 107-114.

Liscovitch, N. and G. Chechik (2013). "Specialization of gene expression during mouse brain development." PLoS Comput Biol **9**(9): e1003185.

Little, G. E., G. Lopez-Bendito, A. E. Runker, N. Garcia, M. C. Pinon, A. Chedotal, Z. Molnar and K. J. Mitchell (2009). "Specificity and plasticity of thalamocortical connections in Sema6A mutant mice." PLoS Biol **7**(4): e98.

Lopez-Bendito, G., A. Cautinat, J. A. Sanchez, F. Bielle, N. Flames, A. N. Garratt, D. A. Talmage, L. W. Role, P. Charnay, O. Marin and S. Garel (2006). "Tangential neuronal migration controls axon guidance: a role for neuregulin-1 in thalamocortical axon navigation." Cell **125**(1): 127-142.

Lopez-Bendito, G., C. H. Chan, A. Mallamaci, J. Parnavelas and Z. Molnar (2002). "Role of Emx2 in the development of the reciprocal connectivity between cortex and thalamus." J Comp Neurol **451**(2): 153-169.

Lopez-Bendito, G., N. Flames, L. Ma, C. Fouquet, T. Di Meglio, A. Chedotal, M. Tessier-Lavigne and O. Marin (2007). "Robo1 and Robo2 cooperate to control the guidance of major axonal tracts in the mammalian forebrain." J Neurosci **27**(13): 3395-3407.

Lopez-Bendito, G. and Z. Molnar (2003). "Thalamocortical development: how are we going to get there?" Nat Rev Neurosci **4**(4): 276-289.

Lund, R. D. and M. J. Mustari (1977). "Development of the geniculocortical pathway in rats." J Comp Neurol **173**(2): 289-306.

Luo, Y., D. Raible and J. A. Raper (1993). "Collapsin: a protein in brain that induces the collapse and paralysis of neuronal growth cones." Cell **75**(2): 217-227.

Maestrini, E., L. Tamagnone, P. Longati, O. Cremona, M. Gulisano, S. Bione, F. Tamanini, B. G. Neel, D. Toniolo and P. M. Comoglio (1996). "A family of transmembrane proteins with homology to the MET-hepatocyte growth factor receptor." Proc Natl Acad Sci U S A **93**(2): 674-678.

Magdaleno, S., P. Jensen, C. L. Brumwell, A. Seal, K. Lehman, A. Asbury, T. Cheung, T. Cornelius, D. M. Batten, C. Eden, S. M. Norland, D. S. Rice, N. Dosooye, S. Shakya, P. Mehta and T. Curran (2006). "BGEM: an in situ hybridization database of gene expression in the embryonic and adult mouse nervous system." PLoS Biol **4**(4): e86.

Manabe, T., H. Togashi, N. Uchida, S. C. Suzuki, Y. Hayakawa, M. Yamamoto, H. Yoda, T. Miyakawa, M. Takeichi and O. Chisaka (2000). "Loss of cadherin-11 adhesion receptor enhances plastic changes in hippocampal synapses and modifies behavioral responses." Mol Cell Neurosci **15**(6): 534-546.

Marcos-Mondejar, P., S. Peregrin, J. Y. Li, L. Carlsson, S. Tole and G. Lopez-Bendito (2012). "The lhx2 transcription factor controls thalamocortical axonal guidance by specific regulation of robo1 and robo2 receptors." J Neurosci **32**(13): 4372-4385.

Marie, P. J., E. Hay, D. Modrowski, L. Revollo, G. Mbalaviele and R. Civitelli (2014). "Cadherin-mediated cell-cell adhesion and signaling in the skeleton." Calcif Tissue Int **94**(1): 46-54.

Marin, O., J. Baker, L. Puelles and J. L. Rubenstein (2002). "Patterning of the basal telencephalon and hypothalamus is essential for guidance of cortical projections." Development **129**(3): 761-773.

Matsuda, K. and M. Yuzaki (2011). "Cbln family proteins promote synapse formation by regulating distinct neurexin signaling pathways in various brain regions." Eur J Neurosci **33**(8): 1447-1461.

Matsui, A., M. Tran, A. C. Yoshida, S. S. Kikuchi, M. U, M. Ogawa and T. Shimogori (2013). "BTBD3 controls dendrite orientation toward active axons in mammalian neocortex." Science **342**(6162): 1114-1118.

McConnell, S. K., A. Ghosh and C. J. Shatz (1989). "Subplate neurons pioneer the first axon pathway from the cerebral cortex." Science **245**(4921): 978-982.

Metin, C. and P. Godement (1996). "The ganglionic eminence may be an intermediate target for corticofugal and thalamocortical axons." J Neurosci **16**(10): 3219-3235.

Meyer, H. S., R. Egger, J. M. Guest, R. Foerster, S. Reissl and M. Oberlaender (2013). "Cellular organization of cortical barrel columns is whisker-specific." Proc Natl Acad Sci U S A **110**(47): 19113-19118.

Miller, B., L. Chou and B. L. Finlay (1993). "The early development of thalamocortical and corticothalamic projections." J Comp Neurol **335**(1): 16-41.

Mitrofanis, J. and G. E. Baker (1993). "Development of the thalamic reticular and perireticular nuclei in rats and their relationship to the course of growing corticofugal and corticopetal axons." J Comp Neurol **338**(4): 575-587.

Miura, E., T. Iijima, M. Yuzaki and M. Watanabe (2006). "Distinct expression of Cbln family mRNAs in developing and adult mouse brains." Eur J Neurosci **24**(3): 750-760.

Mizuno, H., W. Luo, E. Tarusawa, Y. M. Saito, T. Sato, Y. Yoshimura, S. Itohara and T. Iwasato (2014). "NMDAR-regulated dynamics of layer 4 neuronal dendrites during thalamocortical reorganization in neonates." Neuron **82**(2): 365-379.

Molnar, Z., R. Adams, A. M. Goffinet and C. Blakemore (1998). "The role of the first postmitotic cortical cells in the development of thalamocortical innervation in the reeler mouse." J Neurosci **18**(15): 5746-5765.

Molnar, Z. and C. Blakemore (1995). "How do thalamic axons find their way to the cortex?" Trends Neurosci **18**(9): 389-397.

Molnar, Z., S. Garel, G. Lopez-Bendito, P. Maness and D. J. Price (2012). "Mechanisms controlling the guidance of thalamocortical axons through the embryonic forebrain." Eur J Neurosci **35**(10): 1573-1585.

Molnar, Z. and E. Molnar (2006). "Calcium and NeuroD2 control the development of thalamocortical communication." Neuron **49**(5): 639-642.

Molyneaux, B. J., P. Arlotta, J. R. Menezes and J. D. Macklis (2007). "Neuronal subtype specification in the cerebral cortex." Nat Rev Neurosci **8**(6): 427-437.

Mulder, N. J., R. Apweiler, T. K. Attwood, A. Bairoch, A. Bateman, D. Binns, M. Biswas, P. Bradley, P. Bork, P. Bucher, R. Copley, E. Courcelle, R. Durbin, L. Falquet, W. Fleischmann, J. Gouzy, S. Griffith-Jones, D. Haft, H. Hermjakob, N. Hulo, D. Kahn, A. Kanapin, M. Krestyaninova, R. Lopez, I. Letunic, S. Orchard, M. Pagni, D. Peyruc, C. P. Ponting, F. Servant, C. J. Sigrist and C. InterPro (2002). "InterPro: an integrated documentation resource for protein families, domains and functional sites." Brief Bioinform **3**(3): 225-235.

Murray Sherman, S. and R. Guillery (2001). Exploring the thalamus, Academic Press.

Nadella, M., M. A. Bianchet, S. B. Gabelli, J. Barrila and L. M. Amzel (2005). "Structure and activity of the axon guidance protein MICAL." Proc Natl Acad Sci U S A **102**(46): 16830-16835.

Nakagawa, Y. and T. Shimogori (2012). "Diversity of thalamic progenitor cells and postmitotic neurons." Eur J Neurosci **35**(10): 1554-1562.

Nakai, K. and P. Horton (1999). "PSORT: a program for detecting sorting signals in proteins and predicting their subcellular localization." Trends Biochem Sci **24**(1): 34-36.

Nakamura, K., H. Hioki, F. Fujiyama and T. Kaneko (2005). "Postnatal changes of vesicular glutamate transporter (VGluT)1 and VGluT2 immunoreactivities and their colocalization in the mouse forebrain." J Comp Neurol **492**(3): 263-288.

Nakashiba, T., S. Nishimura, T. Ikeda and S. Itohara (2002). "Complementary expression and neurite outgrowth activity of netrin-G subfamily members." Mech Dev **111**(1-2): 47-60.

Nawabi, H., A. Briancon-Marjollet, C. Clark, I. Sanyas, H. Takamatsu, T. Okuno, A. Kumanogoh, M. Bozon, K. Takeshima, Y. Yoshida, F. Moret, K. Abouzid and V. Castellani (2010). "A midline switch of receptor processing regulates commissural axon guidance in vertebrates." Genes Dev **24**(4): 396-410.

Niehrs, C. (2012). "The complex world of WNT receptor signalling." Nat Rev Mol Cell Biol **13**(12): 767-779.

Nielsen, H., J. Engelbrecht, S. Brunak and G. von Heijne (1997). "Identification of prokaryotic and eukaryotic signal peptides and prediction of their cleavage sites." Protein Eng **10**(1): 1-6.

O'Brien, T. F., D. A. Steindler and N. G. Cooper (1987). "Abnormal glial and glycoconjugate dispositions in the somatosensory cortical barrel field of the early postnatal reeler mutant mouse." Brain Res **429**(2): 309-317.

Obst-Pernberg, K., L. Medina and C. Redies (2001). "Expression of R-cadherin and N-cadherin by cell groups and fiber tracts in the developing mouse forebrain: relation to the formation of functional circuits." Neuroscience **106**(3): 505-533.

Ohta, K., A. Mizutani, A. Kawakami, Y. Murakami, Y. Kasuya, S. Takagi, H. Tanaka and H. Fujisawa (1995). "Plexin: a novel neuronal cell surface molecule that mediates cell adhesion via a homophilic binding mechanism in the presence of calcium ions." Neuron **14**(6): 1189-1199.

Ohta, K., S. Takagi, H. Asou and H. Fujisawa (1992). "Involvement of neuronal cell surface molecule B2 in the formation of retinal plexiform layers." Neuron **9**(1): 151-161.

Ohyama, K., K. Tan-Takeuchi, M. Kutsche, M. Schachner, K. Uyemura and K. Kawamura (2004). "Neural cell adhesion molecule L1 is required for fasciculation and routing of thalamocortical fibres and corticothalamic fibres." Neurosci Res **48**(4): 471-475.

Paradis, S., D. B. Harrar, Y. Lin, A. C. Koon, J. L. Hauser, E. C. Griffith, L. Zhu, L. F. Brass, C. Chen and M. E. Greenberg (2007). "An RNAi-based approach

identifies molecules required for glutamatergic and GABAergic synapse development." Neuron **53**(2): 217-232.

Parra, L. M. and Y. Zou (2010). "Sonic hedgehog induces response of commissural axons to Semaphorin repulsion during midline crossing." Nat Neurosci **13**(1): 29-35.

Pascoe, H. G., Y. Wang and X. Zhang (2015). "Structural mechanisms of plexin signaling." Prog Biophys Mol Biol.

Pasterkamp, R. J. (2012). "Getting neural circuits into shape with semaphorins." Nat Rev Neurosci **13**(9): 605-618.

Penny, G. R., K. Itoh and I. T. Diamond (1982). "Cells of different sizes in the ventral nuclei project to different layers of the somatic cortex in the cat." Brain Res **242**(1): 55-65.

Persico, A. M., E. Mengual, R. Moessner, F. S. Hall, R. S. Revay, I. Sora, J. Arellano, J. DeFelipe, J. M. Gimenez-Amaya, M. Conciatori, R. Marino, A. Baldi, S. Cabib, T. Pascucci, G. R. Uhl, D. L. Murphy, K. P. Lesch and F. Keller (2001). "Barrel pattern formation requires serotonin uptake by thalamocortical afferents, and not vesicular monoamine release." J Neurosci **21**(17): 6862-6873.

Petersen, T. N., S. Brunak, G. von Heijne and H. Nielsen (2011). "SignalP 4.0: discriminating signal peptides from transmembrane regions." Nat Methods **8**(10): 785-786.

Powell, T. P. and W. M. Cowan (1954). "The connexions of the midline and intralaminar nuclei of the thalamus of the rat." J Anat **88**(3): 307-319.

Pratt, T., J. C. Quinn, T. I. Simpson, J. D. West, J. O. Mason and D. J. Price (2002). "Disruption of early events in thalamocortical tract formation in mice lacking the transcription factors Pax6 or Foxg1." J Neurosci **22**(19): 8523-8531.

Price, D. J., J. Clegg, X. O. Duocastella, D. Willshaw and T. Pratt (2012). "The importance of combinatorial gene expression in early Mammalian thalamic patterning and thalamocortical axonal guidance." Front Neurosci **6**: 37.

Price, D. J., H. Kennedy, C. Dehay, L. Zhou, M. Mercier, Y. Jossin, A. M. Goffinet, F. Tissir, D. Blakey and Z. Molnar (2006). "The development of cortical connections." Eur J Neurosci **23**(4): 910-920.

Quinlan, R., M. Graf, I. Mason, A. Lumsden and C. Kiecker (2009). "Complex and dynamic patterns of Wnt pathway gene expression in the developing chick forebrain." Neural Dev **4**: 35.

Rakic, S., C. Davis, Z. Molnar, M. Nikolic and J. G. Parnavelas (2006). "Role of p35/Cdk5 in preplate splitting in the developing cerebral cortex." Cereb Cortex **16 Suppl 1**: i35-45.

Rebsam, A., I. Seif and P. Gaspar (2002). "Refinement of thalamocortical arbors and emergence of barrel domains in the primary somatosensory cortex: a study of normal and monoamine oxidase a knock-out mice." J Neurosci **22**(19): 8541-8552.

Rebsam, A., I. Seif and P. Gaspar (2005). "Dissociating barrel development and lesion-induced plasticity in the mouse somatosensory cortex." J Neurosci **25**(3): 706-710.

Renaud, J., G. Kerjan, I. Sumita, Y. Zagar, V. Georget, D. Kim, C. Fouquet, K. Suda, M. Sanbo, F. Suto, S. L. Ackerman, K. J. Mitchell, H. Fujisawa and A. Chedotal (2008). "Plexin-A2 and its ligand, Sema6A, control nucleus-centrosome coupling in migrating granule cells." Nat Neurosci **11**(4): 440-449.

Ribic, A., X. Liu, M. C. Crair and T. Biederer (2014). "Structural organization and function of mouse photoreceptor ribbon synapses involve the immunoglobulin protein synaptic cell adhesion molecule 1." J Comp Neurol **522**(4): 900-920.

Rice, F. L., C. Gomez, C. Barstow, A. Burnet and P. Sands (1985). "A comparative analysis of the development of the primary somatosensory cortex: interspecies similarities during barrel and laminar development." J Comp Neurol **236**(4): 477-495.

Runker, A. E., C. O'Tuathaigh, M. Dunleavy, D. W. Morris, G. E. Little, A. P. Corvin, M. Gill, D. C. Henshall, J. L. Waddington and K. J. Mitchell (2011). "Mutation of Semaphorin-6A disrupts limbic and cortical connectivity and models neurodevelopmental psychopathology." PLoS One **6**(11): e26488.

Saeed, A. I., V. Sharov, J. White, J. Li, W. Liang, N. Bhagabati, J. Braisted, M. Klapa, T. Currier, M. Thiagarajan, A. Sturn, M. Snuffin, A. Rezantsev, D. Popov, A. Ryltsov, E. Kostukovich, I. Borisovsky, Z. Liu, A. Vinsavich, V. Trush and J. Quackenbush (2003). "TM4: a free, open-source system for microarray data management and analysis." Biotechniques **34**(2): 374-378.

Salichon, N., P. Gaspar, A. L. Upton, S. Picaud, N. Hanoun, M. Hamon, E. De Maeyer, D. L. Murphy, R. Mossner, K. P. Lesch, R. Hen and I. Seif (2001).

"Excessive activation of serotonin (5-HT) 1B receptors disrupts the formation of sensory maps in monoamine oxidase a and 5-ht transporter knock-out mice." J Neurosci **21**(3): 884-896.

Satoda, M., S. Takagi, K. Ohta, T. Hirata and H. Fujisawa (1995). "Differential expression of two cell surface proteins, neuropilin and plexin, in Xenopus olfactory axon subclasses." J Neurosci **15**(1 Pt 2): 942-955.

Scholpp, S. and A. Lumsden (2010). "Building a bridal chamber: development of the thalamus." Trends Neurosci **33**(8): 373-380.

Scholpp, S., O. Wolf, M. Brand and A. Lumsden (2006). "Hedgehog signalling from the zona limitans intrathalamica orchestrates patterning of the zebrafish diencephalon." Development **133**(5): 855-864.

Schultz, J., F. Milpetz, P. Bork and C. P. Ponting (1998). "SMART, a simple modular architecture research tool: identification of signaling domains." Proc Natl Acad Sci U S A **95**(11): 5857-5864.

Seibt, J., C. Schuurmans, G. Gradwhol, C. Dehay, P. Vanderhaeghen, F. Guillemot and F. Polleux (2003). "Neurogenin2 specifies the connectivity of thalamic neurons by controlling axon responsiveness to intermediate target cues." Neuron **39**(3): 439-452.

Sherman, S. M. and R. W. Guillery (1998). "On the actions that one nerve cell can have on another: distinguishing "drivers" from "modulators"." Proc Natl Acad Sci U S A **95**(12): 7121-7126.

Shetty, A. S., G. Godbole, U. Maheshwari, H. Padmanabhan, R. Chaudhary, B. Muralidharan, P. S. Hou, E. S. Monuki, H. C. Kuo, V. Rema and S. Tole (2013). "Lhx2 regulates a cortex-specific mechanism for barrel formation." Proc Natl Acad Sci U S A **110**(50): E4913-4921.

Siebold, C., N. Berrow, T. S. Walter, K. Harlos, R. J. Owens, D. I. Stuart, J. R. Terman, A. L. Kolodkin, R. J. Pasterkamp and E. Y. Jones (2005). "High-resolution structure of the catalytic region of MICAL (molecule interacting with CasL), a multidomain flavoenzyme-signaling molecule." Proc Natl Acad Sci U S A **102**(46): 16836-16841.

Song, H., G. Ming, Z. He, M. Lehmann, L. McKerracher, M. Tessier-Lavigne and M. Poo (1998). "Conversion of neuronal growth cone responses from repulsion to attraction by cyclic nucleotides." Science **281**(5382): 1515-1518.

Sonnhammer, E. L., G. von Heijne and A. Krogh (1998). "A hidden Markov model for predicting transmembrane helices in protein sequences." Proc Int Conf Intell Syst Mol Biol **6**: 175-182.

Sunyaev, S. R., F. Eisenhaber, I. V. Rodchenkov, B. Eisenhaber, V. G. Tumanyan and E. N. Kuznetsov (1999). "PSIC: profile extraction from sequence alignments with position-specific counts of independent observations." Protein Eng **12**(5): 387-394.

Suto, F., K. Ito, M. Uemura, M. Shimizu, Y. Shinkawa, M. Sanbo, T. Shinoda, M. Tsuboi, S. Takashima, T. Yagi and H. Fujisawa (2005). "Plexin-a4 mediates axon-repulsive activities of both secreted and transmembrane semaphorins and plays roles in nerve fiber guidance." J Neurosci **25**(14): 3628-3637.

Suto, F., Y. Murakami, F. Nakamura, Y. Goshima and H. Fujisawa (2003). "Identification and characterization of a novel mouse plexin, plexin-A4." Mech Dev **120**(3): 385-396.

Suto, F., M. Tsuboi, H. Kamiya, H. Mizuno, Y. Kiyama, S. Komai, M. Shimizu, M. Sanbo, T. Yagi, Y. Hiromi, A. Chedotal, K. J. Mitchell, T. Manabe and H. Fujisawa (2007). "Interactions between plexin-A2, plexin-A4, and semaphorin 6A control lamina-restricted projection of hippocampal mossy fibers." Neuron **53**(4): 535-547.

Suzuki, S. C., T. Inoue, Y. Kimura, T. Tanaka and M. Takeichi (1997). "Neuronal circuits are subdivided by differential expression of type-II classic cadherins in postnatal mouse brains." Mol Cell Neurosci **9**(5-6): 433-447.

Suzuki-Hirano, A., M. Ogawa, A. Kataoka, A. C. Yoshida, D. Itoh, M. Ueno, S. Blackshaw and T. Shimogori (2011). "Dynamic spatiotemporal gene expression in embryonic mouse thalamus." J Comp Neurol **519**(3): 528-543.

Szabo, N. E., T. Zhao, X. Zhou and G. Alvarez-Bolado (2009). "The role of Sonic hedgehog of neural origin in thalamic differentiation in the mouse." J Neurosci **29**(8): 2453-2466.

Takagi, S., T. Tsuji, T. Amagai, T. Takamatsu and H. Fujisawa (1987). "Specific cell surface labels in the visual centers of Xenopus laevis tadpole identified using monoclonal antibodies." Dev Biol **122**(1): 90-100.

Takao, M., J. Hino, N. Takeshita, Y. Konno, T. Nishizawa, H. Matsuo and K. Kangawa (1996). "Identification of rat bone morphogenetic protein-3b (BMP-3b), a new member of BMP-3." Biochem Biophys Res Commun **219**(2): 656-662.

Tamagnone, L., S. Artigiani, H. Chen, Z. He, G. I. Ming, H. Song, A. Chedotal, M. L. Winberg, C. S. Goodman, M. Poo, M. Tessier-Lavigne and P. M. Comoglio (1999). "Plexins are a large family of receptors for transmembrane, secreted, and GPI-anchored semaphorins in vertebrates." Cell **99**(1): 71-80.

Tawarayama, H., Y. Yoshida, F. Suto, K. J. Mitchell and H. Fujisawa (2010). "Roles of semaphorin-6B and plexin-A2 in lamina-restricted projection of hippocampal mossy fibers." J Neurosci **30**(20): 7049-7060.

Terman, J. R., T. Mao, R. J. Pasterkamp, H. H. Yu and A. L. Kolodkin (2002). "MICALs, a family of conserved flavoprotein oxidoreductases, function in plexin-mediated axonal repulsion." Cell **109**(7): 887-900.

Thompson, C. L., L. Ng, V. Menon, S. Martinez, C. K. Lee, K. Glattfelder, S. M. Sunkin, A. Henry, C. Lau, C. Dang, R. Garcia-Lopez, A. Martinez-Ferre, A. Pombero, J. L. Rubenstein, W. B. Wakeman, J. Hohmann, N. Dee, A. J. Sodt, R. Young, K. Smith, T. N. Nguyen, J. Kidney, L. Kuan, A. Jeromin, A. Kaykas, J. Miller, D. Page, G. Orta, A. Bernard, Z. Riley, S. Smith, P. Wohnoutka, M. J. Hawrylycz, L. Puelles and A. R. Jones (2014). "A high-resolution spatiotemporal atlas of gene expression of the developing mouse brain." Neuron **83**(2): 309-323.

Tong, Y., P. K. Hota, J. Y. Penachioni, M. B. Hamaneh, S. Kim, R. S. Alviani, L. Shen, H. He, W. Tempel, L. Tamagnone, H. W. Park and M. Buck (2009). "Structure and function of the intracellular region of the plexin-b1 transmembrane receptor." J Biol Chem **284**(51): 35962-35972.

Trikalinos, T. A., A. Karvouni, E. Zintzaras, T. Ylisaukko-oja, L. Peltonen, I. Jarvela and J. P. Ioannidis (2006). "A heterogeneity-based genome search meta-analysis for autism-spectrum disorders." Mol Psychiatry **11**(1): 29-36.

Tuttle, R., Y. Nakagawa, J. E. Johnson and D. D. O'Leary (1999). "Defects in thalamocortical axon pathfinding correlate with altered cell domains in Mash-1-deficient mice." Development **126**(9): 1903-1916.

van Kleef, E. S., P. Gaspar and A. Bonnin (2012). "Insights into the complex influence of 5-HT signaling on thalamocortical axonal system development." Eur J Neurosci **35**(10): 1563-1572.

Vieira, C., A. L. Garda, K. Shimamura and S. Martinez (2005). "Thalamic development induced by Shh in the chick embryo." Dev Biol **284**(2): 351-363.

Villanueva, C., S. Jacquier and N. de Roux (2012). "DLK1 is a somato-dendritic protein expressed in hypothalamic arginine-vasopressin and oxytocin neurons." PLoS One **7**(4): e36134.

Vue, T. Y., J. Aaker, A. Taniguchi, C. Kazemzadeh, J. M. Skidmore, D. M. Martin, J. F. Martin, M. Treier and Y. Nakagawa (2007). "Characterization of progenitor domains in the developing mouse thalamus." J Comp Neurol **505**(1): 73-91.

Vue, T. Y., K. Bluske, A. Alishahi, L. L. Yang, N. Koyano-Nakagawa, B. Novitch and Y. Nakagawa (2009). "Sonic hedgehog signaling controls thalamic progenitor identity and nuclei specification in mice." J Neurosci **29**(14): 4484-4497.

Wang, H., P. K. Hota, Y. Tong, B. Li, L. Shen, L. Nedyalkova, S. Borthakur, S. Kim, W. Tempel, M. Buck and H. W. Park (2011). "Structural basis of Rnd1 binding to plexin Rho GTPase binding domains (RBDs)." J Biol Chem **286**(29): 26093-26106.

Wang, Y., H. He, N. Srivastava, S. Vikarunnessa, Y. B. Chen, J. Jiang, C. W. Cowan and X. Zhang (2012). "Plexins are GTPase-activating proteins for Rap and are activated by induced dimerization." Sci Signal **5**(207): ra6.

Wei, P., R. Pattarini, Y. Rong, H. Guo, P. K. Bansal, S. V. Kusnoor, A. Y. Deutch, J. Parris and J. I. Morgan (2012). "The Cbln family of proteins interact with multiple signaling pathways." J Neurochem **121**(5): 717-729.

Welker, E., M. Armstrong-James, G. Bronchti, W. Ourednik, F. Gheorghita-Baechler, R. Dubois, D. L. Guernsey, H. Van der Loos and P. E. Neumann (1996). "Altered sensory processing in the somatosensory cortex of the mouse mutant barrelless." Science **271**(5257): 1864-1867.

Wiencken-Barger, A. E., J. Mavity-Hudson, U. Bartsch, M. Schachner and V. A. Casagrande (2004). "The role of L1 in axon pathfinding and fasciculation." Cereb Cortex **14**(2): 121-131.

Winberg, M. L., J. N. Noordermeer, L. Tamagnone, P. M. Comoglio, M. K. Spriggs, M. Tessier-Lavigne and C. S. Goodman (1998). "Plexin A is a neuronal semaphorin receptor that controls axon guidance." Cell **95**(7): 903-916.

Wolman, M. A., Y. Liu, H. Tawarayama, W. Shoji and M. C. Halloran (2004). "Repulsion and attraction of axons by semaphorin3D are mediated by different neuropilins in vivo." J Neurosci **24**(39): 8428-8435.

Woolsey, T. A. and H. Van der Loos (1970). "The structural organization of layer IV in the somatosensory region (SI) of mouse cerebral cortex. The description of a cortical field composed of discrete cytoarchitectonic units." Brain Res **17**(2): 205-242.

Wright, A. G., G. P. Demyanenko, A. Powell, M. Schachner, L. Enriquez-Barreto, T. S. Tran, F. Polleux and P. F. Maness (2007). "Close homolog of L1 and neuropilin 1 mediate guidance of thalamocortical axons at the ventral telencephalon." J Neurosci **27**(50): 13667-13679.

Wu, C. S., C. J. Ballester Rosado and H. C. Lu (2011). "What can we get from 'barrels': the rodent barrel cortex as a model for studying the establishment of neural circuits." Eur J Neurosci **34**(10): 1663-1676.

Yam, P. T. and F. Charron (2013). "Signaling mechanisms of non-conventional axon guidance cues: the Shh, BMP and Wnt morphogens." Curr Opin Neurobiol **23**(6): 965-973.

Yamada, A., E. Inoue, M. Deguchi-Tawarada, C. Matsui, A. Togawa, T. Nakatani, Y. Ono and Y. Takai (2013). "Necl-2/CADM1 interacts with ErbB4 and regulates its activity in GABAergic neurons." Mol Cell Neurosci **56**: 234-243.

Yamada, T., T. Sakisaka, S. Hisata, T. Baba and Y. Takai (2005). "RA-RhoGAP, Rap-activated Rho GTPase-activating protein implicated in neurite outgrowth through Rho." J Biol Chem **280**(38): 33026-33034.

Yamauchi, K., K. D. Phan and S. J. Butler (2008). "BMP type I receptor complexes have distinct activities mediating cell fate and axon guidance decisions." Development **135**(6): 1119-1128.

Yaron, A., P. H. Huang, H. J. Cheng and M. Tessier-Lavigne (2005). "Differential requirement for Plexin-A3 and -A4 in mediating responses of sensory and sympathetic neurons to distinct class 3 Semaphorins." Neuron **45**(4): 513-523.

Yazdani, U. and J. R. Terman (2006). "The semaphorins." Genome Biol **7**(3): 211.

Yin, Y., J. H. Miner and J. R. Sanes (2002). "Laminets: laminin- and netrin-related genes expressed in distinct neuronal subsets." Mol Cell Neurosci **19**(3): 344-358.

Yoshida, Y. (2012). "Semaphorin signaling in vertebrate neural circuit assembly." Front Mol Neurosci **5**: 71.

Yoshida, Y., B. Han, M. Mendelsohn and T. M. Jessell (2006). "PlexinA1 signaling directs the segregation of proprioceptive sensory axons in the developing spinal cord." Neuron **52**(5): 775-788.

Zhou, C. J., K. I. Pinson and S. J. Pleasure (2004). "Severe defects in dorsal thalamic development in low-density lipoprotein receptor-related protein-6 mutants." J Neurosci **24**(35): 7632-7639.